

Stripping Reactions and the Structure of Light and Intermediate Nuclei*

M. H. MACFARLANE

Argonne National Laboratory, Lemont, Illinois, and University of Rochester, Rochester, New York†

AND

J. B. FRENCH

University of Rochester, Rochester, New York

CONTENTS

I. Introduction.....	567
II. Empirical Reduced Widths.....	569
1. Born-Approximation Differential Cross Section. Definition of Reduced Width..	569
2. Deuteron-Nucleon Reduced Widths; Practical Procedure and Results.....	570
3. Deuteron-Triton Reduced Widths.....	572
4. Area of Applicability, Limitations, and Possible Refinements of the Simple Theory of Stripping.....	573
III. Theoretical Analysis of Reduced Widths...	594
1. Introduction.....	594
2. Nuclear Shell Model.....	594
3. Notation.....	596
4. Antisymmetric States for Nucleons in the Same Shell.....	598
5. Holes, Particles, and Phases.....	599
6. Antisymmetric States for Nucleons in Different Shells.....	605
7. Shell-Model Expressions for $\$$	606
8. Calculation of $\$$ in LSJT Representations.....	612
9. General Comments: Specific Examples.	614
10. Sum Rules and Related Topics.....	620
11. "Weak-Coupling" Formalism.....	629
12. Calculation of $\$$ from Rotational-Model Wave Functions.....	632
13. Calculation of $\$$ from Vibrational-Model Wave Functions.....	635
IV. Stripping and Pickup Reactions on $1p$ -Shell Nuclei.....	636
V. Stripping and Pickup Reactions on ds -Shell Nuclei.....	651
VI. Stripping and Pickup Reactions on Heavier Nuclei ($A > 40$).....	669
VII. Review of the Information Obtained from the Analysis of Empirical Reduced Widths.	679
1. Information about the Properties of Nuclear States.....	679
2. Information about the Mechanism of Stripping Reactions: Single-Particle Reduced Widths.....	682
3. Suggested Experiments for Future Study.	684
Appendix 1.....	686
Appendix 2.....	687
Bibliography.....	688

I. INTRODUCTION

A REDUCED width for the emission of a single nucleon in a transition between two specific nuclear states can be regarded as a product of two factors. Of these factors, the first is a measure of the probability that, in the initial nuclear state, all but one of the nucleons will find themselves in an arrangement corresponding to the final state; the second factor measures the probability that, when this happens, the two components will actually separate. The factorization is formally expressed by

$$\theta^2 = \$ \theta_0^2. \quad (\text{I.1})$$

It is clear that the "spectroscopic factor" $\$$, which depends only on the wave functions of the nuclear states involved, provides a useful basis for comparison between experiment and the predictions of current nuclear models.

There are two different sources of experimental information on nucleon reduced widths. In resonance reactions, they occur as parameters characterizing the rate of decay of levels of the compound system into nucleon channels (La58),¹ while essentially similar quantities appear as multiplicative factors in the differential cross sections of certain "direct" reactions in which a nucleon is transferred, the simplest and best-known example being the (d,p) reaction. For spectroscopic purposes, the second or "stripping" type of reduced width has certain important advantages. Such widths can connect low-lying levels which may be inaccessible to resonance reactions but are of the greatest interest to current nuclear models. Furthermore, a stripping width is a rather easy quantity to measure experimentally and can be extracted from the experimental cross section in a very straightforward fashion, provided that a suitable theory of the stripping process is available.

* Work performed partly under the auspices of the U. S. Atomic Energy Commission.

† Present address: Physics Division, Argonne National Laboratory, Lemont, Illinois.

¹ References to literature are listed alphabetically in the Bibliography at the end of the article.

In the present study, the only empirical reduced widths to be considered are of the stripping and pickup variety. Apart from reduced widths from (d,p) , (d,n) , (p,d) , and (n,d) reactions, we give some consideration to the possibility of obtaining nucleon reduced widths from more complex processes, such as (d,t) , (d,He^3) , (He^3,d) , or (α,t) , in which a single nucleon is transferred. On the other hand, the formal techniques developed in our theoretical analysis of \mathcal{S} are independent of the origin and properties of θ^2 , and are therefore equally applicable in a study of resonant reduced widths.

Holt and Marsham (Ho53, Ho53a-d) were the first to perform a systematic series of stripping experiments as a means of studying the level properties of nuclei. Since then, the work of many authors (for example, La53, Sa54, Au55, Fr56, Sa58) has shown that stripping widths can yield valuable information about the structure of nuclear states. In such studies, empirical reduced widths are extracted from observed differential cross sections with the aid of the original simple theory of Butler (Bu51) or one of its variants (Bh52, Da52). The major difficulty encountered is that these plane-wave Born approximation theories produce disturbingly small reduced widths. It is found that a Butler-Born approximation reduced width is usually smaller by a factor of four or five than would be expected on the basis of some reasonable potential-well model of the nucleon-transfer process, even in cases in which the overlap factor \mathcal{S} should be close to unity. In a few instances, both resonance and stripping widths have been measured for the same two states, the conclusion again being that the (Born approximation) stripping width is markedly the smaller. In other words, the Butler theory overestimates cross sections.

The most obvious way of improving matters would be to employ a better theory of stripping, wherein the incoming and outgoing particles are represented more accurately than they are by the plane waves of the simple theory. It is, in fact, well established that such calculations yield considerably smaller cross sections (Ho53e, Ge53, To55). Nevertheless, these more sophisticated theories do not provide a practicable basis for the present study, wherein hundreds of stripping widths are extracted and analyzed. Since optical-model wave functions must be computed for the incoming and outgoing particles, the numerical solutions then being used in calculating the differential cross section, the extraction of each reduced width would demand a sizable machine calculation. Furthermore, the parameters specifying the relevant optical wells must be regarded as to some extent adjustable. We must therefore reckon with the possibility that the resulting reduced width would not be a sufficiently unambiguous quantity to justify the effort expended in extracting it.

Let us, accordingly, agree to use the simple Butler theory to obtain empirical reduced widths from stripping and pickup reactions. We circumvent diffi-

culties with the absolute magnitude of Born-approximation reduced widths by giving up all pretensions to *a priori* knowledge of the single-particle reduced width θ_0^2 ; it is to be regarded as *an empirical parameter to be evaluated by direct comparison with experiment*. The possibility of using the simple theory in this fashion depends on the fact, as yet imperfectly understood, that its two main sources of error seem to oppose each other systematically, at least so far as their effect on angular distributions near the characteristic stripping peak is concerned.² The tendency of the nuclear distortion is to push this peak toward smaller angles, while Coulomb effects act in the opposite direction; the net effect, as revealed by an imposing body of experimental evidence, is to leave the stripping peak very close to the position predicted by the simple theory. The essential feature of the original Butler theory is thus preserved; the angular distribution of scattered particles in a stripping or pickup reaction may be used as an indicator of the orbital angular momentum l of the transferred nucleon.

What we are trying to do is to absorb the various shortcomings of the simple theory in a single parameter θ_0^2 . We must therefore expect our empirically determined single-particle reduced width to be a function of the quantum numbers of the transferred nucleon, of the Q value of the reaction, of the bombarding energy, and perhaps of other parameters as well. Indeed, we might hope to simulate the main Coulomb and distortion effects neglected in the simple theory by suitable dependences of θ_0^2 on its parameters; in so doing, we try to use the large amount of experimental data presently and potentially available to forge a powerful semi-phenomenological tool for the analysis of stripping widths.

Our analysis is subject to certain inescapable uncertainties. In addition to experimental error, we must take account of the uncertain reliability of reduced widths extracted by means of the Butler formula. It is therefore not possible, nor would it be of much interest, to give a detailed error estimate in each comparison with experiment. Instead, on surveying the quality of agreement obtained between theory and experiment in the entire study, we conclude that agreement to within 25% in any particular case must be considered satisfactory. This does not prevent us from hoping, optimistically, for something better in favorable circumstances.

To summarize, the three main objectives of this study of stripping widths are:

1. to develop a formalism for the theoretical analysis of nucleon reduced widths or, more precisely, of the spectroscopic factor \mathcal{S} defined in Eq. (I.1);
2. to use this formal apparatus and the reduced widths extracted from available stripping and pickup reactions in a detailed study of the structure of the nuclear states involved; and

² This matter is discussed in more detail in a review article by Austern (Au60).

3. to apply the collected results of the preceding study of empirical reduced widths to assessing and, if possible, to increasing the power of the spectroscopic tool furnished by the analysis of stripping widths.

We have already stated our reasons for using the simple Born-approximation theory in extracting stripping widths. The ultimate justification of this step lies in the large amount of consistent information so obtained about the structure of nuclei.

II. EMPIRICAL REDUCED WIDTHS

In this section we give formulas for extracting nucleon reduced widths from the measured differential cross sections of stripping and pickup reactions; the empirical reduced widths so obtained are then tabulated.

We are not concerned with the fundamental properties of the reaction process; such matters are discussed in a number of review articles (Hu53, To56, Bu57, Au60). Our approach is purely empirical. We use the simple Butler-Born approximation theory, neglecting antisymmetrization between the projectile and target nucleons. We do not give a detailed derivation of the Born-approximation differential cross section; for this we refer the reader to a recent article by J. B. French (Fr60, Appendix), which we follow closely in procedure and in notation.

1. Born-Approximation Differential Cross Section. Definition of Reduced Width

We consider the reactions

$$A[J_0 T_0 M_0 M_{T_0}] + a(i_{0t_0} m_0 m_{t_0}) \rightleftharpoons (A+1)[J T M M_T] + (a-1)[i i m m_t], \quad (\text{II.1})$$

where $[a]$ is the lighter of the two initial nuclei, and the spins and isotopic spins are given in square brackets. We sometimes prefer to treat neutrons and protons on a separate footing, in which case the isotopic-spin quantum numbers are omitted. The projection quantum numbers are absent from the final cross section for unpolarized beams.

Particular cases of (II.1) which are of practical interest are

$a=2$ (deuteron-nucleon reactions) $(d,p)(d,n)(p,d)(n,d)$

$a=3$ (deuteron-triton reactions) $(\text{He}^3,d)(d,\text{He}^3)(d,t)$

$a=4$ (alpha-particle reactions) $(\text{He}^4,\alpha)(\alpha,\text{He}^3)(\alpha,t)$.

Forward arrows in (II.1) refer to true stripping, backward arrows to pickup processes.

We then have the following definitions and kinematical relations (taking $\hbar=1$):

$(d\sigma/d\omega)\downarrow, (d\sigma/d\omega)\uparrow$: Center-of-mass differential cross sections for the reaction $A(a, a-1)A+1$ and its inverse.

E : Kinetic energy of $[a]$ in the rest frame of $[A]$.

E : Kinetic energy of $[a-1]$ in the rest frame of $[A+1]$.

Q : Q value of the reaction $A(a, a-1)A+1$. In terms of the binding energies (ϵ) of the four nuclei in (II.1),

$$Q = \epsilon_{A+1} + \epsilon_{a-1} - \epsilon_A - \epsilon_a. \quad (\text{II.2})$$

M : Mass of a nucleon.

r_0 : Butler radius.

k_0 : Relative wave numbers of the pair (A,a) in the center-of-mass frame

$$k_0^2 = 2aE_0M[A^2/(A+a)^2]. \quad (\text{II.3})$$

k : Relative wave number of the pair $(A+1, a-1)$ in the center-of-mass frame

$$k^2 = 2(a-1)EM[(A+1)^2/(A+a)^2]. \quad (\text{II.4})$$

q, κ : Natural momentum variables for the reaction (II.1), q being the momentum-transfer vector

$$q = k_0 - [A/(A+1)]k, \quad (\text{II.5})$$

$$\kappa = [(a-1)/a]k_0 - k. \quad (\text{II.6})$$

$\theta = \cos^{-1}(k_0 \cdot k/k_0 k)$: Center-of-mass scattering angle.

iS : Wave number corresponding to the binding energy in $[a]$ of the transferred nucleon. It is imaginary in all cases of present interest.

$$[a/(a-1)] \cdot (S^2/2M) = \epsilon_a - \epsilon_{a-1}. \quad (\text{II.7})$$

$i\tau$: Wave number corresponding to the binding energy in $[A+1]$ of the transferred nucleon. It is imaginary for capture into bound states of $[A+1]$, for which

$$Q + \epsilon_a - \epsilon_{a-1} > 0.$$

For both bound and unbound states, we have

$$[(A+1)/A] \cdot (l^2/2M) = (Q + \epsilon_a - \epsilon_{a-1}). \quad (\text{II.8})$$

To express the condition of conservation of energy in the center-of-mass frame, we start from the usual expression in terms of k_0 and k and use (II.5) and (II.6) to write

$$2MQ = [a/(a-1)]\kappa^2 - [(A+1)/A]q^2. \quad (\text{II.9})$$

Substitution for Q from (II.7) and (II.8) then yields

$$[a/(a-1)](\kappa^2 + S^2) = [(A+1)/A](q^2 + l^2) \quad (\text{II.10})$$

$$= [(A+1)/A r_0^2](x^2 + y^2), \quad (\text{II.11})$$

where, in the last step, we have introduced the dimensionless quantities

$$x = qr_0, \quad y = tr_0. \quad (\text{II.12})$$

We now proceed to write down the Born-approximation differential cross section for the reaction (II.1). Apart from kinematical and statistical factors which are given explicitly, the final expression involves overlap factors connecting

$$[a] \rightleftharpoons [a-1], \quad [A] \rightleftharpoons [A+1],$$

respectively. Both of these overlap factors are essentially reduced widths, although it is customary to use this terminology only for the second.

To give an explicit definition of the reduced width connecting $[A]$ and $[A+1]$, a convenient coupling scheme must be introduced for the angular momenta in the (A,a) channel. We can choose to specify either the channel spin z or the total angular momentum j of the transferred nucleon. The two representations are connected by the simple unitary transformation (III.55).

Let us use a channel-spin representation and let



symbolize the antisymmetric wave function of the relevant state of $[A]$ (with a similar convention for $[A+1]$). The notation is described fully in Sec. III.3, but for our present purposes it speaks for itself. The overlap integrals which are encountered may then be written in the form

$$\mathcal{S}(z) = \left\langle \begin{array}{c} C \\ J \end{array} \middle| \begin{array}{c} T \\ \ell \end{array} \right\rangle \quad \text{(II.13)}$$

(II.13)

which is manifestly independent of M .

A dimensionless *single-particle reduced width* θ_0^2 is first defined in terms of the radial wave function $R_l(r)$ of the transferred nucleon, evaluated at the nuclear surface by

$$\theta_0^2 = \frac{1}{3} r_0^3 R_l(r_0)^2. \quad (\text{II.14})$$

This would be the correct reduced width if the nucleus $[A]$ could be regarded as presenting an inert potential well to the transferred nucleon. The inert-well picture of $[A]$ is almost always an inadequate approximation. It is therefore necessary to take explicit account of the degree of overlap of the wave functions of $[A]$ and $[A+1]$. To do this we introduce the *relative reduced width* or *spectroscopic factor* s defined by

$$s = (A+1) \sum_z |\mathcal{S}(z)|^2 \quad (\text{II.15})$$

with $\mathcal{S}(z)$ defined as in (II.13). The reduced width for the transition is then

$$\theta^2 = s \theta_0^2. \quad (\text{II.16})$$

Our dimensionless quantity θ^2 is related to the reduced width γ^2 of Lane and Thomas (La58) by

$$\gamma^2 = \frac{3}{2} [(A+1)\hbar^2/MAr_0^2]\theta^2. \quad (\text{II.17})$$

The analogous overlap factor connecting $[a]$ and $[a-1]$ is treated rather differently. Choosing our ter-

minology to reflect this difference in treatment, we refer to it as the *stripping transform* $P_a(\kappa)$. Let ϱ denote the position vector of the transferred nucleon relative to the center of mass of $[a-1]$, while ζ symbolizes a suitable set of internal coordinates of $[a-1]$. Then the stripping transform is

$$P_a(\kappa) = \int \exp(-ik \cdot \varrho) \phi_{a-1}^*(\zeta) \phi_a(\zeta, \rho) d\zeta d^3\rho, \quad (\text{II.18})$$

where ϕ_{a-1} and ϕ_a are the internal (space) wave functions of the nuclei $[a-1]$ and $[a]$.

In terms of these overlap factors, the Born-approximation differential cross section of the reaction $A(a, a-1)A+1$, for a single value of l , is found to be [(A12) of Fr60]

$$\frac{d\sigma}{d\omega} \uparrow = \frac{3}{16\pi} \frac{a^2(a-1)(A+1)^4}{A^2(A+a)^2} \frac{(2J+1)}{(2J_0+1)} \times \left[\frac{(a-1)E}{aE_0} \right]^{\frac{1}{2}} \{C[T_{0\frac{1}{2}}T; M_{T_0}, M_T - M_{T_0}]\}^2 \times [P_a(\kappa)]^2 [W_l(x, y)]^2 (\theta^2/r_0), \quad (\text{II.19})$$

$$W_l(x, y) = \left\{ x \frac{\partial j_l(x)}{\partial x} - \frac{y j_l(x)}{h_l^{(1)}(iy)} \frac{\partial h_l^{(1)}(iy)}{\partial y} \right\}. \quad (\text{II.20})$$

For capture into unbound states of $[A+1]$, we simply replace iy by y in (II.20). In (II.19)

$$\{C[T_{0\frac{1}{2}}T; M_{T_0}, M_T - M_{T_0}]\}$$

is a vector-coupling coefficient (Co35). The cross section of the inverse pickup reaction is

$$\frac{d\sigma}{d\omega} \uparrow = \frac{(2J_0+1)(2i_0+1)}{(2J+1)(2i+1)} \left[\frac{A^2 a E_0}{(A+1)^2 (a-1) E} \right] \frac{d\sigma}{d\omega}. \quad (\text{II.21})$$

If we wish to analyze a reduced width without the isotopic-spin formalism, the diagram (II.13) must be slightly generalized, as discussed in Sec. III.7. The separate question as to whether the isotopic-spin coupling factor $(C)^2$ in (II.19) should be ignored or explicitly divided out in extracting θ^2 is discussed in Appendix 1.

2. Deuteron-Nucleon Reduced Widths; Practical Procedure and Results

In evaluating the stripping transform $P_2(\kappa)$ for deuteron-nucleon reactions, we use the Hulthen form of the deuteron internal wave function. We give only the result, since the details have been described by many authors (for example, Bu57, Au60, Fr60). From (II.18) the deuteron-nucleon stripping transform is

found to be

$$P_2(\kappa) = \left[\frac{4096\pi}{343S^2} \right]^{\frac{1}{2}} \left[\left(1 + \frac{\kappa^2}{S^2} \right) \left(1 + \frac{\kappa^2}{49S^2} \right) \right]^{-\frac{1}{2}}, \quad (\text{II.22})$$

with $S^{-1} = 4.314 \text{ f}$.

Practical calculations may be greatly simplified by the use of numerical tables, prepared by Lubitz (Lu57), of a dimensionless function $\sigma^l_{\text{TAB}}(x,y)$ which is related to quantities appearing in (II.19) by

$$[W_l(x,y)]^2 = (x^2 + y^2)^2 H \sigma^l_{\text{TAB}}(x,y). \quad (\text{II.23})$$

The effect of the term

$$H = \{1 + [(A+1)(x^2 + y^2)/96Ar_0^2S^2]\}^2 \quad (\text{II.24})$$

is so slight that it may be taken into account very accurately by giving A and r_0 any reasonable values. Lubitz took $(A+1)/A \approx 1$ and $r_0 \approx 5 \text{ f}$, so that

$$H^{\frac{1}{2}} = 1 + 0.008(x^2 + y^2). \quad (\text{II.25})$$

The final expressions obtained by substituting from (II.22) and (II.23) in (II.19) and (II.21) are given in (II.29) and (II.30). We first describe the practical procedure for using our formulas to extract reduced widths from experimental data. All energies are expressed in Mev, lengths in fermis, and the final differential cross section in millibarns per steradian.

We consider the reactions

$$A + a \rightleftharpoons (A+1) + (a-1),$$

and postpone the restriction to $a=2$ until the very last step, since the procedure is the same for all the stripping and pickup reactions we consider. We proceed as follows:

(a) Either E_0 or E is given as the laboratory kinetic energy of the bombarding particle. Calculate the other by means of

$$(A+1)E = (A+a)Q + AE_0. \quad (\text{II.26})$$

- (b) Choose values of l and r_0 .
- (c) Calculate y from

$$y = 0.22r_0 \{ [A/(A+1)] |Q + \epsilon_a - \epsilon_{a-1}| \}^{\frac{1}{2}}. \quad (\text{II.27})$$

For the various special cases of interest, $\epsilon_a - \epsilon_{a-1}$ takes the following values:

Deuteron-nucleon reactions: $\epsilon_a - \epsilon_{a-1} = 2.23 \text{ Mev}$,

(d,t) reactions: $\epsilon_a - \epsilon_{a-1} = 6.26 \text{ Mev}$,

(He^3,d) and (d,He^3) reactions: $\epsilon_a - \epsilon_{a-1} = 5.49 \text{ Mev}$,

(α,t) reactions: $\epsilon_a - \epsilon_{a-1} = 19.8 \text{ Mev}$,

(α,He^3) and (He^3,α) reactions: $\epsilon_a - \epsilon_{a-1} = 20.6 \text{ Mev}$.

(d) For each center-of-mass angle θ , calculate x from $x = 0.22r_0A/(A+a)\{aE_0 + (a-1)E - 2[a(a-1)E_0E]^{\frac{1}{2}} \cos\theta\}^{\frac{1}{2}}$. (II.28)

(e) Obtain $\sigma^l_{\text{TAB}}(x,y)$ from Lubitz's tables³ (Lu57).

³ The tabulated values of σ^l_{TAB} for $l=2$ (unbound) are incorrect (Ha59a); the errors in question involve multiplicative factors

The function $\sigma^l_{\text{TAB}}(x,y)$ contains the entire angular dependence of the differential cross section. By appropriately selecting l and by varying r_0 , we try to fit the differential cross section near the first peak as well as possible. Lubitz (Lu 57, pp. 125-126) gives a useful graphical procedure (applicable for bound states with $l \neq 0$) which enables us to determine that value of r_0 which, for given l , places the first peak of the differential cross section at the correct angle.

The final step is to extract the reduced width. The appropriate expressions are found by substituting from (II.22) and (II.23) into (II.19) and (II.21). We obtain

$$\begin{aligned} \frac{d\sigma}{dw} &= 61.19 \cdot \frac{(A+1)^2}{(A+2)^2} \cdot \frac{(2J+1)}{(2J_0+1)} \cdot \left(\frac{E}{E_0} \right)^{\frac{1}{2}} \\ &\times \{C[T_{0\frac{1}{2}}^{\frac{1}{2}} T; M_{T_0}, M_T - M_{T_0}]^2 \\ &\times \sigma^l_{\text{TAB}}(x,y)r_0^3\theta^2 \quad (\text{II.29}) \end{aligned}$$

for (d,p) and (d,n) reactions, and

$$\begin{aligned} \frac{d\sigma}{dw} &= 183.6 \cdot \frac{A^2}{(A+2)^2} \cdot \left(\frac{E_0}{E} \right)^{\frac{1}{2}} \\ &\times \{C[T_{0\frac{1}{2}}^{\frac{1}{2}} T; M_{T_0}, M_T - M_{T_0}]^2 \\ &\times \sigma^l_{\text{TAB}}(x,y)r_0^3\theta^2 \quad (\text{II.30}) \end{aligned}$$

for the inverse (p,d) and (n,d) reactions. Contributions from different l values simply add. In most cases there are significant contributions from only one l value and never from more than two. We repeat that, when r_0 is measured in fermis, (II.29) or (II.30) gives the differential cross section in millibarns per steradian.

Since values of r_0 outside the range 4 to 8 f must be regarded as physically unreasonable, the foregoing procedure usually leads to an unambiguous determination of l ; however, for capture into weakly bound or unbound states of $(A+1)$, Butler curves for adjacent l values are very similar in shape and it may be impossible to distinguish them experimentally. Also, for nuclei with $A > 40$, difficulty is sometimes found in separating adjacent values of l . In such cases the l value may often be determined from other considerations, either experimentally as by studying the appropriate neutron or proton elastic scattering or with the aid of theoretical arguments. By using the l values so determined, we can then extract reduced widths in the usual way.

It appears from consideration of many cases that θ^2 depends significantly on r_0 only when there is some difficulty in obtaining an acceptable fit to the observed angular distribution and in a few special cases in which capture takes place into a level of $(A+1)$ very close to the nucleon separation energy ($Q + \epsilon_a - \epsilon_{a-1} \approx 0$). Spe-

which do not seem to exceed 1.5. Numerous checks of entries in other sections of the tables have failed to reveal any other discrepancies.

cifically, if r_0 is allowed to vary by about 1 fm on either side of its "best" value, θ^2 is usually found to vary by much less than 25% about its central value. Enge (En59) has found reduced widths for $K^{39}(d,p)K^{40}$ depending strongly on r_0 . This is not in conflict with what has just been said about θ^2 , since Enge uses a reduced width γ which has the dimensions of an energy and differs from our dimensionless quantity by a factor proportional to \hbar^2/Mr_0^2 .

Reduced widths extracted from the results of deuteron-nucleon experiments by the foregoing procedure are given in Table I. Many of these experiments include no measurements of absolute cross section; we then give reduced widths in units of the ground-state reduced width (column headed "Relative θ^2 "). When the spin of the final state in a stripping reaction is not known, we list $(2J+1)\theta^2 = [J]\theta^2$. Reduced widths are given to two significant figures; we do so as a matter of arithmetical consistency and do not claim that each entry is significant to this degree of accuracy.

The practice of subtracting a constant isotropic background from the observed differential cross section to represent the "compound nucleus" contribution seems to be without justification. No backgrounds have been subtracted in extracting the reduced widths in Table I. For $A > 40$, we have not divided out the isotopic-spin coupling factor $(C)^2$ in (II.19). In such cases, we list $(C^2)\theta^2$ rather than θ^2 itself (see Appendix 1).

3. Deuteron-Triton Reduced Widths

The technique employed in Sec. II.2 to evaluate the stripping transform for deuteron-nucleon reactions is the first of two alternatives. In the second, instead of choosing explicit wave functions to describe the internal structure of $[a]$ and $[a-1]$, we proceed in the following two steps.

(1) The internal wave function of $[a]$ is expanded formally in terms of the complete set of internal states of $[a-1]$. In the notation introduced in (II.18), this expansion may be written

$$\phi_a(\xi, \rho) = \sum_r A_r f_r(\rho) \phi_{a-1}^{(r)}(\xi), \quad (\text{II.31})$$

where $f_r(\rho)$ describes the relative motion of the transferred nucleon and the mass center of $[a-1]$. By substituting (II.31) into the expression (II.18) for the stripping transform, the integral over ξ can be carried out immediately. Because of the orthonormality of the functions $\phi_{a-1}^{(r)}$ only the term in (II.31) corresponding to the ground state of $[a-1]$ ($r=0$) contributes, yielding

$$P_a(\kappa) = A_0 \int \exp(-i\kappa \cdot \mathbf{e}) f_0(\rho) d^3\rho. \quad (\text{II.32})$$

(2) Since we are interested in the behavior of $[a]$ as it dissociates into $[a-1]$ and a nucleon, it is reason-

able to represent the dependence of the internal wave function of $[a]$ on the relative coordinate ρ approximately by its form at large separation. This asymptotic approximation to the relative motion is correctly achieved by setting

$$f_0(\rho) \sim N_i e^{-S\rho/\rho}, \quad (\text{II.33})$$

where S is defined by (II.7) and N_i is a normalization constant. The stripping transform now becomes

$$P_a(\kappa) = [4\pi(N_i A_0)] / (\kappa^2 + S^2) = 4\pi N_a / (\kappa^2 + S^2). \quad (\text{II.34})$$

For $a=3$ and $a=4$, it is probably better to use the asymptotic approximation than to represent $[a]$ and $[a-1]$ by explicit internal wave functions, such as those of Irving (Ir51), which are designed to be reasonable approximations for small separations of the components but which do not have the correct asymptotic behavior as $\rho \rightarrow \infty$. For deuteron-nucleon reactions, the difference between these two approaches is of no practical consequence.

Let us therefore specialize (II.19) to the case $a=3$ and substitute (II.34) for the stripping transform $P_3(\kappa)$. It is again convenient to introduce the tabulated function $\sigma^l_{\text{TAB}}(x, y)$; we absorb the numerical constants in a single factor Λ , where, in fact,

$$\Lambda = 2545 N_3^2. \quad (\text{II.35})$$

The deuteron-triton differential cross sections are then

$$\begin{aligned} \frac{d\sigma}{d\omega} \Big| = & \left(\frac{3}{2} \right)^{\frac{1}{2}} \Lambda \frac{(A+1)^2}{(A+3)^2} \frac{(2J+1)}{(2J_0+1)} \left(\frac{E}{E_0} \right)^{\frac{1}{2}} \\ & \times \{C[T_{02}^{\frac{1}{2}}T; M_{T_0}, M_T - M_{T_0}]\}^2 \\ & \times H \sigma^l_{\text{TAB}}(x, y) r_0^3 \theta^2 \end{aligned} \quad (\text{II.36})$$

for (t, d) and (He^3, d) reactions, and

$$\begin{aligned} \frac{d\sigma}{d\omega} \Big| = & \left(\frac{3}{2} \right)^{\frac{1}{2}} \Lambda \frac{A^2}{(A+3)^2} \left(\frac{E_0}{E} \right)^{\frac{1}{2}} \\ & \times \{C[T_{02}^{\frac{1}{2}}T; M_{T_0}, M_T - M_{T_0}]\}^2 \\ & \times H \sigma^l_{\text{TAB}}(x, y) r_0^3 \theta^2 \end{aligned} \quad (\text{II.37})$$

for (d, t) and (d, He^3) . If r_0 is given in fermis and Λ in fermis⁻¹, (II.36) or (II.37) gives the differential cross section in millibarns per steradian. H is given by (II.25).

Many (d, t) reactions and a few (d, He^3) and (He^3, d) reactions have now been studied experimentally and found to have angular distributions in good agreement with the predictions of the Born-approximation theory. In fact, there are indications that general agreement is markedly better than for the apparently simpler deuteron-nucleon reactions.

The practical procedure for extracting reduced widths from measured differential cross sections with the help of (II.36) and (II.37) has already been described in

Sec. II.2. The quantity which is obtained directly from experiment is not θ^2 itself but $\Lambda\theta^2$. In order to obtain the desired nucleon reduced width, it is necessary to determine the normalization constant Λ . This we do empirically by comparing deuteron-nucleon and deuteron-triton transitions between the same two states; the deuteron-nucleon cross section gives θ^2 , the deuteron-triton cross section determines $\Lambda\theta^2$, whence Λ may be obtained directly. We hope to determine Λ with sufficient accuracy to enable nucleon reduced widths to be measured equivalently by deuteron-nucleon or deuteron-triton reactions. This would greatly increase the power and flexibility of the analysis of stripping widths as a spectroscopic tool; for example, information obtainable from (d,n) experiments could be obtained from the equivalent (He^3,d) experiments, which can be performed with greater accuracy.

Whether this ideal situation can be realized in practice remains to be seen. Present indications, as we see later, are quite promising, although many more measurements are needed, particularly of absolute cross sections. Our empirical normalization constant Λ may be found to vary with the quantum numbers of the transferred nucleon, with Q , and perhaps also with A , as a consequence of the different effects of Coulomb and nuclear distortions on deuteron-nucleon and deuteron-triton cross sections. Since such distortion effects, although different in the two cases, probably depend on the relevant parameters in qualitatively similar fashion, Λ is expected to vary to a considerably smaller extent than θ^2 . By the same token, we would not be surprised to find a difference between the normalization factors for (d,t) and (He^3,d) .

The present method of analyzing deuteron-triton stripping reactions has been discussed and applied to specific examples by several authors (We56, Bu57, Na58). The first systematic study is that of Hamburger (Ha60a) to which we refer the reader for further details.

Table II contains deuteron-triton reduced widths extracted with the aid of (II.36) and (II.37). The quantity which emerges directly from the experimental data is $\Lambda\theta^2$. If the reduced width θ^2 has been measured by the corresponding deuteron-nucleon reaction, we enter it in square brackets in the appropriate column of Table II, and use it to determine Λ from $\Lambda\theta^2$. When no deuteron-nucleon reduced width is available, we sometimes enter a suitable value of Λ found in the manner just described, in square brackets, in the appropriate column of Table II and use it to determine θ^2 from $\Lambda\theta^2$. Reduced widths for nuclei with $A \leq 26$ are extracted with the aid of the isotopic-spin formalism; for $A > 40$, we list $(C)^2\theta^2$ (see Appendix 1).

There are clearly far too few direct determinations of Λ for us to say much about its dependence on its parameters. There are, however, definite indications of a decrease in Λ between Li and Mg, but it is not clear whether or not this apparent variation with A masks a dependence on some other parameter. All the values of

Λ quoted in Table II are consistent with

$$\Lambda = 190 \pm 40 \text{ fm}^{-1} \quad (\text{II.38})$$

with the exception of the values obtained from $F^{19}(d,t)F^{18}$ and from the data on $C^{13}(d,t)C^{12}$ at 3.29 Mev. Our reasons for regarding the $F^{19}(d,t)F^{18}$ determination as unreliable are given in footnote h to Table II. The fact that the peak cross section of the $C^{13}(d,t)C^{12}$ ground-state transition varies by a factor of 1.6 between deuteron energies of 2.19 and 3.29 Mev suggests either a resonance effect or an error in the measured cross sections.

The foregoing values of Λ are sufficiently consistent to suggest that it may indeed be possible to measure nucleon reduced widths by means of reactions involving triton and He^3 ions. On the other hand, it is obvious that our knowledge of the normalization constant is very primitive and that no firm conclusions can be drawn without a great deal of further experimental study. In particular, we must remember four important limitations:

- (1) There is no direct information about Λ for t values other than 1 and 2.
- (2) The normalization constant Λ has not been determined at all for $A > 25$. In view of the large number of (d,t) studies (Ze60) now being undertaken in the mass region $40 < A < 70$, this is a serious shortcoming.
- (3) The $Li^7(d,He^3)He^6$ and $O^{16}(d,t)O^{15}$ results are very puzzling. They are discussed in Sec. IV.
- (4) We have already mentioned that the normalization factor Λ for (d,t) reactions may differ from that for (d,He^3) and (He^3,d) reactions. Thus, Λ_t and Λ_{He^3} should be evaluated separately. There is, at present, insufficient data on (d,He^3) and (He^3,d) reactions to make this possible.

4. Area of Applicability, Limitations, and Possible Refinements of the Simple Theory of Stripping

In our discussion of the empirical reduced widths, we have bypassed a number of points which require further comment. These concern such matters as the range of bombarding energies to which our treatment is applicable, some special situations in which the Born-approximation theory is inadequate, possible refinements of the simple theory, and the significance of the empirical constant Λ which normalizes the deuteron-triton differential cross section.

(a) Limitations on Bombarding Energies

It is well known that at very low bombarding energies, the differential cross sections of (d,p) reactions lose their characteristic stripping form and, furthermore, vary widely in shape and absolute magnitude with small changes in bombarding energy. Under such circumstances, an empirical reduced width extracted with the aid of the Born approximation would have little meaning.

TABLE I. Reduced widths from deuteron-nucleon stripping reactions.

Incident energy (Mev)	Q (Mev)	Final state excitation	J^π	l	r_0	Relative $[J]\theta^2$	Relative θ^2	Absolute $[J]\theta^2$	Absolute θ^2	Footnotes
$\text{Li}^6(d,p)\text{Li}^7$ $(J_0=1^+)$ 2	5.027	(Ni54) 0 0.478	$\frac{3}{2}^-$ $\frac{1}{2}^-$	1 1	4.1 4.1		1 1.4			
$\text{Li}^6(d,p)\text{Li}^7$ $(J_0=1^+)$ 3	5.027	(Ni54) 0 0.478	$\frac{3}{2}^-$ $\frac{1}{2}^-$	1 1	4.1 4.1		1 2.2			
$\text{Li}^6(d,p)\text{Li}^7$ $(J_0=1^+)$ 8	5.027	(Ho53c) 0 0.478	$\frac{3}{2}^-$ $\frac{1}{2}^-$	1 1	4.9 4.9		1 1.5			
$\text{Li}^6(d,p)\text{Li}^7$ $(J_0=1^+)$ 14.4	5.027	(Le55, Ha59) 0 0.478	$\frac{3}{2}^-$ $\frac{1}{2}^-$	1 1	5.4 5.4		1 1.3		0.048 0.063	
	14.8	4.63 6.54 7.47	
$\text{Li}^7(p,d)\text{Li}^6$ $(J=\frac{3}{2}^-)$ 17.5	-5.027	(Re56) 0 2.184	1+ 3+	1 1	5.5 5.5		1 0.68		0.053 0.036	
$\text{Li}^7(p,d)\text{Li}^6$ 18.6	-5.027	(Be58, Be59) 0 2.184 3.560	1+ 3+ 0+	1 1 1	4.5 5 5		1 0.52 0.54		0.053 0.027 0.028	a
$\text{Li}^7(d,p)\text{Li}^8$ 8	-0.192	(Ho53c) 0	2+	1	4.9				0.011	
$\text{Li}^7(d,p)\text{Li}^8$ $(J_0=\frac{3}{2}^-)$ 14.4	-0.192	(Le55, Ha59) 0 0.98 2.28	2+ 1+ 3+	1 1 1	4.2 4.2 4		1 0.53 0.28		0.053 0.028 0.015	
$\text{Be}^9(p,d)\text{Be}^8$ 12	0.560	(Su58) 0	0+	1	3.1				0.023	b
$\text{Be}^9(p,d)\text{Be}^8$ $(J_0=\frac{3}{2}^-)$ 16.5	0.560	(Re56) 0	0+	1	3				0.024	b
$\text{Be}^9(d,p)\text{Be}^{10}$ $(J_0=\frac{3}{2}^-)$ 3.6	4.585	(Fu52) 0 3.368	0+ 2+	1 1	4.5 4.5		1 0.17	0.046 0.041	0.046 0.008	
$\text{Be}^9(d,p)\text{Be}^{10}$ 7.7	4.585	(El52) 0 3.368	0+ 2+	1 1	4.8 4.8		1 0.23			
$\text{Be}^9(d,p)\text{Be}^{10}$ 8.2	4.585	(Ze58) 0 3.368	0+ 2+	1 1	5 5	1 1.1	1 0.22			
$\text{Be}^9(d,p)\text{Be}^{10}$ 9	4.585	(Gr56) 0 3.368 5.96 6.16 6.28 7.37	0+ 2+ (1-) ...(2-) (3-)	1 1 0 ...	5 4.2 4 4.5 4.5	1 1.1 7.1 ...	1 0.23 2.4 ...			c
$\text{Be}^9(d,p)\text{Be}^{10}$ 9.2	4.585	(Ze58) 0 3.368	0+ 2+	1 1	5 5	1 1.5	1 0.29			d
$\text{Be}^9(d,p)\text{Be}^{10}$ 10	4.585	(Ze58) 0 3.368	0+ 2+	1 1	5 5	1 1.0	1 0.20			

TABLE I.—Continued.

Incident energy (Mev)	Q (Mev)	Final state excitation	J^π	l	r_0	Relative $[J]\theta^2$	Relative θ^2	Absolute $[J]\theta^2$	Absolute θ^2	Foot-notes
$\text{Be}^9(d,p)\text{Be}^{10}$		(Eb54)								
11.9	4.585	0 3.368	0+ 2+	1 1	5.1 4	1 0.90	1 0.18			
$\text{Be}^9(d,p)\text{Be}^{10}$		(Rh54, Ca58)								
14.8	4.585	0 3.368 5.96 6.16 6.28 7.37	0+ 2+ (1-) ... (2-) (3-)	1 1 0 ... 0 2	4.5 4 4 ... 4.5 5.5	1 0.60 5.4 ... 9.5 3.1	1 0.12 1.8 ... 1.9 0.44	0.093 0.055 0.51 ... 0.88 0.29	0.093 0.011 0.17 ... 0.18 0.041	c d
$\text{Be}^9(d,n)\text{B}^{10}$		(Aj52)								
$(J_0 = \frac{3}{2}^-)$										
3.4	4.358	0 0.72 1.74 2.15 3.58	3+ 1+ 0+ 1+ 2+	1 1 1 1 1	4.5 4.5 4.5 4.5 4.5		1 2.1 1.4 0.65 0.44			
$\text{B}^{10}(p,d)\text{B}^9$		(Re56)								
18.9	-6.212	0 1.4 2.326	$\frac{3}{2}^-$ $\frac{1}{2}^+$ $\frac{3}{2}^-$	1 ... 1	4.5 ... 4.5		1 ... 0.8			
$\text{B}^{10}(n,d)\text{Be}^9$		(Ri54)								
14	-4.358	0 1.75 2.431	$\frac{3}{2}^-$ $\frac{1}{2}^+$ $\frac{3}{2}^-$	1 ... 1	4.5 ... 4.5		1 ... 1.05		0.043 ... 0.045	
$\text{B}^{10}(d,p)\text{B}^{11}$		(Ev54)								
$(J_0 = 3^+)$										
7.7	9.234	0 2.14 4.46 5.03 6.76 6.81	$\frac{3}{2}^-$ $\frac{3}{2}^-$ $\frac{3}{2}^-$ 1 1 $(\frac{3}{2}^-)$	1 (1) 1 1 1 1	1 4 1.5 0.51 5.6		1 ... 0.25			e
$\text{B}^{10}(d,p)\text{B}^{11}$		(Bi58)								
$(J_0 = 3^+)$										
7.8		8.93 9.19 9.28	$\frac{5}{2}^+$ $(\frac{7}{2}^+)$ $(\frac{5}{2}^+)$	0 0 0	6.7 6 6	12 28 40	2.0 4.8 6.6			g
$\text{B}^{10}(d,n)\text{C}^{11}$		(Ma56)								
$(J_0 = 3^+)$										
9	6.473	0 2.01	$\frac{3}{2}^-$ $\frac{1}{2}^-$	1 (1)	4.33		1		0.023	h e
$\text{B}^{10}(d,n)\text{C}^{11}$		(Ce56)								
$(J_0 = 3^+)$										
7.55	6.473	0 2.01 4.24 4.75	$\frac{3}{2}^-$ $\frac{1}{2}^-$ 1 1	1 (1) 5.8 5.8	5.8 5.8 1.2 0.54	4 1				e
$\text{B}^{11}(d,p)\text{B}^{12}$		(Ho53c)								
8	1.138	0 0.95 1.67 2.62 2.72 3.38 3.76 4.54	1+ 1 0 (0) 2+ 3-	1 1 0 4.4 4.4	4.4 4.4 4.4 4.4 4.4		0.071 0.098 0.219 0.34 0.34		0.024 0.050	c i c
$\text{B}^{11}(d,n)\text{C}^{12}$		(Gi54)								
$(J_0 = \frac{3}{2}^-)$										
8.1	13.731	0 4.435	0+ 2+	1 1	4.4 4.4		1 0.55			

TABLE I.—Continued.

Incident energy (Mev)	Q (Mev)	Final state excitation	J^π	l	r_0	Relative $[J]\theta^2$	Relative θ^2	Absolute $[J]\theta^2$	Absolute θ^2	Footnotes	
$B^{11}(d,n)C^{12}$ $(J_0 = \frac{3}{2}^-)$ 9	13.731	(Ma56)	0	0 ⁺	1	4.3	1	0.26	0.26	j	
			4.435	2 ⁺	1	4.3	1.1	0.21	0.28		
			7.653	0 ⁺	2	4.3	1.0	0.26	0.055		
			9.63								
$C^{12}(d,p)C^{13}$ 2.68	2.719	(Be56)	0	$\frac{1}{2}^-$	1	7.1			0.022		
$C^{12}(d,p)C^{13}$ 3.29	2.719	(Ho54a)	0	$\frac{1}{2}^-$	1	6.15			0.025		
$C^{12}(d,p)C^{13}$ 8	2.719	(Ro51, 51a, Ho53c)	0	$\frac{1}{2}^-$	1	4.2			0.056	k	
			3.09	$\frac{1}{2}^+$	0	4.2			0.18		
			3.68	$\frac{3}{2}^-$	1	4.2			0.006		
			3.85	$\frac{5}{2}^+$	2	4.2			0.098		
$C^{12}(d,p)C^{13}$ 9	2.719	(Gr56)	0	$\frac{1}{2}^-$	1	4.5			0.042		
			3.09	$\frac{1}{2}^+$	0	4.5			0.19		
			3.68	$\frac{3}{2}^-$	1	4.5			0.013		
			3.85	$\frac{5}{2}^+$	2	4.5			0.073		
$C^{12}(d,p)C^{13}$ 14.8	2.719	(Mc56, Ha59)	0	$\frac{1}{2}^-$	1	4			0.031	l	
			3.09	$\frac{1}{2}^+$	0	4			0.15		
			3.68	$\frac{3}{2}^-$	1	4			0.006		
			3.85	$\frac{5}{2}^+$	2	5.4			0.071		
			5.51								
			6.10								
			6.86	$\frac{5}{2}^+$	2	4.6			0.002		
			7.47								
			7.53								
			7.64	$\frac{3}{2}^+$	2	4.6			0.005		
$C^{12}(d,n)N^{13}$ 2.68	-0.286	(Be56)	0	$\frac{1}{2}^-$	1	4.7			0.024		
$C^{12}(d,n)N^{13}$ 3.26	-0.286	(Be56)	0	$\frac{1}{2}^-$	1	4.7			0.021		
$C^{12}(d,n)N^{13}$ 9	-0.286	(Mi53, Ca57)	0	$\frac{1}{2}^-$	1	4.5			0.047	c n	
			2.37	$\frac{1}{2}^+$	0	4.5					
			3.51	$\frac{3}{2}^-$							
			3.56	$\frac{5}{2}^+$							
$C^{12}(p,d)C^{12}$ $(J = \frac{1}{2}^-)$ 17	-2.719	(Be58)	0	0 ⁺	1	4.2					
			4.435	2 ⁺	1	5		1	0.95		
$C^{13}(d,p)C^{14}$ $(J_0 = \frac{1}{2}^-)$ 3.89	5.947	(Be53)	0	0 ⁺	1	4.8		1			
			6.09	1 ⁻	0	4.8		4.4			
$C^{13}(d,p)C^{14}$ 14.8	5.947	(Mc56)	0	0 ⁺	1	5.4		1	0.063		
			6.09	1 ⁻	0	4.5		3.2	0.59		
			6.59	(0 ⁺)	1	5			0.007		
			6.72	3 ⁻	2	5.4			0.47		
			6.89	0 ⁻	0	4.5					
			7.01	(2 ⁺)		
			7.35	2 ⁻	2	5.4		0.30	0.06		
$N^{14}(p,d)N^{13}$ 18.5	-8.324	(St56, Be58)	0	$\frac{1}{2}^-$	1	5.4		1	0.046	q	
			2.365	$\frac{1}{2}^+$	0	5		0.03	0.002		
			3.51	$\frac{3}{2}^-$	1	5		0.54	0.026		

TABLE I.—Continued.

Incident energy (Mev)	Q (Mev)	Final state excitation	J^π	l	r_0	Relative $[J]\theta^2$	Relative θ^2	Absolute $[J]\theta^2$	Absolute θ^2	Footnotes
$N^{14}(n,d)C^{13}$		(Ca57a)								
14	-5.319	0	$\frac{1}{2}^-$	1	4.5		1		0.05	
		3.09	$\frac{1}{2}^+$	
		3.68	$\frac{3}{2}^-$	1	4.5		(3.2)		(0.16)	r
$N^{14}(d,p)N^{15}$		(Sh55)								
$(J_0=1^+)$	7	3.335	5.28	$\frac{5}{2}^+$	2	5.5	1			
		5.305	$\frac{1}{2}^+$	s
		6.33	$\frac{3}{2}^-$	1	5.5	0.72				
		7.165		2	5.5	6.6				
		7.314	0		5.5	7.6				
		7.575	{ (0)?		5.5	7.7				t
			{ +2							
		8.316	0		5.5	6.5				
		8.571	{ 0		5.5	0.31				
			{ +2		5.5	0.76				
$N^{14}(d,p)N^{15}$	9	(Gr56)	5.28	$\frac{5}{2}^+$	2	4.7	1	0.049	0.008	s, u
	3.335	5.305	$\frac{1}{2}^+$	
		6.33	$\frac{3}{2}^-$	1	4.7	0.69	0.034	0.008		
		7.165		2	4.7	7.9	0.39			
		7.314	0		4.7	6.7	0.33			
		7.575		2	5.7	7.1	0.35			t
		8.316	0		4.7	4.9	0.24			
		8.571		0+2						v
$N^{14}(d,p)N^{15}$	14.8	(Wa57)	0	$\frac{1}{2}^-$	1	5	(1) see w	0.098	0.049	w, x
	8.615	5.28								y
		5.305								y
		6.33	$\frac{3}{2}^-$	1	4.5	0.55	(0.14)	0.027	0.007	x
		7.165								y
		7.314								y
		7.575	{ (0)		5	8.3		0.41		t
			{ +2							
		8.316	0		4.7	9.7		0.48		
		8.571	{ 0		5	0.39		0.019		
			{ +2		5	0.82		0.043		
$N^{14}(d,n)O^{16}$		(Ev 53)								
$(J_0=1^+)$	7.7	5.073	0	$\frac{1}{2}^-$	1	4.7	2	1		
		5.26			2	4.7	0.77			
		6.15	$\frac{3}{2}^-$	1	4.7	0.32	0.08			
		{ 6.79		0	4.7					c
		{ 6.86								c
$C^{14}(d,p)C^{15}$		(Mo59)								
$(J_0=0^+)$	14.9	-1.007	0	$\frac{1}{2}^+$	0	4.1	1	0.19	0.093	z
		0.745	($\frac{5}{2}^+$)		2	5.3	0.48	0.27	0.045	
$C^{14}(d,n)N^{15}$		(Ri57)								
$(J_0=0^+)$	3.53	7.987	0	$\frac{1}{2}^-$	1	5.8	...	1	0.017	
		5.28	$\frac{1}{2}^+$				
		5.31	$\frac{3}{2}^+$	0	5.8					
		6.33	$\frac{3}{2}^-$	1	5.8		0.32		0.006	
$N^{15}(p,d)N^{14}$		(Be58)								
$(J=\frac{1}{2}^-)$	18.6	-8.615	0	1^+	1	5.4	1		0.045	
		2.312	0^+	1	5.4		0.64		0.029	
		3.945	1^+	1	5.4		0.18		0.008	
$N^{15}(d,p)N^{16}$		(Wa57)								
$(J_0=1^+)$	14.8	0.267	0	2^-	2	5.5			0.054	
		0.119	0^-	0		4.2			0.19	
		0.295	3^-	2		5			0.047	
		0.393	1^-	0		4.2			0.18	

TABLE I.—Continued.

Incident energy (Mev)	Q (Mev)	Final state excitation	J^π	l	r_0	Relative $[J]\theta^2$	Relative θ^2	Absolute $[J]\theta^2$	Absolute θ^2	Footnotes
$O^{16}(d,p)O^{17}$ 2.1	1.048	(Gr56a) 0.871	$\frac{1}{2}^+$	0	5				0.013	a'
$O^{16}(d,p)O^{17}$ 3.43	1.919	(St55) 0 0.871	$\frac{5}{2}^+$ $\frac{1}{2}^+$	2 0	5 5				0.035	a'
$O^{16}(d,p)O^{17}$ 3.49	1.919	(Ba57) 0 0.871	$\frac{5}{2}^+$ $\frac{1}{2}^+$	2 0	6.3 6.3				0.047	a'
$O^{16}(d,p)O^{17}$ 4.11	1.919	(Ba57) 0 0.871	$\frac{5}{2}^+$ $\frac{1}{2}^+$	2 0	6.3 6.3				0.053	a'
$O^{16}(d,p)O^{17}$ 8	1.919	(Bu51a, Ho53e) 0 0.871	$\frac{5}{2}^+$ $\frac{1}{2}^+$	2 0	5.1 5.1	1 1.9			0.058 0.11	
$O^{16}(d,p)O^{17}$ 9	1.919	(Gr56) 0 0.871 3.055 3.846 4.553 5.08	$\frac{5}{2}^+$ $\frac{1}{2}^+$ $\frac{1}{2}^-$ $\frac{5}{2}^-$ $\frac{3}{2}^-$ $\frac{3}{2}^+$	2 0 ... 3 1 2	4.8 4.8 ... 4.8 4.8 4.8	1 2.2 ... 0.23 0.25 0.80				c c c
$O^{16}(d,p)O^{17}$ 19	1.919	(Fr53) 0 0.872						0.044		b'
$O^{16}(d,n)F^{17}$ 8	-1.631	(Mi53) 0 0.500	$\frac{5}{2}^+$ $\frac{1}{2}^+$	2 0	4.8 4.8	1 4.3				c c
$O^{17}(d,p)O^{18}$ 7.8	5.842	(Bi57) 0 1.99 3.55	0^+ 2^+ 4^+	{ +2 2	5.9 5.1 5.5	1 0.16 0.72 1.1				
$F^{19}(p,d)F^{18}$ 18.5	-8.187	(Re56, Be58) 0 0.94 1.042 1.087 1.129 1.699 2.105 2.525 3.063 3.131 3.352 3.727 3.790 3.841 4.116 4.227 4.358 4.400	1^+ 3^+ (0^-) 0^+ 5^+ 1^+ (2^+) (3^+) 2^+ ?	0 2 0 0 0 0 ?	6 6 6 6 6 6 ?	1 (1.5) (1.4) 0.12 0.12 0.12 0.12 0.12 0.12 0.12 0.12 0.12 0.12 0.12 0.12 0.12 0.12 0.12 0.12 0.12		0.017	c' d' d' d' d' d'	
$F^{19}(n,d)O^{18}$ 14.1	-5.729	(Ri57a) 0 1.99	0^+ 2^+	0	5.1		(0.5)			f'
$F^{19}(d,p)F^{20}$ ($J_0 = \frac{1}{2}^+$) 8.9	4.379	(El56) 0 0.652 0.828 0.988 1.059 1.309 1.970	(2^+) 2 2 2 0	5.01 5.01 5.01 5.01 0.07	3 0.28 0.22 0.07 ...	0.065 0.005 0.005 0.0015	h'	

TABLE I.—Continued.

Incident energy (Mev)	Q (Mev)	Final state excitation	J^π	l	r_0	Relative $[J]\theta^2$	Relative θ^2	Absolute $[J]\theta^2$	Absolute θ^2	Footnotes
$F^{19}(d,p)F^{20}$ ($J_0 = \frac{1}{2}^+$)		(El56)								
8.9		2.048		2	5.01	2.8		0.061		
		2.195		2	5.01	0.95		0.021		
		2.870		3	5.01	2.0		0.043		
		2.966		1	5.01	0.21		0.005		
		3.491		0	5.01	2.5		0.054		
		3.528		0	5.01	2.5		0.054		
		3.586		
		3.681		
		3.961		
		4.079		0	5.01	0.70		0.015		
		4.275		
		4.310		0	5.01	1.2		0.026		
		5.04		1	5.01	0.24		0.005		
		5.19		1	5.01	0.33		0.007		
		5.27		1	5.01	0.57		0.013		
		5.72		
		5.87		1	5.01	1.4		0.030		
		5.95		1	5.01	2.8		0.060		
		6.25		i'
		6.63		1	5.01	1.6		0.034		
		6.81		1	5.01	3.4		0.074		
		6.98		
		7.20		1	5.01	2.4		0.053		
$F^{19}(d,n)Ne^{20}$ ($J_0 + \frac{1}{2}^+$)		(Ca55a)								
9.06	10.645	0	0^+	0	5		1	0.013	0.013	
		1.632	2	2	5		1.1	0.069	0.014	
		4.248	(4^+)	
		4.969	(1^-)	
		5.631	
		6.745	
		7.19	0	5						
		7.23	0	5						j'
		7.46	2							
		7.86								
		9.3	1^-	1	5					
$Ne^{20}(d,p)Ne^{21}$ ($J_0 = 0^+$)		(Bu56, Mi52)								
8.5	4.53	0	$\frac{3}{2}^+$	
		0.34	($\frac{5}{2}^+$)	2	6	6	1			
		1.735	
		2.79	$\frac{1}{2}^+$	0	5.5	6.4	3.2			
		3.73	
		4.58		2	5	2.7				
		4.81		1	5	8.6				
		5.43		2	5	3.2				
		5.63		2	5	2.9				
		5.78		1	5	3.2				
		5.89	
		6.10	
		6.72		2	5	3.1				i'
$Ne^{22}(d,p)Ne^{23}$ ($J_0 = 0^+$)		(Bu56)								
8.5	2.965	0	($\frac{5}{2}^+$)	2	5.1	6	1			
		0.98	($\frac{3}{2}^+$)	0	5.3	8	4			
$Na^{23}(p,d)Na^{22}$ ($J_0 = \frac{3}{2}^+$)		(Be58)								
18.0	-10.192	0	3^+	2	5.3		1		0.021	
		0.59		2	5.3		1		0.021	
$Na^{23}(d,p)Na^{24}$ ($J_0 = \frac{3}{2}^+$)		(Sh54)								
3	4.731	0	4^+	2	5.65		1			
		0.472	1^+	2	5.65		3.9			k'
		0.56	{ 2^+	0	5.65		0.35			k'
		1.341	1^+	0	5.65		2.5			

TABLE I.—Continued.

Incident energy (Mev)	Q (Mev)	Final state excitation	J^π	l	r_0	Relative $[J']\theta^2$	Relative θ^2	Absolute $[J]\theta^2$	Absolute θ^2	Footnotes
$\text{Na}^{23}(d,p)\text{Na}^{24}$ 8.9	4.731	(Da60)								
		0	4^+	2	5.2	9	1			
		0.472	1^+	2	5.2	4.6	1.5			
		0.56	2^+	0	5.2	2.1	0.41			
		1.341	1^+	0	5.2	13.6	4.6			
		1.844		1	5.2	0.93				
		1.884		+2	5.2	6.3				
		3.409		0	5.2	11.5				
				+2	5.2	12.4				
		3.582								
		3.623								
		3.648								
		3.738								
		3.850								
		3.899								
		3.929								
		4.184								
		4.202								
		4.219								
		4.41								
		4.558								
		4.72								
		4.91								
		5.02								
		5.13								
		5.31								
		5.42								
$\text{Na}^{23}(d,p)\text{Na}^{24}$ 14.8	4.731	(Vo58)							0.036	
		0	4^+	2	6					
		0.472	1^+							y
		0.56	2^+							y'
		1.341	1^+	0	6.2					
$\text{Na}^{23}(d,n)\text{Mg}^{24}$ 7.75	5.332	(El57)								
		4.122	4^+	2	5.2	9	1			
		4.24	2^+	0	5.2	1.7	0.34			m'
		7.4		0	5.2	5.4				
		8.5		0	5.2	10.1				
		10.46		0	5.2	32				
$\text{Na}^{23}(d,n)\text{Mg}^{24}$ $(J_0 = \frac{3}{2}^+)$ 9	9.462	(Ca55)								
		0	0^+							
		1.368	2^+							
		4.122	4^+	2	5.2			0.044	0.0049	m'
		4.24	2^+	0	5.2			0.012	0.0023	
		4.8								
		5.24	(3^-)							
		6.4								
		(?)6.9								
		7.4		0(2)	5.2			0.03(0.07)		n'
		8.5		0	5.2			0.038		
$\text{Mg}^{24}(d,p)\text{Mg}^{25}$ $(J_0 = 0^+)$ 8	5.107	(Ho53d)								
		0	$\frac{5}{2}^+$	2	5.3		1		0.0091	
		0.58	$\frac{1}{2}^+$	0	5.3		2.0		0.018	
		0.98	$\frac{3}{2}^+$	2	5.3		0.75		0.0068	
		1.61	$\frac{7}{2}^+$							
		1.96	$\frac{5}{2}^+$	2	5.3		0.44		0.0040	
		2.56	$\frac{1}{2}^+$							
		2.74	$\frac{5}{2}^+$							
		2.80	$\frac{3}{2}^+$	0	5.3					
		3.40	$\frac{3}{2}^-$	1	5.3		2.3		0.021	
$\text{Mg}^{24}(d,p)\text{Mg}^{25}$ 8.9	5.107	(Hi58)								
		0	$\frac{5}{2}^+$	2	5.2		1	0.057	0.0096	o'
		0.58	$\frac{1}{2}^+$	0	5.2		2.1	0.042	0.021	
		0.98	$\frac{3}{2}^+$	2	5.2		0.76	0.029	0.0072	
		1.61	$\frac{7}{2}^+$							
		1.96	$\frac{5}{2}^+$	2	5.2		0.45	0.026	0.0043	

TABLE I.—Continued.

Incident energy (Mev)	Q (Mev)	Final state excitation	J^π	l	r_0	Relative $[J]\theta^2$	Relative θ^2	Absolute $[J]\theta^2$	Absolute θ^2	Footnotes
$Mg^{24}(d,p)Mg^{25}$		(Hi58)								
8.9		2.56	$\frac{1}{2}^+$	0	5.2		1.0	0.019	0.0096	
		2.74	$\frac{3}{2}^+$	
		2.80	$\frac{3}{2}^+$	2	5.2		1.3	0.048	0.012	
		3.40	$\frac{3}{2}^-$	1	5.2		2.0	0.076	0.019	
		3.90		2	5.2			0.040		
		3.97	$(\frac{7}{2}^-)$	3	5.2		1.1	0.080	0.010	
		4.05		
		4.27		1	5.2			0.022		
		4.42		
		4.72		3	5.2			0.019		
		4.86		
		4.96		
		5.15		
		5.27	$\frac{1}{2}^+$	0			0.29	0.0056	0.0028	
		5.49	$\frac{1}{2}^+$	0	5.2		5.0	0.0945	0.047	
		5.79								p'
		6.09		
		6.25		
		6.54		
		6.80		1	5.2			0.014		
		6.85		(>1)						
		6.95		
		7.18		2	5.2			0.025		
		7.23	$(\frac{5}{2}^-)$	3	5.2			0.079		
		7.40		1	5.2			0.048		
		7.58		(1)	5.2			(0.042)		
		7.8		
		8.05		(2)	5.2			(0.032)		
$Mg^{24}(d,p)Mg^{25}$	14.8	(Ha60)								
	5.107	0	$\frac{5}{2}^+$	2	5		1		0.0085	q'
		1.61	$\frac{7}{2}^+$							
		1.96	$\frac{3}{2}^+$	2	4.3		0.37		0.0031	
$Mg^{24}(d,n)Al^{25}$	4	(Go53)								
	0.06	0	$\frac{5}{2}^+$	2	5.3		1		0.0028	c
		0.45	$\frac{1}{2}^+$	0	5.3		2.5		0.0073	c
		0.95	$\frac{3}{2}^+$	2	5.3		1.1		0.0030	c
		1.61	$\frac{7}{2}^+$	
		1.81	$\frac{5}{2}^+$							p'
		2.51	$\frac{1}{2}^+$	(0)						r'
		2.69	$\frac{3}{2}^+$	(2)	5.3					r'
		2.72	$\frac{7}{2}^+$	
		3.08	$\frac{3}{2}^-$	(1)	5.3					r'
$Mg^{25}(p,d)Mg^{24}$	(Be58)									
$(J=\frac{5}{2}^+)$	17	-5.107	0	0^+	2	5.2	1		0.0079	
		1.368	2^+	2	5.2		2.7		0.022	
		4.122	4^+							
		4.24	2^+	2	5.2		1.2		0.012	s'
$Mg^{25}(d,p)Mg^{26}$	(Ho53d)									
$(J_0=\frac{5}{2}^+)$	8	8.893	0	0^+	(2)	5.3		(0.04)	(0.04)	t'
		1.83	2^+	0^+2	5.3			0.019	0.21	0.0038 0.041
		2.97	2^+	0	5.3			0.17		0.034
		3.97		0	5.3			0.17		
		4.35	2^+	0	5.3			0.19		0.037
		4.86								
		4.92								
		5.27		$1>0$						
		5.32								
		5.50								
		6.15		0	5.3			(0.12)		v'
$Mg^{26}(d,p)Mg^{27}$	(Ho53d)									
$(J_0=0^+)$	8	4.214	0	$\frac{1}{2}^+$	0	5.3		0.02	0.01	w'
		0.987			2	5.3		0.02		

TABLE I.—Continued.

Incident energy (Mev)	Q (Mev)	Final state excitation	J^π	l	r_0	Relative $[J]\theta^2$	Relative θ^2	Absolute $[J]\theta^2$	Absolute θ^2	Footnotes
Mg ²⁶ (d,p)Mg ²⁷		(Hi58)								
8.9	4.214	0	$\frac{1}{2}^+$	0	5.3	2		0.045	0.022	x'
		0.987		2	5.8	2.1		0.048		
		(1.66)		?				?		p'
		3.50	$\frac{1}{2}^+$	0	5.3	1.8		0.040	0.020	
		3.56	(-)	1	5.3	6.5		0.14		
		3.76		2	5.3	4.0		0.09		
		4.13		
		4.75		(1)			?			p'
Al ²⁷ (d,p)Al ²⁸		(Ho53a)								
($J_0 = \frac{5}{2}$)										
8	5.498	0	3^+	0	6.15		1		0.021	
		0.031	2^+	0	6.15		0.72		0.015	y'
		0.97	
		1.02	3^+	2(0)	6.15		0.96(0.13)		0.020(0.0027)	y'
Al ²⁷ (d,p)Al ²⁸		(En56)								
($J_0 = \frac{5}{2}^+$)										
6	5.498	0	3^+	0	6.6	7	1	0.15	0.021	
		0.031	2^+	0	6.6	3.61	0.72	0.08	0.015	
		0.97	
		1.02	3^+	2(0)	5.4	6.27	0.90	0.13	0.019	
		1.37		
		1.63		
		2.14		0	6.6	2.28		0.05		
		2.21		2	5.4	2.08		0.04		
		2.28		2(0)	5.4	5.37		0.11		
		2.49		0	6.6	0.42		0.01		
		2.59		
		2.66		2	5.4	5.13		0.11		
		2.99		
		3.01		
		3.10		
		3.29		0	6.6	0.22		0.005		
		3.345		0	6.6	0.18		0.004		
		3.461		1	5.4	4.01		0.08		
		3.535		
		3.59		1	5.4	5.96		0.13		
		3.67		0	6.6	0.11		0.002		
		3.70		0	6.6	0.38		0.008		
		3.88		1	5.4	1.42		0.03		
		3.90		
		3.93		
		4.03		2	5.4	4.28		0.09		
		4.12		
		4.24		0	6.6	0.21		0.004		
		4.32		2	5.4	1.59		0.03		
		4.38		
		4.46		
		4.52		
		4.69		1	5.4	7.28		0.15		
		4.74		
		4.77		1	5.4	5.72		0.12		
		4.85		
		4.90		1	5.4	3.80		0.08		
		4.93		
		5.00		
		5.03		
		5.14		1	5.4	3.84		0.08		
Al ²⁷ (d,n)Si ²⁸		(Ru57)								
($J_0 = \frac{5}{2}^+$)										
6	9.363	0	0^+	2	5.1	1	1			
		1.78	2^+	0	5.1	0.37	0.07			
		4.61								b''
		5.0								b''
		6.2		0	5.1	0.35				
		6.9		1	5.1	0.30				
		7.3								
		7.9		0	5.1	0.36				b''
		8.3		(0)						c''
		8.6								
		9.3		0	5.1	1.25				d''

TABLE I.—Continued.

Incident energy (Mev)	Q (Mev)	Final state excitation	J^π	l	r_0	Relative $[J]\theta^2$	Relative θ^2	Absolute $[J]\theta^2$	Absolute θ^2	Footnotes
$\text{Al}^{27}(d,n)\text{Si}^{28}$ ($J_0 = \frac{5}{2}^+$)										
9	9.363	0	0^+	2	5.36	1	1	0.039	0.001	e''
		1.78	2^+	0	5.36	0.15	0.03			b''
		4.61								b''
		5.0								b''
		6.2								b''
		6.9		0						b''
		7.3	
		7.9		0	5.36	0.73		0.028		
		8.3		0	5.36					
		8.6		0	5.36	7.9		0.31		
		9.3		0	5.36					
$\text{Si}^{28}(d,n)\text{P}^{29}$ ($J_0 = 0^+$)										
9	0.499	0	$\frac{1}{2}^+$	0	5.4		1	0.034	0.017	
		1.30	($\frac{3}{2}^+$)	2	5.4		0.55	0.037	0.009	
		1.92	($\frac{5}{2}^+$)	2	5.4		0.26	0.027	0.005	
$\text{Si}^{28}(d,p)\text{Si}^{29}$										
8	6.249	0	$\frac{1}{2}^+$	0	5.4		1	0.044	0.022	
		1.28	$\frac{3}{2}^+$	2	5.4		0.86	0.076	0.019	
		2.03	$\frac{5}{2}^+$	2	5.4		0.21	0.027	0.005	
		2.43	$\frac{7}{2}^+$	
		3.07		2	5.4			0.012		
		3.62	($\frac{7}{2}^-$)	3	5.4		(0.60)	0.102	(0.013)	f''
		4.08	
		4.84	
		4.90								
		4.93	($\frac{3}{2}^-$)	1	5.4		(1.31)	0.117	(0.029)	f'', g''
		6.38	($\frac{1}{2}^-$)	1	5.4		(1.04)	0.047	(0.023)	f''
$\text{P}^{31}(p,d)\text{P}^{30}$ ($J_0 = \frac{1}{2}^+$)										
18.6	-10.108	0	1^+	0	5.6			0.013		
		0.685	0^+	0	5.6			0.012		h''
		0.707	(1) ⁺							
$\text{P}^{31}(d,p)\text{P}^{32}$ ($J_0 = \frac{1}{2}^+$)										
8.9	5.695	0	1^+	2	5.53	3	1			i''
		0.077	2^+	2	5.53	4.25	0.85			i''
		0.515		0	5.53	0.7				
		1.15		0	5.53	1.2				
		1.32	
		1.75	
		2.18		0	5.53	0.6				b''
		2.23								
		2.65	
		2.74	
		3.00	
		3.14	
		3.26								
		3.32		1	5.53	8				b''
		3.45								
		4.03		1	5.53	7				
		4.21		0	5.53	0.8				
		4.43		1	5.53	1				
		4.90		1	5.53	5				
		5.11								b''
		5.37		1	5.53	7				
		5.53		1	5.32	2				
		5.82		1	5.53	8				
		6.09		1	5.53	3				
		6.34		1	5.53	1				
		6.56		1 (or 2)	5.53					
$\text{P}^{31}(d,p)\text{P}^{32}$ ($J_0 = \frac{1}{2}^+$)										
7.8	5.695	0	1^+	2	2	3	1			
		0.077	2^+	+ (0)	(7.5)	(0.195)	(0.065)			
				2	5.7	4.25	0.85			

TABLE I.—Continued.

Incident energy (Mev)	Q (Mev)	Final state excitation	J^π	l	r_0	Relative $[J]\theta^2$	Relative θ^2	Absolute $[J]\theta^2$	Absolute θ^2	Footnotes
$P^{31}(d,n)S^{32}$ ($J_0 = \frac{1}{2}^+$)										
9	6.616	(Ca55)	0 ⁺	0	5.53	1	1	0.006	0.006	
		2.24		2	5.53	2.7	0.54	0.016	0.0003	
		3.81								
		4.30		0						
		4.47								
		4.70	
		4.98	
		5.76		2	5.53	5.58		0.033		
$S^{32}(d,p)S^{33}$ ($J_0 = 0^+$)										
8	6.421	(Ho53)	0	$\frac{3}{2}^+$	2	5.6	4	1		
		0.84	$\frac{1}{2}^+$	0	5.6	1.1	0.56			
		1.96	
		2.31	
		2.87								
		2.94	($\frac{7}{2}^-$)	3	5.6	15.6	1.9			j''
		2.97								
		3.22	$\frac{3}{2}^-$	1	5.6	10.5	2.6			
		3.83	
		3.94	
		4.05	
		4.10								
		4.15		1	5.6	1.6				
		4.21								
		4.38	
		4.43	
		4.87								
		4.92		1	5.6	0.82				
		4.95								
		5.71	($\frac{1}{2}^-$)	1	5.6	7.3	3.6			
		6.42								
		6.48								
		6.51								k''
		6.53								
$S^{32}(d,n)Cl^{33}$										
8	0.06	(Mi53)	0	$\frac{3}{2}^+$	2	5.6		1		c
		0.806	$\frac{1}{2}^+$	0	5.6		3.0			
		2.86	$\frac{3}{2}^+$							l''
		4.12	$\frac{3}{2}^-$	1	5.6		(5.5)			m''
$K^{39}(d,p)K^{40}$ ($J_0 = \frac{3}{2}^+$)										
6	5.57	(En59)	0	4 ⁻	3	6.5	9	1	0.086	0.0096
		0.028	3 ⁻	3	6.5	7.7	1.1	0.073	0.010	
		0.795	2 ⁻	3	6.5	5.8	1.2	0.055	0.011	
		0.885	5 ⁻	3	6.5	10.4	0.95	0.10	0.0091	
		1.634		1	4.5	0.08		0.0007		
		1.954			
		2.042	(3 ⁻)	1	4.5	9.0	1.3	0.086	0.012	
		2.064	(2 ⁻)	1	4.5	8.2	1.6	0.078	0.016	
		2.099	(1 ⁻)	1	4.5	5.6	1.9	0.053	0.018	
		2.256		>1						
		2.286		(1)	4.3	0.17		0.0016		
		2.393		1	4.3	0.10		0.0010		
		2.415		1	4.3	0.27		0.0026		
		2.565			
		2.622	(0 ⁻)	1	4.3	1.8	1.8	0.018	0.018	
		2.743		1	4.0	0.70		0.0067		
		2.781	
		2.802		1	4.0	0.18		0.0018		
		2.948	
		2.983	
		3.021								
		3.104		0	5.6	0.11		0.0010		
		3.125	
		3.144		(1)	4.0	(0.16)		(0.0015)		
		3.225		1	4.0	2.3		0.022		
		3.367		1	4.0	0.66		0.0063		
		3.385		(1)	4.0	(0.26)		(0.0025)		

TABLE I.—Continued.

Incident energy (Mev)	Q (Mev)	Final state excitation	J^π	l	r_0	Relative $[J]\theta^2$	Relative θ^2	Absolute $[J]\theta^2$	Absolute θ^2	Foot-notes
$K^{39}(d,p)K^{40}$ ($J_0 = \frac{3}{2}^+$)										
6										
3.412		(En59)		0	5.0	0.07		0.0007		
3.479				1	4.0	0.51		0.0049		
3.599				1	4.0	0.15		0.0014		
3.629				1	4.0	3.1		0.030		
3.657			
3.715			
3.738										
3.766				1	3.8	0.28		0.0027		
3.790				0	5.0	0.13		0.0013		
3.820				1	3.8	0.17		0.0016		
3.838			
3.869			
3.883										
3.898										
3.920				
4.017				1	3.8	1.0		0.0097		
4.102				1	3.8	1.7		0.016		
4.253				1	3.8	3.5		0.033		
4.396				1	3.8	1.8		0.017		
4.462				1	3.8	1.8		0.017		
4.539				1	3.8	1.8		0.017		
4.582			(1)		3.8	(0.66)		(0.0063)		
4.658			1		3.8	0.99		0.0094		
4.788			1		3.8	0.76		0.0073		
4.801			1		3.8	1.3		0.012		
4.902			1		3.8	0.93		0.0089		
$K^{39}(d,p)K^{40}$										
8.9										
(Da59)										
5.57										
0		4 ⁻		3	5.8	9	1			
0.028		3 ⁻		3	5.8	7	1			n'', o''
0.795		2 ⁻		3	5.8	5.5	1.1			
0.885		5 ⁻		3	5.8	12.5	1.1			
1.634		
2.042		(3 ⁻)								
2.064		(2 ⁻)		1	5.0	23.7				p''
2.099		(1 ⁻)								
2.622		(0 ⁻)		1	5.8	2.7	2.7			
2.743				1	5.8	0.66				
3.225				1	4.5	3.2				
3.367				1	5.8	0.96				p''
3.385				1	5.8	0.96				
4.017				1	3.8	1.5				
4.102				1	4.6	1.8				
4.253				1	4.3	3.7				
4.788				1	4.9	2.2				p''
4.801				1	4.9	2.2				
4.902				1	4.4	1.7				
5.14		
5.34		
$Ar^{40}(d,p)Ar^{41}$ ($J_0 = 0^+$)										
8.5										
(Bu56, Hi57, Gi52)										
3.88										
0		$\frac{7}{2}^-$		3	5.87	8		0.08	0.01	
0.57				1	5.87	1.7		0.016		
1.1				2	5.87	0.56		0.005		
1.39				1	5.6	8.3		0.08		
1.9		$\frac{1}{2}^+$		0	5.87	0.85		0.008	0.004	q''
2.46				1	5.6	1.9		0.018		
2.79				1	5.6	1.7		0.016		
3.01				1	5.6	1.8		0.018		
3.36				1	5.6	3.3		0.032		
3.98				1	5.87	3.2		0.030		
$Ca^{40}(d,p)Ca^{41}$ ($J_0 = 0^+$)										
8										
(Ho53)										
6.139										
0		$\frac{7}{2}^-$		3	5.87	8	1	0.114	0.014	
1.947		$\frac{3}{2}^-$		1	5.87	5.6	1.4	0.079	0.020	
2.469				1	5.87	2.2		0.032		
3.95				1	5.87	1.0		0.015		
4.76				2	5.87	3.5		0.050		
5.72				2	5.87	3.1		0.045		r''

TABLE I.—Continued.

TABLE I.—Continued.

Incident energy (Mev)	<i>Q</i> (Mev)	Final state excitation	<i>J</i> ^π	<i>l</i>	<i>r</i> ₀	Relative [<i>J</i>]θ ²	Relative θ ²	Absolute [<i>J</i>]θ ²	Absolute θ ²	Footnotes
Ca⁴⁴(<i>d,p</i>)Ca⁴⁶ (<i>J</i>₀=0⁺)										
7	5.188	(Co57)								
		1.432		1	6	2.05		0.011		
		1.475	
		1.557	
		1.902		1	6	9.7		0.054		
		1.971	
		2.249		1	6	1.7		0.009		
		2.356	
		2.394	1 ⁺	0	6	0.42	0.21	0.0025	0.001	
		2.597	
		2.681	
		2.763	
		2.844		1	6	1.6		0.009		r''
		2.950	
		2.970	
		3.032	
		3.148	
		3.244		1	6	0.77		0.004		r''
		3.296	
		3.319	
		3.419		1	6	2.8		0.017		r''
Ti⁴⁶(<i>d,p</i>)Ti⁴⁷ (<i>J</i>₀=0⁺)										
7.8	6.33	(Ri60)								
		0	5 ⁻	
		0.16	7 ⁻	3	5.5	8	1			
		0.55	(3 ⁻)	
		1.56	(3 ⁻)	1	6	6.3	1.6			
		1.80	(2 ⁻)	1	6	2.5	0.6			
		2.58		1	5	1.8				
		2.83		1	5	1.3				
		3.31		1	5	0.8				
Ti⁴⁸(<i>d,p</i>)Ti⁴⁹ (<i>J</i>₀=0⁺)										
7.8	5.92	(Ri60)								
		0	7 ⁻	3	6	8	1			
		1.38	(3 ⁻)	1	6	14	3.5			
		1.72		1	6	6	1.5			
		1.76	
		2.49								
		3.17								
		3.26		1	5	6				
V⁵¹(<i>d,p</i>)V⁵² (<i>J</i>₀=1⁻)										
8.7	5.075	(El58)								
		0	(2,3) ⁺	1	6.25	7				u'', v''
		0.14		1	6.25	1.4				
		0.43		1	6.25	0.26				
		0.78	{	1	6.25	3.1				
		0.834	{	1	6.25					
		1.402	{	1	6.25	0.32				
		1.475	{	1	6.25					
		1.545		1	6.25	2.2				
		1.753		1	6.25	0.54				
		1.785		+3		3.6				
		1.841								
		2.088		1	6.25	1.1				
		2.131		+3		3.3				
		2.150								
		2.307		1	6.25	0.46				
V⁵¹(<i>d,p</i>)V⁵²										
8.9	5.075	(Da50a)								
		0		1	6	7		0.32		u''-w''
		0.14		1	5.9	1.9		0.084		
		0.43		1	5.7	0.33		0.015		
		0.78	{	1	6	3.9		0.18		
		0.834	{	1	5.3	0.51		0.023		
		1.402	{	1	5.5					
		1.475	{	
		1.545		1	5.5	2.6		0.12		
		1.753	{	1	5	1.1		0.048		x''
		1.785	{							

TABLE I.—Continued.

Incident energy (Mev)	Q (Mev)	Final state excitation	J^π	l	r_0	Relative $[J]\theta^2$	Relative θ^2	Absolute $[J]\theta^2$	Absolute θ^2	Foot-notes
V ⁶¹ (d,p)V ⁶² 8.9		(Da50a) 1.841 2.088 2.131 2.150 2.307 2.415 2.458 2.525 2.76		1 (1) (1) (1)	6.2 4.5 4.9 5.1	0.27 1.7 0.62 0.27		0.012 0.076 0.028 0.012		x''
Cr ⁶² (d,p)Cr ⁶³ ($J_0=0^+$) 10	5.704	(El58b) 0 0.57 0.97 2.31	$\frac{3}{2}^-$ 1 $(\frac{5}{2}^-)$ 1	1 1 3 1	6.25 6.25 5.6 5.6	4 2.1 4.0 2.6	1			y'' z''
Cr ⁶³ (d,p)Cr ⁶⁴ ($J_0=\frac{3}{2}^-$) 10	7.482	(El58b) 0 0.86 1.31 2.67 3.19 3.79	0^+ 2^+ 1 1 1 1	1 1 1 1 1 1	6.25 6.25 6.25 6.25 6.25 6.25	1 2.2 0.88 3.6 3.6 3.4	1 0.44			y''
Co ⁶⁹ (d,p)Co ⁶⁰ ($J_0=\frac{7}{2}^-$) 8.7	5.227	(El58a) 0 0.058 0.282 0.432 0.501 0.541 0.612 0.738 0.782 1.006	5^+ 2^+ 1 1 1 1 1 1 1	1 1 5 5 5 5 5 5 5	5 5 3.8 4.0 11.2 9.7	17.5				a'''
Zn ⁶⁴ (d,p)Zn ⁶⁵ ($J_0=0^+$) 10	5.650	(Sh59) 0 0.052 0.82 0.82 1.28 1.85 2.40	$\frac{5}{2}^-$ $(\frac{3}{2}^-)$ $(\frac{3}{2}^-)$ $(9^+/2)$ $(\frac{5}{2}^+)$ $(\frac{5}{2}^+)$ 0	3 1 1 4 2 0	6.6 6.6 6.6 6.6 6.6 6.6	6 2.4 1.1 11 3.6 0.80	1 0.59 0.53 1.1 0.60 0.40			b''' b''', c''' b''', d''' b''', d''' c''' c'''
Zn ⁶⁶ (d,p)Zn ⁶⁷ ($J_0=0^+$) 10	4.689	(Sh59) 0 0.092 0.182 0.38 0.38 0.88	$\frac{5}{2}^-$ $\frac{3}{2}^-$ +1 $(\frac{1}{2}^-)$ $(9^+/2)$ $(\frac{5}{2}^+)$	3 1 1 1 4 2	6.6 6.6 6.6 6.6 6.6 6.6	6 2.3 1.7 16 5.3	1 0.57 0.85 1.6 0.89			b''' b''' b''' b''', d''' b''', d''' c'''
Zn ⁶⁷ (d,p)Zn ⁶⁸ ($J_0=\frac{5}{2}^-$) 10	7.985	(Sh59) 0 1.11 1.88 3.49	0^+ 2^+	3 1	6.7 6.7	1 0.40	1 0.08			
Zn ⁶⁸ (d,p)Zn ⁶⁹ ($J_0=0^+$) 10	4.266	(Sh59) 0 0.44 0.82	$\frac{1}{2}^-$ $9^+/2$ $(\frac{5}{2}^+)$	1 4 2	6.7 6.7 6.7	2 18 5.9	1 1.8			c'''
Zn ⁶⁸ (d,p)Zn ⁶⁹ 11.9	4.266	(Eb54) 0 0.44 0.82	$\frac{1}{2}^-$ $9^+/2$ $(\frac{5}{2}^+)$	1 4 2	6.7 7.1 7.1	2 11 5.6	1 1.1			c'''

Notes to Table I.

^a Absolute values of the reduced widths were estimated from the ground-state data of Re56.

^b The ridiculously low r_0 needed to fit the angular distribution is probably connected with "internal" or "volume" effects.

^c Levels at this excitation lie close to the nucleon separation energy ($O+2.23=0$), where the behavior of the Butler formula is sometimes erratic.

^d Both $l=1$ and $l=2$ give a reasonably good fit, with $l=2$ slightly favored, particularly in the case of Ca58. Both relevant experiments were originally fitted with $l=1$. See Sec. IV for further discussion of the point, which was brought to our attention by E. W. Hamburger (private communication).

^e Although the curve shows a peak in the characteristic $l=1$ location, the direct $l=1$ transition is forbidden by conservation of angular momentum. The background is very high, however, and there is a marked backward maximum. The mechanism of this transition has been analyzed in terms of the so-called "exchange" and "spin-flip" stripping. (See Au60 for discussion and references.)

^f These levels are not resolved in Ev54. An upper limit of 15% is set in Co57 to the contribution from the 6.81-Mev level, enabling us to give a rough reduced width for the 6.76-Mev level.

^g Reduced widths relative to ground-state reduced width, as usual.

^h Neutrons to eight other levels below 9 Mev were observed, two strong unresolved $l=1$ groups being found. No quantitative reduced-width data could be obtained.

ⁱ No measurements for θ c.m. $<35^\circ$, so that no reliable reduced width could be extracted.

^j The neutron group corresponding to this transition was too weak to be analyzed.

^k Only the ground-state cross section was remeasured in Ho53c. Since no measurements were reported for θ c.m. $<20^\circ$, the Butler curves, particularly for this $l=1$ transition, had to be fitted at undesirably high angles, and the reduced widths are, accordingly, subject to large errors.

^l McGruer *et al.* (Mc56) quote an error of $\pm 50\%$ in the absolute cross sections. Recent measurement by E. W. Hamburger and S. Mayo (quoted in Ha59) indicates that the cross sections of Mc56 are too high by 30%. This correction has been made in extracting the relevant reduced widths. It also affects the $C^{12}(d,p)C^{12}$ results of Mc56.

^m These levels lie far above the neutron separation energy ($O+\epsilon_d=0$). The Butler curves for different l ($=0, 1, 2$) are no longer very different. The l values, however, are obtained unambiguously in $C^{12}(n,n)C^{12}$ experiments (Wi58). The 7.47- and 7.53-Mev levels do not appear in the neutron experiments. These matters were brought to our attention by E. W. Hamburger (private communication).

ⁿ Unresolved. Probably a superposition of $l=1$ and $l=2$.

^o The best fit (not a good one) to the angular distribution is obtained by a superposition of $l=1$ and $l=3$ (Wa58a, Table IX). However, an $l=1, l=3$ admixture is ruled out by conservation of angular momentum since the target spin is $\frac{1}{2}$. We take $l=1$ as the most satisfactory assignment.

^p $l=0$ gives the best fit to the angular distribution (Wa58a, Table IX). Detailed agreement, however, is poor and no reduced width could be extracted.

^q Absolute cross section measured in St56 and used in Be58 to "normalize" measured relative cross sections.

^r The $l=1$ curve, which fits the data very poorly, leads to a reduced width at serious odds with the result quoted in Be58 for the mirror transition. The (p,d) data seem to be much more trustworthy.

^s Since the transition to the N^{15} ground state was not analyzed in either Sh55 or Gr56, we have to modify our usual procedure and normalize relative reduced widths so that $[J]^{0g}$ for the 5.28-Mev level is unity.

^t Concerning the 0+2 mixture in this transition, the $l=0$ component is too doubtful to justify the extraction of a width. Gr56 discard the $l=0$ component as arising from O^{16} percent in the target while Wa57 also consider that their $l=0$ component can arise from this source. Sh55 (unpublished) make no comment.

^u Gr56 did not resolve his doublet of levels. This was done in preparing the table with the aid of results of Sh55.

^v The tentative $l=1$ assignment of Gr56 is almost certainly incorrect.

^w To facilitate comparison with Sh55 and Gr56, the entries in the relative $[J]^{0g}$ column were normalized by multiplying the corresponding absolute $[J]^{0g}$ by the same quantity (20.3) used in the results from Gr56.

^x For comparison with $N^{14}(d,n)O^{16}$, the bracketed entries in the relative 0^2 column are expressed relative to the ground-state reduced width as unity.

^y Not analyzed in this experiment.

^z Several transitions to higher levels, all well above the neutron separation energy, were observed. As noted in footnote m, the Butler curves then do not distinguish between l values (0 to 3).

^{a'} At low energies the ground-state transition does not behave in the characteristic "stripping" fashion. This is not true for the $l=0$ transition.

^{b'} Insufficient low-angle data to justify the extraction of a reduced width.

^{c'} Energy levels measured at Chalk River by $O^{16}(He^4, \gamma)$ (Ku58).

^{d'} This quartet of levels was unresolved in Be58. The reduced widths are accordingly tentative and are bracketed.

^{e'} The combined angular distribution for this unresolved triplet of levels has a peak intermediate between the characteristic $l=1$ and $l=2$ locations. No adequate fit is possible.

^{f'} A good $l=2$ transition is seen to one or more levels (possibly the lowest) of this unresolved quartet.

^{g'} Data too poor to justify any curve fitting.

^{h'} Originally analyzed (Br53) as an $l=0+2$ mixture. It appears (Se57) that this was unjustified. No evidence for any stripping to the F^{20} ground state has been found.

^{i'} Despite the fact that $O+\epsilon_d=0$ in this vicinity, the Butler formula shows no sign of behaving oddly. We note that no $l=0$ transitions are involved.

^{j'} Unresolved group corresponding to at least three levels in Ne^{20} .

^{k'} Unresolved. Separation and the $l=2$ assignment were made on the basis of known positions and spins, although the secondary maximum is intermediate in position between $l=1$ and $l=2$ locations.

^{l'} The angular fit, especially at low angles, is poor. Since the absolute cross section is given at 14° —far below the peak—no absolute reduced width can be quoted with confidence.

^{m'} Unresolved. Separation was again made on basis of spins, which are known otherwise.

^{n'} The $l=2$ component is subject to large errors.

^{o'} Other studies leave open the possibility that there may be levels other than those listed in the table, in the 4- to 8-Mev region.

^{p'} Angular distribution could not be analyzed accurately because of contaminants in the target.

^{q'} At a deuteron energy of 14.8 Mev, Ha60 find a sharp rise in the angular distribution of $Mg^{24}(d,p)Mg^{25}$ (ground state), suggestive of an $l=0$ contribution; $l=0$ is clearly excluded by conservation of angular momentum. No such anomaly is observed at a deuteron energy of 8.9 Mev (Hi58). Ha60 show that the deuteron energy is reduced from 14.8 to 9 Mev, the anomalous peak slowly dies away.

^{r'} No satisfactory fit could be obtained to these angular distributions. This is not surprising since the outgoing neutrons are of 1 Mev or less. No reduced widths can be quoted with confidence.

^{s'} Unresolved. The quoted width is $0.4^2 + 0.2^2$.

^{t'} The proton group is too weak for angular-distribution analysis. We expect $l=2$, however, so that, with this assumption, we can use the measured cross section to give us an upper limit to the corresponding reduced width.

^{u'} Unresolved group of levels. No $l=0$ components.

^{v'} Superposed on $l=0$ group from $C^{12}(d,p)C^{12}$. Since the amount of C^{12} in the target was not known, the accuracy of the subtraction procedure is doubtful.

^{w'} The error in this reduced widths is large since the transition appears as a minor admixture in $Mg^{24}(d,p)Mg^{25}$ (0.98 Mev).

^{x'} Several levels studied in this experiment are not listed in En57.

^{y'} The ground-state doublet was not resolved in Ho53a, nor was the doublet around 1 Mev. The separation was made with the help of En56.

^{z'} Isotropic backgrounds were subtracted in calculating relative reduced widths in the quoted reference. We have simply accepted these values but corrected for the background.

^{z''} The results of Ho53a were used to normalize the relative reduced widths of En56.

^{b''} Could not be fitted in reasonable fashion by any superposition of Butler curves.

^{d''} Unresolved. Probably mostly from the 8.6-Mev level (Ru57).

^{d'''} May be the unresolved doublet-analog of the Al^{28} ground-state doublet. In this case we have listed $70J_{-3} - 5\theta_{-2}$.

^{e''} The listed energy levels were taken from En57b. They are sufficiently different from those given in Ca55 to cast slight doubt on level identification in the 5- to 8.6-Mev region.

^{f''} Bracketed spins are assigned on the basis of the large reduced widths, identifying these with large components of $f_{7/2}$, $p_{3/2}$, and $p_{1/2}$.

^{g''} Unresolved. We mean that (at least) one of these levels contains a large $p_{3/2}$ component.

^{h''} This number is, in fact, $\frac{1}{2}\theta_{-2} - \theta_{-1}$, since Bennett does not resolve the doublet. (The factor of $\frac{1}{2}$ comes from the isotopic-spin coupling.)

^{i''} The ground-state doublet was not resolved by Da57. This has been done in the table using the cross-section ratio of Pa58.

^{j''} Unresolved levels, the combined angular distributions being well fitted by $l=3$. Any appreciable admixture of lower l would, if present, obscure an $l=3$ distribution. One of the three levels is, perhaps, predominantly $f_{7/2}$.

^{k''} Unresolved. No reasonable fit could be obtained to combined distribution.

^{l''} Mi53 suggest $l=1$ for this transition. The spin $\frac{3}{2}^+$ for the level at 2.8 Mev, which is convincingly established by $S^{32}(p,\gamma)Cl^{33}$ (Le56), rules out $l=1$. Possibly, as in the corresponding region of the S^{33} spectrum, we are dealing with an unresolved group of levels.

^{m''} The fit to the observed angular distribution is poor.

^{n''} We list only those transitions for which definite l values and relative cross sections are given in Da59. (With the exception of the levels at 1.634, 5.14, and 5.34 Mev). Several transitions studied in En59 are not reported in Da59. The excitation energies quoted are those of En59.

^{o''} The ground-state doublet being unresolved in Da59, only $[J=3]^{0g} + [J=4]^{0g}$ could be extracted directly. The reduced widths in the table were separated by setting $\theta_{-2} = \theta_{-1}$, which is expected theoretically and borne out well by the results of En 59.

^{p''} Unresolved levels. The entry in the $[J]^{0g}$ column is $\Sigma [J]^{0g}$.

^{q''} Improved measurements, confirming the tentative conclusions of Bu56, are given in Hi57. The reduced widths were normalized with the aid of Gi52.

^{r''} The indicated transitions have angular distributions peaked at angles intermediate between those characteristic of adjacent l values. In each case we have chosen the smaller value of l , for reasons (mainly theoretical) which are discussed in Sec. VI.

^{s''} Only relative cross sections are given in Bo57a. We have used the results of Ho53 to normalize roughly.

^{t''} In Bo57, the $Ca^{40}(d,p)Ca^{40}$ cross sections are given relative to the $Ca^{40}(d,p)Ca^{41}$ ground-state cross section (Bo57a). We can use this and the absolute cross sections of Ho53 to normalize roughly. A similar comment applies to the $Ca^{40}(d,p)Ca^{45}$ results of Co57.

^{u''} Energy levels from Sc53, Q values calculated from the atomic-mass excesses tabulated in Wa58.

^{v''} The spin of V^{62} ground state is doubtful, existing data leaving open the possibility of both 2^+ and 3^+ . In the table, the relative reduced widths are normalized—completely arbitrarily—to the value 7 for $[J]^{0g}$.

^{w''} Five more strong stripping transitions, to levels of V^{62} up to 4.43 Mev, are reported in Da60a. The l values, while probably $l=2$, are not clearly identified by the Butler theory. The matter is discussed in Sec. VI.

^{x''} These angular distributions almost certainly contain large $l=3$ components.

^{y''} Q values are calculated from Wa58.

^{z''} The spin assignment is based on the supposition that the major component in this level is the $f_{5/2}$ single-particle state.

^{a'''} $Co^{59}(d,p)Co^{60}$ is currently being studied by H. A. Enge at MIT with much higher resolution. The excitation energies of the various levels of Co^{60} given in the table (some of which are unresolved in El58a) are taken from a preliminary report of this work (Mass. Inst. Technol. Lab. for Nuclear Sci. Ann. Progr. Rept., June, 1956-May, 1957). With better resolution it seems that some of the $l=1$ groups of El58a contain substantial $l=3$ admixtures.

^{b'''} Although the transitions to the various bracketed levels are not resolved, it is known, from the fact that the target nucleus has spin zero in each case, that the different l values correspond to distinct transitions. An $l=1+3$ superposition, for example, cannot be obtained in transitions involving a spin-zero target.

^{c'''} Spins which are given in round brackets have been assigned on the (reasonable) assumption that we are dealing, successively, with fragments of the $1f_{5/2}$, $2p_{3/2}$, $2p_{1/2}$, $1g_{9/2}$, $2d_{5/2}$, and $3s_{1/2}$ single-particle levels. See Sec. VI for further discussion.

^{d'''} Pairs of levels of opposite parity are found near 0.82 Mev in Zn^{65} and near 0.38 Mev in Zn^{67} , probably $2p_{1/2}$ and $1g_{9/2}$ single-particle levels. The relative positions of these levels are not known.

Many careful studies have been made of the low-energy behavior of deuteron-nucleon cross sections, nearly all of them referring to (d,p) reactions on light nuclei ($A < 30$). [See, for example, Sm57, Re51, Ca52, and Co57, in which the proton angular distributions from $\text{Be}^9(d,p)\text{Be}^{10}$ have been measured at 19 deuteron energies from 0.1 to 3 Mev.] Such studies indicate that, at a deuteron energy of 5 Mev, we are usually clear of the region of rapid energy variation, the cross section being reasonably stable, in both angular distribution and absolute magnitude, as the deuteron energy is further increased. Close to the nucleon separation

energy ($Q = -2.23$ Mev), stable stripping peaks appear at rather lower bombarding energies (Wi57), sometimes as low as 1 Mev.

We take the position that a meaningful reduced width can be extracted from a measured differential cross section only if it possesses a stable "stripping" form and can be reasonably fitted by a suitable Butler curve (or superposition of Butler curves). The results of the foregoing low-energy stripping experiments then indicate that our analysis of stripping widths is applicable to transitions in light nuclei (with $A < 30$) in which the energy of neither the incoming or outgoing

TABLE II. Reduced widths from deuteron-triton stripping reactions.

Incident energy (Mev)	Q (Mev)	Final state excitation	J_0^π	l	r_0	$\Delta\theta^2$	Relative θ^2	Λ	θ^2	Foot-notes
$\text{Li}^7(d,t)\text{He}^6$ (Le55, Ha59) ($J = \frac{3}{2}^-$)										
15	-4.512	0 1.71	0^+ 2^+	1 1	7 7	5.8 1.9	1 0.33	[230] [230]	0.025 0.008	a
$\text{Li}^7(d,t)\text{Li}^6$ (Le55, Ha59)										
15	-0.994	0 2.184 3.560 4.52 5.35 5.4	1^+ 3^+ 0^+ 2^+ 2^+ 1^+	1 1 1 ... 1 ...	5.6 5.6 6.5 ... 5.6 ...	11.1 8.0 7.4 ... 5.7 ...	1 0.73 0.66 ... 0.52 ...	230 225 [230] ... [230] ...	[0.048] [0.036] 0.032 ... 0.025 ...	b c
$\text{C}^{13}(d,t)\text{C}^{12}$ (Ho54) ($J = \frac{3}{2}^-$)										
2.19 3.19	1.313 1.313	0 0	0^+ 0^+	1 1	4.5 5	4.5 7.3		205 290	[0.024] [0.025]	d d
$\text{C}^{13}(d,t)\text{C}^{12}$ (Ma60)										
14.8	1.313	0 4.435 7.653	0^+ 2^+ 0^+	1 1 1	4.6 5 6	5.9 4.5 0.24	1 0.76 0.04	190 [190] [190]	[0.031] 0.024 0.0012	e
$\text{C}^{14}(d,t)\text{C}^{13}$ (Mo58) ($J = 0^+$)										
14.9	-1.915	0 3.09 3.68 3.86	$\frac{1}{2}^-$ $\frac{1}{2}^+$ $\frac{3}{2}^-$ $\frac{5}{2}^+$	1 0 1 2	5.5 5 5.9 5	10.4 0.28 7.0 1.2	1 0.027 0.68 0.18	165 [165] [165] [165]	[0.063] 0.0017 0.041 0.011	f
$\text{O}^{16}(d,t)\text{O}^{15}$ (Ke60) ($J = 0^+$)										
14.9	-9.396	0	$\frac{1}{2}^-$	1	4.8	2.4				
$\text{O}^{18}(d,t)\text{O}^{17}$ (Ar60) ($J = 0^+$)										
14.9	-1.810	0 0.871 3.058 3.846 4.555 5.08 5.22	$\frac{5}{2}^+$ $\frac{3}{2}^+$ $\frac{1}{2}^-$ $\frac{3}{2}^-$ $\frac{1}{2}^+$ $\frac{3}{2}^+$ $\frac{5}{2}^-$	2 0 (1) 3 1 2 1	5 5 5 5 5 5 5	5.7 2.2 0.21 0.22 0.25 0.38	1 0.39 0.038 0.038 0.044 0.065			g
$\text{F}^{19}(d,t)\text{F}^{18}$ (Ha60a) ($J = \frac{3}{2}^-$)										
15	-4.155	0	1^+	0	6	1.7		105	[0.017]	h
$\text{Na}^{23}(d,t)\text{Na}^{22}$ (Vo58) ($J = \frac{3}{2}^+$)										
14.8	-6.16	0 0.59 0.89 1.54	3^+	2 2 2 2	6 6 6.5 6.5	3.3 1.1 1.9 0.61	1 0.33 0.57 0.19	160 [160] [160] [160]	[0.021] 0.007 0.012 0.004	i

TABLE II.—Continued.

Incident energy (Mev)	Q (Mev)	Final state excitation	$J_0\pi$	l	r_0	$\Delta\theta^2$	Relative θ^2	Λ	θ^2	Foot-notes
$Mg^{25}(d,t)Mg^{24}$ (Ha60) ($J=\frac{3}{2}^+$)										
14.8	-1.07	0	0^+	2	5.4	1.3	1	150	[0.0085]	j
		1.368	2^+	2	6	2.6	2.0	[150]	0.017	
		4.122	4^+	2	6	0.42	0.33		0.0028	
		4.24	2^+	2	6	0.11	0.09		0.0008	
		5.24	
		6.01	
		7.33	
		7.60	
$Mg^{26}(d,t)Mg^{25}$ (Ha60) ($J=0^+$)										
14.8	-4.86	0	$\frac{5}{2}^+$	2	6	4.6	1	[150]	0.031	k
		0.58	$\frac{1}{2}^+$	0	7	0.37	0.080		0.0025	
		0.98	$\frac{3}{2}^+$	2	7	0.06	0.013		0.0004	
		1.61	$\frac{7}{2}^+$	
		1.96	$\frac{3}{2}^+$	2	7	0.27	0.058		0.0018	
		2.56	$\frac{1}{2}^+$	0	7	0.11	0.023		0.0007	
		2.74	$\frac{3}{2}^+$	
		2.80	$\frac{3}{2}^+$	2	7	0.14	0.029		0.0009	
		3.40	$\frac{5}{2}^-$	
$V^{51}(d,t)V^{50}$ (Ze60) ($J=\frac{3}{2}^-$)										
21.5	-4.78	0.4]		3	7.1	3.5				l, m, n
		1.1]		3	7.1	2.9				
		3.1]		3	7.1	2.5				
$Cr^{52}(d,t)Cr^{51}$ (Ze60) ($J=0^+$)										
21.5	-5.79	0	$\frac{7}{2}^-$	3	7.1	5.7				m, n
		0.75		3	7.1	0.78				
$Mn^{55}(d,t)Mn^{54}$ (Ze60) ($J=\frac{5}{2}^-$)										
21.5	-3.95	0		1	7.4	5.7				l, m, n
		1.1]		{+3}	7.4	1.0				
		2.7]		1	7.1	1.9				
		4.0]		3	7.4	1.0				
					7.1	0.39				
$Fe^{56}(d,t)Fe^{55}$ (Ze60) ($J=0^+$)										
21.5	-4.94	0	$\frac{3}{2}^-$	1	7.4	3.1				l, m, n
		0.42	($\frac{3}{2}^-$)	1	7.4	0.78				
		1.4]		{+3}	7.4	0.40				
		2.0]		1	7.1	2.7				
		2.5]		3	7.4	0.20				
					7.1	0.20				
$Fe^{57}(d,t)Fe^{56}$ (Ze60) ($J=\frac{3}{2}^-$)										
21.5	-1.38	0	0^+	1	7.4	0.74				l, m, n
		0.845	2^+	{+3}	7.4	1.5				
		2.085	4^+	...	7.1	1.4				
		2.660	2^+	
		2.9]		1	7.4	3.5		
		4.0]		3	7.1	1.8				
$Co^{59}(d,t)Co^{58}$ (Ze60) ($J=\frac{7}{2}^-$)										
21.5	-4.24	0.3]		{+3}	7.4	10.3				l, m, n
				(+3)	7.1	≤ 4.3				
$Zn^{64}(d,t)Zn^{63}$ (Ze60) ($J=0^+$)										
21.5	-5.59	0	$(\frac{3}{2}^-)$	1	7.4	6.4				l, m, n
		0.19	($\frac{5}{2}^-$)	(3)	7.1	≤ 2.9				
		0.64		1	7.4	1.8				
		1.1]		{+3}	7.4	0.78				
					7.1	≤ 0.40				

TABLE II.—Continued.

Incident energy (Mev)	Q (Mev)	Final state excitation	J_0^π	l	r_0	$\Delta\theta^2$	Relative θ^2	Λ	θ^2	Foot-notes
$\text{Cu}^{65}(d,t)\text{Cu}^{64}$ (Ze60) ($J=\frac{3}{2}^-$)										
21.5	-3.65	0.4]		{ 1 (+3)	7.4 7.1	12.5 ≤ 6.2				l, m, n
$\text{Zn}^{68}(d,t)\text{Zn}^{65}$ (Ze60) ($J=0^+$)										
21.5	-4.77	0]		{ 1 (+3)	7.4 7.1	7.3 ≤ 4.6				l, m, n
		0.86]		{ 1 (+3)	7.4 7.1	1.5 ≤ 0.1				
$\text{Zn}^{67}(d,t)\text{Zn}^{66}$ (Ze60) ($J=\frac{5}{2}^-$)										
21.5	-0.80	0	0^+	3	7.1	0.48				m, n
	1.05	2+		{ 1 +3	7.4 7.1	0.68 0.39				
	2.40	4+		
	2.75			{ 1 +3	7.4 7.1	1.3 1.8				
	3.24	
	3.41			{ 1 +3	7.4 7.1	2.9 1.5				
	3.78									
	4.10									
$\text{Zn}^{68}(d,t)\text{Zn}^{67}$ ($J=0^+$)										
21.5	-3.93	0.3]		{ 1 +3	7.4 7.1	8.8 7.2				l, m, n

^a We use the value of Λ obtained from $\text{Li}^{17}(d,t)\text{Li}^{16}$ (Ha59).

^b θ^2 from the $\text{Li}^{17}(d,p)\text{Li}^{17}$ ground-state data of Ha59.

^c θ^2 from the $\text{Li}^{17}(p,d)\text{Li}^{16}$ data of Re56.

^d θ^2 from the $\text{C}^{12}(d,p)\text{C}^{13}$ data of Ho54.

^e θ^2 from the $\text{C}^{12}(d,p)\text{C}^{13}$ data of Ha59.

^f θ^2 from the $\text{C}^{13}(d,p)\text{C}^{14}$ data of Mc56 and Ha59.

^g Although this triton group is obscured by elastically scattered deuterons, it is clear that there is a strong stripping transition. By conservation of angular momentum, such a transition must have $l=1$.

^h There is a discrepancy (involving a factor of two) between the reduced width determined from the $\text{F}^{19}(p,d)\text{F}^{18}$ data of Re56 and Be58. The value of Λ obtained is accordingly uncertain. We use the data of Be58.

projectile is less than 5 Mev. This lower limit, which obviously has only qualitative significance, should probably be somewhat higher for reactions on heavier nuclei ($A > 30$) or for deuteron-triton reactions.

All available data on deuteron-nucleon reactions involve deuterons of 15 Mev or less. At the highest energies studied, the simple theory gives a satisfactory account of the observed angular distributions, so that we are not in a position to set an upper limit to the range of usable projectile energies. There are, however, indications (Ze60a) that the proton angular distributions from the bombardment of Be^9 , Be^{10} , and C^{12} by 21.5-Mev deuterons, although exhibiting very clear "stripping" peaks, cannot be fitted by the simple theory with reasonable interaction radii. In contrast, the simple theory works very well for the triton angular distributions from (d,t) reactions induced by 21.5-Mev deuterons (Ze60). Experimental study of these matters would be worthwhile.

(b) Ambiguities in Determining l

We sometimes encounter transitions which exhibit very marked "stripping" peaks but from which it is impossible to determine l unambiguously.

ⁱ θ^2 from the $\text{Na}^{23}(p,d)\text{Na}^{22}$ data of Be58.

^j θ^2 from the $\text{Mg}^{24}(d,p)\text{Mg}^{25}$ data of Ha60.

^k We use the value of Λ obtained from $\text{Mg}^{25}(d,t)\text{Mg}^{24}$.

^l Individual states of the residual nucleus not resolved. We use the symbol $\bar{\epsilon}$ to signify the mean excitation energy $\bar{\epsilon}$ of a group of unresolved levels.

^m Q values are taken from As59.

ⁿ For $A > 40$, we have not divided out the isotopic-spin coupling factor $(C)^2$ in (II.19). In such cases we list $(C)^2 \theta^2$ rather than θ^2 itself (see Appendix 1).

The first type of situation where this occurs involves capture into unbound levels of the final nucleus. In such cases, Butler curves for adjacent l values are almost identical in shape (see Mc56). The l values can sometimes be determined indirectly, either by arguments concerning reduced widths or by carrying out the appropriate neutron or proton elastic-scattering experiment.

Secondly, (d,p) experiments with 6- to 8-Mev deuterons on heavier nuclei ($A > 40$) (for example, Bo57, Bo57a, Da60a) have repeatedly encountered difficulties in distinguishing $l=1$ from $l=2$, or $l=2$ from $l=3$. The trouble here may stem from the rather low deuteron energies used; it would be interesting to see if the ambiguities persist in experiments with 15-Mev deuterons.

(c) Capture into Weakly Bound Levels of the Residual Nucleus

The simple theory encounters serious difficulties in dealing with $l=0$ capture into levels of the final nucleus close to the nucleon separation energy. There are numerous indications [for example, in $\text{F}^{19}(d,p)\text{F}^{20}$ (El56) and $\text{Mg}^{24}(d,p)\text{Mg}^{25}$ (Hi58)] that the simple

theory remains adequate close to the nucleon separation energy for l values other than 0.

The examples most often quoted in the present connection are (Ca57, Mi53)

$$\begin{aligned} C^{12}(d,n)N^{13} & (2.37 \text{ Mev}), \quad Q + \epsilon_d = -0.425 \text{ Mev}, \\ O^{16}(d,n)F^{17} & (0.51 \text{ Mev}), \quad Q + \epsilon_d = +0.085 \text{ Mev}, \end{aligned}$$

both $l=0$ transitions. Here the difficulty is particularly pronounced; the angular distributions predicted by the simple theory bear little resemblance either to the usual stripping curves or to the experimental cross sections. Not surprisingly, the reduced widths so extracted are valueless, since they vary wildly with the angle at which we normalize the theoretical curve and with r_0 .

No comparably extreme cases have been found among (d,p) reactions, probably because no (d,p) transitions with $l=0$ have been observed so close to $Q+\epsilon_d=0$; however, in

$$Be^9(d,p)Be^{10} (6.28 \text{ Mev}),$$

where $Q+\epsilon_d=0.565$ Mev (Gr56, Rh54), the fact that the $l=0$ reduced width varies strongly with r_0 (by a factor of more than two as r_0 varies by 1 f about its "best" value) indicates that all is not well, although an acceptable fit to the angular distribution can be obtained.

Butler (Bu57, p. 70; see also Au60) has shown that a very simple Coulomb correction rectifies matters in the case of (d,n) transitions to weakly bound final states. The correction in question concerns the second term in the form factor $W_l(x,y)$ (II.20), which contains the logarithmic derivative

$$\{[1/h_l^{(1)}(ir)](\partial/\partial r)h_l^{(1)}(ir)\}_{r=r_0} \quad (\text{II.39})$$

evaluated at the nuclear surface, of a free-particle wave function. This factor is introduced by matching the free-particle logarithmic derivative at $r=r_0$ to that of the radial wave function $R_l(r)$ of the captured nucleon in the potential well of the capturing nucleus. Now in a (d,n) reaction, the captured nucleon is a proton and the solution of the appropriate radial wave equation beyond the range of the nuclear potential is not a free-particle function but a Coulomb function. For the limited purpose of evaluating the logarithmic derivative at $r=r_0$, we may simulate this Coulomb correction by replacing t in (II.39) by \tilde{t} , where

$$\tilde{t}^2 = t^2 + \{2AM/[(A+1)\hbar^2]\}(Ze^2/r_0) \quad (\text{II.40})$$

and Ze is the charge on the target nucleus. It is obvious that this correction, which involves replacing the value of t determined from the binding energies by an "effective" value in calculating the form factor (II.20), is a step in the right direction. In fact, as can be seen from Figs. 6 and 7 in Appendix I of Ma59, it provides an excellent fit to the experimental data on $C^{12}(d,n)N^{13}$ (2.37 Mev), $O^{16}(d,n)F^{17}$ (0.51 Mev) and other similar transitions, with reasonable values of r_0 .

It should, in fact, be appropriate to use the modified procedure for all (d,n) transitions; however, it appears (Appendix I of Ma59) to make little practical difference whether or not we use it unless $Q+\epsilon_d$ is close to zero ($Q+\epsilon_d < 1$ Mev). Accordingly, we use (II.40) only when compelled to do so.

The approximate Coulomb correction (II.40) is inapplicable to (d,p) reactions; however, its success and its character suggest that, in considering (d,p) reactions to weakly bound levels, it might be appropriate to replace the value of t obtained from (II.8) by a suitable effective value. In other words, as suggested by Austern (Au60), it might be better to fit (d,p) cross sections by fixing r_0 and varying t .

We have preferred not to adopt this course in the present study. For (d,p) transitions with $l=0$ and $Q+\epsilon_d \approx 0$, we proceed, as usual, by choosing a best-fit radius and extracting a reduced width on this basis. Since the reduced width so obtained is abnormally sensitive to r_0 , we do not place much reliance on $l=0$ reduced widths close to the nucleon separation energy.

The first Born-approximation calculation for deuteron-nucleon reactions was performed by Bhatia *et al.* (Bh52). They obtained a result which differed from the Butler formula in the occurrence of a simple Bessel function $j_l(qr)$ in place of the factor $W_l(xy)$ given by (II.20). This came about because, in evaluating the relevant radial integral, Bhatia *et al.* assumed that $j_l(qr)$ varies so slowly that it may be replaced by its value at r_0 . This is known to be a poor approximation.

For most transitions, the Bhatia and Butler formulas predict very similar angular distributions, provided that a somewhat larger radius is used in conjunction with the former. Reduced widths extracted by means of the two theories, on the other hand, sometimes differ markedly. The apparent superiority of the Bhatia expression in dealing with transitions to weakly bound levels stems from the fact that their approximate evaluation of the relevant radial integral introduces errors which simulate the correction (II.40). This being fortuitous and the approximation unnecessary because the integral in question can be evaluated exactly, we argue against the use of the Bhatia formula as a substitute for the Butler formula.

In the preceding discussion we have referred specifically to deuteron-nucleon reactions. It is clear that similar comments apply to more complex reactions in which a single nucleon is transferred.

(d) Amado's Procedure for Extracting Reduced Widths

Amado (Am59) has recently described a modified procedure for extracting stripping widths, also relying on the simple Born-approximation theory. Both measured and Born-approximation differential cross sections are first plotted as functions of $\cos\theta$. The value of the quotient

$$(d\sigma/d\omega) \text{ (measured)} / (d\sigma/d\omega) \text{ (B.A.)} \quad (\text{II.41})$$

extrapolated to the (unphysical) value of $\cos\theta$ which satisfies

$$q^2 + t^2 = 0 \quad (\text{II.42})$$

is then taken to be the correct Born-approximation reduced width. Since the Born-approximation cross section has a pole at the value of $\cos\theta$ satisfying (II.42), while other contributions to the observed cross section remain finite, it is hoped that the Born approximation is then exact.

It is clear that, when the appropriate Butler curve fits the experimental data at forward angles very closely, the quotient (II.42) is essentially constant and the extrapolated reduced width does not differ much from the value obtained by the procedure of Sec. II.2. Amado's technique leads to significantly different results only when the Born-approximation angular distribution deviates markedly from the experimental cross section. In such cases, however, the reduced width obtained depends quite sensitively on the exact way in which the extrapolation is performed, a matter which involves considerable ambiguity.

Thus, although Amado's procedure may turn out to be very useful (quite apart from its theoretical implications), we have preferred to base our study of stripping widths on the simple method of Sec. II.2.

(e) *Empirical Normalization Constant in Deuteron-Triton Cross Sections*

The expressions (II.36) and (II.37) for the deuteron-triton differential cross sections contain an empirical constant Λ . This factor is related by (II.35) to the asymptotic normalization constant N_s of the $a=3$ internal wave function. In view of the crudity of the entire Born-approximation procedure, we do not believe that our empirical value of N_s^2 can tell us much about the structure of the $a=3$ nuclei.

It should be observed that the reaction



is both a (d,p) and a (d,t) reaction. If we assume that the $a=2$ stripping transform is known, (II.43) provides a direct measurement of the $a=3$ transform. We refer the reader for discussion of this point to Hamburger's paper (Ha60a). Notice that Hamburger uses a normalization constant B^2 which is related to the quantity N_s^2 used here and in Fr60 by

$$B^2 = 4\pi N_s^2. \quad (\text{II.44})$$

In conclusion, we observe that (II.19), with the stripping transform $P_{a(\kappa)}$ given by (II.34), can be specialized immediately to the case $a=4$ when occasion arises.

(f) *Limitations of the Present Study*

In this study we do not give any systematic discussion of the spectroscopic information to be obtained from

$(d,p\gamma)$ angular-correlation studies or from measurements of the polarization of protons from (d,p) reactions. The latter restriction is a natural consequence of our decision to use the simple Butler theory, since plane-wave Born-approximation theories predict zero polarization.

We have confined our attention to "light and intermediate nuclei" ($A < 70$) simply because available data, with few exceptions, involve such nuclei. It seems certain that stripping and related reactions will eventually be used to probe the structure of heavier nuclei, although it is far from certain that our simple Born-approximation procedure, as it stands, will provide an adequate means of analyzing the data.

III. THEORETICAL ANALYSIS OF REDUCED WIDTHS

1. Introduction

A reduced width θ^2 for the emission of a nucleon in a transition between two nuclear states was introduced in Sec. I and emerged in Sec. II as a factor in the differential cross section of stripping reactions. This reduced width is a product of two factors, the single-particle reduced width θ_0^2 and the spectroscopic factor S , which are defined explicitly in (II.13)–(II.15). We have agreed to treat θ_0^2 as an empirical parameter. We now study the spectroscopic factor S , which contains the information we seek about the structure of the nuclear states involved.

As is later seen explicitly, the evaluation of S consists in calculating overlap integrals between the initial and final nuclear states. The present section is largely devoted to an explicit consideration of such overlap integrals, wherein the nuclear states are represented by the wave functions of appropriate nuclear models. Although the bulk of our detailed applications involve various species of shell model, we also examine the weak-coupling collective model and the rotational model.

It should be emphasized that the present analysis of S is independent of the use of the Butler formula. Our results are equally applicable in studying reduced widths extracted on the basis of more sophisticated theories of the stripping process or from the analysis of resonance reactions. A more descriptive and less explicit account of many of the considerations of this section may be found in a recent article by French (Fr60).

2. Nuclear Shell Model

The basic assumptions, the predictions, and the limitations of the nuclear shell model are discussed in detail in a number of excellent monographs and review articles (Fe55, Ma55, El57). Such matters do not concern us here. Suffice it to say that the many successes of the shell model in the mass region of most interest to us ($A \leq 70$) make it a natural choice in calculating relative reduced widths.

The main physical content of any shell model, whatever its degree of sophistication, resides in two basic assumptions:

(1) There exist single-nucleon orbits, each being characterized by a radial quantum number n and an orbital angular momentum l .

(2) A strong spin-orbit interaction depresses each $j=l+\frac{1}{2}$ level relative to the corresponding $j=l-\frac{1}{2}$ level, where $\mathbf{j}=\mathbf{s}+\mathbf{l}$. These basic postulates are given formal expression by writing the nuclear shell-model Hamiltonian in the form

$$H = H_0 + H_c + H_{so} \quad (\text{III.1})$$

$$= \sum_{i=1}^A V(r_i) + \sum_{i < j=1}^A H_{ij} + a \sum_{i=1}^A \mathbf{l}_i \cdot \mathbf{s}_i. \quad (\text{III.2})$$

The central "shell-model potential" $V(r)$ is assumed throughout to possess a harmonic-oscillator radial dependence. This assumption is made because it is known to be a good approximation for light nuclei and because harmonic oscillator eigenfunctions are particularly convenient in calculations. H_{ij} is an effective two-body interaction operator, while H_{so} is a one-body spin-orbit potential.

The two-body interaction parameters and the strength a of the spin-orbit potential are adjusted so that the model Hamiltonian (III.2) gives as good a description as it can of the observable properties of the nucleus. It is therefore to be expected that the appropriate values of the various parameters will vary with A , n , l , and possibly with other quantities (e.g., $N-Z$).

No experimental data has been found, to date, whose interpretation demands conclusively that H_{ij} be anything other than central, static, and charge-independent (neglecting Coulomb forces). There is no reason why the effective two-body interaction should bear a close resemblance to the interaction experienced by two free nucleons in a scattering process. For heavier nuclei, the assumption that H_{ij} is central is not very strong, since, in most cases of interest in jj coupling, it can be shown that any two-body interaction is effectively central.

H_{so} is diagonal in a jj representation, the diagonal elements being evaluated by direct comparison with experiment. We can therefore avoid introducing H_{so} explicitly when working in a jj representation, absorbing its effects in specifying the single-particle level spacings. We often discuss the positions of single-particle levels in our subsequent analysis of stripping experiments.

The eigenfunctions of H_0 provide a complete set of antisymmetric A -nucleon functions. Since a number of operators commute with H , the functions of such complete sets may be characterized by the corresponding good quantum numbers, amongst which we always find the total angular momentum J , the parity π , and (as long as Coulomb effects are reasonably small) the isotopic-spin T . We do not discuss the important

problem of finding such additional quantum numbers as may be necessary to furnish a complete specification of the basic functions of a representation.

Ideally, we would use the representation so constructed to set up and diagonalize the matrix of H . This energy matrix is a direct sum of disjoint submatrices, each block corresponding to one set of values of J , π , T ; however, this ideal procedure encounters enormous complications and it is necessary, in practice, to restrict the number of basic states which enter the calculation. This restriction is achieved by including only the states of a few of the lowest "configurations," regarding the A nucleons as filling the single-particle states of $V(r)$ in ascending order and in accordance with the demands of the exclusion principle.

The eigenvalues and eigenfunctions of this restricted energy matrix are then used in comparisons with the spectra and other observable properties of nuclei. The parameters in H_c and H_{so} are adjusted—largely by trial and error—so as to produce optimal accord between theory and experiment.

We refer repeatedly to "equivalent nucleons" and to "configurations," terms which ought to be defined with some care. Several nucleons are said to be equivalent if they have the same value of n , l , and also of j if we use a representation wherein j is specified. A configuration is a definite set of values of (nl) or of (nlj) if j is specified.

At the outset of a shell-model calculation, we must decide which configurations to take into account. In practice, we rely on experience tempered by the necessity of keeping the dimensions of the matrices involved within reasonable bounds. In Sec. III.11 a formalism is presented whereby many reduced widths can be analyzed independently of any choice of configurations for the nuclear states involved. It is then seen clearly that a reduced width measures an amplitude corresponding to a given value of l , and often also of j , of the transferred nucleon, quite apart from the success or failure of any model in describing the relevant states.

It should be remarked that the choice of representation is a matter of convenience. Thus, for example, the use of a jj representation has nothing whatever to do with the validity or otherwise of jj coupling, the latter statement being concerned with the properties of the nuclear wave function. The use of a jj representation may not be convenient unless the nuclear states under consideration are reasonably "close to jj coupling."

It is seen from what has been said that one⁴ of the main formal problems of shell-model spectroscopy

⁴ The other two main problems involve the evaluation of the matrix elements of symmetric one- and two-body operators

$$T = \sum_{i=1}^n T(i), \quad G = \sum_{i < j=1}^n G(ij) \quad (\text{III.3})$$

between antisymmetric n -particle states. We do not give a systematic discussion of such matrix elements and their evaluation in the present study.

is the construction of antisymmetric n -particle wave functions. This problem is discussed in detail in Secs. III.4–6, with particular attention to the unambiguous specification of all (relative) phases. Section III.3 contains a preliminary exposition of our notation, while in Sec. III.7 we apply the antisymmetric n -particle wave functions to the central task of calculating the spectroscopic factor S .

3. Notation

The conventional way of writing a wave function is simply to exhibit every quantum number necessary for its complete specification. In treating the spectroscopy of several particles, especially if more than one configuration is involved, such a procedure can be incredibly cumbersome. We prefer to introduce a symbolic notation wherein the structure of a wave function is compactly delineated, often describing groups of quantum numbers by a single symbol. What is gained by so doing becomes apparent on translating some of the considerations of Secs. III.6 and III.7 into conventional language. Many features of our graphical notation⁵ have previously been described by Halbert (Ha56) and by French (Fr60).

Let us start by considering two commuting angular momentum operators \mathbf{j}_1 and \mathbf{j}_2 , with $\mathbf{j}_1 + \mathbf{j}_2 = \mathbf{J}$. We then write, for the function obtained by vector coupling \mathbf{j}_1 and \mathbf{j}_2 ,

$$\psi(j_1 j_2 JM) \equiv \begin{array}{c} \text{Diagram of a triangle with vertices } j_1, j_2, \text{ and } JM \end{array} . \quad (\text{III.4})$$

The diagram on the right-hand side of (III.4) does not merely indicate the mode of angular momentum coupling in ψ , it is an alternative symbolic expression for ψ itself. This is the central feature of our notation.

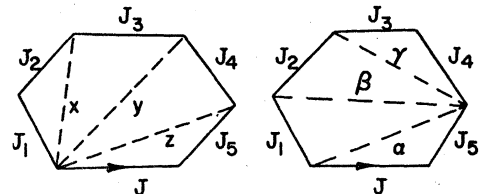
If it is now desired to couple n commuting angular momenta, the diagram of the same type as (III.4) which springs to mind is

$$\begin{array}{c} \text{Diagram of a regular pentagon with vertices } J_1, J_2, J_3, J_4, J_5 \end{array}$$

But this function exhibits only $n+2$ angular-momentum quantum numbers, whereas $2n$ are needed for a complete specification, as can be seen by considering the “direct product” (Ra42) $J_1 M_1, J_2 M_2 \cdots J_n M_n$ representation. It is easy to prove that any set of $n-2$ non-

intersecting coupling lines constitutes a permissible way of completing the desired specification.

Taking the preceding specific case by way of illustration, two possible sets of *internal* coupling lines are



We nearly always omit the projection quantum number M , since it has no bearing on the considerations of this section. In addition, it is clear that only one arrow need be drawn in any diagrammatic wave function.

Functions with the same ordering of the J_i and the same internal coupling lines, where the internal quantum numbers run through all possible values, constitute a complete set of orthogonal functions in the appropriate $\prod_{i=1}^n (2J_i + 1)$ -dimensional vector space. We demand that each such function be normalized.

The complete sets of orthonormal functions belonging to any two schemes for the same angular momenta must be connected by a suitable unitary transformation. Any such transformation may be expressed explicitly and in a finite number of steps in terms of the three fundamental recoupling rules

$$\begin{array}{c} \text{Diagram of a triangle with vertices } a, b, c \end{array} = (-1)^{a+b-c} \begin{array}{c} \text{Diagram of a triangle with vertices } b, a, c \end{array} \quad (\text{III.5})$$

$$\begin{array}{c} \text{Diagram of a rectangle with vertices } a, b, c, d \end{array} = \sum_f U(abcd; ef) \begin{array}{c} \text{Diagram of a rectangle with vertices } a, f, c, d \end{array} \quad (\text{III.6})$$

$$\begin{array}{c} \text{Diagram of a rectangle with vertices } a, b, c, d \end{array} = \sum_e U(abcd; ef) \begin{array}{c} \text{Diagram of a rectangle with vertices } a, e, c, d \end{array} \quad (\text{III.7})$$

$U(abcd; ef)$ is a normalized Racah coefficient (Ra42, Ed57, Ro57, Fr58).

When a wave function is antisymmetric, we indicate this by a circular arc. For example, an antisymmetric state of the configuration (nl) in a $TSL(M_T M_S M_L)$ representation is written as

$$\begin{array}{c} \text{Diagram of a semicircle with vertex } l^n \end{array} \quad \begin{array}{c} \text{Diagram of a semicircle with vertex } s^n \end{array} \quad \begin{array}{c} \text{Diagram of a semicircle with vertex } t^n \end{array} \quad (\text{III.8})$$

$$\begin{array}{c} \text{Diagram of a semicircle with vertex } l_{2...n}^n \end{array} \quad \begin{array}{c} \text{Diagram of a semicircle with vertex } s_{2...n}^n \end{array} \quad \begin{array}{c} \text{Diagram of a semicircle with vertex } t_{2...n}^n \end{array} \quad (\text{III.9})$$

⁵ A diagrammatic notation for wave functions seems to have been first used by Fano (Fa51).

It is usually unnecessary to exhibit the particle numbers explicitly, but this may be done as in (III.9) if there is any danger of ambiguity. The antisymmetrization symbol refers to the entire wave function and not to its separate space, spin, and isotopic-spin parts. In general, let us agree that antisymmetrization symbols appearing in the same wave function act together (in the preceding sense) if and only if they refer to the same particle numbers.

Finally, a "direct product" notation is introduced which enables us to carry out most of our formal manipulations independently of the particular representation to be used. Expressions so derived apply to both LS and jj representations, with or without the isotopic-spin formalism, with one exception to be noted in the following.

Let us write

$$\begin{aligned} \beta^n = & \quad l^n_L \quad s^n_S \quad t^n_T \quad \text{or} \quad l^n_L \quad s^n_S \\ \text{or} \quad & j^n_J \quad \text{or} \quad j^n_J \quad t^n_T \end{aligned} \quad (\text{III.10})$$

$\beta = \{nl, s\}$ or $\{nl, s, t\}$ or nlj or $\{nlj, t\}$,

$\beta = \{L, S\}$ or $\{L, S, T\}$ or J or $\{J, T\}$.

Greek letters are used consistently to refer to such composite quantum numbers.

The recoupling techniques based on (III.5)–(III.7) can be adapted to the direct-product notation, in precisely their original form, by means of an appropriate interpretation of the coefficients. For example,

$$\begin{array}{c} \gamma \\ \beta \quad \tau \\ \Gamma \end{array} \delta = \sum_r U(\beta\gamma\delta: \epsilon\tau) \begin{array}{c} \gamma \\ \epsilon \\ \Gamma \end{array} \delta, \quad (\text{III.11})$$

$$\begin{array}{c} l^n \\ L \quad S \quad s^n \\ JM \end{array} = \sum_{ML} C[LSJ; M_L, M - M_L] \begin{array}{c} l^n \\ LM_L \\ J \end{array} \begin{array}{c} s^n \\ M - M_L \end{array} . \quad (\text{III.14})$$

Although each separate function on the right-hand side of (III.14) fits the direct-product notation, the vector-coupled function does not, since a linear combination of products is itself not necessarily expressible as a product. Nevertheless, we can introduce the symbolic convention

$$\begin{array}{c} \rho^n \\ \beta(J) \end{array} = \begin{array}{c} l^n \\ L \quad S \quad s^n \\ J \end{array} \quad (\text{III.15})$$

provided that the Racah coefficient has the significance

$$U(\beta\gamma\delta: \epsilon\tau) = U(\beta_L\gamma_L\Gamma_L\delta_L: \epsilon_L\tau_L) \times U(\beta_S\gamma_S\Gamma_S\delta_S: \epsilon_S\tau_S) \quad (\text{III.12})$$

in the particular case of an LS representation. In the same representation

$$\begin{aligned} (-1)^\beta &= (-1)^{\beta_L + \beta_S}, \\ [\beta] &= (2\beta + 1) = [LS] = (2L + 1)(2S + 1). \end{aligned} \quad (\text{III.13})$$

The corresponding statements for the other representations in (III.10) can be written down in the same way. The compact symbol $[\beta]$ for the frequently occurring factor $(2\beta + 1)$ is particularly convenient and is used throughout.

The complete specification of a state may demand the presence of quantum numbers which are not angular momenta (e.g., space symmetry). In such an eventuality, the additional quantum numbers may either be written out explicitly

$$\begin{array}{c} \rho^n \\ x, \beta \end{array}$$

or, in a further foreshortening of the notation, simply absorbed in β . In writing out composite symbols, such as Racah coefficients or $(-1)^\beta$, which have been assigned a meaning only for angular-momentum quantum numbers, we must ignore the nonangular-momentum part of β .

The functions

$$\begin{array}{c} l^n \\ L \quad S \quad s^n \\ J \end{array} \quad \begin{array}{c} t^n \\ T \end{array}$$

of an LSJ representation do not fall naturally into a direct-product notation. This can be readily understood from the explicit expression

the additional vector coupling, whose presence prevents the use of the ordinary direct-product notation, being symbolized by the bracketed J .

The formal modification (III.15) owes its usefulness to the circumstance that the manipulations we wish to perform commute with the process of vector coupling. These manipulations—recoupling, and, as we see later, antisymmetrization—involve the formation of specific linear combinations, and the order of two finite summations can always be interchanged.

By introducing the notion of "multiple tensor"

(Ra42), we can calculate the matrix elements of operators in a direct-product notation.⁶ Let T^r , U^s be irreducible tensor operators in disjoint spaces. We may then define the "double tensor"

$$(TU)^{rs} = T^r U^s$$

whose rank is specified by the pair of numbers (rs) and which operates in the direct-product space. A tensor of any multiplicity can be introduced in the same way.

It is natural to write T^Δ for such a multiple tensor in the direct-product notation, the composite rank being designated by the set of numbers Δ . Since the various factors of T^Δ operate independently, each in its own space, matrix elements can be calculated by means of the standard formulas (Ed57, Chap. 5), written in the direct-product notation. In particular, the Wigner-Eckart theorem becomes

$$\langle \rho m_p | T_\gamma^\Delta | \rho' m_{p'} \rangle = \frac{(-1)^{2\Delta}}{[\rho]^{\frac{1}{2}}} C[\rho' \Delta \rho; m_p \gamma m_{p'}] \langle \rho | T^\Delta | \rho' \rangle. \quad (\text{III.16})$$

Often T^Δ does not operate in some of the component spaces of the direct-product manifold, the corresponding factors of T^Δ being unit operators in their spaces. In evaluating the reduced matrix elements $\langle \rho | T^\Delta | \rho' \rangle$ in such cases, we must remember that the reduced matrix element of a unit operator, defined according to (III.16), is not simply unity, being given, instead, by

$$\langle j | 1 | j' \rangle = [j] \delta(jj'). \quad (\text{III.17})$$

Suppose, for example, that we require the reduced matrix element of a spherical harmonic $Y_q^{(k)}$ —the prototype spherical tensor—in the direct product of orbital and spin spaces.

Then $\rho = \{ls\}$ with $s = \frac{1}{2}$,

$$\begin{aligned} T_\gamma^\Delta &= T_{q,0}^{k,0} = Y_q^{(k)}(\mathbf{r}), \\ \langle \rho | T^\Delta | \rho' \rangle &= \langle l | Y^{(k)} | l' \rangle \langle \frac{1}{2} | 1 | \frac{1}{2} \rangle \\ &= \sqrt{2} \langle l | Y^{(k)} | l' \rangle. \end{aligned}$$

The extra factor so introduced ($\sqrt{2}$ in the example) is canceled by a similar factor in the denominator in the Wigner-Eckart theorem. This minor irritation can therefore be avoided by agreeing that, when Latin indices are written explicitly, leaving out unit operators (e.g., T_q^k instead of T_γ^Δ or $T_{q,0}^{k,0}$), integrations in the omitted spaces are ignored.

4. Antisymmetric States for Nucleons in the Same Shell

Let us consider n equivalent particles or "particles in the same shell." We wish to construct completely anti-

⁶ It is worthwhile to complete our discussion of the direct-product notation by applying it to the calculation of matrix elements of tensor operators, in spite of the fact that we evaluate no such matrix elements in our study.

symmetric states

(III.18)

of specified β and x . Suppose that the corresponding problem for $n-1$ equivalent particles has been solved, that

is known. The functions

(III.19)

are antisymmetric in particles #1, 2, ..., $n-1$. They are not, in general, totally antisymmetric, nor do they have specified x . It is, however, clear that the antisymmetric functions (III.18) belong to a restricted subspace of the linear vector space spanned by the functions (III.19). We may therefore write

(III.20)

The expansion coefficients are called "coefficients of fractional parentage" or simply "cfp." The concept of fractional parentage was introduced by Goudsmid and Bacher (Go34) in atomic spectroscopy and was subsequently developed in a far more general form by Racah (Ra43, Ra49). We often adopt the abbreviated notation

$$\langle \rho^n : x\beta | \rho^{n-1} : y\gamma \rangle \equiv \langle \rho^n \beta | \rho^{n-1} \gamma \rangle. \quad (\text{III.21})$$

Orthonormality of functions of different x yields the sum rule

$$\sum_{\nu\gamma} \langle \rho^n : x\beta | \rho^{n-1} : y\gamma \rangle \langle \rho^n : x'\beta | \rho^{n-1} : y\gamma \rangle = \delta(xx'). \quad (\text{III.22})$$

Since β is a good quantum number on both sides of (III.20), there is no sum rule expressing the orthogonality of functions of different β . The abbreviation (III.21) thus must be used with this reservation in mind when dealing with sum rules.

If the cfp are known, (III.20) establishes an inductive chain, starting from $n=1$, which determines the functions of ρ^n for $n=1, 2, \dots, (2\rho+1)$. The

relative signs of all such functions are thereby completely specified; the only freedom left by the parentage expansion is that of a single undetermined sign, referring simultaneously to all functions of the ρ shell. For all practical purposes, this single free sign is irrelevant.

Conversely, the functions (III.18) for $n=1, 2, \dots, (2\rho+1)$ define, by (III.20), a set of cfp leaving no signs undetermined; however, it is usually both cumbersome and unnecessary to give a specification of shell-model wave functions more explicit than that implied by the appropriate parentage expansion.

Before proceeding, let us settle the matter of relative phases for functions with the same β and x . When we wish to refer to that unique and fully determined antisymmetric state of n equivalent particles, with a given β and x , which is defined by a particular set of cfp, we write

$$\begin{array}{c} \rho^n \\ \diagdown \\ 12 \dots n \\ \diagup \\ x\beta \end{array} = \Phi(123 \dots n) \quad (\text{III.23})$$

with the particle numbers in ascending order. The over-all sign which the cfp fail to specify is of no consequence here, since we are interested in the relative signs of functions arising from the same set of cfp.

By operating on (III.23) with any permutation $P \in S_n$, another antisymmetric state of n particles, with the same β and x , is generated. This new function is identical to (III.23) if P is an even permutation and differs in sign if P is odd.

What we have done is to attach a meaning, including a sign, to a function symbol wherein the particle numbers are written out explicitly, in any order.

For example, consider the symbol

$$\begin{array}{c} \rho^4 \\ \diagdown \\ 1432 \\ \diagup \\ x\beta \end{array}$$

Since $\{1432\} = P\{1234\}$, where $P = (42)$ is odd,

$$- \begin{array}{c} \rho^4 \\ \diagdown \\ 1432 \\ \diagup \\ x\beta \end{array} = \begin{array}{c} \rho^4 \\ \diagdown \\ 1234 \\ \diagup \\ x\beta \end{array} .$$

In a complete logical development of the theory of fractional parentage, we would now have to discuss two further topics.

(1) The precise meaning of the additional quantum numbers x in various representations. We have occasion to make some comments on this subject in Sec. III.5, although no systematic treatment is attempted.

(2) Techniques for calculating the cfp which contain all our knowledge of the wave functions. This important subject is bypassed. The cfp are regarded as already calculated and at our disposal.

These facets of the theory of fractional parentage are

treated in detail by Racah (Ra42, Ra43, Ra49, Ra51), by Jahn and van Wieringen (Ja50, Ja51) for $LSJT$ representations and by Flowers and Edmonds (Fl52, Ed52) for jj representations. These references include extensive tabulations of cfp, including the cases

$(l^n)LST$: $1p$ shell, all n (Ja51),

$(j^n)J$: $j=\frac{3}{2}, \frac{5}{2}, \frac{7}{2}$, all n (Ed 52),

$(j^n)JT$: $j=\frac{3}{2}$, all n ; $j=\frac{5}{2}, n \leq 4$; $j=\frac{7}{2}, n=3, 4$ with maximum T (Ed 52).

Concerning the cfp in Ja51 and the question of phases, see the discussion at the end of Sec. III.5.

There is no reason why some particle other than $\#n$ should not be separated in the parentage expansion (III.20). The conventional usage of selecting one particular particle—usually $\#n$ —in this connection has the advantage of eliminating ambiguities in sign. If we wish to separate some particle other than $\#n$ in a parentage expansion, we say so explicitly.

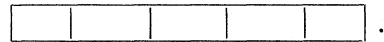
The concept of fractional parentage can be adapted without difficulty to the removal of more than one particle. Since the present study is confined to processes wherein a single nucleon is transferred, the extended theory is of no interest to us.

5. Holes, Particles, and Phases

A shell is characterized by the quantum numbers ρ of its constituent nucleons. In this section, a detailed formulation is given of the hole-particle correspondence for states of a given nuclear shell. For such purposes, the most convenient representation is one in which the magnetic quantum numbers m_ρ of each nucleon are specified. We use a direct-product notation, as described in Sec. III.3. Our general results hold for both LS and jj representations, with or without the isotopic-spin formalism.

The general notions of the hole-particle correspondence were discussed by Condon and Shortley (Co35), while the first formal development was given by Racah (Ra42). We start from a tentative definition (III.24) of “complementary states” appropriate only in an m_ρ representation. Proceeding to a more general representation by a suitable unitary transformation, we are led quite naturally to the relation in terms of which Racah formulated the hole-particle correspondence (Ra42). This relation [our (III.35)] is thereafter adopted as a definition of “complementary states.”

There are $[\rho]$ available states for each nucleon. It is helpful to think of each such state as a cell or slot, which, because of the exclusion principle, can contain no more than one nucleon:



$$[\rho] = 5$$

States of ρ^n can then be constructed by distributing the n nucleons among $N = [\rho]$ available cells. Let us refer

to each such choice of n cells as a “distribution for ρ^n .” A distribution determines one and only one antisymmetric state of n particles, a unique linear combination of the $n!$ distinct product functions obtained by permuting the particle numbers associated with the occupied cells. Thus, every antisymmetric state of ρ^n can be labeled, in the m_ρ representation, by a distribution λ and possesses a specified value of the total projection quantum number $\beta = \sum m_\rho$. By counting the number of distributions of n particles among N cells, it is seen that the number of allowed antisymmetric states of ρ^n is given by the binomial coefficient

$$\binom{N}{n}.$$

Since the number of nucleons cannot exceed the number of available states, it is clear that the ρ shell is “complete” or “closed” when it contains $N = [\rho]$ particles. There is only one distribution for ρ^N and, accordingly, only one allowed antisymmetric state. This closed-shell state, which is unique to within a sign, has all angular-momentum quantum numbers 0 and is denoted by $\Psi(S^*)$.

The $N-n$ cells left unoccupied in any distribution λ of ρ^n determine a distribution λ^c of ρ^{N-n} . Thus, to every antisymmetric state $\Phi_\lambda^B(n)$, there corresponds one and only one antisymmetric state $\Phi_{\lambda^c-B}(N-n)$, a one-one correspondence which is reflected in the relation

$$\binom{N}{n} = \binom{N}{N-n}$$

between binomial coefficients. The two states

$$\Phi_\lambda^B(n) \text{ of } \rho^n, \quad \Phi_{\lambda^c-B}(N-n) \text{ of } \rho^{N-n} \quad (\text{III.24})$$

are said to be “complementary.” It is to this correspondence that we allude when we refer to the states of ρ^{N-n} as “ n -hole” states. The word hole can thus be interpreted in a rather literal fashion, a feature which is all but lost in passing to a representation other than the m_ρ representation.

The relation of complementarity is clearly symmetric in the sense that (λ, B) is the complement of its own complement $(\lambda^c, -B)$.

The allowed antisymmetric states of ρ^n span a certain linear vector space \mathfrak{L} , \mathfrak{R} being the corresponding space for ρ^{N-n} . The unique closed-shell function $\Psi(S^*)$ can obviously be expressed as a linear superposition of products

$$\Phi_\lambda^B(n)\Phi_{\lambda^c-B}(N-n) \quad (\text{III.25})$$

of vectors from \mathfrak{L} and \mathfrak{R} . Only those products in which $\lambda'^c = \lambda^c$ can occur in this expansion, since, otherwise, terms would appear with more than one nucleon to a slot. We can therefore write

$$\Psi(S^*) = \sum_{\lambda} \kappa_{\lambda} \Phi_\lambda^B(n)\Phi_{\lambda^c-B}(N-n), \quad (\text{III.26})$$

and each term (λ, λ^c) in (III.26) corresponds to one pair of complementary distributions.

In order to evaluate the coefficients κ_{λ} , it is necessary to study the behavior of the terms in (III.26) under permutations of the particle labels. This is done most naturally in terms of the “order-preserving permutations” introduced in Sec. III.6. We simply state the result we require, referring the reader for proof to Appendix 3 of Ma59. The desired expression for the closed-shell wave function is

$$\Psi(S^*) = \binom{N}{n}^{-\frac{1}{2}} \sum_B (-)^{B-B_m} \sum_{\{\lambda : B_{\lambda}=B\}} \Phi_{\lambda^c-B}(N-n), \quad (\text{III.27})$$

where the symbol $\{\lambda : B_{\lambda}=B\}$ stands for “the set of all distributions λ such that $B_{\lambda}=B$,” and $B_m=\beta$, the largest possible value of B .

Equation (III.27) exhibits $\Psi(S^*)$ as an invariant product of two vectors, one from \mathfrak{L} and one from \mathfrak{R} , and is invariant in the sense that, since the closed-shell function is unique, it must retain the form (III.27) under suitably related changes of basis in \mathfrak{L} and \mathfrak{R} . Functions arising from (III.24) under these related transformations are then defined to be complementary in the new representation. The “suitable relation” which must hold between the changes of basis in \mathfrak{L} and \mathfrak{R} , such that the expression for $\Psi(S^*)$ retains its form, is clearly⁷ that of contragredience. Indeed, this is precisely the manner in which the transformation contragredient to a given transformation is defined.

Let us, then, perform a unitary change of basis

$$\begin{array}{c} \mathfrak{L} \\ \text{12...n} \\ \times \beta \end{array} = \sum_{\{\lambda : B_{\lambda}=B\}} C_{x\beta:\lambda} \Phi_{\lambda^c-B}(N-n) \quad (\text{III.28})$$

in \mathfrak{L} , introducing a new representation specifying the total angular momenta β whose projections are B . x symbolizes a set of quantum numbers chosen in any suitable fashion so as to complete the specification of the state. Since C is unitary,

$$\sum_{\{\lambda : B_{\lambda}=B\}} C_{x\beta:\lambda}^* C_{\lambda:x'\beta'} = \delta(xx')\delta(\beta\beta'), \quad (\text{III.29})$$

where, as usual, $C^\dagger = (C^*)^T$.

⁷ Let $u_i \in U$, $v_i \in V$ be vectors in two different spaces. Defining the “inner product” (We31, p. 12) $u_i v_i$ of these vectors, we ask how changes of basis

$$u'_i = A_{ik} u_k, \quad v'_i = B_{ik} v_k \quad (\text{i})$$

in U and V , respectively, must be related in order that the inner product remains invariant. In fact, $u'_i v'_i = A_{ik} B_{il} u_k v_l = u_i v_i$ if and only if

$$A_{ik} B_{il} = \delta_{kl}. \quad (\text{ii})$$

In matrix form,

$$A^T B = I \quad \text{or} \quad B = (A^T)^{-1}. \quad (\text{iii})$$

This matrix (or transformation) B , constructed *explicitly* so that the inner product is invariant under a change of basis in U and a suitably related change of basis in V , is referred to as the matrix (or transformation) *contragredient* to A .

If A is unitary, as is the case in quantum-mechanical applications, we have, by definition $(A^T)^* = A^{-1}$, and the contragredient matrix (or transformation) (iii) becomes

$$B = (A^T)^{-1} = A^*. \quad (\text{iv})$$

The contragredient change of basis must now be carried out in the linear vector space \mathfrak{R} . We therefore define the state of ρ^{N-n} complementary to (III.28) to be

$$\text{Diagram: } \begin{array}{c} \text{R} \\ \text{n+l...N} \\ \text{x}^c \beta - \beta \end{array} = \sum_{\{\lambda^c: B_{\lambda^c} = -B\}} C_{x\beta; \lambda}^* \Phi_{\lambda^c - B}(N-n). \quad (\text{III.30})$$

It might be argued that (III.24) already implies a definition of complementary states in a general representation, simply by taking the same linear combinations of states of ρ^n and ρ^{N-n} which are complementary in the m_p representation. We would then have defined the same term in two different ways, not obviously equivalent. Two attitudes are possible.

(1) We may regard (III.24) as applying specifically and exclusively to m_p representations and refuse to admit the word "complementary" has any meaning in more general representations. We are then at liberty to assign such a meaning through (III.28) and (III.30).

(2) We can, alternatively, treat (III.24) as a tentative definition of complementary states to be superseded by (III.30).

It is not important which of these attitudes we adopt. Our main concern is with showing that the intuitive picture of the hole-particle correspondence in the m_p representation leads to Racah's relation (III.35). Our subsequent work uses (III.35) exclusively.

Equations (III.28) and (III.30) can now be inverted and substituted in (III.27) to obtain

$$\begin{aligned} \Psi(S^*) &= \binom{N}{n}^{-\frac{1}{2}} \sum_B (-1)^B \sum_{\substack{x\beta \\ x'\beta'}} C_{x\beta; \lambda}^* (C^*)_{x'\beta'; \lambda}^* \text{Diagram: } \begin{array}{c} \mathcal{L} \\ |2\dots n| \\ x\beta B \end{array} \text{ and } \begin{array}{c} \mathfrak{R} \\ n+l\dots N \\ x' \beta' - B \end{array} \\ &= \binom{N}{n}^{-\frac{1}{2}} \sum_B (-1)^B \sum_{\substack{x\beta \\ x'\beta'}} (-1)^{\beta} \delta(x\beta : x'\beta') \text{Diagram: } \begin{array}{c} \mathcal{L} \\ |2\dots n| \\ x\beta B \end{array} \text{ and } \begin{array}{c} \mathfrak{R} \\ n+l\dots N \\ x' \beta' - B \end{array} \end{aligned} \quad (\text{III.31})$$

$$= \binom{N}{n}^{-\frac{1}{2}} \sum_{x\beta B} (-1)^{B-\beta} \text{Diagram: } \begin{array}{c} \mathcal{L} \\ |2\dots n| \\ x\beta B \end{array} \text{ and } \begin{array}{c} \mathfrak{R} \\ n+l\dots N \\ x^c \beta - B \end{array}, \quad (\text{III.32})$$

noting that $(C^*)^\dagger = C^T$ and using (III.29) to obtain (III.31).

We introduce, finally, a coupled representation

$$\begin{aligned} \Psi(S^*) &= \binom{N}{n}^{-\frac{1}{2}} \sum_{x\beta B} (-1)^{B-\beta} C[\beta\beta 0; B, -B] \text{Diagram: } \begin{array}{c} \mathcal{L}' \\ |2\dots n| \\ x\beta B \end{array} \text{ and } \begin{array}{c} \mathfrak{R} \\ n+l\dots N \\ x^c \beta - B \end{array} \\ &= \binom{N}{n}^{-\frac{1}{2}} \sum_{x\beta} [\beta]^{-\frac{1}{2}} \sum_B \text{Diagram: } \begin{array}{c} \mathcal{L} \\ |2\dots n| \\ x\beta \end{array} \text{ and } \begin{array}{c} \mathfrak{R} \\ n+l\dots N \\ x^c \beta \end{array} \quad (\text{III.33}) \end{aligned}$$

$$= \binom{N}{n}^{-\frac{1}{2}} \sum_{x\beta} [\beta]^{\frac{1}{2}} \text{Diagram: } \begin{array}{c} \mathcal{L} \\ |2\dots n| \\ x\beta \end{array} \text{ and } \begin{array}{c} \mathfrak{R} \\ n+l\dots N \\ x^c \beta \end{array}. \quad (\text{III.34})$$

Equation (III.33) is obtained from

$$C[\beta\beta 0; B, -B] = (-1)^{B-B} [\beta]^{-\frac{1}{2}},$$

while (III.34) emerges on noting that the summand in (III.33) is independent of B , \sum_B giving the number $[\beta]$ of distinct values of B for a given β . In abbreviated form,

$$\Psi(S^*) = \binom{N}{n}^{-\frac{1}{2}} \sum_{\alpha} [\alpha]^{\frac{1}{2}} \text{Diagram: } \begin{array}{c} \mathcal{L} \\ |2\dots n| \\ x\beta \end{array} \text{ and } \begin{array}{c} \mathfrak{R} \\ n+l\dots N \\ x^c \beta \end{array}. \quad (\text{III.35})$$

Equations (III.34) and (III.35) are identical to the expression in terms of which Racah (Ra42) originally formulated the hole-particle correspondence.

In (III.28), a new representation is introduced in the linear vector space \mathcal{L} spanned by the allowed states of ρ^n by means of a transformation which is unitary and specifies the angular-momentum quantum numbers β , but which is otherwise arbitrary. Once a choice of representation in \mathcal{L} has been made, however, (III.34) or (III.35) completely fixes the contragredient representation in the vector space \mathfrak{R} spanned by the allowed states of ρ^{N-n} . In other words, although the relation

between representations in \mathfrak{L} and \mathfrak{R} is uniquely determined, considerable freedom remains in selecting either one.

The customary way of constructing the antisymmetric states of the ρ shell involves the use of a parentage chain and has been described in Sec. III.4. In this section we have been proceeding quite differently. The functions of ρ^n have been formed explicitly by writing them in an m_ρ representation and then applying a specific unitary transformation of the form (III.28). It is obvious that the hole-particle theorem just derived does not depend on how we choose to specify the states of ρ^n . If we do so in terms of a given set of cfp, then (III.34) or (III.35) specifies the contragredient representation in ρ^{N-n} , just as before. As n runs through all values appropriate to the ρ shell, so does $N-n$, and (III.34) or (III.35) implicitly defines a "contragredient" set of cfp in terms of the original set. We shortly express this relation between cfp quite explicitly. The single sign, pertaining to all functions in the ρ shell, left free by the original set of cfp, can now be regarded as that of the closed-shell function $\Psi(S^*)$.

Let us therefore suppose that we possess a standard set of cfp covering the entire ρ shell. A complete set of functions, to which we refer as the "normal" or \mathfrak{L} set, is thereby defined, to without a single unimportant sign, for all values of n appropriate to the given shell. A general function of the \mathfrak{L} set may be written

$$\Psi_{\alpha}^{\mathfrak{L}}(n) \equiv \begin{array}{c} \text{L} \\ \text{I} 2 \dots n \\ \alpha \end{array} \equiv \begin{array}{c} \text{L} \\ \text{I} 2 \dots n \\ \alpha^c \\ \times \beta \end{array}. \quad (\text{III.36})$$

Equation (III.34) or (III.35) defines a second complete set of functions, the "contragredient" or \mathfrak{R} set, in terms of the \mathfrak{L} set. A general function of the contra-

gradient set is

$$\Psi_{\alpha}^{\mathfrak{R}}(N-n) \equiv \begin{array}{c} \text{R} \\ \text{n+1} \dots N \\ \alpha^c \end{array} \equiv \begin{array}{c} \text{R} \\ \text{n+1} \dots N \\ \times^c \beta \end{array}. \quad (\text{III.37})$$

$\Psi_{\alpha}^{\mathfrak{R}}(N-n)$ is the complement of $\Psi_{\alpha}^{\mathfrak{L}}(n)$.

Let us now extract from (III.35) an explicit expression for each \mathfrak{R} cfp in terms of the cfp in \mathfrak{L} connecting the complementary states. The desired expression is independent of the sign of $\Psi(S^*)$. We start from (III.37) by separating particle # $n+1$ from the function

$$\begin{array}{c} \text{R} \\ \text{n+1} \dots N \\ \alpha^c \end{array}.$$

To do so, let us observe that

$$\{n+2, n+3, \dots, N-1, N, n+1\} = P\{n+1, n+2, \dots, N-1, N\},$$

where P is a permutation operator which passes $n+1$ over the other $N-n-1$ numbers. Thus, P is a product of $N-n-1$ interchanges and its parity is

$$(-1)^{N-n-1} = (-1)^{n+1}.$$

Thus, according to the prescription described in Sec. III.4, following (III.23),

$$\begin{array}{c} \text{R} \\ \text{n+1} \dots N \\ \alpha^c \end{array} = (-1)^{n+1} \begin{array}{c} \text{R} \\ \text{n+2, N, n+1} \\ \alpha^c \end{array}. \quad (\text{III.38})$$

We therefore have, from (III.35),

$$\Psi(S^*) = \binom{N}{n}^{-\frac{1}{2}} \sum_{\alpha} [\alpha]^{\frac{1}{2}} \begin{array}{c} \text{L} \quad \text{R} \\ \text{I} 2 \dots n \quad \text{n+1} \dots N \\ \alpha \quad \alpha^c \end{array} \quad O$$

$$= \binom{N}{n}^{-\frac{1}{2}} \sum_{\alpha\epsilon} [\alpha]^{\frac{1}{2}} \langle \rho^{N-n} \alpha^c | \rho^{N-n-1} \epsilon^c \rangle^{\mathfrak{R}} (-1)^{n+1}$$

$$\begin{array}{c} \text{L} \quad \text{R} \\ \text{I} 2 \dots n \quad \text{n+2} \dots N \\ \alpha \quad \alpha^c \end{array} \quad O \quad \rho(n+1)$$

$$= \binom{N}{n}^{-\frac{1}{2}} \sum_{\alpha\epsilon\epsilon'} [\alpha]^{\frac{1}{2}} \langle \rho^{N-n} \alpha^c | \rho^{N-n-1} \epsilon^c \rangle^{\mathfrak{R}} U(\alpha\rho 0\epsilon : \epsilon'\alpha) (-1)^{\rho + \epsilon - \alpha + n + 1}$$

$$\begin{array}{c} \rho(n+1) \\ \text{L} \quad \alpha' \quad \epsilon' \quad \epsilon^c \quad \text{R} \\ \text{I} 2 \dots n \quad \alpha \quad \epsilon \quad \epsilon^c \quad \text{n+2} \dots N \\ O \end{array},$$

where the first step utilizes (III.20) and (III.38), and the last is a simple application of the recoupling rules (III.5) and (III.7). But the Racah coefficient is given by $U(\alpha\rho\epsilon: \epsilon'\alpha) = \delta(\epsilon\epsilon')$, whence

$$\Psi(S^*) = \binom{N}{n}^{-\frac{1}{2}} \sum_{\alpha\epsilon} [\alpha]^{\frac{1}{2}} \langle \rho^{N-n}\alpha^c | \rho^{N-n+1}\epsilon^c \rangle (-1)^{\rho+\epsilon-\alpha+n+1} \quad (III.39)$$

Observe that, since the pairs $(\alpha\epsilon)$ and $(\alpha^c\epsilon^c)$ are in one-one correspondence, we can omit the superscript c in summations over α^c , ϵ^c .

Let us now replace n in (III.35) by $n+1$ and apply (III.20). We obtain

$$\begin{aligned} \Psi(S^*) &= \binom{N}{n+1}^{-\frac{1}{2}} \sum_{\epsilon} [\epsilon]^{\frac{1}{2}} \langle \rho^{n+1}\epsilon | \rho^n\alpha \rangle^R \\ &= \binom{N}{n+1}^{-\frac{1}{2}} \sum_{\alpha\epsilon} [\epsilon]^{\frac{1}{2}} \langle \rho^{n+1}\epsilon | \rho^n\alpha \rangle^L \quad (III.40) \end{aligned}$$

It is clear that (III.39) and (III.40) have the same form. Equating coefficients, we obtain the desired expression

$$\begin{aligned} &\frac{\langle \rho^{N-n}\alpha^c | \rho^{N-n-1}\epsilon^c \rangle^R}{\langle \rho^{n+1}\epsilon | \rho^n\alpha \rangle^L} \\ &= (-1)^{n+1+\alpha-\epsilon-\rho} \left[\frac{(n+1)(2\epsilon+1)}{(N-n)(2\alpha+1)} \right]^{\frac{1}{2}}. \quad (III.41) \end{aligned}$$

A considerable freedom of choice has been left in defining the functions of the normal or \mathcal{L} set, corresponding to the many possible ways of defining the nonangular-momentum symbol x in $\alpha = (x\beta)$. We might try to turn this freedom to advantage by demanding that the entire set (for all n) of basic functions $\Psi_{\alpha}^R(n)$ be characterized by the same array of quantum numbers α as the entire set of functions $\Psi_{\alpha}^L(n)$.

Let us state this requirement in a different way. Each state of ρ^n in the \mathcal{L} representation is characterized by a set of quantum numbers $\alpha \equiv (x\beta)$. The complementary state of ρ^{N-n} in the \mathcal{R} representation then has the quantum numbers $\alpha^c \equiv (x^c\beta)$. We demand that x be so defined that $(x^c\beta)$ also labels a state of ρ^{N-n} in the \mathcal{L} representation. If this can be done for all states $(x\beta)$ in the ρ shell, then the basic functions in \mathcal{L} and \mathcal{R} can differ only in sign. It is not obvious that such a choice of representation is possible.

In practice, the symbol x nearly always refers to irreducible representations of the unimodular unitary

group or of one of its orthogonal and symplectic subgroups (Ra49, Ja51, Ra51, Fl52).⁸ The desired relation between bases in \mathcal{L} and \mathcal{R} is then fulfilled as a direct consequence of the way in which complementary representations are defined. A full discussion of this point would require a description of techniques (Li50) for the reduction of outer products of representations into irreducible components, and is therefore omitted.

Representations which do not satisfy this extra requirement are very inconvenient and are therefore seldom used. Each list of cfp employed in this study defines a normal set \mathcal{L} and, by (III.35), a contragredient set \mathcal{R} whose basic functions are labeled by the same sets of quantum numbers.

All allowed states of the ρ shell now fall into two classes according to whether

$$\begin{aligned} (A) \quad \Psi_{\alpha}^L(n) &= \Psi_{\alpha}^R(n) \\ \text{or} \quad (B) \quad \Psi_{\alpha}^L(n) &= -\Psi_{\alpha}^R(n). \quad (III.42) \end{aligned}$$

This classification is uniquely defined by (III.35) (for suitably specified x), independently of the sign of $\Psi(S^*)$. Reversing the sign of $\Psi(S^*)$ interchanges the two classes (A) and (B) but leaves the division into classes invariant.

It would be quite practical to express the \mathcal{R} cfp in terms of the \mathcal{L} cfp simply by listing explicitly the

⁸The space symmetry quantum number is included in this statement by virtue of the intimate connection (We28, Bo55) between irreducible representations of the unitary and symmetric groups.

assignment of each state in the shell to the appropriate class (A) or (B). This, we prefer not to do; Eq. (III.41) turns out to be a more useful link between \mathcal{L} and \mathcal{R} . In fact, we are less interested in possessing two alternative representations than in making the cfp of one standard set, for $n \leq \frac{1}{2}N$, suffice in all our considerations throughout the entire shell. We now examine this possibility in more detail.

In Sec. III.2 it was remarked that the three central problems in performing shell-model calculations are the construction of antisymmetric functions and the evaluation of the matrix elements of symmetric one- and two-body operators. Having discussed the hole-particle correspondence in the light of the first of these problems, let us, for completeness, turn our attention briefly to the other two.

$$\left\langle \left(\begin{array}{c} \rho^n \\ \alpha \end{array} \right) \middle| T_{\mathcal{L}}^{\Delta} \middle| \left(\begin{array}{c} \rho^n \\ \alpha' \end{array} \right) \right\rangle = \left[(-1)^{\Delta+1} + \frac{N}{N-n} \delta(\Delta 0) \right] \left\langle \left(\begin{array}{c} \rho^{N-n} \\ \alpha_c \end{array} \right) \middle| T_{\mathcal{R}}^{\Delta} \middle| \left(\begin{array}{c} \rho^{N-n} \\ \alpha'_c \end{array} \right) \right\rangle, \quad (\text{III.44})$$

a result first obtained by Racah (Ra42).

Equation (III.41) leads to a similar relation for the symmetric two-body operator

$$\left\langle \left(\begin{array}{c} \rho^n \\ \alpha \end{array} \right) \middle| G_{\mathcal{L}} \middle| \left(\begin{array}{c} \rho^n \\ \alpha' \end{array} \right) \right\rangle = \delta(\alpha\alpha') \left[\frac{2n-N}{N} \right] \sum_{\gamma} [\gamma] g_{\gamma}^{(2)} + \left\langle \left(\begin{array}{c} \rho^{N-n} \\ \alpha_c \end{array} \right) \middle| G_{\mathcal{R}} \middle| \left(\begin{array}{c} \rho^{N-n} \\ \alpha'_c \end{array} \right) \right\rangle \quad (\text{III.45})$$

where

$$G[\mathcal{L}] = \sum_{i < j=1}^n G_{ij}, \quad G[\mathcal{R}] = \sum_{i < j=n+1}^N G_{ij}, \quad g_{\gamma}^{(2)} = \left\langle \left(\begin{array}{c} \rho^2 \\ \gamma \end{array} \right) \middle| G_{12} \middle| \left(\begin{array}{c} \rho^2 \\ \gamma \end{array} \right) \right\rangle,$$

and the summation extends over all the allowed states of ρ^2 . Notice that $G[\mathcal{L}]$ is a scalar operator so that all matrix elements nondiagonal in the angular momentum part of α vanish. Furthermore, the diagonal elements are entirely independent of α and are, for many purposes, of no consequence.

We conclude this section with a summary of the procedure to be followed in shell-model calculations within the ρ shell. The first step is to define a complete set of antisymmetric states in terms of a suitable standard set of cfp. This we define in the following fashion:

(1) $n \leq \frac{1}{2}N$. In the first half of the ρ shell, the standard cfp are taken to be those of some suitably chosen normal or \mathcal{L} set.

(2) $n > \frac{1}{2}N$. In the second half of the ρ shell, the standard cfp are those of the corresponding contragredient or \mathcal{R} set, given explicitly in terms of the complementary standard cfp for $n \leq \frac{1}{2}N$ by (III.41).

Consider, then, a symmetric one-body operator

$$T^{\Delta} = \sum_{i=1}^N T^{\Delta}(i).$$

If we define

$$T^{\Delta}[\mathcal{L}] = \sum_{i=1}^n T^{\Delta}(i), \quad T^{\Delta}[\mathcal{R}] = \sum_{i=n+1}^N T^{\Delta}(i),$$

then

$$T^{\Delta} = T^{\Delta}[\mathcal{L}] + T^{\Delta}[\mathcal{R}], \quad (\text{III.43})$$

where $T^{\Delta}(i)$ is a multiple tensor of rank Δ in the (product) space of the i th nucleon, and the bracketed \mathcal{L} and \mathcal{R} refer to the vector spaces and not to the particular bases selected therein. Starting directly from (III.35), it is easy to derive a relation⁹ between the reduced matrix elements of $T^{\Delta}[\mathcal{L}]$ evaluated in the \mathcal{L} set and those of $T^{\Delta}[\mathcal{R}]$ in \mathcal{R} :

$$\left\langle \left(\begin{array}{c} \rho^n \\ \alpha \end{array} \right) \middle| T_{\mathcal{L}}^{\Delta} \middle| \left(\begin{array}{c} \rho^n \\ \alpha' \end{array} \right) \right\rangle = \left[(-1)^{\Delta+1} + \frac{N}{N-n} \delta(\Delta 0) \right] \left\langle \left(\begin{array}{c} \rho^{N-n} \\ \alpha_c \end{array} \right) \middle| T_{\mathcal{R}}^{\Delta} \middle| \left(\begin{array}{c} \rho^{N-n} \\ \alpha'_c \end{array} \right) \right\rangle, \quad (\text{III.44})$$

In the $1p$ shell, the standard cfp for $n \leq 6$ are conventionally taken to be those given by Jahn and van Wieringen (Ja51), with the amendments enumerated by Elliott, Hope, and Jahn (E154). These amendments must be made both vertically and horizontally in the original table of cfp. For various configurations j^n , we use the cfp tabulated by Edmonds and Flowers (Ed52).

Having thus specified a suitable basic set of antisymmetric states of the ρ shell, we proceed in the usual way to construct and diagonalize the matrix of the Hamiltonian (III.2) and to use the eigenfunctions so obtained to calculate the matrix elements of operators of physical interest. All the necessary calculations in the second half of the shell can be reduced to the complementary

⁹ Strictly, (III.44) holds only for Hermitian tensor operators, those whose components satisfy $T_q^{ik} = (-1)^q (T_q^{ik})^*$. For non-Hermitian tensors, the right-hand side of (III.44) should be modified by $T^{\Delta}[\mathcal{R}] \rightarrow T^{\dagger\Delta}[\mathcal{R}]$ and $\langle \cdot | \cdot \rangle \rightarrow \langle \cdot | \cdot \rangle^*$. We do not have occasion to deal with non-Hermitian tensors, so that (III.44) is of adequate generality.

ones in the first half of the shell with the aid of (III.41), (III.43), and (III.44). It is therefore clear that standard cfp need be tabulated only for $n \leq \frac{1}{2}N$.

Some specific examples of the techniques and theorems of this section are given in Sec. III.9. Possible ways of checking calculations against phase errors are discussed. In particular, we demonstrate the value of $LS \rightarrow jj$ transformations in locating errors in calculations performed in an LS representation.

6. Antisymmetric States for Nucleons in Different Shells

Let us now consider a group of particles not all of which belong to the same shell. In principle, we could construct antisymmetric states by adapting the percentage formalism of Sec. III.4. We use, instead, a hybrid procedure wherein fractional parentage is used within the equivalent groups, while antisymmetry between these groups is handled directly.

We start with the set of functions

$$(III.46)$$

which are mutually orthogonal and normalized. It is important that ρ and ρ' define orthogonal single-particle states. This would not be the case, for example, if ρ referred to neutrons and ρ' to protons, and a different radial dependence were assumed for neutrons and protons.

The antisymmetrizing operator for the symmetric group S_n is

$$A_n = \left(\frac{1}{n!} \right)^{\frac{1}{2}} \sum_{r \in S_n} (-)^r P_r. \quad (III.47)$$

We can construct an antisymmetric function from (III.46) directly by applying the antisymmetrizer A_{n+m} for S_{n+m} . But of the $(n+m)!$ functions which are generated from (III.46) by permutations of S_{n+m} , all those sets wherein the same n particles are in the ρ shell and therefore the same m particles are in ρ' , contain

$$= \left[\frac{n!m!}{(n+m)!} \right]^{\frac{1}{2}} \sum_{r \in S_{n+m}} (-)^r P_r. \quad (III.51)$$

The extension of this technique when there are more than two groups of equivalent particles can be carried out immediately.

In practical applications—those which involve the setting up and diagonalization of energy matrices—the

functions identical to within a sign. This fact, which stems from the antisymmetry of the separate equivalent groups, suggests that a simplified antisymmetrizer can be found in this case.

Let us, therefore, define an order-preserving permutation as one which, when operating on $\Phi_1(12 \cdots n) \times \Phi_2(n+1 \cdots n+m)$, leaves the integers inside Φ_1 and Φ_2 separately in ascending order. Thus, if all $(n+m)!$ permutations of S_{n+m} be divided into sets such that two permutations belong to the same set if and only if the functions arising through them from (III.46) are the same, then it is obvious that each set contains one and only one order-preserving permutation. S_{n+m} contains

$$\binom{n+m}{n}$$

order-preserving permutations with respect to the partition $\{12 \cdots n : n+1 \cdots n+m\}$.

Let us introduce the operator

$$\alpha_{n+m} = \left[\frac{n!m!}{(n+m)!} \right]^{\frac{1}{2}} \sum'_{r \in S_{n+m}} (-)^r P_r, \quad (III.48)$$

where \sum' indicates a summation over order-preserving permutations in S_{n+m} . The composite permutation operator

$$\alpha_{n+m} A_n A_m \quad (III.49)$$

consists of a linear combination of permutations of S_{n+m} . Manifestly, each term is distinct and there are

$$\binom{n+m}{n} n!m! = (n+m)!$$

terms. Since the parity $(-)^r$ looks after itself, the terms in the linear combination (III.49) are identical with those in A_{n+m} . Finally, the normalization factors are the same, yielding the operator identity

$$\alpha_{n+m} A_n A_m = A_{n+m}. \quad (III.50)$$

However, since the wave functions for the groups ρ^n , ρ'^m in (III.46) are separately antisymmetric, A_n and A_m reduce, effectively, to unit operators. Thus, α_{n+m} is itself a simplified antisymmetrizing operator for the function (III.46), yielding for the desired normalized antisymmetric function,

large dimensionalities encountered render (III.51) somewhat academic, with two important exceptions:

- (1) when one of the shells contains a very few (≤ 3) nucleons or holes;
- (2) when $n+m$ itself is small (≤ 3 , or 4 at most).

In the first case, (III.51) is both usable and convenient. In the second case, (III.51) is also quite practical, but it may be preferable to use an extension of the percentage techniques of Sec. III.4 [see, for example, the work of Elliott and Flowers (El55a) on $A=18$ and $A=19$].

We also see, in Sec. III.7, that (III.51) and its generalizations can readily be used to set up general expressions for relative reduced widths.

$$\mathcal{S}(z) = \left\langle \begin{array}{c} C \\ \nearrow J \\ \downarrow T \\ \end{array} \middle| \begin{array}{c} t^n \\ \nearrow T \\ \downarrow J \\ \end{array} \right\rangle \quad (III.52)$$

$t(n)$ and $\mathcal{S}(n)$ refer to the transferred nucleon, c^{10} and c_0 symbolize the precise representation used in constructing wave functions, and z is the channel spin. n is the number of antisymmetrically coupled particles in the heavier nucleus identical to the transferred nucleon.

In this and ensuing sections we solve the problem of evaluating \mathcal{S} with a variety of assumptions concerning the shell-model wave functions. Simple explicit expressions are given. It is important to bear in mind that the simplicity involved refers to the calculation of relative reduced widths from wave functions which are already known. Often, the more difficult problem is that of calculating reasonable wave functions. There are therefore many transitions for which we cannot obtain reliable relative reduced widths, in spite of the existence of very general expressions for \mathcal{S} .

The task of constructing shell-model wave functions, particularly for nuclei with $A > 30$, is frequently made easier by treating neutrons and protons on a separate

7. Shell-Model Expressions for \mathcal{S}

It is recalled that the relative reduced width, or spectroscopic factor \mathcal{S} , was defined in Sec. II, Eq. (II.15), as

$$\mathcal{S}(l) = n \sum_z |\mathcal{S}(z)|^2 \quad (III.52)$$

with

$$\left\langle \begin{array}{c} C_0 \\ \nearrow J_0 \\ \downarrow Z \\ \end{array} \middle| \begin{array}{c} t^{n-1} \\ \nearrow T_0 \\ \downarrow T \\ \end{array} \right\rangle \quad (III.53)$$

footing. The definitions (III.52) and (III.53) can then still be used, with these qualifications:

(1) The isotopic-spin coupling factor (C)² in (II.19) must be handled in the fashion described in Appendix 1.

(2) The diagram in (III.53) or (III.54) must be generalized [see (III.78)].

(3) Due regard must be paid to the fact that n , in (III.52), signifies the number of antisymmetrically coupled particles *identical to the transferred nucleon*. If we are using the isotopic-spin formalism, n is the total number of active nucleons in [$A+1$]. Treating neutrons and protons on a separate footing and considering, for example, a (d,p) reaction, n is the number of active neutrons in [$A+1$].

Another convenient representation is that in which $j(n)$ rather than z is specified. $\mathcal{S}(z)$ is then replaced by

$$\mathcal{S}(j) = \left\langle \begin{array}{c} C \\ \nearrow J \\ \downarrow T \\ \end{array} \middle| \begin{array}{c} t^n \\ \nearrow T \\ \downarrow J \\ \end{array} \right\rangle \quad (III.54)$$

The necessary change of representation is achieved by

$$\left\langle \begin{array}{c} C_0 \\ \nearrow J_0 \\ \downarrow Z \\ \end{array} \right| \mathcal{S}(n) = \sum_j (-1)^{J+\frac{1}{2}-j-z} U(l\frac{1}{2}J_0J : zj) \left\langle \begin{array}{c} C_0 \\ \nearrow J_0 \\ \downarrow j(n) \\ \end{array} \right| \mathcal{S}(n). \quad (III.55)$$

Substituting from (III.55) in (III.52) and (III.53), we have

$$\begin{aligned} \mathcal{S}(l) &= n \sum_z \mathcal{S}(z)^* \mathcal{S}(z) \\ &= n \sum_{zj} (-1)^{j-i'} U(l\frac{1}{2}J_0J : zj) \\ &\quad \times U(l\frac{1}{2}J_0J : j'z) \mathcal{S}^*(j) \mathcal{S}(j') \\ &= n \sum_{jj'} (-1)^{j-i'} \delta(jj') \mathcal{S}^*(j) \mathcal{S}(j'), \end{aligned}$$

¹⁰ This meaning of c should not be confused with its significance in connection with complementary states.

making use of the unitarity of the transformation induced by normalized Racah coefficients. Performing the summation over j yields

$$\mathcal{S}(l) = n \sum_j |\mathcal{S}(j)|^2, \quad (III.56)$$

with no interference between different values of j . We often rewrite (III.56) in the form

$$\mathcal{S}(l) = \sum_i \mathcal{S}(lj) \quad (III.57)$$

or some modification thereof.

General expressions for \mathcal{S} are now derived which apply to the antisymmetric states of any pure configuration. We use the j rather than the z representation. Some special cases of interest are mentioned explicitly. It is then demonstrated that the separate treatment of neutrons and protons introduces no new complication, and a very simple prescription is given for dealing with mixed configurations. Throughout, the direct-product notation of Sec. III.3 is used. Although the same might be achieved by means of an appropriate formal modification [see Sec. III.3, Eqs. (III.14) and (III.15)], we prefer to consider separately the case of LSJ representations.

A case which is sufficiently general to embrace most situations of practical interest may be symbolized by

$$\left\{ \begin{array}{c} \text{Initial State: } \rho_1^{n_1} \rho_2^{n_2} \rho_3^{n_3} \\ \xrightarrow{\Gamma} \text{Final State: } \rho_1^{n_1} \rho_2^{n_2} \rho_3'^{n_3'} \rho_3'^{n_3'} \end{array} \right\}, \quad (\text{III.58})$$

where $\{\times\}_\Gamma$ indicates vector coupling to a resultant Γ , and, as explained in Sec. III.3, ρ stands for either of the sets Nlj or $Nljt$. Let us emphasize that the single-particle states ρ_1 , ρ_2 , and ρ_3 are taken to be mutually orthogonal. From (III.54) and (III.56), the relative reduced width for this transition is given by

$$\mathcal{S}(\rho_3) = (n_1 + n_2 + n_3) |\mathcal{J}(\rho_3)|^2, \quad (\text{III.59})$$

where

$$\mathcal{J}(\rho_3) = \left(\rho_3(n_1 + n_2 + n_3) \right) \quad (\text{III.60})$$

Let us first manipulate the wave function on the left:

$$\begin{aligned} \mathcal{J}(\rho_3) &= \alpha_{n_1+n_2+n_3} \sum_{\sigma_3} \langle \rho_3^{n_3} \alpha_3 | \rho_3^{n_3-1} \sigma_3 \rangle \\ &= \alpha \sum_{\sigma_3 \gamma} \langle \rho_3^{n_3} \alpha_3 | \rho_3^{n_3-1} \sigma_3 \rangle U(\beta \sigma_3 \Gamma \rho_3 : \gamma \alpha_3) \\ &= \alpha_{n_1+n_2+n_3} \quad (\text{III.61}) \end{aligned}$$

The appropriate antisymmetrizer is defined, as in (III.48), by

$$\alpha_{n_1+n_2+n_3} = \left[\frac{n_1! n_2! n_3!}{(n_1 + n_2 + n_3)!} \right]^{\frac{1}{2}} \sum'_{r \in S_{n_1+n_2+n_3}} (-1)^r P_r.$$

The last two steps leading to (III.61) involve, successively, application of Eqs. (III.20) and (III.7).

Again modifying (III.48) in a suitable way, the function on the right-hand side of (III.60) becomes

$$\alpha_{n_1+n_2+(n_3-1)} \quad (\text{III.62})$$

where

$$\alpha_{n_1+n_2+(n_3-1)}$$

$$= \left[\frac{n_1! n_2! (n_3-1)!}{(n_1+n_2+n_3-1)!} \right]^{\frac{1}{2}} \sum'_{s \in S_{n_1+n_2+n_3-1}} (-)^s P_s.$$

It only remains to decide how many of the regular permutations on each side of (III.60) can contribute, and to add all contributions. Let us do so in five steps.

(1) In the wave function on the left-hand side of (III.61), only those regular permutations can contribute which leave particle $(n_1+n_2+n_3)$ in the ρ_3 shell. This is a direct consequence of the orthogonality of different single-particle states.

(2) For the same reason, all contributions to the overlap integral are diagonal in the permutations P_s .

(3) These diagonal contributions are all equal since they cannot depend on the particular way in which the particles are labeled.

(4) According to (1), the contributing terms on the left-hand side are simply those permutations which are order-preserving relative to

$$\{1, 2, 3, \dots, n_1: n_1+1, n_1+2, \dots, n_1+n_2: n_1+n_2+1, \dots, n_1+n_2+n_3\}$$

and leave $n_1+n_2+n_3$ invariant. These permutations are obviously order-preserving with respect to

$$\{1, \dots, n_1: n_1+1, \dots; n_1+n_2+1, \dots, n_1+n_2+n_3-1\},$$

and are therefore in one-one correspondence with the terms, given by (III.62), on the right-hand side of (III.60). There are, accordingly,

$$(n_1+n_2+n_3-1)! / n_1! n_2! (n_3-1)!$$

equal contributions.

(5) Each equal contribution involves the overlap integral of the wave functions on the right-hand side of (III.61) and (III.62), and this is clearly equal to

$$\delta(\alpha_1 \alpha'_1) \delta(\alpha_2 \alpha'_2) \delta(\beta \beta') \delta(\sigma_3 \sigma'_3) \delta(\gamma \gamma').$$

Collecting points (1) to (5) and remembering the normalizing factors in the antisymmetrizers, (III.60) leads to

$$\begin{aligned} g(\rho_3) &= \left[\frac{n_1! n_2! n_3!}{(n_1+n_2+n_3)!} \frac{n_1! n_2! (n_3-1)!}{(n_1+n_2+n_3-1)!} \right]^{\frac{1}{2}} \\ &\times \frac{(n_1+n_2+n_3-1)!}{n_1! n_2! (n_3-1)!} \sum_{\sigma \sigma'} \langle \rho_3^{n_3} \alpha_3 | \rho_3^{n_3-1} \sigma_3 \rangle \\ &\times U(\beta \sigma_3 \Gamma \rho_3: \gamma \alpha_3) \\ &\times \delta(\alpha_1 \alpha'_1 \beta \sigma_3 \gamma: \alpha'_1 \alpha'_2 \beta' \sigma'_3 \gamma'). \quad (\text{III.63}) \end{aligned}$$

We have introduced the abbreviated notation

$$\delta(a_1 a_2 a_3 \dots : a'_1 a'_2 a'_3 \dots) = (\delta(a_1 a'_1) \delta(a_2 a'_2) \delta(a_3 a'_3) \dots)$$

for a product of Kronecker deltas.

The summation in (III.63) can be performed explicitly, and the final result is

$$\begin{aligned} g(\rho_3) &= [n_3 / (n_1+n_2+n_3)]^{\frac{1}{2}} \delta(\alpha_1 \alpha'_1 \beta: \alpha'_1 \alpha'_2 \beta') \\ &\times \langle \rho_3^{n_3} \alpha_3 | \rho_3^{n_3-1} \sigma_3 \rangle U(\beta \sigma_3 \Gamma \rho_3: \gamma' \alpha_3). \quad (\text{III.64}) \end{aligned}$$

From (III.59), the desired spectroscopic factor is

$$\begin{aligned} S(\rho_3) &= n_3 \langle \rho_3^{n_3} \alpha_3 | \rho_3^{n_3-1} \sigma_3 \rangle^2 \\ &\times U(\beta' \sigma_3 \Gamma \rho_3: \gamma' \alpha_3) \delta(\alpha_1 \alpha'_1 \beta: \alpha'_1 \alpha'_2 \beta'). \quad (\text{III.65}) \end{aligned}$$

That an orthogonality condition for the quantum numbers of the inert groups of nucleons must emerge is obvious. All the relative reduced widths which we write down in the remainder of the article are diagonal in such quantum numbers.

With this minor reservation, we see from (III.65) that the inert groups of nucleons ($\rho_1^{n_1}$ and $\rho_2^{n_2}$) influence the spectroscopic factor S only through their total quantum number β . In particular, although the total number of antisymmetrically coupled particles appears in the original definition (III.56) of S , it is the number of equivalent nucleons *in the group to which the transferred nucleon belongs* that emerges as a multiplying factor in the final expression. In other words, with an obvious notation,

$$\begin{aligned} S &\left\{ \begin{array}{c} \text{Diagram showing } \rho_1^{n_1}, \rho_2^{n_2}, \rho_3^{n_3} \text{ and } \alpha_1, \alpha_2, \alpha_3 \text{ in a circle } \Gamma. \end{array} \rightarrow \begin{array}{c} \text{Diagram showing } \rho_1^{n_1}, \rho_2^{n_2}, \rho_3^{n_3} \text{ and } \alpha_1, \alpha_2, \sigma_3' \text{ in a circle } \gamma'. \end{array} \right. \times \rho_3 \} \\ &= S \left\{ \begin{array}{c} \text{Diagram showing } \beta, \rho_3^{n_3} \text{ and } \alpha_3 \text{ in a circle } \Gamma. \end{array} \rightarrow \begin{array}{c} \text{Diagram showing } \beta, \sigma_3', \rho_3^{n_3-1} \text{ and } \rho_3 \text{ in a circle } \gamma'. \end{array} \right. \times \rho_3 \}. \end{aligned}$$

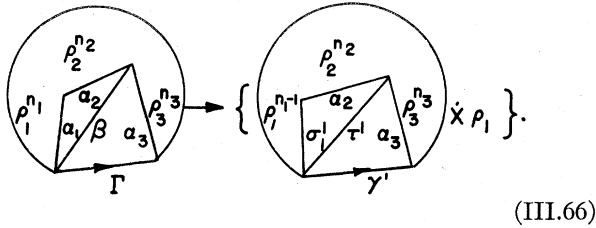
If the inert groups happen to be coupled to zero ($\beta=0$), it is obvious that the relative reduced width for the transition (III.58) reduces to

$$S \left\{ \begin{array}{c} \text{Diagram showing } \alpha_3 \text{ and } \rho_3 \text{ in a circle } \Gamma. \end{array} \rightarrow \begin{array}{c} \text{Diagram showing } \sigma_3', \rho_3 \text{ and } \beta^{-1} \text{ in a circle } \gamma'. \end{array} \right. \times \rho_3 \}.$$

Thus a set of zero-coupled inert groups of nucleons is devoid of influence on the relative reduced width. The most frequently encountered case of zero-coupled groups is that of a number of closed shells.

A slightly modified version of the general case just treated might emerge if we wished to transfer a particle

from the ρ_1 or ρ_2 shells. Consider, then, the transition



A few applications of the basic recoupling rules (III.5)–(III.7) suffice to reduce this case to the one whose general solution has just been obtained. Substituting from (III.65), we encounter a one-parameter sum over products of three Racah coefficients, which may be carried out with the aid of Biedenharn's sum rule [Ro57, Eqs. (II.6)–(II.15)]. Let us recall that, because of the commutativity of finite summations, recoupling can be carried out inside the antisymmetrization symbols.

The results are

$$\begin{aligned} g(\rho_1) = & [n_1/(n_1+n_2+n_3)]^{\frac{1}{2}} (-1)^{\alpha_1-\Gamma-\sigma_1'+\gamma'} \\ & \times \langle \rho_1^{n_1} \alpha_1 | \rho_1^{n_1-1} \sigma_1' \rangle U(\beta \alpha_2 \rho_1 \sigma_1' : \alpha_1 \tau') \\ & \times U(\rho_1 \tau' \Gamma \alpha_3 : \beta \gamma') \end{aligned} \quad (\text{III.67})$$

and

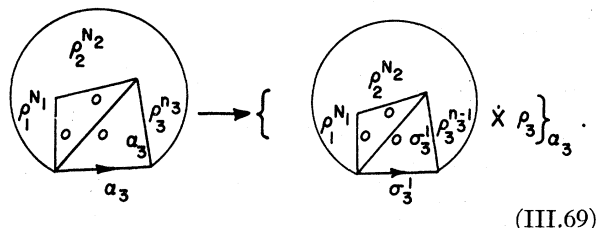
$$\begin{aligned} S(\rho_1) = & n_1 \langle \rho_1^{n_1} \alpha_1 | \rho_1^{n_1-1} \sigma_1' \rangle^2 U(\beta \alpha_2 \rho_1 \sigma_1' : \alpha_1 \tau')^2 \\ & \times U(\rho_1 \tau' \Gamma \alpha_3 : \beta \gamma')^2. \end{aligned} \quad (\text{III.68})$$

It is easy to carry out a similar calculation for the case of transfer of a ρ_2 nucleon or, more simply, we can apply the necessary coupling transformation (only a phase factor) to bring us back to the situation covered by (III.67) and (III.68).

(a) Role of Closed Shells

We have already remarked that any set of inert groups of nucleons, whose total angular momentum quantum numbers are zero, has no influence on relative reduced widths. The commonest case of this type, where the relevant inert groups are closed shells, is worth writing down explicitly.

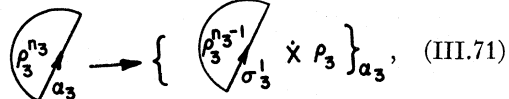
If $n_1 = [\rho_1] = N_1$, $n_2 = [\rho_2] = N_2$, we have seen in Sec. III.5 that the ρ_1 and ρ_2 shells are closed. Equation (III.58) then reduces to



The Racah coefficient in (III.65) being unity, we have

$$S(\rho_3) = n_3 \langle \rho_3^{n_3} \alpha_3 | \rho_3^{n_3-1} \sigma_3' \rangle^2. \quad (\text{III.70})$$

This, however, is precisely the relative reduced width for the transition



as follows immediately on equating both n_1 and n_2 to zero in (III.65). We conclude that, in evaluating relative reduced widths, we are justified in ignoring inert closed shells. We do so consistently in the rest of this study.

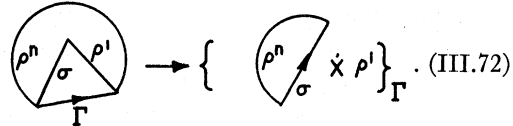
The preceding conclusion is even more apparent if only the ρ_1 shell in (III.58) is closed. In this case, the very form of (III.65) is unchanged.

(b) Addition of an Inequivalent Particle to an Equivalent Group

If, in (III.58), we put

$$\left. \begin{array}{l} n_1=0 \quad n_2=n \quad n_3=1 \\ \rho_2=\rho \quad \rho_3=\rho' \end{array} \right\},$$

Eq. (III.65) gives the spectroscopic factor for the transition



Since the Racah coefficient and the cfp in (III.65) both reduce to unity, we obtain the well-known result

$$S(\rho') = 1. \quad (\text{III.73})$$

In practice, the equivalent nucleons ρ^n in $(\rho^n \rho')_\Gamma$ usually do not couple to a single value of σ , the extra particle ρ' having the effect of exciting the equivalent group.¹¹ Instead, we have

$$\sum_{\sigma} K(\sigma) \left(\begin{array}{c} \rho^n \\ \sigma \\ \rho' \end{array} \right)_{\Gamma},$$

and the relative reduced width for transfer of ρ' becomes

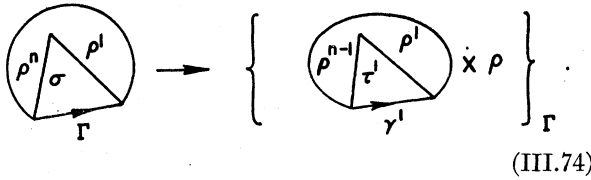
$$S(\rho') = |K(\sigma)|^2 \leq 1. \quad (\text{III.73}')$$

Thus, from a reaction wherein an inequivalent nucleon is separated from (or added to!) an equivalent group, we obtain a direct lower limit for the corresponding single-particle reduced width.

¹¹ Here we are discussing only excitations within a single configuration. We see repeatedly that there is no difficulty in calculating S between linear superpositions of states. The introduction of mixtures of excited configurations is only one such case.

The case $S=1$ occurs when ρ^n contains a unique state, as in all cases where the ρ shell contains a single particle or a single hole. If several amplitudes $K(\sigma)$ occur in the wave function of $[A+1]$, but all except one are very small, then $S \approx 1$. In such a case we may say that the inequivalent nucleon is "weakly coupled" to the equivalent group. We develop this idea of weak coupling, first discussed by Lane (La55a), in detail in Sec. III.11.

While dealing with (III.72), we should also consider the closely related transition



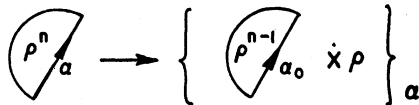
This is one of the special cases embraced by (III.68), whence

$$S(\rho) = n \langle \rho^n \sigma | \rho^{n-1} \tau' \rangle^2 U(\rho \tau' \Gamma \rho : \sigma \gamma)^2 \quad (\text{III.75})$$

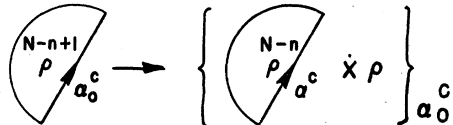
which, apart from the notation, is the same as (III.20) in Fr60.

(c) Hole-Particle Theorems for Reduced Widths

The hole-particle correspondence described in Sec. III.5 leads us to expect a simple connection between the relative reduced width for the transition



and that for the complementary transition



To derive the relevant hole-particle theorem, let us use (III.70) to write

$$\begin{aligned} S(n\alpha \rightarrow n-1, \alpha_0) \\ \overline{S(N-n+1, \alpha_0^c \rightarrow N-n, \alpha^c)} \\ = \frac{n \langle \rho^n \alpha | \rho^{n-1} \alpha_0 \rangle^2}{(N-n+1) \langle \rho^{N-n+1} \alpha_0^c | \rho^{N-n} \alpha^c \rangle^2}. \end{aligned}$$

If we now express the wave functions for ρ^n and ρ^{n-1} in the normal or \mathcal{L} set, those for ρ^{N-n} , ρ^{N-n+1} in \mathfrak{R} , we can use (III.41) for the ratio of the cfp, whence

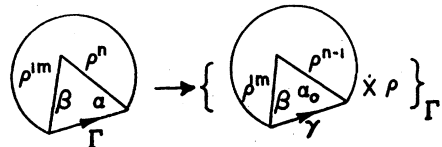
$$\begin{aligned} S(N-n+1, \alpha_0^c \rightarrow N-n, \alpha^c) \\ = [\alpha/\alpha_0] S(n\alpha \rightarrow n-1, \alpha_0) \quad (\text{III.76}) \end{aligned}$$

agreeing with (III.29) of Fr60.

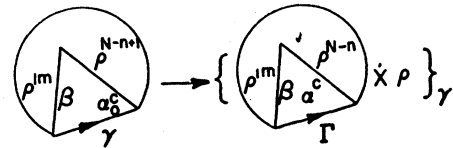
Equation (III.76) reduces the calculation of reduced widths for transitions in the second half of a shell into the complementary problem in the first half. As such, it rounds out the considerations of Sec. III.5.

In addition, (III.76) is very useful in Sec. III.11, where we discuss sum rules.

It is easy to see that the presence of inactive groups of particles in different shells does not disturb the foregoing hole-particle theorem. In fact, the relative reduced widths for the transitions



and



are related by the appropriate modification (III.76') of (III.76). The presence of the group ρ'^m only produces an extra recoupling factor, which is $U(\beta\alpha_0\Gamma\rho : \gamma\alpha)^2$ in the first case, and

$$U(\beta\alpha\gamma\rho : \Gamma\alpha_0)^2 = [\Gamma\alpha_0/\gamma\alpha] U(\beta\alpha_0\Gamma\rho : \gamma\alpha)^2,$$

in the second. For the ρ nucleons, (III.76) holds, so that, taking account of the minor difference in the recoupling factors, we have

$$\begin{aligned} S(N-n+1, \alpha_0^c \gamma \rightarrow N-n, \alpha^c \Gamma) \\ = [\Gamma/\gamma] S(n, \alpha \Gamma \rightarrow n-1, \alpha_0 \gamma). \quad (\text{III.76}') \end{aligned}$$

The appropriate modification therefore consists solely in introducing the total quantum numbers Γ and γ in the multiplicative factor. Otherwise, the inactive groups are devoid of influence. It is interesting to notice [see Sec. III.8, Eq. (III.102)] that a hole-particle theorem of precisely the same form as (III.76) and (III.76') emerges in LSJ representations.

(d) Separate Treatment of Neutrons and Protons

The general results (III.65) and (III.68) can be applied directly only to transitions connecting initial and final states which are antisymmetric in all particles involved. Suppose, next, that a neutron is added to a state of the configuration

$$[\{\omega_1^{r_1} \omega_2^{r_2}\}_p \{\rho_1^{n_1} \rho_2^{n_2}\}_n].$$

Specifically, let us calculate

$$S(\rho_2) = (n_1 + n_2) |\mathcal{J}(\rho_2)|^2, \quad (\text{III.77})$$

where

$$\mathcal{J}(\rho_2) = \left\langle \begin{array}{c} \text{Diagram showing two circles representing wave functions } \Psi_{\Gamma} \text{ and } \Phi_{\Gamma}, \text{ with internal labels } \omega_1^{\nu}, \tau_1, \beta_p, \beta_n, \rho_1^{n_1}, \rho_2^{n_2}, \alpha_1, \alpha_2, \epsilon, \gamma, \beta_2^{n_2-1}, \rho_2(n_1+n_2). \end{array} \right\rangle. \quad (\text{III.78})$$

It is immediately obvious that the inactive group of protons influences \mathcal{S} only through the total quantum number β_p . Let us then contract the proton portion of (III.78) to its bare essentials and consider the overlap integral

$$\mathcal{J}(\rho_2) = \left\langle \begin{array}{c} \text{Diagram showing two circles representing wave functions } \Psi_{\Gamma} \text{ and } \Phi_{\Gamma}, \text{ with internal labels } \beta_p, \beta_n, \rho_1^{n_1}, \rho_2^{n_2}, \alpha_1, \alpha_2, \epsilon, \gamma, \beta_2^{n_2-1}, \rho_2(n_1+n_2). \end{array} \right\rangle. \quad (\text{III.79})$$

In order to reduce this to a case covered by (III.65), it is only necessary to specify β_n rather than γ in the right-hand wave function. According to (III.7), the necessary transformation is expressed by the Racah coefficient $U(\beta_p \epsilon \Gamma \rho_2 : \gamma \beta_n)$. Use of (III.65) with $n_1=0$ then yields

$$\mathcal{S}(\rho_2) = n_2 \langle \rho_2^{n_2} \alpha_2 | \rho_2^{n_2-1} \sigma_2 \rangle^2 U(\beta_p \epsilon \Gamma \rho_2 : \gamma \beta_n)^2 \times U(\alpha_1 \sigma_2 \beta_n \rho_2 : \epsilon \alpha_2)^2. \quad (\text{III.80})$$

This example is sufficiently general to demonstrate that the separate treatment of neutrons and protons is covered by the general results (III.65) and (III.68), to within a recoupling transformation which can be written down at sight. Let us note that in the direct-product symbols in (III.78) and (III.80) no isotopic-spin factors appear, since we are using wave functions in a language which treats neutrons and protons as separate entities.

(e) Superpositions of Basic States

In this section we have shown how to calculate overlap integrals and reduced widths connecting basic states of jj representations. In practice, we usually wish to deal with wave functions which are linear combinations of basis elements. This can be handled very easily, as we now demonstrate.

The overlap integral, and hence, by (III.56), the relative reduced width, for the transition

$$\Phi_{\Gamma}(r) \rightarrow \{\Psi_{\Gamma_0}(s) \dot{\times} \rho\}_{\Gamma}$$

connecting basic states of our representation can be calculated by the methods of this section. We obtain thereby an expression for

$$\mathcal{G}_{rs}(\rho) = \langle \Phi_{\Gamma}(r) | \{\Psi_{\Gamma_0}(s) \dot{\times} \rho\}_{\Gamma} \rangle. \quad (\text{III.81})$$

Let us now suppose that the states Φ_{Γ} and Ψ_{Γ_0} in which we are interested are linear superpositions of the states of the representation, according to

$$\Phi_{\Gamma} = \sum_r K_r^{\Gamma} \Phi_r(r), \quad \Psi_{\Gamma_0} = \sum_s K_s^{\Gamma_0} \Psi_{\Gamma_0}(s). \quad (\text{III.82})$$

Simply substituting (III.82) in (III.81) yields the desired result

$$\mathcal{G}(\rho) = \sum_{rs} K_r^{\Gamma} K_s^{\Gamma_0} \mathcal{G}_{rs}(\rho). \quad (\text{III.83})$$

Since we always deal with real coefficients K , the complex conjugation on K_r^{Γ} in (III.83) has been omitted.

This procedure is by no means restricted to jj representations. It applies to all transitions connecting states whose wave functions are linear combinations of constituents which are connected by known (i.e., calculable) overlap integrals. Indeed, the process of taking linear combinations is so simple and obvious that we usually content ourselves with an evaluation of the individual overlap integrals to the right of (III.83), taking the final step for granted.

We are now in a position to calculate the relative reduced width for any transition connecting states for which shell-model wave functions are available. This last proviso is, as we emphasized at the beginning of this section, an important one, since the problem of obtaining suitable wave functions may well be harder than that of calculating the resulting spectroscopic factor. From a reduced width, however, we can sometimes deduce an amplitude directly, particularly in the case of transitions involving two contributing l values. An example of such a determination is given in Sec. III.9 (see also Pa58 and Fr60, Example 15). Thus, even in mass regions which are spectroscopically obscure, a reduced width may give us information about the nuclear wave functions.

Since the relative reduced width is proportional to the square of $\mathcal{G}(\rho)$, it is clear from (III.83) that the contributions from the various basic states add coherently. This has the important consequence that a small observed reduced width may not be recognizable as due to the operation of some general selection rule.

8. Calculation of \mathcal{S} in LSJT Representations

The cases of practical interest to which the results of Sec. III.7 are directly applicable are those of jjJ representations, with or without the isotopic spin T . We now show how to handle the calculation of relative reduced widths when the relevant overlap integrals involve wave functions in an LSJT or LSJ representation. As we saw in Sec. III.3, such representations do not permit the use of a simple direct-product notation, but can be accommodated by a straightforward formal modification (III.15). We prefer not to use this adapted

product notation here, although it would be entirely feasible to do so.

No formal advantage is gained by specifying the value of j for the transferred nucleon when LS wave functions are used for initial and final states. Furthermore, in situations where the use of an LS representation is more convenient, we usually expect the two different j values for each J to participate on a more or less equal footing. We therefore prefer to use a channel-spin representation [(III.52) and (III.53)], the relevant overlap integral being

$$\mathcal{J}(z) = \left\langle \begin{array}{c} l^n \\ \alpha_L \\ S \\ s \\ \hline J \end{array} \middle| \begin{array}{c} t^n \\ T \end{array} \right\rangle = \left\langle \begin{array}{c} l^{n-1} \\ \alpha_0 L_0 S_0 \\ S(n) \\ \hline J(n) \\ z \\ J_0 \\ \hline J \end{array} \middle| \begin{array}{c} t^{n-1} \\ T_0 \\ T(n) \end{array} \right\rangle, \quad (\text{III.84})$$

where α and α_0 label the quantum numbers necessary, in addition to LSJ , in a complete specification of the states involved.

It is now easy to see why things are a little more complicated than they were in Sec. III.7. The difficulty is simply that when we proceed, as usual, by inserting in (III.84) the parentage expansion

$$\left\langle \begin{array}{c} l^n \\ \alpha_L \\ S \\ s \\ \hline J \end{array} \middle| \begin{array}{c} t^n \\ T \end{array} \right\rangle = \sum_{\alpha_0' L_0' S_0' T_0'} \langle \alpha L S T | \alpha_0' L_0' S_0' T_0' \rangle \left\langle \begin{array}{c} l^{n-1} \\ \alpha_0' L_0' S_0' \\ S(n) \\ \hline J(n) \\ z \\ J_0 \\ \hline J \end{array} \middle| \begin{array}{c} t^{n-1} \\ T_0 \\ T(n) \end{array} \right\rangle, \quad (\text{III.85})$$

for the wave function on the left, we see that neither z nor J_0 is specified. An extra recoupling is therefore necessary. Observe that the parentage expansion (III.85) has not been affected by specifying J .

With the aid of the recoupling rules (III.5)–(III.7), Eq. (III.85) can be suitably transformed to yield, for the wave function on the left of the overlap integral (III.84),

$$\sum_{\substack{\alpha_0' L_0' S_0' T_0' \\ z' J_0'}} (-1)^{l+L_0'+L} \langle \alpha L S T | \alpha_0' L_0' S_0' T_0' \rangle U(l L_0' JS : Lz') U(L_0' S_0' zS : J_0' S)$$

$$\times \left\langle \begin{array}{c} l^{n-1} \\ \alpha_0' L_0' S_0' \\ S(n) \\ \hline J_0 \\ z \\ J_0 \\ \hline J \end{array} \middle| \begin{array}{c} t^{n-1} \\ T_0 \\ T(n) \end{array} \right\rangle. \quad (\text{III.86})$$

The overlap integral between the wave function in (III.86) and that on the right-hand side of $\mathcal{J}(z)$ in (III.84) is

$$\delta(\alpha_0 L_0 S_0 T_0 J_0 z : \alpha_0' L_0' S_0' T_0' J_0' z').$$

so that

$$\mathcal{J}_{rs}(z) = (-1)^{l+L_0+L} \langle \alpha L S T | \alpha_0 L_0 S_0 T_0 \rangle U(l L_0 JS : Lz) U(L_0 S_0 zS : J_0 S), \quad (\text{III.87})$$

where $r = \{\alpha L S T\}$, $s = \{\alpha_0 L_0 S_0 T_0\}$.

In all cases of interest we deal with wave functions of the form

$$\Phi_{TJ}(l^n) = \sum_{\alpha L S} K_{\alpha L S T J} \Phi_{\alpha L S T J}(l^n) \quad (\text{III.88})$$

with a similar equation for $\Psi_{T_0 J_0}(l^{n-1})$. The overlap integral $\mathcal{J}(z)$ between such states can be written down from (III.83), the $\mathcal{J}_{rs}(z)$ between basic states being given by (III.87). We conclude that

$$\mathcal{S}(l) = n \sum_z \mathcal{J}(z)^2 \quad (\text{III.89})$$

and

$$\mathcal{J}(z) = \sum_{\alpha L S \alpha_0 L_0 S_0} K_{\alpha L S T J} K_{\alpha_0 L_0 S_0 T_0}^{J_0} (-1)^{l+L_0+L}$$

$$\langle \alpha L S T | \alpha_0 L_0 S_0 T_0 \rangle U(l L_0 JS : Lz) U(L_0 S_0 zS : J_0 S). \quad (\text{III.90})$$

This expression has been given by Lane (La53), Satchler (Sa54), and Auerbach (Au54, 55). In the latter reference and in Fr60, our $\mathcal{J}(z)$ is referred to as β_z .

Since $\mathbf{z} = \mathbf{J}_0 + \mathbf{s}$ and $s = \frac{1}{2}$, there are at most two terms in the sum over z in (III.89). For example, in the case $\text{Li}^7(d, p)\text{Li}^8$, when $J_0 = \frac{3}{2}$, we can have $z = 1$ or 2, provided that the spin J of the state in Li^8 is such as to satisfy $\Delta(zlJ)$, with $l = 1$. For example, a state with $J = 3$ could only be attained by $z = 2$. When $J_0 = 0$ there is only $z = \frac{1}{2}$.

The fact that contributions from the two different channel spins add incoherently has the consequence that measurements on angular distributions alone cannot distinguish between channel spins. In order to measure relative values of different terms $\mathcal{J}(z)^2$, recourse can be had, in principle, to studies of $(d, p\gamma)$ angular correlations. We encounter an example of this later in our discussion of the $A=8$ polyad.

It is useful to regard (III.90) as a matrix equation

$$\mathcal{J}(z) = K(\beta_z)^\mu K_0^T, \quad (\text{III.91})$$

where K is a row vector, K_0^T is a column vector, and $(\beta_z)^\mu$ is the rectangular matrix

$$(\beta_z)^\mu = (-1)^{l+L_0+L} \langle \alpha LST | \alpha_0 L_0 S_0 T_0 \rangle \\ \times U(lL_0 JS : Lz) U(L_0 S_0 zS : J_0 S). \quad (\text{III.92})$$

The rows and columns of these matrices are labeled by the sets of quantum numbers

$$r = \{\alpha LST\} \quad \text{and} \quad s = \{\alpha_0 L_0 S_0 T_0\}.$$

There is a separate matrix $(\beta_z)^\mu$ for each pair of values $\mu = (JJ_0)$ of the spins of the nuclear states involved. For every μ , r and s can take all sets of values satisfying the triangle conditions $\Delta(LSJ)$, $\Delta(L_0 S_0 J_0)$.

The matrix $(\beta_x^c)^\mu$, whose rows and columns correspond to the sets of complementary quantum numbers r^c and s^c , is given, according to (III.92), by

$$(\beta_x^c)^\mu = (-1)^{l+L+L_0} \langle \alpha_0^c L_0 S_0 T_0 | \alpha^c LST \rangle \\ \times U(lL_0 S_0 : L_0 x) U(L_0 S_0 xS : JS_0). \quad (\text{III.93})$$

A striking relation exists between β_z and β_x^c . In order to obtain this relation, we need two auxiliary results. The first of these involves specializing (III.41) to the case of an LST representation:

$$\begin{aligned} & \langle l^{N-n+1} : \alpha_0^c L_0 S_0 T_0 | l^{N-n} ; \alpha^c LST \rangle \\ & \overline{\langle l^n \alpha LST | l^{n-1} \alpha_0 L_0 S_0 T_0 \rangle} \\ & = (-)^{n+l+1+L+S+T+L_0+S_0+T_0} \\ & \times \left\{ \frac{n[LST]}{(N-n+1)[L_0 S_0 T_0]} \right\}^{\frac{1}{2}}. \end{aligned} \quad (\text{III.94})$$

Secondly, let us write the Biedenharn sum rule [(Bi53,

Ro57 (6-15)] in terms of normalized Racah coefficients:

$$\begin{aligned} & U(lLJ_0 S_0 : L_0 x) U(LSx_{\frac{1}{2}} : JS_0) \\ & = (-)^{L+S+J+L_0+S_0+J_0+1} \left[\frac{JL_0 S_0}{J_0 LS} \right]^{\frac{1}{2}} \\ & \times \sum_z U(J_0 l_{\frac{1}{2}}^1 J : xz) U(lL_0 JS : Lz) \\ & \quad \times U(L_0 S_0 z_{\frac{1}{2}}^1 : J_0 S) \end{aligned} \quad (\text{III.95})$$

noting that $S = \frac{1}{2}$.

Collecting (III.94)–(III.95), and rearranging the phase factors,

$$\begin{aligned} (\beta_x^c)_{rs}^\mu & = (-)^{n+l+1+J+J_0+T+T_0} \left(\frac{n}{N-n+1} \right)^{\frac{1}{2}} \left[\frac{JT}{J_0 T_0} \right]^{\frac{1}{2}} \\ & \times \sum_z U(J_0 l_{\frac{1}{2}}^1 J : xz) \\ & \times [(-)^{l+L_0+L} \langle l^n \alpha LST | l^{n-1} \alpha_0 L_0 S_0 T_0 \rangle \\ & \quad \times U(lL_0 JS : Lz) U(L_0 S_0 z_{\frac{1}{2}}^1 : J_0 S)]. \end{aligned}$$

We see from (III.92) that the bracketed term is simply $(\beta_z)_{rs}^\mu$. The desired relation between corresponding matrix elements of complementary β matrices is therefore

$$\begin{aligned} (\beta_x^c)_{rs}^\mu & = \left(\frac{n}{N-n+1} \right)^{\frac{1}{2}} (-)^{n+l+1+J+J_0+T+T_0} \left[\frac{JT}{J_0 T_0} \right]^{\frac{1}{2}} \\ & \times \sum_z U(J_0 l_{\frac{1}{2}}^1 J : xz) (\beta_z)_{rs}^\mu. \end{aligned} \quad (\text{III.96})$$

The inverse relation follows immediately, by the unitarity of the U function:

$$\begin{aligned} (\beta_z)_{rs}^\mu & = \left(\frac{N-n+1}{n} \right)^{\frac{1}{2}} (-1)^{n+l+1+J+J_0+T+T_0} \left[\frac{J_0 T_0}{JT} \right]^{\frac{1}{2}} \\ & \times \sum_x U(J_0 l_{\frac{1}{2}}^1 J : xz) (\beta_x^c)_{rs}^\mu. \end{aligned} \quad (\text{III.97})$$

Since there are, in general, two allowed values of the channel spins z and x , the unitary transformation (III.96) and (III.97) connecting complementary elements of the β matrices can be regarded as a rotation in a two-dimensional space. We now derive the corresponding relation between the relative reduced widths, bearing in mind that S^c and S , with the same amplitude vectors K and K_0^T , are not usually of interest simultaneously, since, if Ψ represents a state l^n (or l^{n-1}), Ψ^c does not, in most cases, represent a state of l^{N-n} (or l^{N-n+1}), which is physically interesting.

We wish to evaluate the relative reduced width s^c of the transition

$$l^{N-n+1} : J_0 T_0 \rightarrow l^{N-n} : JT \quad (\text{III.98})$$

expressing the respective state vectors K_r , K_s^0 of the states of l^{N-n} and l^{N-n+1} in the \mathcal{G} set. Equations

(III.89)–(III.91) then yield

$$\begin{aligned} S^c &= (N-n+1) \sum_x g^c(x)^2 \\ &= (N-n+1) \sum_{rsr's'} K_r K_{r'} K_s^0 K_{s'}^0 \\ &\quad \times \sum_x (\beta_x^c)_{rs} (\beta_x^c)_{r's'}. \end{aligned} \quad (\text{III.99})$$

But, from (III.96),

$$\begin{aligned} \sum_x (\beta_x^c)_{rs} (\beta_x^c)_{r's'} &= \frac{n}{N-n+1} \left[\frac{JT}{J_0 T_0} \right] \sum_{zzz'} U(J_0 l_2^1 J : xz) \\ &\quad \times U(J_0 l_2^1 J : xz') (\beta_z)_{rs} (\beta_z)_{r's'} \\ &= \frac{n}{N-n+1} \left[\frac{JT}{J_0 T_0} \right] \sum_z (\beta_z)_{rs} (\beta_z)_{r's'}, \end{aligned} \quad (\text{III.100})$$

where the final step makes use of the unitarity of the transformation (III.6). Finally, we use (III.100) in (III.99) to give

$$S^c = \left[\frac{JT}{J_0 T_0} \right] n \sum_{rs} K_r K_{r'} K_s^0 K_{s'}^0 \sum_z (\beta_z)_{rs} (\beta_z)_{r's'}, \quad (\text{III.101})$$

which can be written in the compact form

$$\begin{aligned} S^c(l^{N-n+1}, J_0 T_0 \rightarrow l^{N-n}, JT) &= \left[\frac{JT}{J_0 T_0} \right] S'(l^n, JT \rightarrow l^{n-1}, J_0 T_0). \end{aligned} \quad (\text{III.102})$$

S' is, by definition, the spectroscopic factor calculated according to (III.89) and (III.90) using (1) the amplitudes of the state vectors (in \mathcal{R}) for the nuclear levels connected by the transition

$$l^{N-n+1}, J_0 T_0 \rightarrow l^{N-n}, JT,$$

and, (2) the β matrices (in \mathcal{L}) for the complementary transition

$$l^n, JT \rightarrow l^{n-1}, J_0 T_0.$$

In view of (III.96) and (III.102), we require β matrices only for the first half of the l shell. The considerations of this section leading to (III.102) may therefore be regarded as augmenting our collection of hole-particle theorems [(III.41)–(III.45), (III.76), (III.96), and (III.102)]. Appendix 2 of Ma59 contains, in numerical form, the more useful β matrices for the first half of the $1p$ shell.

9. General Comments: Specific Examples

A reasonable first step in analyzing the empirical reduced widths given in Tables I and II would be to seek general selection rules to explain the smallness of the reduced widths for certain transitions. Apart from the requirements imposed by conservation of angular

momentum and parity, we would be particularly interested in selection rules having their origin in the detailed structure of the nuclear states concerned.

Various selection rules are discussed in this way in Fr60. Here we demand an explicit expression for each reduced width rather than a qualitative statement as to its order of magnitude. Particular selection rules are mentioned when and where they are encountered.

A few numerical examples are now examined. These are useful later in their own right, but serve in this section to demonstrate how we intend to use the formal expressions for reduced widths derived in Secs. III.7 and III.8.

Example 1.

$$\begin{aligned} C^{12}(d, p) &\rightarrow C^{13}(\text{g.s.}) \quad l=1 \quad \theta_g^2 \sim 0.04 \\ 0^+ &\quad \frac{1}{2}^- \\ &\rightarrow C^{13}(3.68 \text{ Mev}) \quad l=1 \quad \theta^{2*} \sim 0.01. \end{aligned}$$

These reactions were first discussed from the viewpoint of the shell model by Lane (La53).

Let us introduce the symbol S_g for the relative reduced width of the ground-state transition, the corresponding quantity for the $\frac{1}{2}^-$ excited state being S^* .

In extreme jj coupling, the C^{12} ground state is represented by the closed-shell wave function $(p_{\frac{1}{2}}^8)_0$. The C^{13} ground state is, similarly, $(p_{\frac{1}{2}}^8)_0 p_{\frac{1}{2}}$, yielding

$$S_g = 1,$$

with the aid of (III.73). The jj -coupling wave function for the $\frac{1}{2}^-$ excited state must involve excitation of the $p_{\frac{1}{2}}$ closed shell, so that

$$S^* = 0.$$

From the small value ($\approx \frac{1}{4}$) of the observed reduced-width ratio θ^{2*}/θ_g^2 , we might be tempted to conclude that jj coupling is a good approximation for the relevant wave functions. We would not be justified in drawing such a conclusion, since, as we shortly prove and illustrate in Fig. 2, the calculated reduced-width ratio remains small for considerable departures from extreme jj coupling. This and several other examples show that it is dangerous to make statements about modes of coupling on the basis of single numbers, unsupported by other evidence.

We now examine the behavior of S_g and S^* as functions of the spin-orbit parameter $\xi = |a|/|K|$ ¹² considering,

¹² The “single-particle spin-orbit” shell model has been used extensively in studies of the $1p$ shell (In53, La53, La54, and many others). The formalism of the model is discussed, for example, in El57 and Fr58. The matrix elements of the two-body central interaction in the $1p$ shell have been given explicitly by Racah (Ra50) and by Elliott *et al.* (El54), completing earlier work of Hund (Hu37) and of Feenberg, Wigner, and Phillips (Fe37, Fe37a). These central-force matrix elements can be expressed in terms of two radial integral parameters L and K (In53, Fr58). The results of calculations of quantities of interest—for example, energy spacings and reduced widths—are insensitive to changes in L and K around the values 5 to 7 for L/K and -1 Mev for K . We use $L/K=6$, $K=-1.25$ Mev unless we state otherwise.

first, the ground-state transition

$$l^{N-n+1}, J_0 T_0 \leftarrow l^{N-n}, JT,$$

where $n=4$, $J=T=0$ and $J_0=T_0=\frac{1}{2}$. The rather peculiar step of labeling the final state of a (d,p) transition with a subscript zero is taken in order to conform in every detail with the notation of (III.99).

The relevant basic states of $(1p^8)$ and $(1p^9)$, in an LST representation, are

$$C^{12}: {}^{11}S^{[44]} {}^{13}P^{[431]} {}^{11}S^{[422]} {}^{15}D^{[422]} {}^{13}P^{[332]}, \quad (\text{III.103})$$

$$C^{13}: {}^{22}P^{[441]} {}^{22}P^{[432]} {}^{24}P^{[432]} {}^{24}D^{[432]} {}^{22}S^{[333]},$$

where $[\alpha]$ labels the space symmetry (Fe37, Ja51, Fr58).

The calculation of wave functions and reduced widths is carried out in the standard representation defined in Sec. III.5. This representation is spanned by the functions of the normal or \mathcal{L} set for $n \leq 6$ and by those of the contragredient or \mathcal{R} set for $n > 6$, where n is the number of $1p$ particles and the \mathcal{L} and \mathcal{R} sets were defined in Sec. III.5. The most important property of this standard representation is that its defining cfp satisfy the Racah hole-particle relation (III.41). Consequently, in calculating matrix elements and reduced widths in the second half of the shell, we usually do not need explicit cfp for $n > 6$, instead expressing each quantity of interest directly in terms of its complement in the first half of the shell by the appropriate hole-particle theorem.

Using this procedure, we first construct and diagonalize the matrix of the Hamiltonian (III.2). The appropriate hole-particle theorems in this case are (III.44) and (III.45), the results being presented,¹³ in the form of tables covering all configurations $1p^n$, in Appendix C of Fr58.

By using a Rosenfeld exchange mixture (Ro58, El57, Fr58), with $L/K=6$, $K=-1.25$ Mev, we obtain the wave functions for a few values of ξ :

$$\begin{bmatrix} 1 & 0 & 0 & 0 & 0 \end{bmatrix} \xi=0 \quad (\text{LS limit})$$

$$\begin{aligned} C^{12}: K = & [0.945 \ 0.309 \ 0.084 \ -0.065 \ 0.039] \quad \xi=3 \\ & [0.823 \ 0.500 \ 0.151 \ -0.190 \ 0.115] \quad \xi=5 \\ & [0.249 \ 0.609 \ 0.314 \ -0.497 \ 0.471] \quad \xi \rightarrow \infty \end{aligned} \quad (jj \text{ limit})$$

$$\begin{aligned} C^{13}: K_0^T = & \begin{pmatrix} 1 \\ -0.044 \\ 0 \\ 0 \\ 0 \end{pmatrix} \begin{pmatrix} 0.930 \\ -0.214 \\ 0.148 \\ 0.257 \\ -0.038 \end{pmatrix} \begin{pmatrix} 0.805 \\ -0.359 \\ 0.212 \\ 0.415 \\ -0.087 \end{pmatrix} \begin{pmatrix} 0.430 \\ -0.544 \\ 0.272 \\ 0.609 \\ -0.272 \end{pmatrix} \\ & \xi=0 \quad \xi=3 \quad \xi=5 \quad \xi \rightarrow \infty \end{aligned} \quad (\text{III.104})$$

¹³ Our standard representation corresponds to the "complementary" or (C) phases of Fr58, Appendix C.

The rows and columns of these vectors are labeled by the basic states ordered as in (III.103).

The C^{12} wave functions are taken from Bennett's thesis (Be58), where they are given¹⁴ in a representation defined by the cfp of Ja51 without the modifications of El54. To express the C^{12} functions in our \mathcal{L} set, we must make these modifications, which, as can be seen from Appendix 2 of Ma59, involve a change of sign in Bennett's ${}^{11}S^{[44]}$ and ${}^{13}P^{[431]}$ amplitudes relative to the other three. Since all five states belong to the same class [(B) in Appendix 2 of Ma59], no further changes of sign are necessary in passing to \mathcal{R} and therefore to our standard representation.

The C^{13} wave functions are given by Auerbach and French (Au56) in the \mathcal{L} representation. Passage to \mathcal{R} is achieved (Appendix 2 of Ma59) by reversing the sign of the ${}^{24}D^{[432]}$ and ${}^{22}S^{[333]}$ amplitudes.

The transition in which we are interested,

$$(1p^9), (T_0 J_0) = \left(\frac{1}{2} \frac{1}{2}\right) \leftarrow (1p^8), (TJ) = (00),$$

obviously has only one channel, with $z=\frac{1}{2}$. Instead of computing the relevant β matrix (III.92), we make use of the hole-particle theorem (III.102) in order to go over to the complementary transition

$$(1p^4), (TJ) = (00) \leftarrow (1p^3), (T_0 J_0) = \left(\frac{1}{2} \frac{1}{2}\right),$$

which also has only one channel, with channel spin $x=1$.

To evaluate the matrix β_1^e in our standard representation for the complementary transition, we insert the modified (El54) cfp of Ja51 in (III.92). The result, from Appendix 2 of Ma59, is

$$\begin{bmatrix} {}^{22}P^{[3]} & {}^{22}P^{[21]} & {}^{24}P^{[21]} & {}^{24}D^{[21]} & {}^{22}S^{[111]} \\ {}^{11}S^{[4]} & -\sqrt{3}/3 & 0 & 0 & 0 \\ {}^{13}P^{[31]} & -\sqrt{2}/3 & \sqrt{5}/6 & -\sqrt{5}/12 & -1/4 & 0 \\ {}^{11}S^{[22]} & 0 & \sqrt{3}/3 & 0 & 0 & 0 \\ {}^{15}D^{[22]} & 0 & 0 & \sqrt{30}/12 & \sqrt{6}/4 & 0 \\ {}^{13}P^{[211]} & 0 & \sqrt{3}/6 & \sqrt{3}/12 & -\sqrt{15}/12 & \sqrt{3}/3 \end{bmatrix}. \quad (\text{III.105})$$

The rows and columns of this matrix are labeled by the states complementary to (III.103) with unchanged ordering.

To evaluate S_g as a function of ξ , we follow (III.92) and (III.101), forming the matrix product

$$J(1) = K(\beta_1^e) K_0^T$$

operating fore-and-aft on (III.105) with the row and column vectors (III.104). Then, following (III.102),

$$S_g = [JT/J_0 T_0] S' = \frac{1}{4} \cdot 4 J(1)^2 = J(1)^2$$

¹⁴ Strictly, the C^{12} wave function in the LS limit should contain a small admixture of ${}^{11}S^{[422]}$, arising from the weak central interaction between states of the same LST and different $[\alpha]$. The relevant minute amplitude would not influence the normalization to the necessary accuracy, and since, in addition, the corresponding element in the β matrix vanishes, is without influence on the value of S .

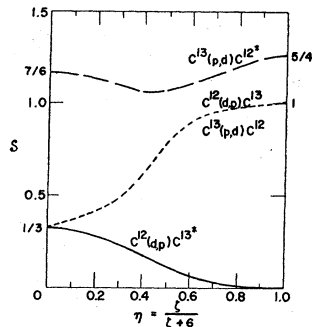


FIG. 1. Spectroscopic factors for $A=12 \rightleftharpoons 13$ as a function of the spin-orbit parameter η .

or

$$S_g = \{K(\beta_1^c)K_0^T\}^2. \quad (\text{III.106})$$

The procedure involved in evaluating S^* is precisely the same as that just described; we do not go into it in detail. On performing the necessary matrix multiplications, we obtain the results shown in Fig. 1, where S^* and S_g are plotted as functions of $\eta = \xi/(\xi+6)$. Figure 2 exhibits S^*/S_g as a function of the same parameter. A number of points demand further comment.

(A) We observe that

$$\begin{aligned} S_g &\rightarrow 1 \quad \text{as } \xi \rightarrow \infty \\ S^* &\rightarrow 0 \quad \text{as } \xi \rightarrow \infty \end{aligned}$$

agreeing with the values otherwise obtained in the jj limit at the beginning of this discussion. The agreement so obtained furnishes a valuable check on

- (1) the correctness of the β matrices given in Appendix 2 of Ma59,
- (2) the consistency of the phases of wave functions and β matrices.

(B) It would be just as easy to calculate S_g for the transition

$$(1p^9), (T_0J_0) = (\frac{1}{2} \frac{1}{2}) \leftarrow (1p^8), (TJ) = (00)$$

directly from (III.93), using the cfp which we have agreed on as standard. For the second half of the $1p$ shell, as in this example, the standard cfp are those of the \mathfrak{R} set, obtained from the complementary $\langle 4|3\rangle$ cfp in \mathfrak{L} with the help of (III.41). S_g would then be obtained, by (III.91), on matrix multiplication by the row and column vectors— K and K_0^T of (III.104). The results are the same as before.

In every calculation of reduced widths in an LSJ representation, it is desirable to check consistency of phases and the correctness of the β matrices by going to the jj limit. The relative reduced width under consideration should be computed by substituting the appropriate eigenvectors of the spin-orbit matrices for $(1p)^n$ and $(1p)^{n-1}$ in (III.91) and comparing with the value of $S(jj)$ obtained by an independent calculation in a jj representation. This was done in Example 1.

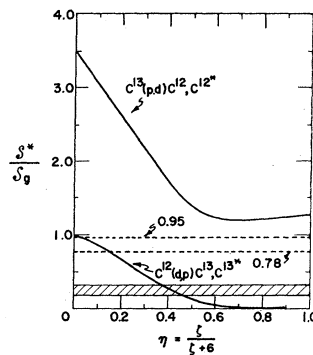


FIG. 2. Ratios of spectroscopic factors for $A=12 \rightleftharpoons 13$ as a function of the spin-orbit parameter η . Experimental $\theta^{2*}/\theta_0^2(d,p) = 0.25 \pm 0.06$; experimental $\theta^{2*}/\theta_0^2(p,d) \approx 0.95$; experimental $\theta^{2*}/\theta_0^2(d,t) \approx 0.78$.

Example 2.

$$O^{17}(d,p) \rightarrow O^{18}(1.98 \text{ Mev}) \quad l=0+2$$

$$\theta^2(2)/\theta^2(0) \approx 4.4.$$

Our analysis is very similar to that of Bilaniuk and Hough (Bi57) who first studied the preceding transition. It illustrates how a reduced-width ratio can lead to a direct determination of an amplitude in a wave function.

From the structure of O^{17} , which has a $\frac{5}{2}^+$ ground state, a $\frac{1}{2}^+$ state at 0.872 Mev, and no $\frac{3}{2}^+$ states until 5.08 Mev, we expect $1d_{\frac{5}{2}}$ and $2s_{\frac{1}{2}}$ to compete closely in the low-lying levels of nearby nuclei, $1d_{\frac{5}{2}}$ being relatively unimportant. Let us, therefore, write for the wave function of the preceding 2^+ state in O^{18} ,

$$A_{55}(d_{\frac{5}{2}})_2 + A_{51}(d_{\frac{1}{2}}s_{\frac{1}{2}})_2, \quad (\text{III.107})$$

neglecting the small amounts of $(d_{\frac{3}{2}}d_{\frac{3}{2}})$, $(d_{\frac{3}{2}}s_{\frac{1}{2}})$, and $(d_{\frac{3}{2}}^2)$ which may be present.

Since the O^{17} ground state is simply $d_{\frac{5}{2}}$, it is obvious that

$$S(l=0) = |A_{51}|^2, \quad S(l=2) = 2|A_{55}|^2. \quad (\text{III.108})$$

Remembering that $\theta^2 = S\theta_0^2$, we have

$$\frac{\theta^2(l=2)}{\theta^2(l=0)} = 2 \frac{|A_{55}|^2}{|A_{51}|^2} \frac{\theta_0^2(1d)}{\theta_0^2(2s)}. \quad (\text{III.109})$$

The single-particle reduced widths are, unfortunately, not known very precisely in this mass region; however, the results of various $O^{16}(d,p)O^{17}$ experiments (see Table I for references) and indirect evidence from other nearby nuclei strongly suggest that

$$2 \leq \frac{\theta_0^2(2s)}{\theta_0^2(1d)} \leq 3. \quad (\text{III.110})$$

By using (III.110) and the observed value 4.4 of the reduced-width ratio in (III.109), we find

$$0.43 \geq |A_{51}| \geq 0.36, \quad 0.89 \leq |A_{55}| \leq 0.93. \quad (\text{III.111})$$

In other words, the relevant 2^+ state in O^{18} contains between 13% and 18% of $(d_{\frac{3}{2}}s_{\frac{1}{2}})$.¹⁵ This is to be compared with the rather larger value of around 40% which emerges from intermediate-coupling calculations (Re54, Re58). The neglect of the small amplitudes involving $d_{\frac{3}{2}}$ has no effect on this disparity. Bilaniuk and Hough (Bi57), who used a different method of accounting for the difference between the $l=0$ and $l=2$ single-particle reduced widths, found

$$(|A_{55}|, |A_{51}|) = (0.81, 0.48),$$

which is not very different from (III.111). The amplitudes are quite insensitive to the uncertainty in the single-particle widths and similarly to inaccuracy in the measured reduced-width ratio.

Experimental results (Bi57) are available only for the transitions to the three lowest states in O^{18} , at 0 (0^+), 1.99 (2^+), and 3.55 (4^+) Mev, respectively. A determination of the position of the next 2^+ state, whose wave function is approximately

$$-A_{55}(d_{\frac{3}{2}})_2 + A_{51}(d_{\frac{3}{2}}s_{\frac{1}{2}})_2,$$

would yield an estimate of the interaction matrix element

$$H_{51} = \langle (d_{\frac{3}{2}})_2 | H | (d_{\frac{3}{2}}s_{\frac{1}{2}})_2 \rangle.$$

The relevant 2^+ state could be identified by its dominant $l=0$ stripping component from O^{17} , the small $l=2$ admixture being, in all probability, too weak to be detected. If the observed separation of the two 2^+ levels is ΔE (we know that $\Delta E > 1.5$ Mev), first-order perturbation theory yields

$$|H_{51}| \sim |A_{51}| / \Delta E,$$

the amplitude being measured by the reduced widths.

In the preceding example it is of no consequence whether or not we use the isotopic-spin formalism, since we are dealing with states of maximum isotopic spin.

Example 3.

$$K^{39}(d, p) \rightarrow K^{40} \quad l=3.$$

Four $l=3$ transitions are observed leading to the ground and first four excited states of K^{40} (En59). In considering these transitions it is most convenient to work without the isotopic-spin formalism.

The work of Goldstein and Talmi (Go56) and of Pandya (Pa56) has demonstrated that the four K^{40} levels in question may be identified, to considerable accuracy, with the quadruplet

$$\{[(d_{\frac{3}{2}})_2]_p \times [1f_{7/2}]_n\}_J, \quad J=2, 3, 4, 5^-. \quad (\text{III.112})$$

This wave function has the form of an $f_{7/2}$ neutron coupled to the K^{39} ground state ($d_{\frac{3}{2}}$ proton hole) function. The closed shell $(d_{\frac{3}{2}})_0$ of neutrons has been

¹⁵ Percentage refers to the square of the amplitude.

TABLE III.

Excitation (Mev) in K^{40}	J^π	l	θ^2 (relative to θ_0^2)
0	4^-	3	1
0.028	3^-	3	1.1
0.795	2^-	3	1.2
0.885	5^-	3	0.95

ignored; we see later that this involves no additional physical assumption because of the uniqueness of the proton and neutron states concerned. Since the number of antisymmetrically coupled neutrons is simply 1, it is obvious from the definitions (III.54) and (III.56) that each of the four $l=3$ transitions in question has $s=1$. This result is also contained in (III.80), as can be seen by putting $n_1=0$, $n_2=1$ and observing that each of the Racah coefficients and the cfp has the value unity.

That these predictions agree quite well with what is observed for the transitions in question is apparent from the list of experimental results in Table III (En59), taken from Table I.

Of the four states listed in Table III, those with spins 4^- and 5^- , the ground and 0.885-Mev excited states, respectively, of K^{40} , cannot be reached from K^{39} by $l=1$ transitions because of angular-momentum conservation. For the 2^- and 3^- levels, however, the possibility of $l=1$ components is open and might arise by interaction with the appropriate members of the tetrad

$$\{[(d_{\frac{3}{2}})_2]_p \times [(2p_{\frac{3}{2}})_n\}_J, \quad J=0, 1, 2, 3^-. \quad (\text{III.113})$$

The major portions of these $2p_{\frac{3}{2}}$ states are found to lie around 2 Mev in K^{40} , as evidenced by prominent $l=1$ stripping (En59).

The $l=1$ admixtures found in the $l=3$ transitions to the levels 0.028 Mev(3^-) and 0.795 Mev(2^-) of K^{40} are certainly small. For the 3^- state, En59 give, as a result of a very careful analysis, a lower limit

$$\theta^2(l=3)/\theta^2(l=1) \geq 50, \quad (\text{III.114})$$

with an even larger limit for the 2^- state.

If we write

$$K_1 \{[(d_{\frac{3}{2}})_2]_p \times [f_{7/2}]_n\}_{J=3} + K_2 \{[(d_{\frac{3}{2}})_2]_p \times [2p_{\frac{3}{2}}]_n\}_{J=3}$$

for the K^{40} (0.028 Mev) wave function, it is clear that

$$S(l=3)/S(l=1) = |K_1|^2/|K_2|^2. \quad (\text{III.115})$$

Now, as we see in Secs. V and VI, an analysis of many transitions in the mass region $24 \leq A < 70$ indicates that

$$\theta_0^2(2p)/\theta_0^2(1f) \approx 2$$

is a reliable estimate, whence, using (III.114) and (III.115),

$$|K_1|^2/|K_2|^2 \geq 100.$$

We therefore conclude that $K_1 \leq 0.1$ and that the

relevant 3^- state contains less than 1% of

$$\{[d_{\frac{3}{2}}]_p [f_{7/2}]_n\} J=3^-,$$

an upper limit which applies *a fortiori* to the 2^- state.

In order to produce a 1% $l=1$ admixture in the 3^- transition by interaction with the appropriate $2p_{\frac{3}{2}}$ level, which appears at 2.042 Mev in K^{40} , a matrix element of the order of magnitude of 200 kev is necessary, as follows from the first-order perturbation theory. A plausible calculation of this matrix element (Pa57b) yields a value of 330 kev. The difference between these two values is not surprising in view of the uncertainty as to the exchange character of the effective two-body interaction.

It is important to observe that the separate proton and neutron states in (III.112) and (III.113) are unique. Thus, it is not necessary to make an additional physical assumption to the effect that the neutron and proton angular momenta are each good quantum numbers. This is to be contrasted with the situation in Example 5, Sec. III.10.

By treating neutrons and protons separately in this example, we were enabled to ignore the closed $d_{\frac{3}{2}}$ neutron shell. The problem was thereby reduced to the simplest of two-body cases (strictly, one hole and one particle), where we do not have to worry about antisymmetry between the two particles concerned.

Example 4.

$$N^{15}(d,n) \rightarrow O^{16}(\text{g.s.}) \quad l=1.$$

This reaction has not yet been studied experimentally. Adopting a jj representation (the result is the same with an LS representation, as we see later), this transition involves filling a hole in the $1p_{\frac{3}{2}}$ shell. It follows at once from the uniqueness of the states concerned that the appropriate cfp is unity. Thus, from (III.70),

$$S(\text{closed shells} \rightarrow p_{\frac{3}{2}}^{-1}) = 4, \quad (\text{III.116})$$

the number of nucleons in the $p_{\frac{3}{2}}$ shell. In Sec. III.10 we have more to say on the subject of large spectroscopic factors for transitions wherein a shell is completed.

Without isotopic spin, the foregoing transition fills the $p_{\frac{3}{2}}$ neutron shell, for which, by the same argument, $S=2$.

The apparent discrepancy is removed on recalling the isotopic spin coupling factor in the Butler formula (II.19). In the present instance it is

$$\{C[\frac{1}{2} \frac{1}{2} 0; \frac{1}{2} -\frac{1}{2} 0]\}^2 = \frac{1}{2}.$$

If we are not using the isotopic-spin formalism, the coupling factor would, naturally, be ignored. The reduced width θ^2 extracted with the isotopic-spin formalism is thus twice what is obtained without it, a factor which is reflected in the preceding S values.

The N^{15} ground state is a single-hole $p_{\frac{1}{2}}$ state in the jj picture. There is a similar $p_{\frac{1}{2}}$ state at 6.33 Mev in N^{15} . A transition connecting this $p_{\frac{1}{2}}$ hole state to the ground state of O^{16} , which could be realized experimentally by $O^{16}(n,d)N^{15}$, would have

$$S(\text{closed shells} \rightarrow p_{\frac{1}{2}}^{-1}) = 8. \quad (\text{III.116}')$$

In an $LSJT$ representation, (III.116) and (III.116') are trivial consequences of (III.103). The two transitions we have just discussed are

$$(1p)^{12}, (T_0 J_0) = (00) \rightarrow (1p^{11}), \quad (TJ) = (\frac{1}{2}J),$$

with $J=\frac{1}{2}$ and $\frac{3}{2}$. The complementary transitions are

$$(1p)^1, (TJ) = (\frac{1}{2}J) \rightarrow (1p)^0,$$

where, obviously, $S=1$ for both values of J . Since the relevant states are unique and there are therefore no amplitudes to take into account, (III.103) immediately gives

$$S(\text{closed shells} \rightarrow p_J^{-1}) = [JT/J_0 T_0] \cdot 1 = 2(2J+1), \quad (\text{III.117})$$

a result which includes both (III.116) and (III.116') as special cases with $J=\frac{1}{2}, \frac{3}{2}$, respectively.

Equation (III.117) is also obtained, perhaps in a more revealing fashion, on consideration of the extra recoupling transformation which, as we saw in Sec. III.8, is the one extra complication which led to the separate treatment of $LSJT$ representations. The appropriate Racah coefficient is

$$U(LSz_{\frac{1}{2}}:JS_0)^2 = U(1\frac{1}{2}1\frac{1}{2} J_0)^2 = (2J+1)/6.$$

It is obvious that the remaining Racah coefficient and the cfp in (III.92) are both unity. The relative reduced width is therefore given by the product of the recoupling coefficient and the number of particles (12) in the complete $1p$ shell:

$$S(\text{closed shells} \rightarrow p_J^{-1}) = 12 \cdot [(2J+1)/6] = 2(2J+1),$$

which agrees with (III.117). It is instructive to observe the combined effect of the extra recoupling factor and the difference in the number of nucleons in LS and jj closed shells.

Example 5.

$$\begin{aligned} Ca^{40}(d,p) &\rightarrow Ca^{41}(\text{g.s.}) \\ Ca^{42}(d,p) &\rightarrow Ca^{43}(\text{g.s.}) \\ Ca^{44}(d,p) &\rightarrow Ca^{45}(\text{g.s.}) \end{aligned} \Big\} l=3.$$

The lowest levels of the Ca isotopes are expected to belong to the configurations $f_{7/2}^n$. As in Example 2, it is immaterial whether or not we use the isotopic-spin formalism, since all states concerned would have maximum T .

The ground-state transitions, with their respective

relative reduced widths, are

$$\left. \begin{array}{l} f_{7/2} \leftarrow [\text{closed shells}], \quad s=1 \\ (f_{7/2}^3)_{7/2} \leftarrow (f_{7/2}^2)_0, \quad s=3\langle f_{7/2}^3 \frac{7}{2} | f_{7/2}^2 0 \rangle^2 = \frac{3}{4} \\ (f_{7/2}^5)_{7/2} \leftarrow (f_{7/2}^4)_0, \quad s=5\langle f_{7/2}^5 \frac{7}{2} | f_{7/2}^4 0 \rangle^2 = \frac{1}{2} \end{array} \right\},$$

obtaining the necessary cfp from the tables of Ed52, with the help of (III.41) for the last one. These spectroscopic factors can also be obtained very simply from the sum rules to be discussed in Sec. III.10. (See Example 2 of Sec. III.10.) The observed ground-state reduced widths (Bo57, Ca57, Bo57a) are seen, from Table I, to be in the ratio

$$4:2.9:1.6,$$

in satisfactory agreement with the predicted values

$$4:3:2.$$

These transitions furnish useful illustrative examples in a preliminary discussion of single-particle levels. Although there is a variety of possible definitions, the underlying physical picture is the same in all of them. We think of a nucleon moving in a potential well generated by the other constituents of the nucleus [A]. These other constituents must be well described as being in some definite state of the nucleus [A-1]. A state of [A] which can be represented in such a fashion lends itself very naturally to the description "single-particle level." It is characterized by a specified value of l (or both l and j) of the extra particle and can be identified by its prominent appearance in transitions involving the transfer of a single nucleon. According to the intuitive description of a reduced width given in Sec. I, a single-particle level of [A] would be one which, by definition, has $s=1$ and $\theta=\theta_0$ for decay to its particular parent state of [A-1]. Single-particle levels are naturally encountered in nuclear reactions on [A-1] as target. The term "single-particle level" is usually confined to states of the foregoing description whose parent is the ground state of [A-1]. We follow this custom in the present study since we deal with target nuclei in their ground states. The case of excited parent states could be of interest in connection with the decay of levels of the compound nucleus in resonance reactions.

In expressing these ideas more precisely, we can distinguish two different situations according to whether the effective potential field does or does not number among its generating nucleons some which are equivalent to the loose "single" particle. At the very outset, we demand freedom to express our definition in a number of different ways, since which one is most convenient depends on the context. The various alternatives do not conflict with each other.

Bearing in mind the ground states of the Ca isotopes, let us define a single-particle level of the first kind as

one whose dominant configuration is $(j^{2n+1})_{J=j}$.¹⁶ Transitions leading from $(j^{2n})_0$ to such levels do not necessarily have $s=1$; however, as in the foregoing examples, the reduced widths for the single-particle transitions,

$$(j^{2n+1})_{J=j, v=1} \leftarrow (j^{2n})_{J_0=0, v_0=0}, \quad (\text{III.118})$$

are usually of the same order of magnitude as the single-particle width, and, in fact, we always have $s \leq 1$ in such cases. On the other hand, transitions of the type

$$(j^{2n+2})_{J=0, v=0} \leftarrow (j^{2n+1})_{J_0=j, v_0=1}, \quad (\text{III.118}')$$

wherein a nucleon is added to rather than removed from a single-particle state, do, in fact, have¹⁷ $s > 1$. Explicit spectroscopic factors for the foregoing transitions are derived in Sec. III.10, Example 2.

The configuration j^{2n+1} contains several states other than the lowest-seniority single-particle state. It would be natural to refer to $(j^{2n+1})J \neq j$ or $(j^{2n+1})J=j, v \neq 1$ as "multiparticle" states. The configuration $(j^{2n+1})_{J \neq j}$ cannot be reached from $(j^{2n})_0$ by a stripping transition because of angular-momentum conservation, the same being true for $(j^{2n+1})J=j, v \neq 1$ as a result of the seniority selection rule¹⁸ $\Delta v=1$. For $(f_{7/2})^{2n+1}$ (identical nucleons), no states with $J=j, v \neq 1$ occur, as is also the case for $j=\frac{3}{2}$ and $\frac{5}{2}$. An example of a multiparticle level is the 0.373-Mev level in Ca⁴³, whose dominant configuration is probably $(f_{7/2}^3)_{\frac{5}{2}}$ and which shows no stripping from the $(f_{7/2}^2)_0$ ground state of Ca⁴².

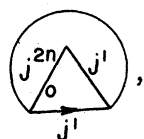
The basic idea of the Mayer-Jensen single-particle model (Ha49, Ma49, Ma50, Ha50), where the notion of single-particle levels originated, is that the properties of low-lying states of odd- A nuclei are determined by the last odd nucleon. We might try to express this formally by assigning a wave function $(j^{2n})_0 j(\# 2n+1)$ to a single-particle level of j^{2n+1} . As was realized in the very early stages of the single-particle model (Ma50a), this would violate the exclusion principle. On antisymmetrizing $(j^{2n})_0 j$ components involving $(j^{2n})_{J \neq 0}$ appear. The natural substitute for $(j^{2n})_0 j$ is $(j^{2n+1})_{J=j, v=1}$, which has many of the characteristic properties of states of the Mayer-Jensen model and satisfies the primary demand of antisymmetry.

¹⁶ This definition applies to a configuration of both neutrons and protons, or to an odd group of particles of one kind (neutrons or protons) only. If the configuration j^{2n+1} contains more than one state with $J=j$, the single-particle level is defined to be that of lowest seniority. ($v=1$. See Ra49, Fl52, Ed52.)

¹⁷ An absolute upper limit on all spectroscopic factors is provided by the inequality $s \leq n$, where n is the number of nucleons in the heavier nucleus equivalent to the transferred nucleon. The case of equality, wherein the upper limit is attained, corresponds to the transition (III.118').

¹⁸ For stripping from $(j^{2n})_0$, this seniority selection rule does more than forbid transitions already forbidden by angular-momentum conservation only when j^{2n+1} contains $J=j, v \neq 1$. We must then make the assumption (which is probably reasonable) that seniority is a good quantum number.

On the other hand, the wave function



which we may abbreviate to $(j^{2n})_0 j'$, contains no components wherein the $2n$ equivalent j nucleons are coupled to nonzero spin. This state is of precisely the sort envisaged by the Mayer-Jensen model, and may be referred to as a single-particle level of the second kind. It follows from (III.73) that the transition

$$(j^{2n})_0 j' \leftarrow (j^{2n})_0$$

has $S=1$, its reduced width being the single-particle width $\theta_0^2(l'j')$.

We expect to find single-particle levels of the second kind, with configurations $(f_{7/2}^{2n})_0 2p_{\frac{1}{2}}, (f_{7/2}^{2n})_0 2p_{\frac{3}{2}}$, among the low-lying¹⁹ levels of the Ca isotopes. Instead of the expected two such levels, we find in each of Ca⁴¹, Ca⁴³, and Ca⁴⁵, some half-dozen $l=1$ transitions, most of which are far short of single-particle strength. Indeed, the only two levels which can possibly be predominantly $(j^{2n})_0 j'$ are the $p_{\frac{1}{2}}$ levels at 1.947 Mev in Ca⁴¹ and at 2.048 Mev in Ca⁴³. The appearance of appreciably more transitions of given l than would be expected on the basis of simple counting is not necessarily indicative of a failure of the model used for the relevant nuclear states. Interactions between final states can give rise to a fragmentation of single-particle levels into several components, each of which may show a sizeable stripping width. This idea of spreading out a single-particle reduced width over a number of levels is the basis of Lane, Thomas, and Wigner's (La55) treatment of cross sections averaged over many resonances.

From the viewpoint of this study, the most significant property of a single-particle level (of the second kind) of a nucleus [A] is that it is connected to [$A-1$] by a transition with $S=1$. Our discussion has, until now, been confined to the case where A is odd and the relevant state of [$A-1$] is coupled to zero. It is clear from (III.73) that we can have transitions with $S=1$, involving an inequivalent nucleon, wherein neither of the restrictions just mentioned applies. It would be desirable to include such cases in our definition of single-particle level. For example, we would like to think of the K³⁹(d,p)K⁴⁰ transitions discussed in Example 3 as leading to single-particle levels. The necessary generalized definition, still in accordance with the physical picture discussed earlier, is given in Sec. III.10 in a manner which does not rely upon definite configuration assignments. It contains $(j^{2n})_0 j'$ as a special case and does not conflict with $(J^{2n+1})_{J=j}$.

¹⁹ By "low" we mean at an excitation of 5 Mev or less.

Concluding Remarks

In Secs. III.7-9, especially when working in jj representations, we concentrated much of our attention on the calculation of relative reduced widths between single basic states of pure configurations. It should now be clear that this imposes no limitations on the applicability of our results. If we can calculate these elementary constituents of reduced widths, the general case follows without difficulty by taking linear combinations in the manner described at the end of Sec. III.7. It is to be noted that the various contributions to the reduced width are coherent.

Finally, it is of interest to mention the possibility of working in a mixed LS and jj representation. For example, the $\frac{5}{2}^+$ and $\frac{7}{2}^+$ levels near 8 Mev in B¹¹, which we discuss in detail at the beginning of Sec. III.11, may be described in terms of a $1d_{\frac{5}{2}}$ or $2s_{\frac{1}{2}}$ nucleon coupled to the ground state of B¹⁰, whose wave function can be given in an LS representation.

10. Sum Rules and Related Topics

By using normalization and factorization properties of cfp, various sum rules for relative reduced widths can be written down from the expressions given in Secs. III.7 and III.8. In this section we discuss such rules, once again treating jj and $LSJT$ representations separately. The sum rule which we use most frequently emerges from the weak-coupling formalism to be described in Sec. III.11.

jj Representations

To begin with, let us use the direct-product notation described in Sec. III.3 and adopted throughout Sec. III.7. We deal with transitions between states of a single shell, phrasing our results so as to apply either to jj or to jjT representations. Specifically,

$$\begin{aligned}\rho &= (j, t=\frac{1}{2}) \text{ or } j, \\ \Gamma &= (x, J, T) \text{ or } (x, J), \\ \Gamma_0 &= (x_0, J_0, T_0) \text{ or } (x_0, J_0),\end{aligned}$$

where x and x_0 symbolize all necessary nonangular-momentum quantum numbers.

Rewriting (III.70), we have

$$S(n, \Gamma \rightarrow n-1, \Gamma_0) = n \langle \rho^n \Gamma | \rho^{n-1} \Gamma_0 \rangle^2. \quad (\text{III.119})$$

The condition that the relevant wave function $(\rho^n)\Gamma$ be normalized yields, as in (III.22),

$$\sum_{\Gamma_0} \langle \rho^n \Gamma | \rho^{n-1} \Gamma_0 \rangle^2 = 1.$$

Using this to sum over Γ_0 in (III.119), we obtain our first sum rule:

$$\sum_{\Gamma_0} S(n, \Gamma \rightarrow n-1, \Gamma_0) = n. \quad (\text{III.120})$$

From the standpoint of a (d,p) reaction, (III.120) involves a summation over initial states. It is, accordingly, of interest mainly²⁰ in connection with pickup reactions. More interesting would be a sum rule involving summation over Γ in (III.119), since this would concern final states in true stripping reactions, to which most available experiments refer. (See Table I.) A sum rule of the desired nature can be deduced from (III.120) with the aid of the hole-particle theorem (III.76) for relative reduced widths. In fact, rewriting (III.76) and summing over Γ , we have

$$\sum_{\Gamma} [\Gamma] S(n, \Gamma \rightarrow n-1, \Gamma_0) = [\Gamma_0] \sum_{\Gamma} S(N-n+1, \Gamma_0^c \rightarrow N-n, \Gamma^c).$$

The summation over Γ on the right-hand side can now be carried out by (III.120), giving a second sum rule

$$\sum_{\Gamma} [\Gamma] S(n, \Gamma \rightarrow n-1, \Gamma_0) = (N-n+1)[\Gamma_0], \quad (\text{III.121})$$

where $N = [\rho]$ is the number of particles in the complete ρ shell.

Let us now adopt a jjT representation, wherein further sum rules can be derived by expressing the cfp as products of spin-orbit and isotopic-spin factors. The factorized sum rules can be combined to reconstruct (III.120) and (III.121), as is seen explicitly in Example 3. Thus, the new sum rules really contain the ones already written down.

The wave functions for j^n are characterized by xJT , where x symbolizes irreducible representations of the symplectic group (Fl52) together with any additional quantum numbers which may be necessary. The value of T determines the transformation properties of the isotopic-spin part of the wave function under permutations in charge space and hence, through the exclusion principle, also the symmetry of the spin-orbit function. In fact, the isotopic-spin function transforms according to the irreducible representation of the symmetric group S_n corresponding to the partition $[\frac{1}{2}n+T, \frac{1}{2}n-T]$ of n , while the symmetry of the spin-orbit function is characterized by the partition $[2^{1/2}n-T, 1^{2T}]$ obtained by interchanging the rows and columns of $[\frac{1}{2}n+T, \frac{1}{2}n-T]$. The dimension of either of these irreducible representations is easily found from We46 (p. 201) to be

$$\nu = \frac{n!(2T+1)}{(\frac{1}{2}n+T+1)!(\frac{1}{2}n-T)!}. \quad (\text{III.122})$$

We now express the full wave functions as sums of products of spin-orbit and charge functions, each of which is separately normalized. Correspondingly, spin-orbit and charge cfp are defined by the appropriate

²⁰ Equation (III.120) also refers to a stripping reaction if the summation over Γ_0 reduces to a single term which corresponds to a ground state. We encounter such a situation, for example, in $\text{Mg}^{28}(p,d)\text{Mg}^{25}$ (g.s.), described in pure jj coupling.

modifications of (III.20), the full cfp also appearing as products.

This factorization procedure is well known in both LS and jj representations (Ja51, Ed52), following from a theorem enunciated and proved by Racah (Ra42). The description given in Secs. 2-4 of Ja51 is very thorough and readable; although it applies specifically to LST representations, only minor modifications in notation are necessary in carrying it over to the jjT case. The results we need are given in Ed52, Eqs. (1), (2), and (4). In using these equations, it should be noted that the summations over the symmetry quantum number for j^{n-1} (λ' in the notation of Ed52) in Eqs. (2) and (4) are redundant. This comes about because (again using the notation of Ed52) the Yamanouchi symbol k labeling the spin-orbit and charge functions for n particles determines the $n-1$ particle Yamanouchi symbol k' which is obtained from it by removing particle label # n ,²¹ k' , in turn, determines the irreducible representation λ' of S_{n-1} to which it belongs. Thus the summations over λ' each reduce to a single term. In particular, the isotopic-spin function is defined by Eq. (4) of Ed52, which reduces to a simple product. In fact,

$$\langle t^n T | t^{n-1} T_0 \rangle = \langle t^n T | t^{n-1} T_0 \rangle [(t^{n-1})_{T_0, k_0} \dot{\times} t(n)]_T, \quad (\text{III.123})$$

where the Yamanouchi symbols k and k_0 label particular functions of the basic sets which span the relevant ν , ν_0 -dimensional representations in isotopic-spin space of S_n and S_{n-1} , respectively. Since the isotopic spin functions are normalized, we have

$$\langle t^n T | t^{n-1} T_0 \rangle^2 = 1. \quad (\text{III.124})$$

The full cfp can then be written in the factorized form (Ja51, p. 503)

$$\langle j^n x J T | j^{n-1} x_0 J_0 T_0 \rangle = (\nu_0/\nu)^{\frac{1}{2}} \langle j^n x J(T) | j^{n-1} x_0 J_0(T_0) \rangle \times \langle t^n T | t^{n-1} T_0 \rangle, \quad (\text{III.125})$$

where, according to (III.124), $\langle t^n T | t^{n-1} T_0 \rangle$ has only two possible values, namely, +1 or -1. The bracketed symbols T and T_0 in the spin-orbit cfp label the symmetry of the corresponding functions in the manner just described. The dimensions ν and ν_0 of the relevant irreducible representations of the symmetric group are given by (III.122).

Again we start from (III.70) using (III.125) to express the spectroscopic factor in the form

$$\begin{aligned} S(n, x J T \rightarrow n-1, x_0 J_0 T_0) \\ = n(\nu_0/\nu) \langle j^n x J(T) | j^{n-1} x_0 J_0(T_0) \rangle^2. \end{aligned} \quad (\text{III.126})$$

By using (III.124) and the normalization condition

$$\sum_{x_0 J_0} \langle j^n x J(T) | j^{n-1} x_0 J_0(T_0) \rangle^2 = 1$$

of the spin-orbit functions, we can sum over $x_0 J_0$ in

²¹ Yamanouchi symbols and their significance in the present context are described in Sec. 1 of Ja51.

(III.126) to obtain a third sum rule

$$\sum_{x_0 J_0} S(n, xJ T \rightarrow n-1, x_0 J_0 T_0) = n(\nu_0 / \nu). \quad (\text{III.127})$$

Another sum rule follows from (III.127) in the same way as (III.121) was obtained from (III.120). Rewriting (III.76) and summing over xJ , we have

$$\begin{aligned} \sum_{xJ} [J] S(n, xJ T \rightarrow n-1, x_0 J_0 T_0) \\ = \left[\frac{J_0 T_0}{T} \right] \sum_{xJ} S(N-n+1, x_0^c J_0 T_0 \rightarrow N-n, x^c J T). \end{aligned}$$

Equation (III.127) can now be used to perform the summation over xJ on the right-hand side, giving a fourth sum rule:

$$\begin{aligned} \sum_{xJ} [J] S(n, xJ T \rightarrow n-1, x_0 J_0 T_0) \\ = \frac{\nu^c}{\nu_0^c} (N-n+1) \left[\frac{J_0 T_0}{T} \right], \quad (\text{III.128}) \end{aligned}$$

where

$$\begin{aligned} \nu^c &= \frac{(N-n)!(2T+1)}{\left[\frac{1}{2}(N-n)+T+1 \right]! \left[\frac{1}{2}(N-n)-T \right]!}, \\ \nu_0^c &= \frac{(N-n+1)!(2T_0+1)}{\left[\frac{1}{2}(N-n+1)+T_0+1 \right]! \left[\frac{1}{2}(N-n+1)-T_0 \right]!}. \end{aligned}$$

The sum rules (III.127) and (III.128) can be further refined by splitting the spin-orbit cfp into two factors. We have already stated that x stands for irreducible representations σ of the symplectic group $Sp(2j+1)$, together with any other quantum numbers which may be necessary. In other words, $x = (\sigma\alpha)$. The factorization in question, which follows from a theorem of Racah (Ra49), is expressed by Edmonds and Flowers (Ed52) in the form

$$\begin{aligned} \langle j^n xJ(T) | j^{n-1} x_0 J_0(T_0) \rangle &= \langle \sigma(T) | \sigma_0(T_0) \rangle \\ &\times \langle \sigma\alpha J | \sigma_0\alpha_0 J_0 \rangle, \quad (\text{III.129}) \end{aligned}$$

where the first factor is independent of α and J , the second of the representation (T) of the symmetric group to which α and J belong. The two terms in (III.129) are exhibited separately in the tables of cfp in Ed52. They obey the normalization conditions

$$\sum_{\sigma} \langle \sigma(T) | \sigma_0(T_0) \rangle^2 = 1, \quad (\text{III.130})$$

$$\sum_{\alpha_0 J_0} \langle \sigma\alpha J | \sigma_0\alpha_0 J_0 \rangle^2 = 1, \quad (\text{III.131})$$

which combine to give the normalization condition for $\langle j^n xJ(T) | j^{n-1} x_0 J_0(T_0) \rangle$.

On substituting (III.129) for the spin-orbit cfp in the expression (III.126) for the relative reduced width, and summing over $\alpha_0 J_0$ by means of (III.131), we

obtain a fifth sum rule:

$$\begin{aligned} \sum_{\alpha_0 J_0} S(n, \sigma\alpha J T \rightarrow n-1, \sigma_0\alpha_0 J_0 T_0) \\ = \frac{\nu_0}{\nu} \langle \sigma(T) | \sigma_0(T_0) \rangle^2. \quad (\text{III.132}) \end{aligned}$$

The technique whereby a sixth sum rule can be obtained from (III.132) has already been described twice, following (III.120) and (III.127). We need reciprocity theorems connecting the factors of the spin-orbit cfp with their complements. Such theorems depend on the fact (We28, p. 281; Fl52) that n -particle spin-orbit functions which spread out the irreducible representation of the symmetric group labeled by the partition $[2^{\frac{1}{2}n-T}, 1^{2T}]$, also transform according to that irreducible representation of the unimodular unitary group $SU(2j+1)$ which is characterized by the partition in question. They are special cases of a general theorem connecting the coefficients which reduce a product of contragredient representations with the coefficients reducing the original product representation (see Ja51, p. 518). In the present case, we have

$$\frac{\langle \sigma_0^c \alpha_0^c J_0 | \sigma^c \alpha^c J \rangle}{\langle \sigma\alpha J | \sigma_0\alpha_0 J_0 \rangle} = (-1)^{J+J_0+j} \left[\frac{J}{J_0} \right]^{\frac{1}{2}} \left(\frac{d'(\sigma_0)}{d'(\sigma)} \right)^{\frac{1}{2}}, \quad (\text{III.133})$$

$$\frac{\langle \sigma_0^c(T_0) | \sigma^c(T) \rangle}{\langle \sigma(T) | \sigma_0(T_0) \rangle} = \left(\frac{d^{2j+1}(T_0)}{d^{2j+1}(T)} \cdot \frac{d'(\sigma)}{d'(\sigma_0)} \right)^{\frac{1}{2}}, \quad (\text{III.134})$$

where $d^{(2j+1)}(T)$ is the dimension of the irreducible representation $[2^{\frac{1}{2}n-T}, 1^{2T}]$ of $SU(2j+1)$, $d'(\sigma)$ being the dimension of the irreducible representation σ of $Sp(2j+1)$.

On multiplying (III.133) and (III.134), we obtain the reciprocity theorem satisfied by the spin-orbit cfp. It contains no reference to the dimensions of representations of the symplectic group. If we then multiply this reciprocity theorem for the spin-orbit cfp by the corresponding result,

$$\langle t^{N-n+1} T_0 | t^{N-n} T \rangle / \langle t^n T | t^{n-1} T_0 \rangle = (-1)^{T+T_0+\frac{1}{2}}, \quad (\text{III.135})$$

for the isotopic-spin cfp, introduce the correct weight factors as in (III.125), and use (III.122) and We28 (p. 383) for the various dimension factors which occur, we arrive at the hole-particle theorem (III.41) for the full cfp. This provides a useful check on our procedure.

To obtain the sixth and final sum rule, we write down (III.76) summed over αJ , using (III.132) to carry out the summation on the right-hand side of the equation. α symbolizes all quantum numbers necessary in addition to σ , J , and T . We have, then,

$$\begin{aligned} \sum_{\alpha J} [J] S(n, \sigma\alpha J T \rightarrow n-1, \sigma_0\alpha_0 J_0 T_0) \\ = (N-n+1) \left[\frac{J_0 T_0}{T} \right] \frac{\nu^c}{\nu_0^c} \langle \sigma_0^c(T_0) | \sigma^c(T) \rangle^2. \quad (\text{III.136}) \end{aligned}$$

For transitions in the second half of a shell this result is convenient as it stands. In the first half of a shell we can use (III.134) to write, alternatively,

$$\begin{aligned} \sum_{\alpha J} [J] S(n, \sigma \alpha J T \rightarrow n-1, \sigma_0 \alpha_0 J_0 T_0) \\ = (N-n+1) \left[\frac{J_0 T_0}{T} \right]^{\nu^c} \frac{d^{(2j+1)}(T_0)}{d^{(2j+1)}(T)} \cdot \frac{d'(\sigma)}{d'(\sigma_0)} \\ \times \langle \sigma(T) | \sigma_0(T_0) \rangle^2. \quad (\text{III.137}) \end{aligned}$$

The dimensions of irreducible representations of $SU(2j+1)$ and $Sp(2j+1)$, which are commonly of interest in practical applications, are listed by Flowers (Fl52), Tables I and III, respectively.

In a true stripping reaction, the differential cross section is proportional to $[J]\theta^2$. Only if the spin of the relevant final state is known can the actual reduced width be extracted. On inspection of the sum rules, however, we see that (III.121), (III.128), and (III.137), which refer to final states in stripping reactions, already have the spin factor $[J]$ inside the summation. They have the form $\sum [J]S$. On the other hand, no spin statistical factors appear in the expression for the differential cross section of a pickup reaction, the reduced width θ^2 emerging directly. Correspondingly, the pickup sum rules (III.120), (III.127), and (III.132) contain no spin factors, having the form $\sum S$.

Thus, the statistical factors in the cross section and the internal spin factors in the relative reduced width are intimately related. We encounter this connection in other parts of this study, notably in connection with hole-particle theorems for reduced widths and in the discussion of Example 2 in this section. The various factors combine in such a way that the sum rules can be applied even if the spins of the final states concerned are unknown. Indeed, the possibility is opened of using our sum rules in discussing unresolved or poorly resolved groups of final states. It should also be noted that sum rules can sometimes be used when, because of ignorance of spins, we cannot proceed by calculating individual spectroscopic factors.

Sum Rules for More Complicated Configurations

We saw in Secs. III.7 and III.8 that the form of the hole-particle theorem for relative reduced widths [(III.76) and (III.103)] is the same in jj and LS representations, and that, moreover, it is not disturbed by the presence of inactive groups of nucleons with nonzero total spin. Let us now examine the corresponding situation for sum rules. We find again that the extra recoupling coefficients have the effect of replacing the spins of the active groups by the total spins, the form of the sum rules remaining the same as before.

Consider the transition

$$\sum_{\Gamma} S(n, \sigma_0 \alpha_0 J_0 T_0 \rightarrow n-1, \beta_2 \Gamma_0) \rightarrow \left\{ \sum_{\Gamma_0} S(n, \sigma_0 \alpha_0 J_0 T_0 \rightarrow n-1, \beta_2 \Gamma_0) \right\}_{\Gamma} \quad (\text{III.138})$$

for which, according to (III.64),

$$S = n_2 U(\alpha_1 \beta_2 \Gamma \rho_2 : \Gamma_0 \alpha_2)^2 \langle \rho_2^{n_2} \alpha_2 | \rho_2^{n_2-1} \beta_2 \rangle^2. \quad (\text{III.139})$$

The summation over Γ_0 is immediate, yielding

$$\sum_{\Gamma_0} S(n, \alpha_2 \Gamma \rightarrow n-1, \beta_2 \Gamma_0) = n_2 \langle \rho_2^{n_2} \alpha_2 | \rho_2^{n_2-1} \beta_2 \rangle^2.$$

We can now sum over β_2 as before, using the normalization of $\langle \rho_2^{n_2} \rangle_{\beta_2}$, whence

$$\sum_{\beta_2 \Gamma_0} S(n, \alpha_2 \Gamma \rightarrow n-1, \beta_2 \Gamma_0) = n_2, \quad (\text{III.140})$$

of the same form as (III.120).

To obtain the sum rule for α_2 and Γ , let us first note that

$$U(\alpha_1 \beta_2 \Gamma \rho_2 : \Gamma_0 \alpha_2)^2 = [\Gamma_0 \alpha_2 / \Gamma \beta_2] U(\alpha_2 \alpha_1 \rho_2 : \Gamma \beta_2)^2,$$

so that

$$\begin{aligned} \sum_{\Gamma} [\Gamma] S(n, \alpha_2 \Gamma \rightarrow n-1, \beta_2 \Gamma_0) \\ = n_2 [\Gamma_0 \alpha_2 / \Gamma \beta_2] \langle \rho_2^{n_2} \alpha_2 | \rho_2^{n_2-1} \beta_2 \rangle^2 \\ = (N_2 - n_2 + 1) [\Gamma_0] \langle \rho_2^{N_2 - n_2 + 1} \beta_2 | \rho_2^{N_2 - n_2} \alpha_2 \rangle^2, \end{aligned}$$

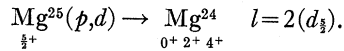
the second step using (III.41). The normalization of the cfp then leads to

$$\begin{aligned} \sum_{\Gamma \alpha_2} [\Gamma] S(n, \alpha_2 \Gamma \rightarrow n-1, \beta_2 \Gamma_0) \\ = (N_2 - n_2 + 1) [\Gamma_0], \quad (\text{III.141}) \end{aligned}$$

of exactly the same form as (III.121). The four additional sum rules obtained by factorizing the cfp can obviously be derived as before.

We conclude that the way in which statistical factors in the cross section keep step with spin factors in the reduced width is not spoiled by the presence of inactive groups of nucleons, even if these are not coupled to zero.

Example 1.



The transitions in question to the three lowest states of Mg^{24} have been studied experimentally by Bennett (Be58). The transition to the 4^+ level, however, was not definitely resolved. We assume that Bennett's third deuteron group corresponds entirely to the 4^+ state for the purposes of this example.²² We use the

²² We return to this matter in Sec. V. (a) Physically, this may not be a good approximation. Our main interest here is in showing how the sum rules work.

isotopic-spin formalism and assume that jj coupling is a reasonable approximation. This is a procedure of uncertain accuracy in the mass region in question, but we can hardly avoid adopting it in order to be able to treat the foregoing reactions within the framework of the shell model.

The transitions in which we are interested are

$$(d_{\frac{5}{2}}^{-3})_{\frac{5}{2}, T=\frac{1}{2}} \rightarrow (d_{\frac{5}{2}}^{-4})_{J_0, T_0=0}.$$

The unfactorized sum rule (III.120) does not interest us here because it includes $T_0=1$ states. We therefore start by considering the first factorized sum rule (III.127), which connects states of fixed isotopic spin.

$(d_{\frac{5}{2}}^{-3})_{J_0, T_0=\frac{1}{2}}$ contains two states, with $\sigma=(100)$ and (210) (Fl52). We further assume that symplectic symmetry is a good quantum number and agree to describe the Mg^{25} ground state by $J=\frac{5}{2}$, $T=\frac{1}{2}$, $\sigma=(100)$.^{22a}

$(d_{\frac{5}{2}}^{-4})_{J_0, T_0=0}$ includes thirteen states:

$$\begin{aligned} \sigma_0 = (000) & \quad J=0 \\ (110) & \quad 2 \ 4 \\ (220) & \quad 0 \ 2^2 \ 3 \ 4^2 \ 5 \ 6^2 \ 8. \end{aligned} \quad (\text{III.142})$$

Let us, then, apply (III.127), with $n=9$, and

$$\nu/\nu_0 = \nu(n=9, T=\frac{1}{2})/\nu_0(n=8, T_0=0) = \frac{1}{3} \text{ from } (\text{III.122}). \text{ Therefore,}$$

$$\sum_{\sigma_0 J_0}^{(T_0=0)} S(\sigma_0 J_0) = 9 \cdot \frac{1}{3} \cdot 1 = 3, \quad (\text{III.143})$$

the summation extending over all 13 states (III.142). We omit the additional symbol α_0 in (III.143) because, as we see, $\sigma_0=(220)$ does not enter, the remaining states being completely specified by σ_0 and J_0 .

Next we pass on to the doubly factorized sum rule (III.132), which connects states of fixed isotopic spin and also of fixed symplectic symmetry. First, consider $T=\frac{1}{2}$, $\sigma=(100) \Rightarrow T_0=0$, $\sigma_0=(000)$. The final state being unique, we obtain a direct evaluation of a relative reduced width. We have already evaluated all the factors in (III.132) except $\langle (100)[54] | (000)[44] \rangle^2$, where we introduce the partition $[\frac{1}{2}n+T, \frac{1}{2}n-T]$ instead of T . With the help of (III.134), Tables I and III of Fl52, and the cfp of Ed52, we have

$$\begin{aligned} \langle (100)[54] | (000)[44] \rangle^2 &= \frac{d^{(6)}[(21)]d'(000)}{d^{(6)}[(22)]d'(100)} \langle (000)[22] | (100)[21] \rangle^2 \\ &= 70/156 \cdot \frac{1}{6} \cdot 1 = \frac{1}{9}. \end{aligned}$$

Thus

$$S[(000)0] = S_0 = \frac{1}{9} \cdot 3 = \frac{1}{3}. \quad (\text{III.144})$$

Similarly, for $T=\frac{1}{2}$, $\sigma=(100) \rightarrow T_0=0$, $\sigma_0=(110)$, we need

$$\langle (100)[54] | (110)[44] \rangle^2 = 8/9,$$

whence

$$S_2 + S_4 = 8/3. \quad (\text{III.144}')$$

Equations (III.144), (III.144'), and (III.143) then yield

$$\sum_{\sigma_0 J_0}^{(T_0=0)} S(\sigma_0 J_0) = 3. \quad (\text{III.145})$$

It is clear, from a comparison of (III.143) and (III.145), that the other 10 states in (III.142) do not contribute. Obviously, the transitions $(100) \rightarrow (220)$ must be forbidden by a selection rule. The nature of this selection rule, however, is easy to find; quite generally, from the reduction of the direct product

$$(\sigma_1 \sigma_2 \sigma_3 \cdots \sigma_k) \times (100 \cdots 0)$$

of irreducible representations of $Sp(2k)$, $(\sigma_1 \sigma_2 \sigma_3 \cdots \sigma_k)$ can only be connected to those representations of the set $(\sigma_1+1, \sigma_2, \dots, \sigma_k)$, $(\sigma_1, \sigma_2+1, \dots, \sigma_k)$, $(\sigma_1, \sigma_2, \dots, \sigma_k+1)$ which are allowed²³ (see Fl52, also We46, p. 218).

The observed ground-state reduced width (Be58) is $\theta_g^2 = 0.008$, whence, using $S_g = \frac{1}{3}$ from (III.144), we have $\theta_g^2(1d) \approx 0.024$ for the relevant single-particle reduced width. This value is in satisfactory agreement with other estimates in this mass region.

The situation is much less satisfactory for the 2^+ and 4^+ states. The observed reduced widths (Be58) give

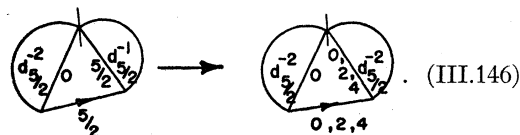
$$\theta_2^2 + \theta_4^2 = 0.022 + 0.012 = 0.034 \approx 4.5 \theta_g^2,$$

which is to be compared with

$$S_2 + S_4 = 8S_g$$

from (III.144) and (III.144'). It is not clear to what extent this discrepancy is due to the crudity of the model or to uncertainties in the experiment and its interpretation. A remeasurement of the $J_0=4$ reduced width, resolving the two levels around 4.2 Mev in Mg^{24} , would be valuable.

If we wanted to treat neutrons and protons separately, we might make the further approximation, a very common but doubtful one, of neglecting excitations of the even group of protons in the Mg isotopes. The transition in question would then be



Applying the unfactorized sum rule (III.120) without isotopic spin yields

$$S_0' + S_2' + S_4' = 5, \quad (\text{III.147})$$

quite different from (III.145). The difference is due to the fact that, in (III.146), the relevant states are represented by wave functions quite different from the ones

²³ $(\sigma_1 \sigma_2 \cdots \sigma_k)$ is said to be allowed if $\sigma_1 \geq \sigma_2 \geq \cdots \geq \sigma_k$. In jjT representations we are interested only in cases where $\sigma_i \leq 2$.

used in the earlier part of this discussion. They are, in fact, unacceptable because they do not possess definite isotopic spin. We encounter a similar situation in Example 4.

Example 2. Fluctuations in reduced widths. The sum rules (III.120) and (III.121) yield expressions for individual reduced widths when the summations reduce to a single term. Let us make use of this property to demonstrate fluctuations in S throughout a shell.

Consider identical nucleons without isotopic spin. The essential point is that $(j^{2n})_{J=v=0}$ is linked, in both stripping and pickup, to the unique seniority $v=1$ states with $J=j$ of the adjacent odd configuration nuclei.

Apply (III.121) to the transition $(j^{2n+1})_{J=j} \rightarrow (j^{2n})_0$, where we omit the seniority labels. Noting that $N=2j+1$, we have

$$(2j+1)S(2n+1 \rightarrow 2n) = (2j+1) - 2n \quad (\text{III.148})$$

or

$$S(2n+1 \rightarrow 2n) = 1 - [2n/(2j+1)].$$

Equation (III.120) yields, in similar fashion, the relative reduced width for the transition $(j^{2n})_0 \rightarrow (j^{2n-1})_{J=j}$:

$$S(2n \rightarrow 2n-1) = 2n. \quad (\text{III.149})$$

Thus, for the chain of transitions

$$(nJ) = (00) \leftarrow (1j) \leftarrow (20) \leftarrow (3j) \dots \text{etc.},$$

expressions (III.148) and (III.149) combine to give

$$\begin{aligned} S(n \rightarrow n-1) &= n \quad (n \text{ even}), \\ S(n \rightarrow n-1) &= 1 - [(n-1)/(2j+1)] \quad (n \text{ odd}). \end{aligned} \quad (\text{III.150})$$

For $j=\frac{7}{2}$, the sequence of S values so obtained is

$$S = 1, 2, \frac{3}{4}, 4, \frac{1}{2}, 6, \frac{1}{4}, 8.$$

We have, incidentally, rederived two earlier results.

(1) Putting $n=N=(2j+1)$ in (III.123), we find $S=N$ for a transition in which a shell is completed. This was pointed out in connection with Example 4, Sec. III.9.

(2) The chain of S values for $j=\frac{7}{2}$ includes the three S values $(1, \frac{3}{4}, \frac{1}{2})$ connecting ground states in the Ca experiments, mentioned in Example 5, Sec. III.9.

Although a transition in which a hole is filled has $S=N$, it does not have a correspondingly larger cross section than a transition involving a single particle. This comes about through the influence of the spin factors in the expression for the differential cross section (see Sec. II.2). Let us, then, compare single-particle and single-hole transitions at opposite ends of the j shell. On omitting everything but the relative reduced width and the spin factors, we have, at the end of the shell,

$$\begin{aligned} \sigma^{d,p}(j^{N+1} + j \rightarrow j^N) &\propto (2j+1)^{-1} S(N \rightarrow N-1) = 1, \\ \sigma^{p,d}(j^N \rightarrow j^{N-1} + j) &\propto S(N \rightarrow N-1) = 2j+1, \end{aligned} \quad (\text{III.151})$$

the p,d cross section involving no spin factors. For the

corresponding transitions involving a single particle,

$$\begin{aligned} \sigma^{d,p}(j^0 + j \rightarrow j) &\propto (2j+1)S(1 \rightarrow 0) = 2j+1, \\ \sigma^{p,d}(j \rightarrow j^0 + j) &\propto S(1 \rightarrow 0) = 1. \end{aligned} \quad (\text{III.152})$$

The cross sections, from (III.151) and (III.152), are therefore in one-one correspondence in spite of the difference in reduced widths. Notice that in a pickup transition involving a single hole no cancellation can occur and the large reduced width manifests itself as a correspondingly large cross section.

In a true stripping reaction, on the other hand, the compensation by spin factors of the large reduced width associated with the filling of a shell is inescapable. To make this point clear, consider the transition²⁴

$$\{ \quad \text{final state} \quad \} \quad (\text{III.153})$$

wherein we might hope to avoid the cancellations of (III.151) and (III.152). Expression (III.139) can be reduced to the case $j_2^{N_2} \rightarrow j_2^{N_2-1} + j_2$ by means of a single recoupling whose Racah coefficient is

$$U(j_1 j_2 j_1 j_2; J0).$$

The relative reduced width for (III.153) is, accordingly,

$$\begin{aligned} S(j_1^{N_1-1}, j_2^{N_2}, j_1 \rightarrow j_1^{N_1-1}, j_2^{N_2-1}, J) \\ = [J/j_1 j_2] [j_2] = [J/j_1] \end{aligned} \quad (\text{III.154})$$

using (III.139) and the explicit value of the squared Racah coefficient. The differential cross section for the transition (III.153) is therefore

$$\sigma^{d,p} \propto [j_1/J] S_1 = 1,$$

from (III.154). Thus, although cancellation can no longer be supplied by the total spin factors, the deficiency is made up by the additional recoupling coefficient.

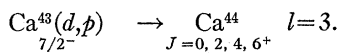
Experimental results with a bearing on the predictions of (III.136) are disappointingly scarce. The predicted large reduced width ($S=8$) does seem to be observed in $B^{11}(d,n)C^{12}$ (g.s.) (Ma56), but not, apparently in $Al^{27}(d,n)Si^{28}$ (Ru57); or $P^{31}(d,n)S^{32}$ (Ca55). The ground-state reduced width for $Mg^{25}(d,p)Mg^{26}$ is between five and six times that for $Mg^{24}(d,p)Mg^{25}$ (Ho53d). The S values predicted by (III.150) for the tail of the $j=\frac{5}{2}$ chain being $\frac{1}{3}$ and 6, the observed fluctuation is in the expected direction but considerably smaller. In view of the approximations involved (see Example 1, Sec. III.10), this result is quite encouraging.

²⁴ The ensuing argument is the same if we replace $j_1^{N_1-1}$ by j_1 . The essential point is that the separate neutron and proton states are unique, the doubtful "odd-group assumption" (see Example 4) being, therefore, unnecessary.

The best prospect for improving this situation and of testing (III.150) is probably furnished by the Ca isotopes. We have already seen that the (d,p) experiments on Ca⁴⁰, Ca⁴², and Ca⁴⁴ yield ground-state reduced widths in satisfactory agreement with the S values of 1, $\frac{3}{4}$, and $\frac{1}{2}$ predicted by (III.150) with $n=1, 3$, and 5, respectively. Expression (III.150) gives $S=2$ and $S=4$, respectively, for the ground-state (p,d) or (d,t) transitions on Ca⁴² and Ca⁴⁴. These transitions should be quite easy to observe.

By assuming that symplectic symmetry is a good quantum number and considering transitions connecting unique states of lowest symplectic symmetry, we could exhibit similar fluctuations throughout a shell containing both neutrons and protons, using the isotopic-spin formalism. We do not go into this matter here because of the lack of pertinent experimental data and because the qualitative features are the same as in the case of identical nucleons.

Example 3.



We first use (III.121) without the isotopic-spin formalism. Noting that $(f_{7/2}^3)_{7/2}$ necessarily has good seniority $v_0=1$ (there are no other $\frac{7}{2}$ states in $f_{7/2}^3$), the transitions are

$$(f_{7/2}^4)_{Jv} \leftarrow (f_{7/2}^3)_{7/2} \quad v=1.$$

The selection rule $\Delta v=1$ limits the $f_{7/2}^4$ states of interest to $v=0$, $J=0$, and $v=2$, $J=2, 4, 6$. Noting that $n=4$, $N=8$, (III.120) yields

$$\sum_{J=0,2,4,6} [J]S_J = 40. \quad (\text{III.155})$$

Since $S_0=4$ (from Example 2), we have also a sum rule for $v=2$ states:

$$\sum_{J=2,4,6}^{(v=2)} [J]S_J = 36. \quad (\text{III.156})$$

Let us now verify that, introducing the isotopic-spin formalism and applying the factorized sum rule (III.128) to transitions between states of maximum isotopic spin ($T=2$, $T_0=\frac{3}{2}$), we simply rederive (III.155). The result is so obvious that we are really checking the consistency of our sum rules.

On applying (III.128) to

$$(f_{7/2}^4)_{T=2, J=0} \leftarrow (f_{7/2}^3)_{T_0=3/2, J_0=7/2^-},$$

we note that the summation again contains $J=0, 2, 4$, and 6. Since $N=16$, $n=4$, and

$$\begin{aligned} \nu^e/\nu_0^e &= \nu^e(N-n=12, T=2)/\nu_0^e(N-n+1=13, T_0=\frac{3}{2}) \\ &= 25/4.13 \end{aligned}$$

[from (III.122)], (III.128) gives

$$\sum_{J=0,2,4,6} [J]S_J = 13 \cdot \frac{8.4}{5} \cdot \frac{25}{4.13} \cdot 1 = 40, \quad (\text{III.156}')$$

which agrees with (III.155).

There is a similar sum rule for transitions to $T=1$ states, which would appear in $\text{Ca}^{43}(d,n)\text{Sc}^{44}$. Expression (III.128) gives, for the transitions

$$(f_{7/2}^4)_{T=1} \leftarrow (f_{7/2}^3)_{T_0=3/2, J_0=7/2},$$

$$\sum_{J(T=1)} [J]S_J = 13 \cdot \frac{8.4}{3} \cdot \frac{27}{4.13} \cdot 1 = 72. \quad (\text{III.157})$$

We conclude our discussion of this example by verifying that the $T=1$ sum rule (III.157) and the $T=2$ sum rule (III.156) combine to give the result obtained with the aid of the unfactorized sum rule (III.121). In fact, from (III.157) and (III.156),

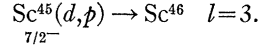
$$\begin{aligned} \sum_{J,T=1,2} [JT]S_{JT} &= 3 \sum_{J(T=1)} S_J + 5 \sum_{J(T=2)} S_J \\ &= 216 + 200 = 416, \quad (\text{III.158}), \end{aligned}$$

while (III.121), with $[\Gamma_0] = [J_0 T_0] = 8.4$, yields

$$\sum_{J,T=1,2} [JT]S_{JT} = 13.32 = 416, \quad (\text{III.159})$$

the same result as before.

Example 4.



There is no pertinent experimental data, although $\text{Sc}^{45}(d,p)\text{Sc}^{46}(\text{g.s.})$ has been observed. (See Wa55 for references.) Using the isotopic-spin formalism, the transitions under consideration are

$$(f_{7/2}^6)_{T=2} \leftarrow (f_{7/2}^5)_{T_0=3/2, J_0=7/2, \sigma_0=(1000)},$$

connecting states of the lowest isotopic spin ($\frac{3}{2}$ and 2, respectively) in Sc⁴⁵ and Sc⁴⁶. We assume that symplectic symmetry is a good quantum number. Possible final states are (Fl52)

$$\begin{aligned} \sigma &= (2000) \quad J=1, 3, 5, 7 \\ \sigma &= (1100) \quad J=2, 4, 6. \end{aligned}$$

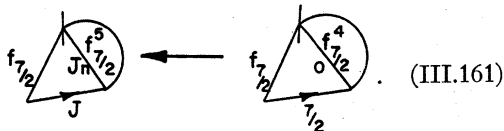
Other $T=2$ states of $f_{7/2}^6$ are forbidden by the symplectic selection rule encountered in Example 1 and, in some cases, by conservation of angular momentum. Expression (III.128) then yields, with an obvious notation,

$$\sum_{J=1}^7 [J]S_J = 11 \cdot \frac{5}{11} \cdot \frac{8.4}{5} = 32. \quad (\text{III.160})$$

We notice that none of the final states in (III.160) has $J=0$; in fact, $(f_{7/2}^6)_{T=2}$ contains no $J=0$ levels. Since Sc⁴⁶ has $T=2$, we are interested only in $T=2$ and

$T=3$. The unique state $(f_{7/2}^6)_{T=3, J=0}$ is thus the only $J=0$ state of Sc^{46} which can arise from $f_{7/2}^6$.

Let us now consider the $l=3$ transitions in $\text{Sc}^{46}(d, p)$ - Sc^{46} without the isotopic-spin formalism. In order to write down comparably simple wave functions for the relevant nuclear states, we assume that the total angular momenta J_p and J_n of protons and neutrons are, separately, good quantum numbers. This assumption was mentioned briefly in Example 1. The transitions in question are now represented by



The relative reduced width for this transition is

$$5U(\frac{7}{2}0J\frac{7}{2}; \frac{7}{2}J_n)^2 \langle f_{7/2}^6 J_n | f_{7/2}^6 40 \rangle^2,$$

and is zero unless $J_n = \frac{7}{2}$. There are, accordingly, eight final states with $J=0, 1, 2, 3, 4, 5, 6, 7$, each being connected to the five-particle state in (III.161) by a transition with $S=\frac{1}{2}$. We have the sum rule

$$\sum_{J=0}^7 [J] S_J = \frac{1}{2} \sum_{J=0}^7 [J] = 32. \quad (\text{III.162})$$

In spite of the fact that the right-hand sides are the same, the sum rules (III.160) and (III.162) are quite different. In particular, (III.162) contains a $J=0$ state which does not appear in (III.160).

Since, as we have remarked before, there is only one $J=0$ state of $f_{7/2}^6$ with $T=2$, this unique state having $T=3$, we must have

Now this state cannot be attained by transfer of a single nucleon from any state with $T_0 = \frac{3}{2}$; furthermore, we have seen that it is connected to

by a transition with $S=\frac{1}{2}$. We are therefore forced to the conclusion that the function (III.164) is not a pure $T=\frac{3}{2}$ state. The relative reduced widths can be used, as we now show, to evaluate the percentage of $T=\frac{5}{2}$ in (III.164).

Start by writing $\alpha(f_{7/2}^6)_{T_0=3/2} + \beta(f_{7/2}^6)_{T_0=5/2}$ for (III.164). Only the $T_0=\frac{5}{2}$ component can contribute

to the relative reduced width. Thus,

$$S = \{C[\frac{5}{2} \frac{1}{2} 3; \frac{3}{2} \frac{1}{2} 2]\}^2 S[(f_{7/2}^6)_{(TJ)=(30)} \leftarrow$$

$$(f_{7/2}^5)_{(T_0J_0)=5/2 7/2}] \cdot \beta^2 \quad (\text{III.165})$$

$$= \frac{5}{6} \cdot 6(f_{7/2}^6(30) | f_{7/2}^5(\frac{5}{2} \frac{7}{2}))^2 \cdot \beta^2 = 5\beta^2. \quad (\text{III.166})$$

The second step uses (III.70): The third step follows from the fact that the cfp is of magnitude unity because of the uniqueness of the states involved. The isotopic-spin coupling factor takes account of the difference in the spectroscopic factors appropriate to reduced widths extracted with and without the isotopic-spin formalism.

We have already found, by direct evaluation, that this relative reduced width is simply $\frac{1}{2}$. By using (III.166), then, we have

$$\beta^2 = \frac{1}{10}. \quad (\text{III.167})$$

The conclusion is, in other words, that the wave function (III.164) is 90% $T_0 = \frac{3}{2}$ and 10% $T_0 = \frac{5}{2}$.

It is interesting to verify this result by considering the operator T^2 , which, operating on n -nucleon wave functions, can be written in the form

$$T^2 = \frac{1}{4} [n(4-n)] - \sum_{i < j=1}^n P_{ij}, \quad (\text{III.168})$$

where P_{ij} exchanges the space and spin coordinates of nucleons i and j . This form for the "square of the isotopic-spin operator" has a meaning even if the isotopic-spin formalism is not used. The eigenfunctions of (III.168) are, by definition, "states of definite isotopic spin."

The expectation value of T^2 in the state (III.164) can now be calculated in straightforward fashion. The result, which we state with proof because the details are of no interest to the present study, is

$$\langle T^2 \rangle = 17/4. \quad (\text{III.169})$$

By inserting $\alpha\psi(T_0 = \frac{3}{2}) + \beta\psi(T_0 = \frac{5}{2})$ instead of (III.164), we find

$$\langle T^2 \rangle = (15/4)\alpha^2 + (35/4)\beta^2, \quad (\text{III.170})$$

since the expectation value of T^2 in $T_0 = \frac{3}{2}, \frac{5}{2}$ states is $15/4$ and $35/4$, respectively. By using (III.169), (III.170), and the normalization condition, we have two simultaneous equations,

$$(15/4)\alpha^2 + (35/4)\beta^2 = 17/4, \quad \alpha^2 + \beta^2 = 1, \quad (\text{III.171})$$

for the squared amplitudes. The solutions, $\alpha^2 = 9/10$ and $\beta^2 = 1/10$, are exactly what was obtained in the foregoing from the reduced width connecting (III.163) and (III.164).

It should be noted that the possibility of obtaining the percentage isotopic-spin composition of a wave function by considering only a single reduced width, or by evaluating only the expectation value of T^2 in the state in question, depends on the existence of only two possible values of T . When there are more than

two possibilities, or whenever we wish either to evaluate the amplitudes rather than their squares, or, equivalently, to construct explicit states of definite isotopic spin in terms of functions such as (III.163) or (III.164), we must construct the matrix of T^2 and diagonalize it.

The example illustrates the point that a wave function in which neutrons and protons separately possess specified angular momentum may not have a definite isotopic spin. Since there is no evidence to suggest that isotopic spin is not an approximately good quantum number for the low-lying states of all nuclei of interest in the present study (with A less than about 70), such functions may be unacceptable. (In the example just discussed the isotopic-spin impurity is quite small.) There is no reason why such functions may not be used as the basis of a representation, if it be so desired.

Practical applications of the jj sum rules we have been discussing are severely limited by the lack of pertinent experiments. We have seen that, for true stripping reactions on even-even targets, our sum rules result in the direct evaluation of the relevant ground state reduced width. To find cases with more content, we must consider pickup reactions or stripping on odd- A targets. It can be seen from Table I that most of the experiments which have been performed in the mass region of potential interest involve stripping on even-even target nuclei. Some of the exceptions, for example, $P^{31}(d,p)P^{32}$, $K^{39}(d,p)K^{40}$, $V^{61}(d,p)V^{52}$, connect nuclei whose lowest configurations are too simple to be of much interest as far as sum rules are concerned. Experiments such as $Ca^{43}(d,p)Ca^{44}$, $Sc^{45}(d,p)Sc^{46}$, and $Sc^{46}-(He^3,d)Ti^{46}$ are quite feasible and present interesting possibilities. We do not discuss, at this point, the use of our jj sum rules in connection with (d,p) studies of low resolution.

Sum Rules in an LST Representation

It would now be easy to write down the LS analogs of the six sum rules, factorized and unfactorized, which were derived in a jj representation. Such sum rules would be of no more than formal interest because LS coupling is a reasonable approximation only for the very lightest nuclei. We therefore seek $LSJT$ sum rules by attacking the general expression (III.89) and (III.90) for the relative reduced width. This expression, involving as it does two sets of mixing coefficients, can be summed explicitly only in special cases.

One such case has been discussed by French (Fr56a) and applied to stripping and pickup reactions in the $A=14$ polyad. It involves transitions connecting two- and one-hole states

$$l^{N-2}, T_0 J_0 \rightleftharpoons l^{N-1}, TJ,$$

where $T=\frac{1}{2}$, $J=l\pm\frac{1}{2}$. Here we can perform the summation over J because, in view of the uniqueness of the one-hole states, the corresponding mixing amplitudes do not intrude.

Let us start from (III.103), which becomes

$$S(l^{N-2}, T_0 J_0; l^{N-1}, \frac{1}{2}J) = [T_0 J_0]/2[J]S'(l, \frac{1}{2}J; l^p, T_0 J_0),$$

where the prime indicates that we must use the amplitudes $K_{L_0 S_0} T_0 J_0$ for the states $(T_0 J_0)$ of l^{N-2} :

$$\begin{aligned} \sum_J [J]S(T_0 J_0; \frac{1}{2}J) \\ = [T_0 J_0] \sum_{\substack{z L_0 S_0 \\ L_0' S_0' J}} K_{L_0 S_0} T_0 J_0 K_{L_0' S_0'} T_0 J_0 \\ \times U(l L J_0 S_0 : L_0 z) U(l L J_0 S_0' : L_0' z) \\ \times U(l \frac{1}{2} z \frac{1}{2} : JS_0) U(l \frac{1}{2} z \frac{1}{2} : JS_0') (-1)^{L_0 + L_0'} \end{aligned}$$

from (III.103), since $S=\frac{1}{2}$, $L=l$, and the cfp are obviously unity. First, we sum over J using the unitarity of the transformation (III.7), obtaining $\delta(S_0 S_0')$. Using this to eliminate S_0' , we can then sum over z , obtaining $\delta(L_0 L_0')$. The summation then reduces to

$$[T_0 J_0] \sum_{L_0 S_0} (K_{L_0 S_0} T_0 J_0)^2 = [T_0 J_0],$$

since the state $(T_0 J_0)$ of l^{N-2} must be normalized. We obtain the sum rule

$$\sum_J [J]S(l^{N-1}, \frac{1}{2}J \rightarrow l^{N-2}, T_0 J_0) = [T_0 J_0], \quad (\text{III.172})$$

the summation extending over the two values $l\pm\frac{1}{2}$ of J . It is interesting to notice that (III.172) enables us to deduce, from a measurement of the ratio of the two relevant reduced widths, the absolute values of their spectroscopic factors. If the absolute reduced widths are also measured, we obtain a direct determination of the single-particle reduced width $\theta_0^3(l)$. Thus, information which cannot be obtained directly from a single reduced width because of ignorance of the amplitudes in its spectroscopic factor has been gained by considering two related widths.

In the case of the $1p$ shell, there are two types of transitions:

$$\begin{aligned} (T_0 J_0) &= (01); N^{14}(d,p)N^{15}, N^{14}(d,n)O^{15} \\ (T_0 J_0) &= (10); C^{14}(d,n)N^{15} \end{aligned} \quad \left. \right\} J=\frac{1}{2}, \frac{3}{2}.$$

Following Fr56a, let us denote the relative reduced widths of the four transitions under consideration by s_0, s_0^*, s_1, s_1^* , where the subscript indicates the J value of the target nucleus, and the asterisk implies that the transition proceeds to the excited one-hole state with $J=\frac{3}{2}$. Expression (III.172) then becomes

$$s_i + 2s_i^* = \frac{3}{2} \quad (\text{III.173})$$

for $i=0$ and 1.

The sum rules discussed in this section have all referred to transitions connecting low-lying states of the same configuration of equivalent nucleons. In most experiments, such transitions are in a minority. The weak-coupling formalism of Sec. III.11 leads to a dif-

ferent type of sum rule, involving the transfer of a nucleon inequivalent to the constituents of the target. This sum rule asserts that a basic single-particle reduced width can be broken into fragments by final state interactions but cannot be augmented or diminished thereby. Some further sum rules, in which the summations extend over all observed transitions of given l , are discussed at the end of Sec. VI.

11. "Weak-Coupling" Formalism

The considerations of Secs. III.7–10, whereby it is shown how to compute relative reduced widths in the language of the shell model, are not useful when explicit shell-model wave functions cannot be obtained. Since this is true in many cases of practical interest, it is desirable to develop a formalism for analyzing reduced widths with as little reliance as possible on model wave functions.

Lane (La55a) has studied levels in light nuclei of parity opposite to that of the ground state. He suggests that levels of this kind which are excited strongly in reactions involving the transfer of a single nucleon can be well described by vector coupling the appropriate single particle to the ground state of the parent nucleus and antisymmetrizing. We refer to this process as "weak coupling." For example, the $\frac{1}{2}^+$ level at 3.09 Mev in C¹³ may be regarded as mainly

$$[\varphi_0(C^{12}) \dot{\times} 2s_{\frac{1}{2}}]_{\frac{1}{2}^+} = A(\varphi_0(C^{12}) \dot{\times} 2s_{\frac{1}{2}})_{\frac{1}{2}^+},$$

where $(\dot{\times})_{\frac{1}{2}^+}$ symbolizes vector coupling to spin $\frac{1}{2}^+$ and A is the antisymmetrizing operator.

In most cases, the extreme weak-coupling assumption is too restrictive; several low-lying levels of the parent nucleus contribute significantly to the states under consideration. The idea of weak coupling can, however, be extended so as to take such possibilities into account. The weak-coupling formalism which emerges was first used by Lane, Thomas, and Wigner (La55) in their discussion of average cross sections.

We proceed by letting two simple examples speak for themselves, concluding with some general comments.

Example 1. $B^{10}(d, p)B^{11}$. In $B^{10}(d, p)B^{11}$, a group of $l=0$ and $l=2$ transitions is observed leading to levels around 9 Mev in B^{11} . The relative reduced widths in Fig. 3(a) were obtained from the data of Bilaniuk and Hensel (Bi59), the spins having been determined independently (see Aj59).

The spin and the large $l=0$ reduced width of the 9.19-Mev level strongly suggest that it is predominantly $[\varphi_0(B^{10}) \dot{\times} 2s_{\frac{1}{2}}]_{7/2^+}$.²⁵ It can be seen from the spins and spacings of low-lying levels of B^{10} [Fig. 3(b)] that the only other weak-coupling states which can be expected to contribute appreciably are $[\varphi_0 \dot{\times} 1d_{\frac{5}{2}}]$ and $[\varphi_1 \dot{\times} 1d_{\frac{5}{2}}]$.

²⁵ No absolute cross sections have been measured for the levels in question. We know that their reduced widths are of single-particle size from their measured ratio to the $B^{10}(d, p)B^{11}$ ground-state reduced width, whose approximate size is known [from $B^{10}(d, n)C^{11}$].

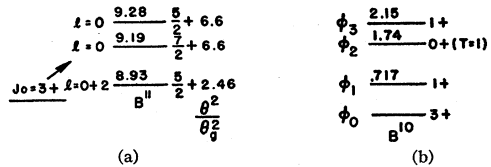


FIG. 3.

For a sizeable component of such a state (more likely the first) to be present in the 9.19-Mev level in B^{11} , it would have to be nearly degenerate with $[\varphi_0 \dot{\times} 2s_{\frac{1}{2}}]$. The two members of this interacting doublet would then be separated by an amount of the order of magnitude of twice the interaction matrix element, so that a second $\frac{7}{2}^+$ level in B^{11} would be expected close to 9.19 Mev, certainly within 1 Mev. This expectation is strengthened by the fact that d - s interactions are not, apparently, very strong²⁶; in fact (Aj59), the nearest $\frac{7}{2}^+$ level in B^{11} to that at 9.19 Mev, is at least 1.2 Mev away and probably further. We conclude that the B^{11} level in question is well described by $[\varphi_0 \dot{\times} 2s_{\frac{1}{2}}]_{7/2^+}$.

Similar arguments apply to possible mixing of $\frac{5}{2}^+$ weak-coupling states. In this case, however, two levels with $J=\frac{5}{2}^+$ are found in B^{11} only 350 kev apart; the $l=0+2$ admixture in the stripping to the 8.93-Mev level confirms that we are dealing with an interaction between $[\varphi_0 \dot{\times} 1d_{\frac{5}{2}}]_{\frac{5}{2}^+}$ and $[\varphi_0 \dot{\times} 2s_{\frac{1}{2}}]_{\frac{5}{2}^+}$. We therefore set up the 2×2 Hamiltonian submatrix

$$\begin{bmatrix} E_1 & H_{12} \\ H_{12} & E_2 \end{bmatrix} \quad (\text{III.174})$$

between the states

$$\chi_1 = [\varphi_0 \dot{\times} 1d_{\frac{5}{2}}]_{\frac{5}{2}^+}, \quad \chi_2 = [\varphi_0 \dot{\times} 2s_{\frac{1}{2}}]_{\frac{5}{2}^+}.$$

Diagonalizing this submatrix, we obtain the eigenvectors and energies

$$\begin{aligned} \Psi_1 &= \alpha \chi_1 + \beta \chi_2, & \mathcal{E}_1 &= 8.93 \text{ Mev}, \\ \Psi_2 &= -\beta \chi_1 + \alpha \chi_2, & \mathcal{E}_2 &= 9.28 \text{ Mev} \end{aligned} \quad (\text{III.175})$$

of the observed B^{11} levels.

The ratio of the $l=0$ and $l=2$ reduced widths of the 8.93-Mev level provides us with a measure of the amplitudes in (III.175); in fact,

$$\frac{\theta^2(l=0)}{\theta^2(l=2)} = \frac{s(0)\theta_0^2(2s)}{s(2)\theta_0^2(1d)} = \frac{\beta^2\theta_0^2(2s)}{\alpha^2\theta_0^2(1d)}. \quad (\text{III.176})$$

The ratio of the $2s$ and $1d$ single-particle reduced widths can be obtained directly from the transitions to the two $\frac{5}{2}^+$ levels in question, whence

$$\frac{\theta^2(l=0: 9.28)}{\theta^2(l=2: 8.93)} = \frac{\alpha^2\theta_0^2(2s)}{\alpha^2\theta_0^2(1d)} = \frac{6.6}{4.6}.$$

²⁶ See, for example, Halbert's calculations (Ha57) for the positive-parity levels of $A=15$.

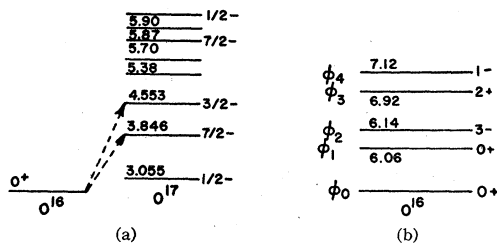


FIG. 4.

On using this and the observed ratio of the $l=0$ and $l=2$ reduced widths of the 8.93-Mev level, (III.176) yields $\beta^2/\alpha^2=0.30$, whence

$$|\alpha|=0.88, \quad |\beta|=0.48.$$

We now know, not only the diagonal form of the matrix (III.174), but also the matrix which carries out the diagonalization, namely,

$$\begin{bmatrix} 0.88 & -0.48 \\ 0.48 & 0.88 \end{bmatrix},$$

making an arbitrary choice of the relative sign of α and β . We can therefore solve for E_1 , E_2 , and H_{12} . A change in the relative sign of α and β merely reverses the sign of H_{12} ; the reduced-width ratio tells us only the magnitude of the interaction matrix element.

The results are

$$H_{12}=150 \text{ kev}, \quad E_1=9.01 \text{ Mev}, \quad E_2=9.20 \text{ Mev}. \quad (\text{III.177})$$

We could equally well use the $l=0$ reduced width of the 9.19-Mev level to obtain the ratio of the $2s$ and $1d$ single-particle reduced widths. This leads to results slightly different from (III.177), reflecting a 20% discrepancy in the total $l=0$ reduced widths of

$$[\varphi_0 \dot{\times} 2s_{\frac{1}{2}}]_{\frac{1}{2}^+} \text{ and } [\varphi_0 \dot{\times} 2s_{\frac{1}{2}}]_{7/2^+}$$

measured by the relevant experiment (Bi59). On using the second normalization, we have

$$H_{12}=160 \text{ kev}, \quad E_1=9.04 \text{ Mev}, \quad E_2=9.17 \text{ Mev}. \quad (\text{III.178})$$

It is interesting that $[\varphi_0 \dot{\times} s_{\frac{1}{2}}]_{\frac{1}{2}^+}$ lies nearly degenerate with or below $[\varphi_0 \dot{\times} s_{\frac{1}{2}}]_{7/2^+}$, although, as a result of the interaction between $\frac{5}{2}^+$ states, the $\frac{5}{2}^+$ level is observed to be 100 kev higher. Any reasonable effective interaction seems to place the $\frac{5}{2}^+$ below the $\frac{7}{2}^+$ member of the $s_{\frac{1}{2}}$ doublet. This matter and what it implies about the effective interaction will be discussed in a forthcoming paper by Bilaniuk and French (Bi60).

Example 2. $l=1$ and $l=3$ transitions in $O^{16}(d,p)O^{17}$. Here we have a larger number of competing weak-coupling states than was the case in Example 1. We can do no more than enumerate the states which can contribute, using this and the observed level structure

of O^{17} to make quantitative statements about the $\frac{3}{2}^-$, $\frac{1}{2}^-$, and $\frac{7}{2}^-$ states in question.

The relevant states of O^{17} , together with the next known levels of the same spin and parity, are shown in Fig. 4(a). The level-structure of O^{16} below 8 Mev is illustrated in Fig. 4(b).

We consider the $\frac{7}{2}^-$ levels first. The large $l=3$ reduced width of the 3.846-Mev level indicates that it contains a large fragment of the $[\varphi_0(O^{16}) \dot{\times} f_{7/2}]$ single-particle component. Although no stripping data is yet available on the next $\frac{7}{2}^-$ level, the fact that it is at 5.70 Mev is in itself a compelling argument that the lower $\frac{7}{2}^-$ level is a good single-particle state.²⁷ For, "spreading" measurable $l=3$ components over 2 Mev would, in this case, demand existence of a weak-coupling state close in energy to $[\varphi_0 \dot{\times} 1f_{7/2}]$ and an interaction matrix element of 1 Mev. This is improbably large, particularly in view of the fact that such an interaction would involve inequivalent pairs (f and d , or f and s). We predict, then, that the 5.70-Mev level will show weak stripping; the corresponding reduced width, if measurable, would give an estimate of the interaction matrix element.

The existence of a $1f_{7/2}$ single-particle level only 4 Mev above the $1d_{\frac{5}{2}}$ ground state of O^{17} is surprising. On the basis of the potential-well model of the interaction of an extra nucleon with the nucleons of O^{16} , using the customary harmonic-oscillator radial dependence, the $d_{5/2} - f_{7/2}$ separation is expected to be more than 10 Mev.

From the spins and parities of low-lying levels of O^{16} , we see that only $[\varphi_2 \dot{\times} 1d_{\frac{5}{2}}]$, $[\varphi_2 \dot{\times} 2s_{\frac{1}{2}}]$, and $[\varphi_4 \dot{\times} 1d_{\frac{5}{2}}]$ can possibly give $\frac{7}{2}^-$ states low enough to interact with $[\varphi_0 \dot{\times} 1f_{7/2}]$. To estimate the relevant energies, we note that the expectation value of the nuclear Hamiltonian in the weak-coupling state $[\varphi_i \dot{\times} u_k]$ breaks into two parts:

{internal energy of φ_i }

+ {energy of interaction of nucleon u_k with φ_i }.

The first term is simply the observed energy of the state φ_i of the parent nucleus; to estimate the second, we make the crude approximation that the interaction energy of u_k is roughly the same as its interaction energy with the ground state φ_0 , which can then be obtained from the observed single-particle level position. On applying this procedure to the $\frac{7}{2}^-$ levels of O^{17} , we find that the preceding three $d_{\frac{5}{2}}$ and $s_{\frac{1}{2}}$ weak-coupling states are expected about 2 to 3 Mev above $[\varphi_0 \dot{\times} 1f_{7/2}]$. This is consistent with our conclusion, based on the O^{17} level structure, that the 3.846-Mev level is a good single-particle $f_{7/2}$ state.

Let us similarly consider $\frac{3}{2}^-$ levels. The sizeable $l=1$ reduced width of the 4.553-Mev level indicates a $[\varphi_0 \dot{\times} 2p_{\frac{1}{2}}]$ component. It is, at present, not clear what proportion of the whole this component constitutes. Firstly, the next $\frac{3}{2}^-$ level is only about 800 kev away,

²⁷ For a definition of "single-particle level," see the discussion following the examples.

quite close enough to permit substantial mixing. In the second place, although we know very little about $\theta_0^2(2p)$ in this mass region, data later in the ds shell ($A \geq 20$; see Sec. V) indicate that the $l=1$ reduced width of the 4.553-Mev level is considerably smaller²⁸ than the full single-particle value.

Weak-coupling states with $J = \frac{3}{2}^-$ which might interact with $[\varphi_0 \dot{\times} 2p_{\frac{1}{2}}]$ obviously include $[\varphi_2 \dot{\times} d_{\frac{3}{2}}]$ and $[\varphi_4 \dot{\times} d_{\frac{1}{2}}]$; however, since the 6.92-Mev 2^+ level of $O^{16}(\varphi_3)$ almost certainly involves excitation of the $1p_{\frac{1}{2}}$ shell, $[\varphi_3 \dot{\times} 1p_{\frac{1}{2}}]$ must also be considered. φ_3 is probably well represented by

$$\begin{aligned}\varphi_3 \simeq & \alpha(1p_{\frac{1}{2}}^{-2})_0(1d_{\frac{3}{2}})_2 + \beta(1p_{\frac{1}{2}}^{-2})_0(1d_{\frac{1}{2}})_2 s_1 \\ & + \gamma(1p_{\frac{1}{2}}^{-1})_0(2p_{\frac{1}{2}})_2\end{aligned}\quad (\text{III.179})$$

while (El57b)

$$\begin{aligned}\varphi_2 \simeq & (1p_{\frac{1}{2}}^{-1})_0(1d_{\frac{3}{2}})_2 + (\text{minor components}), \\ \varphi_4 \simeq & (1p_{\frac{1}{2}}^{-1})_0(2s_1)_2 + (\text{minor components}).\end{aligned}$$

We therefore see that $[\varphi_3 \dot{\times} 1p_{\frac{1}{2}}]$, which is given by

$$\alpha(1p_{\frac{1}{2}}^{-1})_0(1d_{\frac{3}{2}})_2 + \beta(1p_{\frac{1}{2}}^{-1})_0(1d_{\frac{1}{2}})_2 + \gamma(1p_{\frac{1}{2}}^{-1})_0(2p_{\frac{1}{2}})_2$$

has large overlaps with $[\varphi_0 \dot{\times} 2p_{\frac{1}{2}}]$, $[\varphi_2 \dot{\times} d_{\frac{3}{2}}]$, and $[\varphi_4 \dot{\times} d_{\frac{1}{2}}]$. The weak-coupling states, in other words, are not orthogonal, in fact, they are not linearly independent.

This difficulty, which comes about because the relevant excited states of O^{16} belong to configurations other than that of the ground state, is a central one in constructing a formal theory of weak coupling. We can clearly proceed by step-by-step orthogonalization, constructing a new set of functions χ_i as follows:

$$\begin{aligned}\chi_0 &= [\varphi_0 \dot{\times} 2p_{\frac{1}{2}}], \quad \chi_1 = [\varphi_2 \dot{\times} 1d_{\frac{3}{2}}], \quad \chi_2 = [\varphi_4 \dot{\times} 1d_{\frac{1}{2}}], \\ \chi_3 &= \mathcal{N} \{ [\varphi_3 \dot{\times} 1p_{\frac{1}{2}}] - (\chi_0, [\varphi_3 \dot{\times} 1p_{\frac{1}{2}}]) \chi_0 - \dots \\ &\quad - (\chi_2, [\varphi_3 \dot{\times} 1p_{\frac{1}{2}}]) \chi_2 \} \dots, \quad \text{etc.},\end{aligned}$$

where \mathcal{N} is a normalizing coefficient. This new set is orthonormal because we have made it so, but no longer has the property of unique parentage, in that a state χ_i is not associated with a unique state φ_j of the parent nucleus; however, the ground state φ_0 is still uniquely associated with χ_0 , a significant fact in the discussion of stripping reactions.

On using the crude energy estimate described in connection with the $\frac{7}{2}^-$ levels, we find that any of χ_1 , χ_2 , χ_3 may well interact significantly with $[\varphi_0 \dot{\times} 2p_{\frac{1}{2}}]$, as is suggested by the stripping data. We therefore expect appreciable reduced widths for one or more $\frac{3}{2}^-$ levels between 5 and 6 Mev in O^{17} .

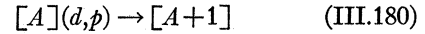
The salient feature of known $\frac{1}{2}^-$ levels in O^{17} is the existence of an isolated low-lying level of this nature at 3.058 Mev, which apparently shows no stripping from O^{16} . No data are available concerning the reduced widths of higher $\frac{1}{2}^-$ levels. Our rough energy estimates

²⁸ From $F^{19}(d, p)F^{20}$ we obtain the lower limit $\theta_0^2(2p) \geq 0.02$, while the $O^{17} l=1$ reduced width in question has the value 0.013.

suggest that $[\varphi_2 \dot{\times} d_{\frac{3}{2}}]_{-}$ may lie 1 or 2 Mev below $[\varphi_0 \dot{\times} 2p_{\frac{1}{2}}]$.

Further $O^{16}(d, p)O^{17}$ or $O^{16}(\text{He}^3, d)F^{17}$ experiments, studying levels up to 7 or 8 Mev, are clearly needed.

Leaving the examples, we now briefly formalize the arguments which we have been using. Consider the stripping reaction



expressing the wave functions of $[A+1]$ levels in a representation spanned by the weak-coupling states $[\varphi_i \dot{\times} u_k]$, where φ_i ($i=0, 1, 2, \dots$) are the actual states of $[A]$ and the u_k are the single-particle states which belong to the unoccupied subshells in the ground state of $[A]$.

The restriction to nucleons u_k inequivalent to all those in the ground-state configuration of $[A]$ is made because the idea of weak-coupling loses its special character when applied to equivalent nucleons. For example, direct antisymmetrization of $(d_{\frac{3}{2}})_0 d_{\frac{1}{2}}$ introduces components of $\{(d_{\frac{3}{2}})_0 d_{\frac{1}{2}}\}_{\frac{1}{2}}$. In dealing with the transfer of equivalent nucleons, the techniques of Secs. III.7–10 are most convenient.

The functions $[\varphi_i \dot{\times} u_k]$ are not linearly independent. This difficulty was illustrated in Example 2 and is liable to be encountered when the states φ_i belong to configurations other than that of the ground state φ_0 of $[A]$. We therefore construct an orthonormal set χ_{ik} from the functions $[\varphi_i \dot{\times} u_k]$ by the direct procedure described in Example 2. We have

$$\chi_{0k} = [\varphi_0 \dot{\times} u_k] \quad (\text{III.181})$$

for all k . The new states χ_{ik} do not, in general, correspond to unique parent states in $[A]$.

The matrix of the Hamiltonian of $[A+1]$ is now set up in the representation spanned by the states χ_{ik} . Diagonalizing the submatrix \mathcal{H}^{TJ} , we obtain the wave functions of states of $[A+1]$ with the given T and J in the form

$$\Psi_{TJ}^{(s)} = \sum_{ik} C_{ik}^{(s)} (\chi_{ik})_{TJ}, \quad (\text{III.182})$$

where s labels the different eigenvalues and eigenvectors of \mathcal{H}^{TJ} .

Only those states $\Psi_{TJ}^{(s)}$ of $[A+1]$ are observed in the stripping experiment (III.180) which contain appreciable components of some χ_{0k} . The reduced width of $\Psi_{TJ}^{(s)}$ for capture of u_k is obviously

$$S(u_k) = |C_{0k}^{(s)}|^2. \quad (\text{III.183})$$

A *single-particle level* of $[A+1]$ is now profitably defined as one for which the expansion (III.182) contains one predominant term, $C_{0k}^{(s)} \simeq 1$. In other words, a single-particle level is one for which the weak-coupling approximation is good. If we restrict A to be even and represent the ground state φ_0 of $[A]$ by $(j^{2n})_0$, we obtain, as a special case, the second type of single-particle level introduced in Example 5 of Sec. III.9.

The first type, belonging to a configuration of equivalent nucleons, corresponds to a situation explicitly excluded from our discussion of the weak coupling formalism.

In certain cases, a nucleus $[A+1]$ can be reached by (d,p) and (d,n) experiments from nuclei with the same A and different T_z . Let us consider, as an illustration of such a situation, the levels of N^{15} , since both C^{14} and N^{14} are available as targets. The C^{14} ground state is the analog the first excited state φ_1 of N^{14} . Thus, not only $[\varphi_0 \dot{\times} u_k]$ but also $[\varphi_1 \dot{\times} u_k]$ can be reached by stripping experiments. A slight extension of the preceding definition of single-particle component is desirable to accommodate $[\varphi_1 \dot{\times} u_k]$. A weak-coupling representation of the levels of N^{15} must be based on N^{14} and cannot be based on C^{14} .

We now write down, from (III.183), an obvious but important sum rule which simply reassembles the various fragments into which a single-particle reduced width has been split by final-state interactions. The matrix $C_{ik}^{(s)}$ which diagonalizes the Hamiltonian submatrix \mathcal{H}^{TJ} is unitary. This implies, for the column labeled by $i=0, k$, that $\sum_s |C_{0k}^{(s)}|^2 = 1$. Thus, from (III.183),

$$\sum_s S^{(s)}(u_k) = 1, \quad (\text{III.184})$$

the summation embracing all states of $[A+1]$ with the given TJ which contain components of $[\varphi_0 \dot{\times} u_k]_{TJ}$.

In applying the preceding sum rule, we simply add the observed values of $[J]\theta^2$ for transitions involving the single-particle u_k in question. Then (III.184) yields, on further summation over J ,²⁹

$$\sum_{(u_k)} [J]\theta^2 = \theta_0^2(u_k) \sum_J [J] = [jJ_0]\theta_0^2(u_k). \quad (\text{III.185})$$

Much of our information concerning the $2p$, and $1f$ single-particle reduced widths is obtained in this fashion.

In practical applications of (III.185), we encounter a difficulty illustrated by the $l=0$ transitions in $\text{Ca}^{40}(d,p)\text{Ca}^{41}$, discussed in Sec. VI. In this case, $l=0$ transitions to low-lying levels in Ca^{41} contain, in principle, both $2s_1$ and $3s_1$ contributions, the former because of possible core excitation in Ca^{40} . If we now sum $[J]\theta^2$ over all observed $l=0$ reactions, $\sum [J]\theta^2$ includes, in addition to the $3s_1$ terms to which (III.185) applies, extraneous $2s_1$ contributions. Since we cannot disentangle $2s$ and $3s$, we cannot, strictly, apply the sum rule; however, even if the low-lying $l=0$ transitions were pure $2s_1$, they would contribute less than 5% to $\sum [J]\theta^2$.³⁰ Such contributions are of no importance. We conclude therefore, that the sum rule (III.185) can be

²⁹ J_0 is the spin of the target nucleus, and j the transferred j value. If, for example, one cannot distinguish between p_1 and p_2 , we further sum over j .

³⁰ The $3s$ transitions in $\text{Ca}^{40}(d,p)\text{Ca}^{41}$ have not been observed; however, it is known (Sc59) that $\theta_0^2(3s) \approx \theta_0^2(2d)$ and the $2d$ transitions have been observed.

applied to $l=0$ transitions in $\text{Ca}^{40}(d,p)\text{Ca}^{41}$ and, almost certainly, to other cases of interest also.

Taking into account the fact that some weak contributions to stripping involving u_k may escape detection, (III.185) should be replaced by

$$\sum_s S^{(s)}(u_k) \leq 1. \quad (\text{III.186})$$

This inequality applies *a fortiori* to any one transition involving an inequivalent nucleon. This point has already been made in Sec. III.7 (III.73'). When we have reason to believe that a given transition or set of transitions involves almost all of the relevant single-particle component, we often omit the inequality and quote a direct estimate of the single-particle reduced width rather than a lower limit.

In the formalism just developed, an orthonormal set of functions χ_{ik} has been introduced at the expense of the uniqueness of the parentage relation. A state χ_{ik} may be associated with several different states of the parent nucleus $[A]$, although for the special functions χ_{0k} , corresponding to the ground state of $[A]$, the uniqueness of the parentage relation is preserved. Since stripping reactions involve these very components χ_{0k} , the introduction of the set χ is appropriate and convenient in the study of stripping. In contrast, a pickup reaction reveals all possible parent states (in $[A]$) of the ground state of $[A+1]$. Such a situation is not covered by the formalism of this section.

12. Calculation of S from Rotational-Model Wave Functions

Several recent studies (Sh56, Pa57, Ra57, Br57, Li58, Br58) have indicated that the rotational model—direct descendant of Bohr's strong-coupling collective model (Bo52)—is capable of describing with some success many aspects of nuclei in the ds shell. The mass region to which these studies refer— $19 \leq A \leq 31$ —is of direct interest to our analysis. Various features of stripping and collective models have been analyzed by Yoshida (Yo54), Satchler (Sa55, Sa58), and Sawicki (Sa58a). The following discussion is closest to that of Satchler.

It is recalled that one of the main assumptions which led to the form (II.19) for the differential stripping cross section demanded the spherical symmetry of the nuclear potential acting on the transferred nucleon. Without this assumption, separation of the radial and angular portions of the integration in the transition matrix element could not have proceeded in the manner of Sec. II. But the very use of a rotational wave function presupposes that the nucleus so described possesses a sizeable equilibrium deformation, automatically excluding any chance that its potential field can be spherical. Thus, strictly speaking, it would be self-contradictory to insert rotational wave functions for the nuclear states in the overlap integrals (III.53) and (III.54).

Analysis (Sa58b) of these "geometrical" effects has indicated that they are, in general, quite small. We therefore ignore geometrical effects and adopt the apparently illogical course of using rotational wave functions, while retaining the assumption that the transferred nucleon experiences what is, to all intents and purposes, a central potential.

Let us proceed to discuss the overlap integral (III.54), with the intention of representing initial and final nuclei by means of rotational wave functions.

All forms of rotational model which have been used to date begin by segregating the constituent nucleons of a nucleus into two groups. The first group is treated as a whole and referred to as the core of the nucleus. The nucleons of the second group are described as "active" or "extra-core" nucleons. As a result of the competition between the preference of the core itself for a spherical shape and the "polarizing" efforts of the extra-core nucleons, the nucleus assumes a nonspherical equilibrium shape. The deformed nucleus can execute motions of a rotational type which have, as their associated dynamical variables, a suitable set of Euler angles ϑ specifying the orientation of a body-fixed set of axes relative to a frame of reference whose orientation is fixed in space. The motion of the active nucleons in the field of the core is described, in a manner to be discussed, by an "intrinsic" wave function $\chi(i)$, where i signifies the set of all coordinates of the active nucleons referred to the body-fixed axes.

The internal degrees of freedom of the core are discussed, if at all, in terms of a collective vibrational model. We follow the accepted procedure in studies of the rotational model, assuming throughout that the core is in its vibrational ground state, described by the wave function $\phi(\xi)$.

We adopt Nilsson's model of the intrinsic structure (Ni55), wherein each active nucleon moves in a spheroidal potential well. Each Nilsson orbit is characterized by the principal quantum number n , and by the projection Ω of the single-particle angular momentum j on the body-fixed z axis. Nucleons fill these orbits four at a time, in accordance with the exclusion principle, most of the filled orbits being lumped together as the core. l and j are no longer good quantum numbers. $\chi(i)$ is thus a normalized antisymmetric product of Nilsson functions.

Assuming the independence of the particle motion in the deformed nuclear field and the rotation of this field, we can write the wave function of the nucleus [A] in the form

$$\Psi_{J_0 K_0 M_0}(\xi, \vartheta, i) = [(2J_0 + 1)/16\pi^2]^{\frac{1}{2}} \phi_i(\xi) \\ \times \{D_{M_0 K_0}^{J_0}(\vartheta) \chi_{K_0}(i) + (-1)^{J_0 - \Sigma j} D_{M_0, -K_0}^{J_0} \chi_{-K_0}\}. \quad (\text{III.187})$$

$D_{M_0 K_0}^{J_0}$ is the matrix representative of the rotation operator $R(\vartheta)$ (Ro57, Ed57). The precise definition of

the D^J which we use is that of Bohr (Bo52), the complex conjugate of the D functions introduced in Ro57. The requirement of axial symmetry implies that $\Omega = K_0$. Finally, the phase operator $(-1)^i$ must be interpreted according to the equation

$$(-1)^i \chi_k = \sum_j (-1)^j a_{jk} \chi_{jk}. \quad (\text{III.188})$$

A detailed discussion of the wave function (III.187) will be found in the review article by Moszkowski (Mo57). Questions concerning the validity of the adiabatic assumption from which it emerges or the precise significance of the division of nucleons into "core" and "particles outside the core" constitute one of the major unsolved problems of nuclear spectroscopy.

The rotational wave function for the nucleus [A+1] is

$$\Phi_{JKM}(\xi, \vartheta, i\nu) = [(2J + 1/16\pi^2)^{\frac{1}{2}} \phi_J(\xi) \\ \times \{D_{MK}^J(\vartheta) \chi_K(i\nu) \\ + (-1)^{J - \Sigma j_i - j_p} D_{M, -K}^J \chi_{-K}\}], \quad (\text{III.189})$$

where ν is the set of all coordinates of the transferred nucleon referred to the body-fixed axes.

Let us now consider the problem of calculating relative reduced widths. The overlap integral in terms of which S is defined in (III.54) and which emerges from the considerations of Sec. II, can be written

$$S(lj) = \int \Phi_{JKM}^*(\xi, \vartheta, i\nu') \{ \Psi_{J_0 K_0}(\xi, \vartheta, i) \dot{\times} \psi_{nlj}(\nu') \}_{JMD} d\xi d\vartheta di d\nu', \quad (\text{III.190})$$

on suitably modifying the notation of (III.54). $\psi_{nlj}(\nu')$ is the wave function of the transferred nucleon referred to the space-fixed axes. We observe, in particular, that $S(lj)$ is independent of M . This, indeed, was why the spin summation could be performed explicitly.

On the other hand, the overlap which presents itself more naturally in the present context is

$$\langle JKM | J_0 K_0 M_0 \rangle = \int \Phi_{JKM}^*(\xi, \vartheta, i\nu) \Psi_{J_0 K_0 M_0}(\xi, \vartheta, i) \\ \times d\xi d\vartheta di, \quad (\text{III.191})$$

a function of the coordinates of the transferred nucleon. We now prove that $S(lj)$ can be deduced simply and directly from $\langle JKM | J_0 K_0 M_0 \rangle$. It is, accordingly, unnecessary to recalculate the differential stripping cross section *ab initio*.

Indeed (III.190) may be rewritten

$$S(lj) = \int d\nu' \sum_{M_0} C[J_0 j J; M_0, M - M_0] \\ \times \langle JKM | J_0 K_0 M_0 \rangle \psi[M - M_0; nlj]. \quad (\text{III.192})$$

This suggests that we make the formal expansion:

$$\begin{aligned} \langle JKM | J_0 K_0 M_0 \rangle &= \sum_{ij} \alpha_{ij} C[J_0 jJ; M_0, M - M_0] \\ &\quad \times \psi^*[M - M_0; nlj](\nu'). \end{aligned} \quad (\text{III.193})$$

Our assumption that one n can contribute in any instance is in the spirit of Nilsson's calculation. If we now multiply (III.193) by

$$\psi[M - M_0; nlj'] C[J_0 jJ; M_0, M - M_0],$$

integrate over ν' , and sum over M_0 , we obtain, comparing with (III.192),

$$\alpha_{lj} = g(lj),$$

i.e.,

$$\begin{aligned} \langle JKM | J_0 K_0 M_0 \rangle &= \sum_{ij} g(lj) C[J_0 jJ; M_0, M - M_0] \\ &\quad \times \psi^*[M - M_0; nlj](\nu'). \end{aligned} \quad (\text{III.194})$$

Thus, in order to obtain $g(lj)$, we must evaluate $\langle JKM | J_0 K_0 M_0 \rangle$ and select the coefficient of

$$C[J_0 jJ; M_0, M - M_0] \psi^*[M - M_0; nlj](\nu').$$

We wish, therefore, to calculate the overlap of the wave functions (III.187) and (III.189). Let us make, in this connection, three manipulations.

(1) Depending on the Ω value of the transferred nucleon, there are four possible kinds of transition between (III.187) and (III.189). These we may write symbolically

$$\left. \begin{array}{l} K_0 \rightleftharpoons K \\ -K_0 \rightleftharpoons -K \end{array} \right\} |\Omega| = |K - K_0|,$$

$$\left. \begin{array}{l} K_0 \rightleftharpoons -K \\ -K_0 \rightleftharpoons K \end{array} \right\} |\Omega| = K + K_0.$$

It is clear that, whichever case we are handling, the two terms in the overlap integral $\langle JKM | J_0 K_0 M_0 \rangle$ must be equal. Let us consider, first, the case $|\Omega| = |K - K_0|$; the result for $K + K_0$ follows by changing the sign of K_0 in the relevant final formula. As a result of what has just been said, it is permissible to calculate $\langle JKM | J_0 K_0 M_0 \rangle$ with simple product wave functions of the form

$$[(2I+1)/8\pi^2]^{\frac{1}{2}} \phi(\xi) D_{MK^I}(\vartheta) \chi_K, \quad (\text{III.195})$$

allowing for the occurrence of two equal terms by a compensatory change in normalization.

If either K or $K_0 = 0$, (III.195) is the correct wave function, and there is only one term since $-K_0 = K_0$. Our general result holds in this special case, provided that we include a multiplicative factor of $\sqrt{2}$.

(2) Both $\chi_K(i\nu)$ and $\chi_{K_0}(i)$ are antisymmetric in all active nucleons. Let n be the number of active nucleons in the heavier nucleus [A+1]. We may evaluate

$\langle JKM | J_0 K_0 M_0 \rangle$ by writing $\chi_K(i, \nu)$ as a simple product,

$$\chi_K(i, \nu) = \chi_{K-\Omega}(i) \chi_\Omega^{(n)}(\nu), \quad (\text{III.196})$$

where $\chi_{K-\Omega}(i)$ is an antisymmetric function of the first $n-1$ nucleons, provided that we multiply by the normalization factor $n^{-\frac{1}{2}}$ associated with the antisymmetrization of (III.196). It is clear that $\chi_K(i, \nu)$ and $\chi_{K_0}(i)$ have zero overlap if they differ in the orbital of more than one nucleon.

(3) It is seen from (III.194) that the wave function of the transferred nucleon should be referred to axes fixed in space. This can be achieved, with the aid of the rotation matrices, on expanding $\chi_\Omega(\nu)$ in (III.196) as a sum of functions of definite j . Explicitly,

$$\begin{aligned} \chi_\Omega(\nu) &= \sum_{lj} a_{nlj}(\Omega) \chi_{nlj}^\Omega(\nu) \\ &= \sum_{ljm} a_{nlj}(\Omega) D_{m\Omega}^{*i}(\vartheta) \psi_{nlj}^m(\nu'). \end{aligned} \quad (\text{III.197})$$

The a_{nlj} are given in terms of the coefficients $b_{nl\Lambda}$ tabulated by Nilsson (Ni55) by the simple transformation

$$a_{nlj}(\Omega) = \sum_\Lambda C[l\frac{1}{2}j; \Lambda, \Omega - \Lambda] b_{nl\Lambda}(\Omega). \quad (\text{III.198})$$

Then, from (III.191) with the help of (III.196)–(III.198),

$$\begin{aligned} \langle JKM | J_0 K_0 M_0 \rangle &= n^{-\frac{1}{2}} \cdot \rho \frac{[JJ_0]}{8\pi^2} \langle f | i \rangle \int D_{MK}^{*J} \\ &\quad \times D_{m\Omega}^i D_{M_0 K_0}^{J_0} d\vartheta \delta(K_0, K - \Omega) \\ &\quad \times a_{nlj}(\Omega) \psi^*[m; nlj](\nu'), \end{aligned} \quad (\text{III.199})$$

where $\langle f | i \rangle$ is the core overlap, and

$$\begin{aligned} \rho &= \sqrt{2} \text{ if either } K \text{ or } K_0 \text{ is zero} \\ &= 1 \text{ otherwise.} \end{aligned} \quad (\text{III.200})$$

The integral over the Euler angles yields [Ed57, (4.6.2)]

$$\begin{aligned} &[8\pi^2/(2J+1)] C[J_0 jJ; M_0, M - M_0] \\ &\quad \times C[J_0 jJ; K_0, K - K_0] \\ &\quad \times \delta(m, M - M_0) \delta(\Omega, K - K_0). \end{aligned} \quad (\text{III.201})$$

The summation over m can now be carried out explicitly, and (III.199) becomes

$$\begin{aligned} \langle JKM | J_0 K_0 M_0 \rangle &= \sum_{lj} \{ n^{-\frac{1}{2}} \rho \cdot \langle f | i \rangle [J_0 / J]^{\frac{1}{2}} \\ &\quad \times C[J_0 jJ; K_0, K - K_0] a_{nlj}(\Omega) \delta(\Omega, K - K_0) \} \\ &\quad \times C[J_0 jJ; M_0, M - M_0] \\ &\quad \times \psi^*[M - M_0; nlj](\nu'). \end{aligned} \quad (\text{III.202})$$

The overlap integral for the case $|\Omega| = K + K_0$ is obtained from (III.202) by the replacement $K - K_0 \rightarrow$

$K+K_0$, as discussed in the foregoing. Comparing (III.202) with (III.194), we obtain an expression for the overlap integral in which we are really interested:

$$\begin{aligned} g(lj) &= n^{-\frac{1}{2}} \cdot \rho \cdot \langle f | i \rangle [J_0/J]^{\frac{1}{2}} \\ &\times C[J_0 j J; \mp K_0, K \pm K_0] a_{nlj}(|\Omega|) \\ &\times \delta(|\Omega|, |K \pm K_0|). \quad (\text{III.203}) \end{aligned}$$

Finally, let us recall the definition (III.56), $s(lj) = n g(lj)^2$, whence

$$\begin{aligned} s(lj) &= \rho^2 \langle f | i \rangle^2 [J_0/J]^2 \\ &\times C[J_0 j J; \mp K_0, K \pm K_0]^2 a_{nlj}^2(|\Omega|) \\ &\times \delta(|\Omega|, |K \pm K_0|). \quad (\text{III.204}) \end{aligned}$$

The core overlap

$$\langle f | i \rangle = \int \phi_f^*(\xi) \phi_i(\xi) d\xi$$

defies exact calculation. Crude estimates based on the approximate vibrational wave functions of Bohr and Mottelson (Bo53) suggest that

$$\langle f | i \rangle \sim 1 \quad (\text{III.205})$$

is a reasonable value provided that, as is nearly always the case in practice, the nuclei concerned have similar equilibrium deformations (Sa58).

In all cases of interest to us, excited bands are based on intrinsic states of single-particle excitation. The influence of the mixing of bands (R.P.C.) on relative reduced widths can be analyzed as described in Sec. III.8.

Let us conclude this section by deriving a sum rule. We can use the orthonormality of the Clebsch-Gordan coefficients to sum over all states J in the rotational band K in (III.204). The sum rule is

$$\sum_J [J] s(lj) = \rho^2 [J_0] a_{nlj}^2(|\Omega|), \quad (\text{III.206})$$

where we have set $\langle f | i \rangle = 1$ and omitted the Kronecker δ .

The normalization of the intrinsic wave function, expressed by

$$\sum_{lj} a_{nlj}^2 = 1,$$

yields a further sum rule

$$\sum_{Jlj} [J] s(lj) = \rho^2 [J_0]. \quad (\text{III.207})$$

These sum rules were first given by Satchler (Sa58). Their application is discussed in Sec. V, where stripping reactions in the ds shell are analyzed.

Lastly, in the second sum rule, let us put $J_0 = 0$, $J = j$, $\rho = \sqrt{2}$, and $n = 1$, the case of an even-even target nucleus.

We obtain

$$\sum_{lj} [j] s(lj) = 2, \quad (\text{III.208})$$

which is the sum rule written down and used by Litherland *et al.* (Li58).

13. Calculation of s from Vibrational-Model Wave Functions

Another important type of nuclear collective excitation involves shape oscillations about a spherical equilibrium (Bo52, Mo57). The reduced widths of vibrational levels were first discussed by Satchler (Sa58), whose treatment we follow quite closely.

In the most important case of quadrupole or ellipsoidal vibrations, the shape of the nucleus at any moment can be described by

$$R(\theta, \phi) = R_0 [1 + \sum_{\mu=-2}^2 \alpha_{\mu} Y_{\mu}^{(2)}(\theta, \phi)], \quad (\text{III.209})$$

where R_0 is the normal radius of the nucleus and (θ, ϕ) describes the direction of R relative to a set of axes fixed in the nuclear shape. The α_{μ} can now be used as dynamical variables in the shape oscillations, the relevant "vibrational" Hamiltonian being

$$H_c = \frac{1}{2} \sum_{\mu} \{B |\dot{\alpha}_{\mu}|^2 + C |\alpha_{\mu}|^2\}. \quad (\text{III.210})$$

B and C are parameters which may either be calculated on the basis of some more detailed nuclear model or, preferably, treated as empirical constants. H describes a set of uncoupled oscillators, whose quanta we refer to as "phonons." Each such phonon carries two units of angular momentum and possesses an energy $\hbar\omega = \hbar[C/B]^{\frac{1}{2}}$.

If we confine our attention to states involving on more than three phonons, then the eigenfunctions of (III.210) can be completely specified by (NR) , where N is the number of phonons and R is the total angular momentum.

Once again let us start by separating the nucleus into a core and a number n of "loose" nucleons outside the core. Correspondingly, the nuclear Hamiltonian may be written

$$H = H_p + H_c + H_{\text{int}}. \quad (\text{III.211})$$

H_p is the ordinary shell-model Hamiltonian for the loose nucleons, the core being described by the vibrational Hamiltonian H_c given by (III.210). The interaction energy can be expressed (Bo52) as

$$H_{\text{int}} = k \sum_{i=1}^n \sum_{\mu=-2}^2 \alpha_{\mu} Y_{\mu}^{(2)}(\theta_i, \phi_i) \quad (\text{III.212})$$

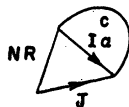
where k is a constant of the order of magnitude 20 Mev for light nuclei. We take

$$H_0 = H_c + H_p \quad (\text{III.213})$$

as a zero-order Hamiltonian, treating H_{int} by first-order perturbation theory.

We begin by discussing reduced widths connecting zero-order states (eigenfunctions of H_0). The perturbed wave functions (eigenfunctions of H) are linear combinations of these zero-order states; the corresponding reduced widths can then be obtained from the zero-order overlap integrals by the method described at the end of Sec. III.7.

Reverting to the notation described in Sec. III.3, the eigenfunctions of H_0 may be written



$$\mathcal{G}_{I\alpha: I_0\alpha_0}(l, j) = \sum_{I'} U(R_0 I_0 J j : J_0 I') \left\langle \begin{array}{c} \text{NR} \\ \diagdown \text{Ia} \\ J \end{array} \middle| \begin{array}{c} \text{NoRo} \\ \diagup \text{Co} \\ I_0 \alpha_0 \\ J_0 \\ j(n) \\ I' \\ J \end{array} \right\rangle = \delta(NN_0)\delta(RR_0)U(R_0 I_0 J j : J_0 I) g^{\text{s.m.}}(l, j), \quad (\text{III.215})$$

where $g^{\text{s.m.}}(l, j)$ is the overlap integral of the shell-model states. Expression (III.215) agrees with Satchler's result [Sa58, Eq. (8)]. As might have been expected, the overlap integral is diagonal in the vibrational states, whose only effect is to multiply the shell-model overlap by an angular-momentum coupling factor.

For a nucleus in its ground state, the zero-order vibrational wave function has $N=R=0$. The vibrational selection rule $\Delta N=0$ then implies that stripping and pickup reactions select members of the ground-state vibrational band in the residual nuclei.

The first-order effect of H_{int} is to mix states whose phonon-numbers differ by one. Such admixtures give rise to small reduced widths for one-phonon states. Two-phonon states only have nonzero reduced widths in second and higher orders. The mixing coefficients are calculated (El57) by standard perturbation theory. $\mathcal{G}(l, j)$ is then expressed in terms of $\mathcal{G}_{I\alpha: I_0\alpha_0}(l, j)$ as in (III.83) and the shell-model overlap calculated with the help of the techniques described in Sec. III.7. The final relative reduced width is

$$S(l, j) = n \mathcal{G}(l, j)^2. \quad (\text{III.216})$$

Situations may be encountered wherein perturbation theory is not valid. This would happen, for example, if an excited level of the ground-state vibrational band lay close to a one-phonon state of the same spin and parity.³¹ The states in question could then interact strongly, producing two levels with sizeable stripping widths.

³¹ Satchler (Sa58) cites, in this connection, two close 2^+ levels in Cd^{114} .

with the eigenvalues $N\hbar\omega + E(nI\alpha)$. c symbolizes an antisymmetric shell-model wave function for the n loose nucleons.

The desired overlap integral is

$$\mathcal{G}_{I\alpha: I_0\alpha_0}(l, j) = \left\langle \begin{array}{c} \text{NR} \\ \diagdown \text{Ia} \\ J \end{array} \middle| \begin{array}{c} \text{NoRo} \\ \diagup \text{Co} \\ I_0 \alpha_0 \\ J_0 \\ j(n) \\ I' \\ J \end{array} \right\rangle. \quad (\text{III.214})$$

On applying the recoupling rule (III.5) to the right-hand wave function,

$$\mathcal{G}_{I\alpha: I_0\alpha_0}(l, j) = \sum_{I'} U(R_0 I_0 J j : J_0 I') \left\langle \begin{array}{c} \text{NR} \\ \diagdown \text{Ia} \\ J \end{array} \middle| \begin{array}{c} \text{NoRo} \\ \diagup \text{Co} \\ I_0 \alpha_0 \\ J_0 \\ j(n) \\ I' \\ J \end{array} \right\rangle = \delta(NN_0)\delta(RR_0)U(R_0 I_0 J j : J_0 I) g^{\text{s.m.}}(l, j), \quad (\text{III.215})$$

There are strong indications (Mo57) that nuclei in the region $70 \leq A \leq 150$ exhibit some of the features predicted by the vibrational model. Not nearly enough is known about this region experimentally; stripping and pickup reactions provide a good means of improving the situation.

IV. STRIPPING AND PICKUP REACTIONS ON $1p$ -SHELL NUCLEI

We now analyze the reduced widths given in Tables I and II, on the basis of suitable nuclear models. This section deals with nuclei in the $1p$ shell, with $4 \leq A \leq 16$.

In this region, many $l=1$ transitions involving $1p$ nucleons are discussed in terms of the intermediate-coupling shell model (In53, Ku56), using the techniques described in Sec. III.8. For the effective two-body interaction we assume either a Rosenfeld (Ro48, Fr58) or an Inglis (In53, Fr58) exchange dependence. These two forms of interaction lead to almost identical results in most cases of interest to us³²; in practical situations we select whichever is more convenient. Later in the $1p$ shell, beyond $A=11$, it is worthwhile to examine the jj coupling predictions.

We also encounter transitions involving $2s$, $1d$, and, possibly, $2p$ nucleons. In such cases it is most convenient to use the weak-coupling approach of Sec. III.11.

Reduced widths in the $1p$ shell have been discussed by Lane [La54: $\text{C}^{12}(d, p)\text{C}^{18}$], Auerbach and French (Au55: Li, C, and N), French (Fr56: $A=14$), French

³² See, however, our discussion of the channel-spin ratio in $\text{Li}^7(p, \gamma)\text{Be}^8$ (17.63 Mev).

and Fujii (Fr57: $A=6-10$), and Bennett³³ [Be58: $C^{18}(p,d)C^{12}$; $N^{15}(p,d)N^{14}$].

When we have occasion to use experimental evidence not concerned with stripping reactions, we do not, in general, give explicit references, referring the reader for such matters to the review article of Ajzenberg-Selove and Lauritsen (Aj59).

$$A=6 \rightleftharpoons 7$$

$$Li^6(d,p)Li^7$$

The ratio θ^{**}/θ_g^2 for the two levels of the ground state P doublet shows no variation as the deuteron energy increases from 2 to 14.4 Mev (Fig. 5).

With the use of a Rosenfeld interaction, we now calculate the ratio S^*/S_g of the P doublet spectroscopic factors as a function of the spin-orbit parameter ξ .³⁴ The low-lying level spectra of both Li^6 and Li^7 are well reproduced with $\xi \sim 1.2$; accordingly, let us set $\xi(Li^6) = \xi(Li^7)$ in studying S^*/S_g . The results are (Au56)

$$\begin{aligned} \xi &= 0 \quad 1.2 \quad 2.4 \quad 3.6 \\ S^*/S_g &= 1 \quad 1.2 \quad 1.4 \quad 1.6, \end{aligned}$$

with a Rosenfeld interaction. The observed ratio $\theta^{**}/\theta_g^2 \sim 1.4$ (Le55) leads to $1.8 \leq \xi \leq 2.8$, slightly larger than the values determined from the spectra. On using the lowest admissible value of $\xi=1.8$, we have $S_g=0.8$. With the absolute ground-state reduced width of Le55 we then have

$$\theta_0^2(1p)=0.060. \quad (IV.1)$$

The 4.63-Mev level is almost certainly the $\frac{7}{2}^-$ member of the F doublet. The corresponding stripping transition from Li^6 is forbidden by angular momentum conservation. The transition to the $\frac{5}{2}^-$ member of the doublet is L -forbidden.³⁵ Since all the evidence indicates that for $A=7$ we are close to LS coupling, we can expect that the predominantly $^{22}F_{\frac{5}{2}}$ level of Li^7 will not appear in $Li^6(d,p)Li^7$.

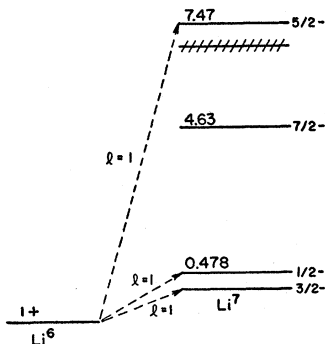


FIG. 5.

³³ Bennett's analysis of $C^{18}(p,d)C^{12}$ is incorrect. He uses different phase conventions (i.e., different basic sets of states) in his C^{12} and C^{18} wave functions.

³⁴ Defined in Example 1 of Sec. III.9.

³⁵ The transition $l^n \rightarrow l^{n-1}$, L_0 is L -forbidden if the triangle condition $\Delta(L_0 L L)$ is not satisfied.

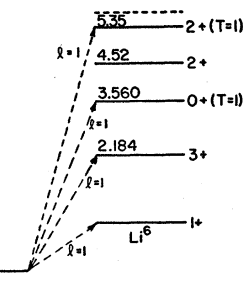


FIG. 6.

The sizeable reduced width of the $\frac{5}{2}^-$ level at 7.47 Mev is thus compelling evidence (Fr57) that it is not predominantly $^{22}F_{\frac{5}{2}}$, but that, instead, $^{24}P_{\frac{1}{2}}$ is the main component, as is now well known (Me56, Ma57). For $\xi=1.8$, the corresponding relative reduced width is $S^{**}=0.65$, whence $S^{**}/S_g=0.81$, in excellent agreement with $\theta^{**}/\theta_g^2=0.83$.

The resonant width of the 7.47-Mev level has been measured by elastic scattering of neutrons on Li^6 (Wi56). The ratio of resonance to stripping widths is found (Ha59) to be

$$\theta^2(\text{res})/\theta^2(\text{str})=0.21/0.04=5.2. \quad (\text{IV.2})$$

$$Li^7(p,d)Li^6; Li^7(d,t)Li^6$$

There are two relevant (p,d) experiments and one (d,t) (Fig. 6). The ratios of the reduced widths so obtained agree to within 20%. The (d,t) ³⁶ reduced widths are normalized as described in Sec. III.3.

Let us consider the two lowest $T=0$ states first. Once more let us take $\xi(Li^6)=\xi(Li^7)$. We have (Fr57)

$$\begin{aligned} \xi &= 0 \quad 1.2 \quad 2.4 \quad 3.6 \quad \infty \\ S^*/S_g &= 0.48 \quad 0.69 \quad 0.89 \quad 1.12 \quad 2.33, \end{aligned}$$

with a Rosenfeld interaction.

The observed³⁷ ratio $\theta^{**}/\theta_g^2=0.70 \pm 0.03$ ³⁸ is consistent with the previous predictions in the reasonable range $0.8 \leq \xi \leq 1.2$.

Serious difficulties are encountered with the $T=1$ levels. The ratio of the spectroscopic factors for the ground and 0^+ , $T=1$ levels is given by (Ha59)

$$\begin{aligned} \xi &= 0 \quad 1.2 \quad 2.4 \quad 3.6 \quad \infty \\ S^{**}/S_g &= 1 \quad 1.06 \quad 1.17 \quad 1.33 \quad 2.78, \end{aligned}$$

using a Rosenfeld interaction. These values, all greater than one, are to be contrasted with $\theta^{**}/\theta_g^2=0.66$ extracted from the (d,t) data (Ha59). The (p,d) mea-

³⁶ $Li^7(d,t)Li^6$ and $Li^7(d,He^3)He^6$ were analyzed by Hamburger (Ha59), his methods and conclusions being similar to ours.

³⁷ We regard the value for this ratio obtained from the (d,t) experiment (Le55) and the (p,d) work of Re56 as being most reliable.

³⁸ We frequently use this way of writing the value of a quantity of which we have several separate determinations (experimental or theoretical). The quoted "errors" indicate the limits within which the various determinations are consistent, and should not be taken to imply that the value so obtained is *reliable* to this accuracy.

urement of this ratio is, unfortunately, subject to large uncertainties. The statement $\theta^{2**}/\theta_g^2 = 0.5 \pm 0.3$ is probably trustworthy and suggests that the difficulty is not mainly due to our technique for extracting (d,t) widths. A more accurate (p,d) measurement of this ratio would be valuable.

The reduced width for the $2^+, T=1$ level at 5.35 Mev is hard to measure accurately because of the presence of the nearby broad ${}^{18}D_1$ level. The "measured" value of 0.5 for the reduced-width ratio is only a rough estimate. We therefore cannot attach much significance to the fact that a satisfactory value of S/S_g can be obtained only with an unreasonably large value of ζ .

In the LS limit, which should be a satisfactory approximation here, the S values of the ${}^{18}D$ levels at 4.52 and 5.5 Mev are 0.15 and 0.02, respectively. The nonappearance of these levels in $\text{Li}^7(d,p)\text{Li}^6$ is thus to be expected.

The absolute ground-state reduced widths measured by $\text{Li}^7(d,p)\text{Li}^6$ and $\text{Li}^6(d,p)\text{Li}^7$ agree well. The estimate (IV.1) of $\theta_g^2(1p)$ is therefore consistent with the pickup results on Li^7 .

$\text{Li}^7(d,\text{He}^6)\text{He}^6$

The first two levels in He^6 are the analog of the $T=1$ states at 3.56 and 5.35 Mev in Li^6 (Fig. 7). The (d,t) and (d,He^6) reduced widths for these levels should be identical. In fact,

$$\begin{aligned}\theta^2(d,\text{He}^6)/\theta^2(d,t) &= 0.8(J=0^+), \\ \theta^2(d,\text{He}^6)/\theta^2(d,t) &= 0.3(J=2^+).\end{aligned}$$

The discrepancy for the 2^+ state is striking, even allowing for a possible uncertainty by a factor of two in the (d,t) reduced width.

The statement that the predicted reduced widths for the $T=1$ levels in Li^6 are markedly smaller than the observed values obviously applied *a fortiori* to the analog levels in He^6 . For the 1.71-Mev state the disagreement involves the alarming factor four.

We regard these difficulties as very serious and can offer no satisfactory explanation. Indeed, they are perhaps the severest single trouble which we encounter in our study. Any (He^6,d) or (d,He^6) studies would help indirectly by revealing whether or not our difficulties, if genuine, stem from an incorrect treatment of the mechanism of (d,He^6) reactions.

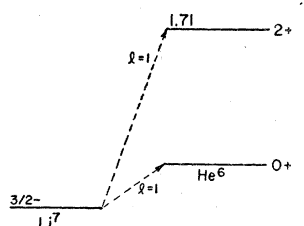


FIG. 7.

$A=7 \rightleftharpoons 8$

$\text{Li}^7(d,p)\text{Li}^8$

The 8- and 14.4-Mev experiments lead to conflicting values for the ground-state reduced widths (Fig. 8). We favor the 14.4-Mev datum since the implied value of $\theta_g^2(1p)$ agrees well with values obtained elsewhere in the $1p$ shell.

The known level spacings of Li^6 , Li^7 , and Li^8 can be adequately fitted with the same two-body interaction with values of ζ which vary very little. It is therefore reasonable to set $\zeta(\text{Li}^7) = \zeta(\text{Li}^8)$ when computing spectroscopic factors S_g , S^* , S^{**} for the three lowest levels in Li^8 . On using a Rosenfeld interaction, we have (Fr57) for the values of ζ of most interest:

ζ	S_g	S^*/S_g	S^{**}/S_g
0	10/9	0.60	0.36
1	1.09	0.50	0.31
2	0.98	0.43	0.34

Since the observed ratios θ^{2*}/θ_g^2 and θ^{2**}/θ_g^2 are 0.53 and 0.28, respectively, good agreement is obtained for any of the values of ζ in the range considered. The absolute

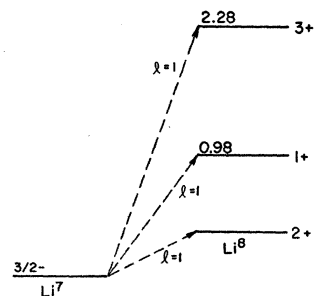


FIG. 8.

value $\theta_g^2 = 0.053$ implies

$$0.05 \leq \theta^2(1p) \leq 0.06, \quad (\text{IV.3})$$

consistent with our earlier estimate (IV.1).

Hamburger (Ha59) examined the region between 2 and 8 Mev excitation in Li^8 , without finding any other sharp levels than the ones discussed afore. It was estimated that levels with widths less than 100 kev, attained by transitions⁴⁰ with cross sections larger than 0.6 mb/sr,⁴¹ would have been detected.

An intermediate coupling calculation using a Rosenfeld interaction with $\zeta \approx 1.2$ indicates that there should be at least seven levels of the configuration $1p^4$ in the 2- to 8-Mev region, several of which have S values of the same order of magnitude as those for the three lowest levels of Li^8 .

The nonappearance of these states, at first sight

³⁹ Relative to the $T=0$ reduced widths for which agreement seems to be good.

⁴⁰ The word "transition" as a synonym for "reaction" seems to be appropriate for direct interaction processes.

⁴¹ The 2.28-Mev level shows a peak cross section of 11 mb/sr (Ha59).

surprising, can be naturally explained on recalling that levels above 2.034 Mev in Li^8 are unbound against neutron emission. The total width of such a level can be easily estimated.⁴² For example, a level as low as 3 Mev in Li^8 with $s \approx 0.5$ and $\theta_0^2(\text{res}) \approx 0.4$ already has $\Gamma > 0.5$ Mev. The widths clearly tend to increase with excitation.

Thus the expected levels with sizeable θ^2 must be broad and overlapping. The proton spectrum obtained by Hamburger (Ha59) is consistent with such an interpretation.

We have seen that the s values in $\text{Li}^7(d,p)\text{Li}^8$ to the first three levels of Li^8 are very insensitive to the spin-orbit parameter. However, on closer inspection of the interaction matrices and the tables of β_s appropriate to the 0.98-Mev level of Li^8 (Appendix 2 of Ma59), we see that the channel-spin ratio⁴³

$$x = \mathcal{J}(2)^2 / \mathcal{J}(1)^2 \quad (\text{IV.4})$$

is quite sensitive to ζ for any reasonable interaction. This arises from a strong interference effect between the $^{33}P^{[31]}$ and $^{31}P^{[31]}$ multiplets, which are expected to be quite close.

The spacing of these two multiplets is itself a parameter of considerable interest in connection with the effective two-body central interaction in the $1p$ shell. We can express all central interaction matrix elements in terms of the two-body multiplet energies $^{13,31}S$, $^{13,31}D$, ^{11}P , and ^{33}P . The channel-spin ratio is a function of these multiplet energies and ζ . Examination of a whole range of $1p$ shell data reveals that we can determine all the multiplet energies quite well with the sole exception of ^{11}P , whose position is related to the preceding Li^8 difference by

$$\begin{aligned} \Delta = ({}^{11}P - {}^{33}P) &= 2({}^{31}P^{[31]} - {}^{33}P^{[31]}) \\ &+ (11/6)({}^{13}D - {}^{31}D) + (5/6)({}^{31}S - {}^{13}S) \\ &\approx 2({}^{31}P^{[31]} - {}^{33}P^{[31]}) - 1.1 \text{ Mev.} \end{aligned} \quad (\text{IV.5})$$

In the second equation, we have used the values of the S and D multiplet separations obtained from the Li^6 spectrum.

All but two of the parameters upon which x depends have now been fixed. It is therefore worthwhile to study the behavior of the channel-spin ratio x as a function of ζ and Δ .

In principle, x might be measurable by the $\text{Li}^7(d,p\gamma)-\text{Li}^8$ (0.98 Mev) angular-correlation experiment, which has not been done. The same parameter has, however, been determined by $\text{Li}^7(p,\gamma)\text{Be}^8$. The 17.63-Mev resonant level of Be^8 which is reached in this reaction is the analog of the 0.98-Mev level in Li^8 . The angular distribution of γ rays to the ground state of Be^8 is given

⁴² See Ha59, p. 46.

⁴³ In general, we define the channel-spin ratio x to be $\mathcal{J}(z_>)^2 / \mathcal{J}(z_<)^2$. In this case, where $J_0 = \frac{3}{2}$, $z_> = 2$ and $z_< = 1$. $\mathcal{J}(z)$ is defined in terms of (β_s) matrix elements by (III.91).

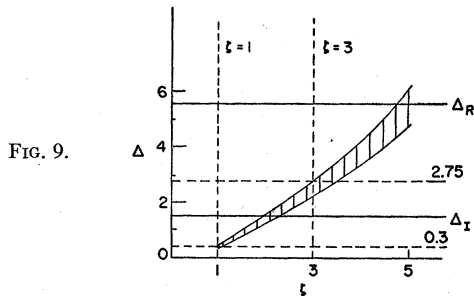


FIG. 9.

by

$$1 + [(5-x)/(5+7x)] \cos^2 \theta. \quad (\text{IV.6})$$

The most recent study of this angular distribution (Ne58) yields

$$3.0 \leq x \leq 3.6. \quad (\text{IV.7})$$

In Fig. 9 the shaded region contains points (ζ, Δ) which yield values of x within the allowed range (IV.7).

If we accept the restriction $1 \leq \zeta \leq 3$ imposed by other data in this region of the $1p$ shell, it is clear from the diagram that the measured channel-spin ratio (IV.7) implies

$$0.3 \leq \Delta \leq 2.75 \text{ Mev.}$$

The Rosenfeld interaction, which has been widely used in $1p$ shell studies, gives $\Delta_R = 5.5$ Mev, far above the allowed range. On the other hand, the Inglis interaction gives the acceptable value $\Delta_I = 1.4$ Mev. The two interactions differ very little in other respects.

It may be objected that such a complete determination treats the effective interaction too literally. Even if this be the case, the example is useful in illustrating how a channel-spin ratio may be able to measure a quantity inaccessible to reduced widths.

In conclusion we remark that the resonant reduced width of the 2.28-Mev level in Li^8 has been measured by elastic scattering of neutrons on Li^7 (Wi56). The ratio of resonant to stripping reduced width is (Ha59)

$$\theta^2(\text{res}) / \theta^2(\text{str}) = 0.072 / 0.015 = 4.8, \quad (\text{IV.8})$$

very similar to the value (IV.2) found for the 7.45-Mev level in Li^7 .

$$A=8 \rightleftharpoons 9$$

$$Be^9(p,d)Be^8$$

It is now certain (Aj59) that the only states in Be^8 below 10 Mev are the 0^+ ground state and the broad 2^+ level at 2.90 Mev. Only the ground-state angular distribution has received accurate experimental study, the two available measurements of the absolute reduced width (Re56, Su58) being in good agreement.

Let us use the wave functions of Fr55 for the Be^9 ground state and treat Be^8 in the LS coupling approximation, which should be reasonably accurate. With $\zeta = 3$, which seems (Fr55) to be a reasonable value for Be^9 , we have $s_0 \approx 0.4$. The ground-state reduced width

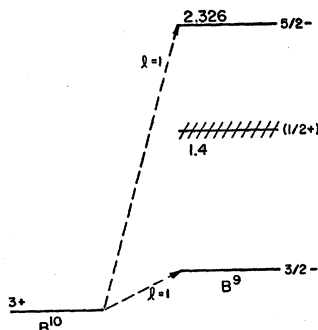


FIG. 10.

being $\theta_0^2 = 0.024$, we have

$$\theta_0^2(1p) \approx 0.06 \quad (\text{IV.9})$$

in good agreement with (IV.1) and (IV.3).

$$A=9 \rightleftharpoons 10$$

$$B^{10}(p,d)B^9$$

Transitions to two of the three lowest states in B^9 have been studied (Re56) (Fig. 10). The spin assignments are based on evidence concerning the mirror nucleus Be^9 , but do not contradict anything known about B^9 itself.

If the 1.4-Mev level has, in fact, spin $\frac{1}{2}^+$, the transition to it is l -forbidden; experimentally, no stripping is observed.

In Table IV are given⁴⁴ values of S/S_g for the $\frac{5}{2}^-$ and $\frac{3}{2}^-$ levels with various pairs of spin-orbit parameters $\zeta(B^9)$ and $\zeta(B^{10})$.

The B^{10} wave function near the LS limit varies very rapidly with ζ , a fact which is reflected in the behavior of S/S_g . Apart from this the ratio S/S_g is insensitive to variations in the spin-orbit parameters. For all values of ζ in Table IV, except the first and possibly the fifth, agreement with the observed ratio $\theta^2/\theta_0^2 = 0.8$ is adequate. In view of the complexity of the wave functions, the general agreement found for the reduced width ratio is pleasing. The favored values of the spin-orbit parameters are $\zeta(B^9) \approx 1.8$, $\zeta(B^{10}) \approx 3.8$, but the wave functions are too complicated for us to place much reliance on this.⁴⁵

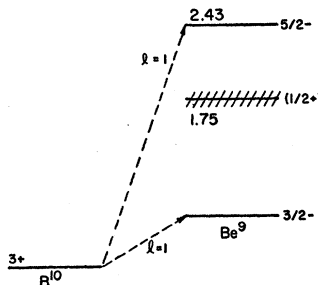


FIG. 11.

There is a general lack of experimental information concerning the $A=9$ polyad. Higher levels in Be^9 and B^9 , their spins, parities, and positions should be studied. In this (and other) connections, careful $B^{10}(d,t)B^9$ and $B^{10}(d,He^3)$ experiments would be valuable.

$$B^{10}(n,d)Be^9$$

The results of this experiment (Ri54) are in satisfactory agreement with those of the mirror experiment. The observed value of θ^2/θ_0^2 for the $\frac{5}{2}^-$ level is 1.05, slightly larger than the (p,d) value (Fig. 11).

The theoretical discussion of $B^{10}(p,d)B^9$ is equally applicable here. The larger value of θ^2/θ_0^2 improves agreement with the calculated S/S_g for higher $\zeta(Be^9)$ and correspondingly strengthens the argument in favor of $\zeta(Be^9) \sim 3$.

The absolute ground-state reduced width of 0.043 leads to

$$0.04 \leq \theta_0^2(1p) \leq 0.06, \quad (\text{IV.10})$$

in satisfactory agreement with earlier estimates.

$$Be^9(d,p)Be^{10}$$

The $l=1$ transitions to the first two states of Be^{10} have been examined at various bombarding energies [Fig. 12(a)]; most observers, unfortunately, did not measure absolute cross sections. The reduced width ratio does not seem to vary with energy [Fig. 12(b)]; on the basis of the 3.6- and 14.4-Mev data, it is tempting to suggest that $\theta_0^2(1p)$ increases with bombarding energy. Systematic measurements, in this or other cases, are badly needed to clarify the behavior of reduced widths as a function of the energy parameters (bombarding energy and Q value).

Calculations of relative reduced widths for the first two levels of Be^{10} predict a strong ground-state transition ($S \approx 2$) and an excited-state transition which is weaker by a factor of 10 ($S \approx 0.2$). These predictions are in satisfactory accord with the experimental reduced width ratio of 0.18 ± 0.07 . On using the absolute ground-state width at 14.8 Mev, we have

$$0.04 \leq \theta_0^2(1p) \leq 0.05, \quad (\text{IV.11})$$

which agrees with earlier estimates.

TABLE IV.

$\zeta(B^9)$	$\zeta(B^{10})$	S_g	S	S/S_g
0	0	0.0012	1.84	~1500
1.4	1.4	1.18	1.35	1.13
2.8	2.8	1.12	1.24	1.11
3.8	3.8	1.09	1.24	1.14
5.7	5.7	1.03	1.26	1.22
1.4	3.8	1.03	0.95	0.92

⁴⁴ From Table III of Fr55.

⁴⁵ If the spin of the first excited state of B^9 and Be^9 is $\frac{1}{2}^+$, as seems to be the case (Aj59), a value $\zeta(B^9) \approx 3$ is preferred. On the

other hand, a $\frac{1}{2}^-$ assignment would favor the smaller value $\zeta \approx 1.8$. See Fr55 for a fuller discussion.

The calculation for the 2^+ state predicts that channel spin 2 should dominate; measurements of (ρ, γ) angular correlations (Aj59) confirm this prediction, giving a value of nine for the channel-spin ratio x defined by (IV.4).

We now turn our attention to negative parity levels of Be^{10} . Two strong $l=0$ transitions proceed to the 5.96- and 6.26-Mev levels of Be^{10} . Since Be^9 has $J_0 = \frac{3}{2}^-$, these levels must have spin 1^- or 2^- . The γ -decay branching ratios to the first two states of Be^{10} (Me58, Aj59) indicate definitely that the 5.96-Mev level has $J=1^-$ and the 6.26-Mev level $J=2^-$. It is likely⁴⁶ that these levels are the members of the $T=1$ $2s$ doublet

$$[\varphi_0(\text{Be}^9) \times 2s_{\frac{1}{2}}]_{J=1^-, 2^-}. \quad (\text{IV.12})$$

Since we are dealing with levels within 800 kev of the neutron separation energy, we cannot place much reliance on the exact values of the reduced widths. It is, however, interesting that

$$[J]\theta^2(6.26) > [J]\theta^2(5.96) \quad (\text{IV.13})$$

in agreement with the foregoing spin assignments, in spite of the fact that the observed peak cross sections (Rh54, Gr56) are in the ratio

$$\sigma(5.96)/\sigma(6.26) \approx 1.5. \quad (\text{IV.14})$$

The intermediate-coupling calculations of Inglis (In53) and Kurath (Ku56) predict that, for any reasonable interaction, the first four $T=1$ levels of $1p^6$ should have $J=0^+, 2^+, 2^+$, and 3^+ . The S values for the second 2^+ and the 3^+ states are zero in the jj limit and are very small for reasonable values of $S(\text{Be}^9)$ and $\zeta(\text{Be}^{10})$. The 6.18-Mev level, whose stripping width is unobservably small, may well be the second 2^+ state.

The 7.37-Mev level has attracted much attention.⁴⁷ From $\text{Be}^9(n,n)$ (Wi55) the spin of this level is definitely three; the angular distribution of neutrons is best fitted on the assumption of p -wave formation (and therefore positive parity), although d -wave capture cannot be ruled out (Wi55, Aj59). The 3^+ assignment was apparently confirmed when Green and Middleton (Gr56) obtained a good fit to the stripping data with $l=1$; the 14.8-Mev data, however, are not nearly as well fitted by $l=1$ (Ca58).

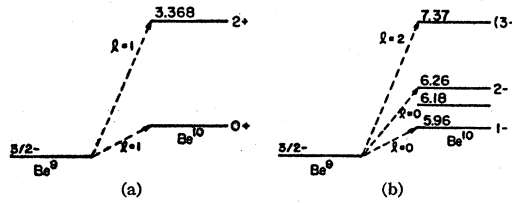


FIG. 12.

⁴⁶ The absence of any other levels below 7.5 Mev in Be^{10} with measurable $l=0$ reduced widths suggests that the $2s$ states (IV.12) are not subject to strong final-state interactions.

⁴⁷ We are indebted to Dr. E. W. Hamburger for much of the ensuing discussion.

Assuming that the $l=1, J=3^+$ assignment is correct, we would have

$$\theta^2(\text{res})/\theta^2(\text{str}) = 0.015/0.042 = 0.36,$$

smaller by an order of magnitude than the ratios [(IV.2) and (IV.8)] found for the 7.47-Mev level in Li^7 and the 2.28-Mev level in Li^8 , which are quite typical. This contradictory situation, whereby the same transitions is strong from the stripping viewpoint and weak as a resonance reaction, constitutes a serious objection to the $l=1, 3^+$ assignment. Furthermore, the $l=1$ reduced width from the stripping data is larger by an order of magnitude than what is expected for the $3^+, T=1$ state.⁴⁸

On closer scrutiny, $l=2, J=3^-$ is much more attractive. Both the elastic neutron scattering data and the stripping distribution of Green and Middleton are not inconsistent with such an assumption, while Cameron's (d,p) results favor $l=2$ quite strongly. We would then have

$$\theta^2(\text{res})/\theta^2(\text{str}) = 0.136/0.041 = 3.3, \quad (\text{IV.15})$$

a very reasonable result.

If the $J=3^-$ assignment is correct, the level must be predominantly $[\varphi_0(\text{Be}^9) \times d_{\frac{3}{2}}]_{3^-}$. The S value for the corresponding transition from Be^9 is then close to unity, whence

$$\theta_0^2(1d) \geq 0.04, \quad (\text{IV.16})$$

which is satisfactorily consistent with other p -shell estimates of this quantity. We conclude that available data strongly suggest that the 7.37-Mev level in Be^{10} has $J=3^-$.

$\text{Be}^9(d,n)\text{B}^{10}$

Only a low-energy experiment (Aj52) with no absolute cross sections is available (Fig. 13). For this reason, and because of the great complexity of the relevant wave functions, we do not consider it worth-

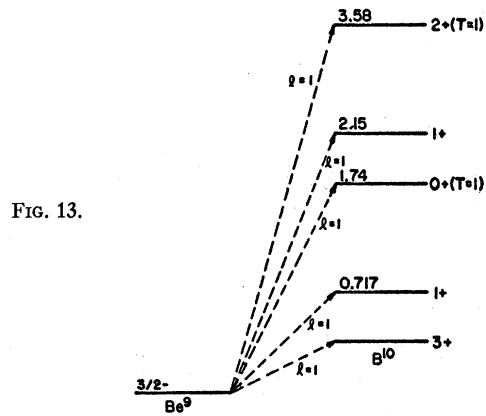


FIG. 13.

⁴⁸ The $l=1$ transition to this level is forbidden in both LS and jj coupling. For $\zeta(\text{Be}^9)=1.5$ and $\zeta(\text{Be}^{10})=4, 5$ we have $S=0.012, 0.011$, respectively (Fr55).

while to undertake a detailed comparison of observed reduced widths and calculated S values.

Since only the lowest $T=1$ level has so far been studied in $\text{Be}^9(d,n)\text{B}^{10}$, no direct comparison can be made between the ratios of the reduced widths of $T=1$ levels in B^{10} and of their analogs in Be^{10} . However, the absolute reduced widths of the ground ($3^+, T=0$) and second excited ($0^+, T=1$) states of B^{10} have been measured by $\text{B}^{10}(n,d)\text{Be}^9$ and $\text{Be}^9(d,p)\text{Be}^{10}$, respectively. The ratio of the reduced widths so obtained, $0.093/0.043 = 2.1$, is to be compared with the value 1.4 measured directly by the (d,n) experiment. In view of the low energy of the (d,n) deuterons, this agreement is perhaps all that could be expected.

An experiment at higher deuteron energy, including absolute cross sections,⁴⁹ would be valuable. We have already noted the existence of possible weak-coupling $2s_1$ levels in Be^{10} . In the 5- to 10-Mev region in B^{10} we expect to find strong $l=0$ transitions to four such levels, two with $T=0$ and two with $T=1$.

$$A = 10 \rightleftharpoons 11$$

$$\text{B}^{10}(d,p)\text{B}^{11}; \text{B}^{10}(d,n)\text{C}^{11}$$

The reduced-width ratios for mirror (d,p) and (d,n) reactions (Ev54, Ce56) to levels below 7 Mev, in B^{11} and C^{11} , respectively, are in good agreement (Fig. 14). No absolute (d,p) reduced widths have been measured.

Quantitative intermediate coupling calculations of spectroscopic factors are of doubtful value in this complex region and are not attempted. It is worthwhile, however, to consider the jj -coupling predictions. In this approximation the low-lying levels of B^{11} and C^{11} belong to the configurations $p_{\frac{1}{2}}^7$ and $p_{\frac{3}{2}}^6 p_{\frac{1}{2}}^1$ which contain, for $T=\frac{1}{2}$, the following states:

$$J = (\frac{1}{2})^2, (\frac{3}{2})^3, (\frac{5}{2})^2, \frac{7}{2}. \quad (\text{IV.17})$$

Three of these states can be reached from $(p_{\frac{1}{2}}^6)$ ($TJ = (03)$), the levels in question having $J = \frac{3}{2}, \frac{5}{2}$, and $\frac{7}{2}$

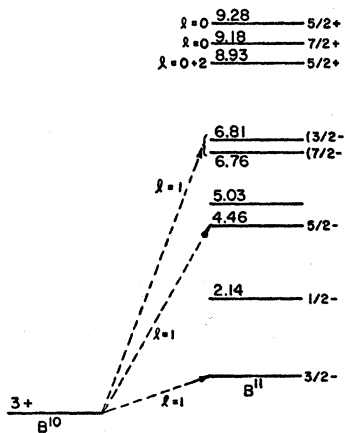


FIG. 14.

TABLE V.

B^{11} excitation	J^π	θ^2 rel	C^{11} excitation	J^π	θ^2 rel
0	$\frac{3}{2}-$	1	0	$\frac{3}{2}-$	1
2.14	$\frac{1}{2}-$...	1.99	$\frac{1}{2}-$...
4.46	$(\frac{5}{2}-)$	0.25	4.26	$(\frac{5}{2}-)$	0.2
5.03	$(\frac{3}{2}-)$	0.17	4.75	$(\frac{3}{2})$	0.14
6.76	$(\frac{7}{2}-)$	0.7			
6.81	$(\frac{3}{2}-)$...			
7.30	$(\frac{5}{2}-)$?			
7.99					

with $S=7/4$, 1 and, 1, respectively. The spins (Aj59, Table 11.1) and $l=1$ reduced widths of negative parity levels below 8 Mev in B^{11} and C^{11} are listed in Table V.

Agreement with the simple jj predictions is fair. The number and what is known of the spins of the low-lying negative parity levels is consistent with the enumeration (IV.17). The reduced-width ratios, although they indicate mixing of the basic $\frac{3}{2}-$ and $\frac{5}{2}-$ states, are also in qualitative agreement with the values 1:0.57:0.57 predicted in jj coupling.

We do not discuss the reactions to the first excited states of B^{11} and C^{11} , which appear to have the characteristic $l=1$ angular distribution although the spins ($3^+ \rightarrow \frac{1}{2}-$) forbid $l=1$ stripping. To resolve this difficulty, various authors⁵⁰ have invoked a spin-flip or a nucleon exchange effect. We later remark on a number of cases where a similar mechanism might have been expected to be important.

The large $l=0$ reduced widths of levels at 9.19 and 9.28 Mev in B^{11} suggest an interpretation in terms of the weak coupling of a $2s$ nucleon to the ground state (φ_0) of B^{10} . In fact, since the relevant spins are known (Aj59) to be $\frac{7}{2}$ (9.19 Mev) and $\frac{5}{2}$ (9.28 Mev), we interpret the levels in question as $[\varphi_0 \times 2s_{\frac{7}{2}}]_{7/2}+$ and $[\varphi_0 \times 2s_{\frac{5}{2}}]_{5}+$. The small energy separation of these states and other aspects of s doublets in light nuclei are discussed in a paper by Bilaniuk and French (Bi60).

The transition to the 8.93-Mev level ($J=\frac{5}{2}$) is identified by Bilaniuk and Hensel (Bi58) as $l=2$ with a smaller $l=0$ admixture. If the positive-parity assignment so obtained is correct,⁵¹ it is clear that we are dealing with a major fragment of the $1d$ single-particle state $[\varphi_0 \times 1d_{\frac{5}{2}}]_{\frac{5}{2}}+$. The $l=0$ admixture in the 8.93-Mev angular distribution then indicates an interaction with $[\varphi_0 \times 2s_{\frac{5}{2}}]_{\frac{5}{2}}+$. In Sec. III.11 we saw how the ratio of the $l=0$ and $l=2$ reduced widths of this level can be used to determine the mixture of the basic single-particle states in the observed $\frac{5}{2}+$ levels.

The fact that no absolute (d,p) cross sections have been measured tends to weaken our arguments in favor

⁴⁹ See Au59 for discussion and references.

⁵⁰ Recent work by Wilkinson (Wi60) on the reaction $\text{B}^{10}(d,p)\text{B}^{11}$ at low deuteron energies (3 to 4.5 Mev) suggests negative parity for the 8.93-Mev level; in a study of $\text{Be}^9(\text{He}^3, p)\text{B}^{11}$, Hinds and Middleton (Hi60b) reach a similar conclusion. If the parity of the level in question is indeed negative, Example 1 of Sec. III.11 should be regarded merely as an illustration of the weak-coupling procedure.

⁵¹ A preliminary report has appeared of a $\text{Be}^9(\text{He}^3, d)\text{B}^{10}$ experiment, using 25-Mev He^3 ions (We60).

of the single-particle nature of the levels in question. In this particular case, however, the high spin of the B^{10} ground state leads us to expect weak coupling of $2s_{\frac{1}{2}}$ to be a very good approximation for $J=\frac{7}{2}^+$ and quite good for $J=\frac{5}{2}^+$.

The foregoing interpretation of the stripping data for levels near 9 Mev in $B^{11}(\text{Bi}^{68})$ implies $\theta_0^2(1d) \approx \theta_0^2(2s)$, whereas, in other cases of capture into weakly bound levels of the final nucleus, we find $\theta_0^2(2s) \geq \theta_0^2(1d)$. The measured $B^{10}(d,n)C^{11}$ ground-state reduced width (Ma56) is smaller than expected on the basis of jj coupling, by a factor of two.

Measurements of absolute cross sections in $B^{10}(d,p)B^{11}$ and independent determinations of the parity of the 8.93-Mev level would be valuable.

$$B^{11}(p,d)B^{10}$$

No pertinent experimental data are available.

In jj coupling we have

$$p_{\frac{1}{2}}^7 : (TJ) = (\frac{1}{2} \frac{3}{2}) \rightarrow p_{\frac{1}{2}}^6 : (T_0 J_0),$$

the spectroscopic factor for which follows immediately from (III.76) and is

$$S(T_0 J_0) = \frac{1}{4}[T_0 J_0]. \quad (\text{IV.18})$$

We thus expect to see four $l=1$ transitions, the states of $p_{\frac{1}{2}}^6$ and their relative reduced widths being, from (IV.18),

$$\begin{aligned} T_0 J_0 &= 03 \quad 01 \quad 10 \quad 12 \\ S(T_0 J_0) &= 7/4 \quad 3/4 \quad 3/4 \quad 15/4. \end{aligned}$$

The jj prediction is therefore that the first three levels of B^{10} should show strong reactions, while the other positive parity levels except the lowest with $T=1$, $J=2$ (probably at 5.16 Mev) should be weak.

Transitions to negative parity levels of B^{10} are forbidden by configuration selection rules and should be weak. Any measured $l=0$ or $l=2$ width would indicate components from higher configurations in the B^{11} ground state.

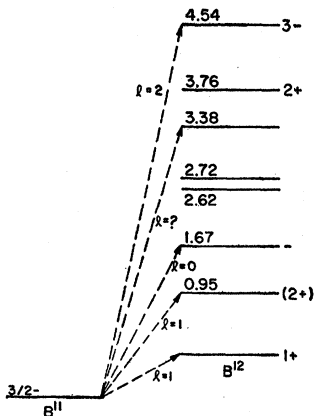


FIG. 15.

$$A=11 \rightleftharpoons 12$$

$$B^{11}(d,p)B^{12}$$

The reliability of the reduced widths from the only available experiment (Ho53c) is doubtful, especially for transitions to the second and higher excited states, because of a lack of low-angle measurements (Fig. 15).

We first inquire whether jj coupling can predict the main features of the observed $l=1$ transitions. Since $p_{\frac{1}{2}}^8$ contains no $T=1$ states, we must have

$$p_{\frac{1}{2}}^7 p_{\frac{1}{2}} \rightarrow (p_{\frac{1}{2}}^7)_{J_0=\frac{1}{2}}.$$

We therefore expect two strong $l=1$ transitions ($s \approx 1$) proceeding to levels in B^{12} with $J=1^+$ and 2^+ .

Two strong $l=1$ reactions proceed to the first two states of B^{12} , the relative values of the reduced widths being consistent with 2^+ for the first excited state. The absolute reduced widths, however, are smaller than expected by a factor close to two. A weak $l=1$ level is found at 3.76 Mev by $B^{11}(n,n)B^{11}$ (Wi55). If there are no other strong $l=1$ transitions, the jj coupling picture is qualitatively correct.

The $l=0$ reduced width of the 1.67-Mev level is subject to considerable uncertainties because no measurements were made below 14° . The strength of the transition suggests $[\varphi_0(B^{11}) \times 2s_{\frac{1}{2}}]_{1^- \text{ or } 2^-}$.

The 3.38-Mev transition was assigned $l=1$ by Holt and Marsham (Ho53c). This assignment is uncertain because they did not measure the differential cross section below 23° . In fact, if we compare the 3.38- and 1.67-Mev angular distributions for $\theta \geq 23^\circ$, we see that they are very similar. Thus $l=0$ is a definite possibility for the 3.38-Mev level. At any rate, the 2.62-, 2.72-, and 3.38-Mev levels probably include at least one strong $l=0$ state, corresponding to the second member of the $[\varphi_0 \times 2s_{\frac{1}{2}}]$ doublet. The situation obviously needs experimental clarification.

The $l=2$ assignment for the 3^- level at 4.54 Mev, not convincing from the stripping data, is confirmed by $B^{11}(n,n)B^{11}$ (Wi55). The next level with $J=3$ is at 5.73 Mev in B^{12} , the l value from $B^{11}(n,n)$ being either one or two. It is not clear whether this level, whose resonant reduced width is small (see Aj59, Table 12.2) for either l value, is a 3^+ , $T=1$ level of $p_{\frac{1}{2}}^8$ or a 3^- level containing a fragment of $[\varphi_0(B^{11}) \times d_{\frac{3}{2}}]$. In any case, we expect weak coupling to be a reasonable approximation for the 4.54-Mev level, since the first excited state of B^{11} , with $J=\frac{1}{2}^-$, is 2 Mev above the ground state. The absolute reduced width for the 4.54-Mev level indicates

$$0.05 \leq \theta_0^2(1d) \leq 0.06. \quad (\text{IV.19})$$

$$B^{11}(d,n)C^{12}$$

The two available experiments (Gi54, Ma56) yield reduced width⁵² ratios for the first two levels of C^{12}

⁵² The reduced widths extracted from the data of Ma56 and given in Table I differ from those quoted in Table 12.8 of Aj59 by a factor of two. The discrepancy arises from the isotopic-spin coupling factor which here has the value $\frac{1}{2}$.

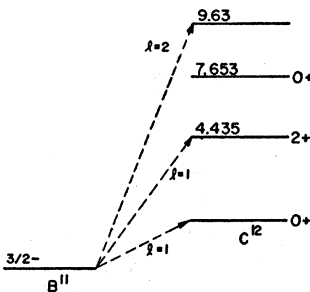


FIG. 16.

differing by a factor of 2.6 (Fig. 16). The ground-state angular distribution in the 8.1-Mev experiment is, however, very crude and the disagreement is probably not significant.

The jj predictions for the $l=1$ transitions are rather interesting. The ground-state transition fills the eight particle $p_{\frac{1}{2}}$ shell and therefore has $S=8$. (See Example 4 of Sec. III.9.) A very large value is, in fact, observed for θ_0^2 . Two other $l=1$ transitions to $T=0$ levels are expected; each involves the addition of a $p_{\frac{1}{2}}$ nucleon and has $S=1$. The reduced width for the 2^+ level at 4.435 Mev is in apparent agreement with such a prediction. The corresponding $J=1^+$ state has not yet been identified.

The strong $l=2$ transition to the 9.63-Mev level indicates that it is predominantly $[\varphi_0(B^{11}) \times d_{\frac{5}{2}}]$. The spin of the state is probably 1^- ; 2^- would give a value of $\theta_0^2(1d)$ more in line with other determinations, but seems to be excluded by the data concerning $C^{12}(e,e')$ and $N^{14}(d,\alpha)$ (see Aj59).

Considerable interest centers on the 0^+ level at 7.653 Mev; intermediate coupling calculations within $1p^8$ (Ku56) predict that the first 0^+ excited state should be at least 3 Mev, and probably 5 Mev, higher. It is therefore of interest to find out what are the dominant configurations in this level. In addition to $1s^4 1p^8$, we could have the doubly excited configurations $1s^4 1p^6 2s^2$, $1s^4 1p^6 1d^2$, and $1s^4 1p^6 2s1d$, and the "breathing modes" $1s^4 1p^7 2p$ and $1s^3 1p^8 2s$.

Both $1s^4 1p^8$ and $1s^4 1p^7 2p$ components can be reached by $B^{11}(d,n)C^{12}$. Unfortunately, present experimental information can only give the upper limit $\theta^2 < 0.02$ on the reduced width, and this is too crude to give us useful information about the configurations.

A careful study of the level under consideration has been made by $C^{18}(d,t)C^{12}$ (Ma60). The reduced width $\theta^2 = 0.0012$ so measured implies $S \approx 0.025$. The simplest interpretation of this S value is that the 7.653-Mev level is about 10% $s^4 p^8$.⁵³ A component of this size could arise by the interaction of a 0^+ state from $s^4 p^8$ with a similar state belonging to excited configurations. Stripping data on this and other levels up to 14 Mev would be interesting and might best be obtained by a careful $B^{11}(He^3,d)$ rather than $B^{11}(d,n)$ experiment.

⁵³ An accidental cancellation is possible but unlikely.

$$A = 12 \rightleftharpoons 13$$

$$C^{12}(d,p)C^{13}$$

Relative and absolute differential cross sections for $C^{12}(d,p)C^{13}$ have been measured at deuteron energies between 2 and 14.8 Mev. (Fig. 17). There is no definite indication of an energy variation in the reduced widths, although the ground state reduced width seems to increase slightly between 2.7 and 9 Mev. The experiments at 8, 9, and 14.8 Mev are in reasonable agreement. We regard the latter two as more reliable⁵⁴ and use the corresponding reduced widths in the following analysis.

For the $l=1$ transitions⁵⁵ to the $\frac{1}{2}^-$ and $\frac{3}{2}^-$ levels, we have $S_g = S^* = \frac{1}{3}$ in LS coupling and $S_g = 1, S^* = 0$ in the jj limit. The experimental ratio $\theta_0^2/\theta_1^2 = 0.25 \pm 0.06$ then indicates immediately that we are far from LS coupling (as is well known anyway). A plot of the S values and their ratio, covering the transition from LS to jj coupling is given in Fig. 1, where we have calculated S_g and S^* as functions of ζ (assumed the same for each nucleus) with an Inglis interaction. The reduced-width ratio is not well enough determined experimentally to fix a value of ζ , but the range $3 \leq \zeta \leq 6$ is satisfactory. For $\zeta = 5$ we find $S_g = 0.7$, whence, using $\theta_0^2 = 0.036 \pm 0.006$, we have

$$0.043 \leq \theta_0^2(1p) \leq 0.06, \quad (IV.20)$$

which agrees with other estimates.

Because the lowest states of C^{12} are widely separated, the levels at 3.09 and 3.85 Mev must be nearly pure single particle $2s_{\frac{1}{2}}$ and $1d_{\frac{5}{2}}$ levels. This expectation is confirmed by the corresponding strong $l=0$ and $l=2$ transitions, from which we obtain reliable estimates of the single-particle reduced widths:

$$\theta_0^2(2s) \approx 0.17, \quad (IV.21)$$

$$\theta_0^2(1d) \approx 0.07. \quad (IV.22)$$

McGruer *et al.* (Mc56) studied several unbound levels between 5 and 9 Mev in C^{13} , but could not assign l values because the relevant Butler curves with $l=0, 1$, and 2 are very similar. The correct values of l

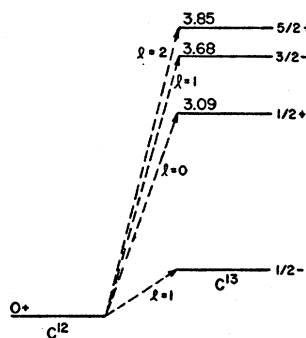


FIG. 17.

⁵⁴ See Table I, footnote k.

⁵⁵ These were first studied by Lane (La54), who also discussed weak coupling for the positive parity levels of C^{13} (La55).

have now been determined by elastic scattering of neutrons on C¹². (See Table 13.5 of Aj59.)

The 5.51- and 6.10-Mev levels are not seen either in the stripping or in neutron scattering experiments. One of them is probably the $\frac{5}{2}^-$ level of p^0 which grows from the $^{22}F^{[441]}$ multiplet.

At 6.86 Mev there is an $l=2$ level with $J=\frac{5}{2}^+$ whose small stripping width $\theta^2=0.0018$ indicates a fragment of the basic single-particle state $[\varphi_0(C^{12}) \times 1d_{\frac{5}{2}}]$, whose major component belongs to the $\frac{5}{2}^+$ level at 3.86 Mev. The 6.86-Mev level must be⁵⁶ predominantly $[\varphi_1(C^{12}: 4.435) \times s_{\frac{1}{2}}]$ (or perhaps $d_{\frac{3}{2}}$), the reduced widths implying that the $[\varphi_0 \times d_{\frac{3}{2}}]$ component amounts to only 2.5% in intensity. Such an admixture demands an interaction matrix element of about 600 kev.

A weak $l=2$ level with $J=\frac{3}{2}^+$ is found at 7.57 Mev by $C^{12}(n,n)C^{12}$ and another such level, with a very large resonant width, at 8.33 Mev. The latter level appears very strongly in $C^{12}(d,p)C^{13}$, but it is too broad to yield an identifiable angular distribution. It is probable that we are dealing here with single particle $d_{\frac{3}{2}}$ components, which would indicate

$$[d_{\frac{3}{2}}] - [d_{\frac{1}{2}}] \approx 4 \text{ Mev.} \quad (\text{IV.23})$$

for the d doublet splitting in C¹³, comparable to the value (≈ 5 Mev) found in O¹⁷.

$$C^{12}(d,n)N^{13}$$

This experiment should yield very similar results to the mirror (d,p) experiment, since the spectra of C¹³ and N¹³ agree very closely. Because of the much poorer resolution in the (d,n) case, no meaningful comparison can be made, apart from noting that the absolute ground state reduced widths agree tolerably well.

$$C^{13}(p,d)C^{12}; C^{13}(d,t)C^{12}$$

There is a large discrepancy between the absolute ground-state reduced widths measured in the only available (p,d) experiment (Be58) and the (d,p) experiments (Fig. 18). The (d,p) reduced width being confirmed by several experiments, we suggest that the (p,d) cross section quoted in Be58 is incorrect.

The ratio of reduced widths for the first two states of C¹² is found to be 0.95 on the (p,d) experiment (Be58) and 0.76 in the (d,t) experiment (Ma59). The two determinations agree well.

In Fig. 1, again calculated with an Inglis interaction, it is clear that

$$s^*/s_g > 1.2,$$

and that the ratio does not vary appreciably for $\zeta > 5$. This agreement is mediocre and no value of ζ can be fixed.

⁵⁶ $[\varphi_3 \times 1p_{\frac{1}{2}}]$, where φ_3 represents the (1^-) state at 9.63 Mev in C¹², would appear energetically to be an even stronger possibility. However, we have already seen that $\varphi_3 \approx [(\rho_1') \times d_{\frac{3}{2}}]$, so that $[\varphi_3 \times 1p_{\frac{1}{2}}] \approx [\varphi_0 \times d_{\frac{3}{2}}]$.

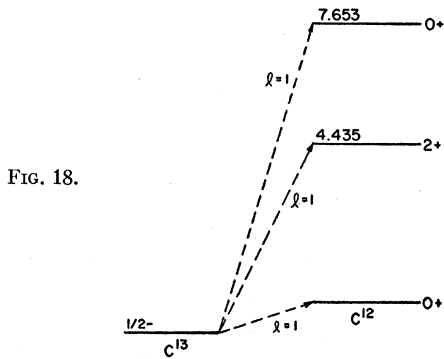


FIG. 18.

We have already pointed out, in discussing B¹¹(d,n)C¹², that the (d,t) reduced width (0.0012) of the 7.653-Mev level probably indicates a component of $s^4 p^8$ about 10% in intensity. Nothing further can be said about the structure of this state until further experimental data are available, concerning stripping from B¹¹ to the level in question and both stripping and pickup to higher levels of C¹².

In spite of the very small reduced width, a clear $l=1$ angular distribution is observed (Ma59) to the 7.653-Mev level. The background in this weak transition is itself surprisingly low, about 0.02 mb/sr. There is, in fact, some evidence that the background in deuteron-triton reactions tends to be lower than in the corresponding deuteron-nucleon reactions. Further experimental study of this point, which could be very significant, is essential. A very interesting experiment in this connection would be the "spin-flip" transition B¹⁰(He³, d)C¹¹ (2.01 Mev). If the nonstripping contributions to deuteron-triton and deuteron-nucleon cross sections differ markedly, this is obviously an ideal case to examine.

$$A = 13 \rightleftharpoons 14$$

$$C^{13}(d,p)C^{14}$$

All low-lying $l=1$ transitions are forbidden in jj coupling except that to the ground state, for which $S=2$. The only strong $l=1$ transition observed is, in fact, the ground-state transition, as predicted (Fig. 19). The 6.59-Mev level is probably weak $l=1$, possibly the $J=2^+$ ($T=1$) level expected in this vicinity.

The level at 6.09 Mev is known to have $J=1^-$ (Aj59), and shows a strong $l=0$ stripping transition. It is undoubtedly $[\varphi_0(C^{13}) \times 2s_{\frac{1}{2}}]_{1^-}$, there being no nearby 1^- levels to suggest strong interactions. From the reduced width we obtain the value

$$\theta_0^2(2s) \approx 0.20. \quad (\text{IV.24})$$

We do not expect the 0^- member of the $s_{\frac{1}{2}}$ doublet to be far away. The only level below 11 Mev with a strong enough stripping transition is a $J=0$ level, of uncertain parity, at 6.89 Mev. This level was assigned $l=1$ in Mc56; however, the reduced width would then

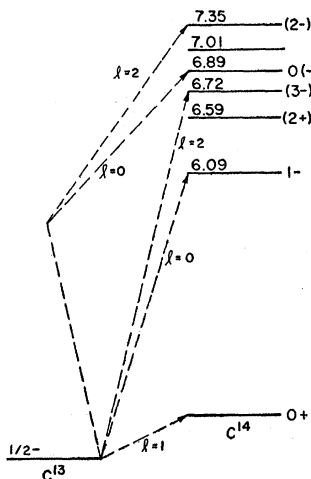


FIG. 19.

be anomalously large for an $l=1$ transition ($\theta^2 \approx 0.09$) and incredibly so for a forbidden one. It is found that $l=0$ gives an acceptable fit to the angular distribution of the transition in question and must surely be the correct assignment. (See Table I, footnote p.) Because of a lack of low-angle measurements, a reliable reduced width could not be extracted. The transition, however, is strong and the 6.89-Mev level probably $[\varphi_0(C^{13}) \times 2s_{\frac{1}{2}}]$.

The strong $l=2$ transitions to states at 6.72 and 7.35 Mev suggest the presence of large components of $[\varphi_0 \times d_{\frac{3}{2}}]_{2^-, 3^-}$. We expect weak coupling for the $1d_{\frac{3}{2}}$ single-particle states of C^{14} . The lowest states in the weak coupling representation (Sec. III.11) which can interact with $[\varphi_0 \times d_{\frac{3}{2}}]_{2^-, 3^-}$, $[\varphi_2 \times d_{\frac{3}{2}}]_{2^-, 3^-}$, and $[\varphi_2 \times 2s_{\frac{1}{2}}]_{2^-}$, where φ_2 represents the $\frac{3}{2}^-$ second excited state of C^{13} , are probably about 3 Mev higher, since the excitation of φ_2 is 3.68 Mev. The assumption that the 6.72- and 7.35-Mev levels are the 3^- and 2^- members, respectively, of the doublet is supported by the reduced-width ratio

$$[J]\theta^2(6.72) : [J]\theta^2(7.35) = 1.55 : 1,$$

very close to the statistical ratio of 1.4:1. The absolute reduced widths yield

$$0.06 \leq \theta_0^2(1d) \leq 0.07. \quad (\text{IV.25})$$

A broad level at 11.9 Mev in C^{14} appears very strongly in $C^{13}(d,p)C^{14}$. Although no l assignment is possible, it is probable that this transition involves one (or both?) single particle $d_{\frac{3}{2}}$ states with $J=1^-$ and 2^- . This would indicate

$$[d_{\frac{3}{2}}] - [d_{\frac{3}{2}}] \approx 5 \text{ Mev}, \quad (\text{IV.26})$$

similar to values found for the d doublet splitting in C^{13} and O^{17} . A firm l assignment might be possible by $C^{13}(n,n)C^{13}$.

$C^{13}(d,n)N^{14}$

There is no data concerning reduced widths, although a few low-energy experiments have been performed (see Aj59). In jj coupling, we expect only two $l=1$ transitions, both with $S=2$, to the first two states of N^{14} . Negative parity $2s_{\frac{1}{2}}$ and $1d_{\frac{3}{2}}$ levels appear with both $T=0$ and $T=1$. The $T=1$ levels, analogs of the C^{14} levels discussed previously, have been identified by $C^{13}(p,p)C^{13}$ (Table 14.8 of Aj59). A high resolution $C^{13}(He^3,d)N^{14}$ experiment, studying levels in N^{14} up to 10 Mev, would be well worthwhile.

$C^{14}(d,t)C^{13}$

The calculated ratio for the $l=1$ reduced widths to the $\frac{3}{2}^-$ and $\frac{1}{2}^-$ levels is found to be insensitive to the spin-orbit parameters, except near the uninteresting LS limit (Fig. 20). With $\zeta(C^{13})=\zeta(C^{14})$, we have

$\zeta=0$	2	5	16	∞
$S^*/S_g=2$	1.47	1.15	1.20	1.23.

Reasonable separate variations of $\zeta(C^{13})$ and $\zeta(C^{14})$ do not change these results appreciably.

The experimental reduced-width ratio (Mo58) is $\theta^*/\theta_g^2 \approx 0.7$, significantly smaller than S^*/S_g for any value of ζ . This disagreement may perhaps indicate a variation in $\theta_0^2(1p)$ between the ground and 3.68-Mev states, which, in turn, may be due to the fact that the reaction is (d,t) rather than the simpler (p,d) .

Since the 3.09- and 3.86-Mev levels have been identified as single-particle $2s_{\frac{1}{2}}$ and $1d_{\frac{3}{2}}$ states, the measured $l=0$ and $l=2$ reduced widths give a measure of admixtures of p^8s^2 and p^8d^2 in the C^{14} ground state. The technique for estimating such admixtures is described in connection with $N^{14}(p,d)N^{13}$. We work in jj coupling and assume $\theta_0^2(2s)=0.17$ and $\theta_0^2(1d)=0.07$ for the relevant single-particle reduced widths. The jj coupling assumption implies neglect of $1p^8s1d$, since $(1p_{\frac{3}{2}})^8_0 2s_{\frac{1}{2}} 1d_{\frac{3}{2}}$ contains no states with $J=0$. The measured reduced widths imply that, assuming

$$\psi(C^{14}) = \alpha 1p^{10} + \beta (1p_{\frac{3}{2}})^8_0 2s_{\frac{1}{2}}^2 + \gamma (1p_{\frac{3}{2}})^8_0 1d_{\frac{3}{2}}^2,$$

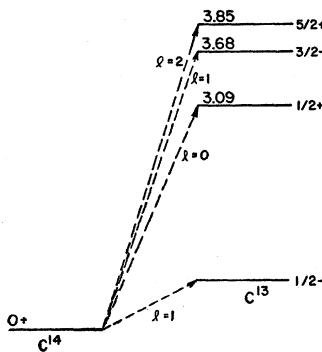


FIG. 20.

the intensities of the various configurations are

$$\alpha^2 = 0.92 \text{ (92\%)}, \quad \beta^2 = 0.005 \text{ (0.5\%)}, \\ \gamma^2 = 0.07 \text{ (7\%).} \quad (\text{IV.27})$$

An analysis similar to the foregoing was first given by Baranger and Meshkov (Ba58), who obtained a p^8d^2 intensity of 12%, about twice that given in (IV.27). Their result differs from ours because of a different way of handling the data. The discrepancy of a factor of two in the p^8d^2 intensity is within the reliability claimed by Baranger and Meshkov and does not influence their qualitative conclusions, which we discuss later.

$$N^{14}(p,d)N^{13}; N^{14}(n,d)C^{13}$$

The ground-state widths (Be58, Ca57a) measured by the two different reactions agree very well, but there is a large discrepancy in the measurements of the $l=1$ reduced width ratio to the $\frac{1}{2}^-$ and $\frac{3}{2}^-$ states (Fig. 21). The $l=1$ curve in the (n,d) experiment fits the data very poorly; any reduced width extracted from such a curve is subject to large uncertainties. Furthermore, the (n,d) width $\theta^2 = 0.16$ for the $\frac{3}{2}^-$ state is incredibly large for an $l=1$ transition whose s value in the jj limit is $2/11$. We conclude that the (n,d) ratio is erroneous and take $\theta^*/\theta_g \approx 0.5$ as the experimental value.

The ratio s^*/s_g of spectroscopic factors, calculated as a function of $\zeta(N^{13}) = \zeta(N^{14})$ within the configurations $1p^n$, is found to decrease monotonically from 2.26 at $\zeta=0(LS)$ to $2/11$ at $\zeta=\infty(jj)$. A few representative values, obtained (Au55) with a Rosenfeld interaction, are

$$\begin{array}{ccccc} \zeta = & 0 & 2 & 5 & 16 \\ s^*/s_g = & 2.26 & 0.97 & 0.15 & 0.12 & 0.09. \end{array}$$

Agreement with the measured ratio is found for $\zeta \approx 3.5$. This value is rather low, but could be modified by varying $\zeta(N^{13})$ and $\zeta(N^{14})$ separately. For $\zeta \approx 3.5$, $s_g \approx 1.3$, whence, using $\theta_g^2 = 0.05$,⁶⁷

$$\theta^*(1p) \approx 0.04. \quad (\text{IV.28})$$

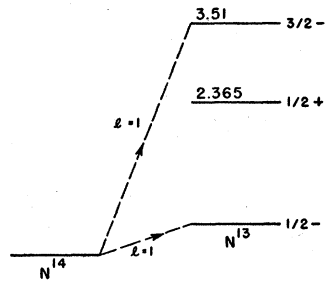
The $l=0$ reduced width to the 2.365-Mev level in N^{13} extracted from Bennett's data (Be58) is subject to large uncertainties, because the transition is very weak and no measurements were taken for $\theta_{e.m.} < 15^\circ$. We should probably regard the "measured" reduced width as setting an upper limit

$$\theta^2 < 0.002. \quad (\text{IV.29})$$

We have identified the $\frac{1}{2}^+$ level of N^{13} in question as $(p_{\frac{1}{2}}^8)_0 2s_{\frac{1}{2}}$. A measurable $l=0$ pickup width must indicate the presence of p^8s^2 in the N^{14} ground state. The configuration p^8s^2 contains a number of states with $J=1$,

⁶⁷ Our ground-state reduced width is twice that quoted on page 174 of Aj59. As in the case of $B^{11}(d,n)C^{12}$, this difference reflects an isotopic-spin coupling factor of $\frac{1}{2}$.

FIG. 21.



$T=0$ and there is therefore the chance of accidental cancellation in the spectroscopic factor. Ignoring this remote possibility, we use the jj coupling approximation, which is probably quite accurate, to estimate an upper limit on the p^8s^2 admixture.

The transition in question is

$$\alpha 1p^{10} + \beta (1p_{\frac{1}{2}})_0^8 (2s_{\frac{1}{2}})_1 \rightarrow (1p_{\frac{1}{2}}^8)_0 2s_{\frac{1}{2}},$$

with $s=2\beta^2$. Taking $\theta_0^2(2s)=0.17$ [see (IV.21) and (IV.22)], we find $\beta^2 < 0.006$. In other words, (IV.29) implies that the $p_{\frac{1}{2}}^8 2s_{\frac{1}{2}}$ admixture in the N^{14} ground state is less than 0.6% in intensity.

$$A=14 \rightleftharpoons 15$$

Since a lot of attention has been paid to the C^{14} and N^{14} ground-state wave functions, we first summarize the present status of this problem and then discuss the relevant stripping data.

Stripping Data and the Ground-State Wave Functions of C^{14} and N^{14}

During the past few years, major interest in the $A=14$ polyad has shifted its focus away from the C^{14} β decay. This problem is now resolved and there is little doubt that the long lifetime of C^{14} is due to an accidental cancellation. The fact that such a cancellation cannot be produced within the framework of the single-particle spin-orbit model, with wave functions restricted to p^{10} , but can be if we introduce a tensor force, has occasioned comments that the long lifetime of C^{14} demonstrates the existence of a tensor interaction.

Two procedures were used in studying this problem. The first, very similar in spirit to conventional intermediate coupling calculations, involved a choice of effective central, tensor, and spin-orbit interactions and the use of these to calculate energy levels, wave functions, and other properties of interest (Ja54, El56, Vi57). The second technique proceeded directly from the experimental data and, assuming again wave functions belonging to p^{10} , obtained a direct solution for the amplitudes in the wave functions of interest (Sh55, Be58). The C^{14} and N^{14} ground-state wave functions determined from the experimental data did not agree with the results of the shell-model calculation and, indeed, appeared to be inconsistent with what is known about p -shell level structures.

It now seems that the fault lies in the assumption of p^{10} wave functions. Baranger and Meshkov (Ba58) have shown that the $C^{14}(d,t)C^{13}$ $l=0$ and $l=2$ reduced widths indicate mixtures of p^8s^2 and especially p^8d^2 ⁵⁸ in the C^{14} wave function which, while negligibly small for most purposes, are large enough to play an important part in the very delicate β -decay cancellation. The long lifetime of C^{14} therefore imposes no simple relation between the p^{10} wave functions of C^{14} and N^{14} . The direct solution of Sherr *et al.* loses its central datum. Moreover, the specific necessity for a tensor force disappears.

It is nevertheless of interest to see what restrictions the stripping data impose on the wave functions

$$\Psi(01) = \alpha\psi(^3S_1) + \beta\psi(^1P_1) + \gamma\psi(^3D_1) \quad (\text{IV.30})$$

of the N^{14} ground state ($T=0, J=1$) and

$$\Psi(10) = \alpha\psi(^1S_0) + \gamma\psi(^3P_0) \quad (\text{IV.31})$$

representing the C^{14} ground state ($T=1, J=0$) and its analog at 2.31 Mev in N^{14} . We consider the $l=1$ transitions connecting these two levels with the $\frac{1}{2}^-$ and $\frac{3}{2}^-$ single-hole states in N^{15} and O^{15} , using the notation described in Example 4 of Sec. III.10. The sum rule derived there yields

$$s_i = 3/2(1 + s_i^*/s_i) \quad (i=0, 1) \quad (\text{IV.32})$$

enabling us to extract s_i directly from a measured ratio of reduced widths. In the following discussion, the phase-convention used for the $A=14$ wave functions is the standard one discussed in Sec. III.5.

We now present the experimental information concerning s_i and s_i^* . Since the relevant (single hole) states in N^{15} and O^{15} are about 6 Mev apart, we must allow for the possibility of an energy variation in $\theta_0^2(1p)$. Since no clear evidence for such a variation is found elsewhere in the $1p$ shell, it seems sensible to restrict this variation in $\theta_0^2(1p)$ to a factor 1.3 in either direction. The effects of such possible energy dependence of $\theta_0^2(1p)$ are included in deriving s_i^*/s_i from measured values of θ_i^{2*}/θ_i^2 :

$N^{14}(d,p)N^{15}$ (Wa57) to levels at 0 and 6.33 Mev in N^{15} :

$$0.10 \leq s_1^*/s_1 \leq 0.20,$$

whence, using (IV.32), we have

$$1.07 \leq s_1 \leq 1.25. \quad (\text{IV.33})$$

$N^{14}(d,n)O^{15}$ (Ev53) to levels at 0 and 6.14 Mev in O^{15} :

$$0.06 \leq s_1^*/s_1 \leq 0.11,$$

yielding

$$1.22 \leq s_1 \leq 1.34. \quad (\text{IV.34})$$

This was one of the first (d,n) stripping experiments to be performed and it may not be as reliable as (IV.34)

⁵⁸ See the earlier discussion of $C^{14}(d,t)C^{13}$ for quantitative estimates.

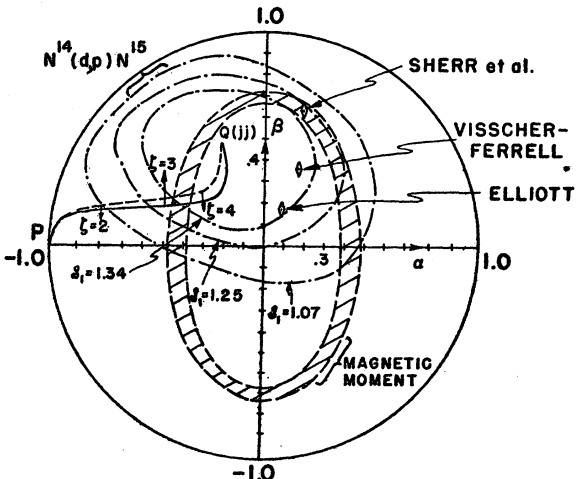


FIG. 22. N^{14} ground-state wave function. Curves PQ : —, with Rosenfeld interaction; ---, with Inglis interaction.

suggests. The agreement between (IV.33) and (IV.34) is therefore quite satisfactory.

$C^{14}(d,n)N^{15}$ (Ri57) to levels at 0 and 6.33 Mev in N^{15} :

$$0.20 \leq s_0^*/s_0 \leq 0.50$$

whence

$$0.75 \leq s_0 \leq 1.07. \quad (\text{IV.35})$$

The relevant experiment used very low energy deuterons ($E_0=3.5$ Mev). There is some evidence [$\text{Be}^9(d,p)\text{Be}^{10}$] to support the hope that a stripping ratio does not vary much with bombarding energy.

$N^{15}(p,d)N^{14}$ (Be58), to ground and 2.31-Mev states in N^{14} :

$$0.5 \leq s_0/s_1 \leq 0.8. \quad (\text{IV.36})$$

Equations (IV.33) to (IV.35) yield the range of values

$$0.56 \leq s_0/s_1 \leq 1,$$

whose agreement with (IV.36) confirms the accuracy of the low-energy $C^{14}(d,n)N^{15}$ estimate of s_0^*/s_0 . We regard the limits

$$0.5 \leq s_0 \leq 1 \quad (\text{IV.37})$$

on s_0 as reliable.

We now examine the restrictions imposed by (IV.33), (IV.34), and (IV.37) on the amplitudes in $\Psi(01)$ and $\Psi(10)$. In this analysis we can safely neglect configurations other than $1p^{10}$, since the admixtures of $1p^8d^2$ and $1p^8s^2$ found in C^{14} from the (d,t) results have no appreciable influence on the $l=1$ reduced widths under consideration. s_1 is given (Fr56) in terms of the amplitudes by

$$2s_1 = 1 + \frac{3}{2}\gamma^2 + 2\beta\left[\left(\frac{5}{6}\right)^{\frac{1}{2}}\gamma - \left(\frac{2}{3}\right)^{\frac{1}{2}}\alpha\right], \quad (\text{IV.38})$$

as can be shown directly from (III.89) and (III.90). Using the normalization condition to eliminate γ^2 , (IV.38) determines a curve in the $\alpha\beta$ plane for each value of s_1 . The loci for $s_1=1.07, 1.25$, and 1.34 are

shown in Fig. 22.⁵⁹ The shaded annular region contains values of α and β consistent with the stripping data.

Since the β decay is no longer regarded as relating α/β and x/y , the only other data yielding a relation between α and β concern the magnetic and quadrupole moments of N^{14} . We do not regard the latter as providing any useful information in the present connection. The magnetic moment locus is the cross-hatched ellipse in Fig. 22 the errors being uncertain. The available data are seen to restrict (α, β) to two zones in the (α, β) plane.

The first is a wide band in the first quadrant, where the wave functions of Sherr *et al.*, Elliott, and Visscher and Ferrell lie (Sh55, El56, Vi57, Be58). The second is a smaller region around $\alpha = -0.4$, $\beta = 0.1$ in the second quadrant. Intermediate coupling calculations with Rosenfeld and Inglis interactions yield the curves PQ as ξ ranges from 0 to ∞ . These curves lie inside the allowed region for the low values $2 \leq \xi \leq 3$. Since a small tensor force changes the calculated values of (α, β) from the second quadrant to the first, we should not expect agreement to be much better. The experimental data do not enable us to choose between the two allowed regions.

Let us now consider S_0 , for which we have [Fr56: (III.89) and (III.90)]

$$2S_0 = 1 + x^2 + 2\sqrt{2}xy. \quad (\text{IV.39})$$

Thus, a value of S_0 , together with the normalization condition, determines two distinct values of (x, y) . The allowed points on the unit circle $x^2 + y^2 = 1$ are exhibited in Fig. 23, corresponding to the range of values (IV.37) for S_0 . The stripping data demand that x and y have the same sign and that either $x/y \geq 2.8$ or $x/y \leq 0.35$.

Any shell-model calculation with a reasonable interaction, with or without a tensor force, predicts⁶⁰ that $x \approx y$, to within a factor two. To obtain $x \geq 2.8y$, we must go to the physically unreasonable LS limit while $x \leq 0.35y$ is quite impossible. Since the limits imposed by the stripping data on x/y are insensitive to variations in S_0 , we have here a clear-cut contradiction.

In summary, we would assert that available experimental evidence⁶¹ does not permit us to choose between alternative means of achieving cancellation in the β -decay matrix element. Ignoring the β decay entirely, we obtain two distinct direct solutions for the N^{14} wave function, lying in different quadrants of the $\alpha\beta$ plane, and we have no way of deciding between these alternatives. The poor agreement between the intermediate coupling N^{14} wave function with the usual value of ξ

⁵⁹ A diagram of this kind was first used by Warburton and McGruer (Wa57).

⁶⁰ This can be seen from the form of the spin-orbit matrix

$$\begin{bmatrix} ^1S_0 & 0 & \sqrt{2}\xi \\ ^3P_1 & \sqrt{2}\xi & \xi \end{bmatrix}$$

and the fact that the central diagonal difference $E(^1S) - E(^3P) \sim 6K$. A small tensor force simply adds a small term to the 3P diagonal matrix element and is of no importance to our argument.

⁶¹ The γ -decay branching ratio of the 3.945-Mev level to the two lowest levels in N^{14} could also be analyzed in this connection.

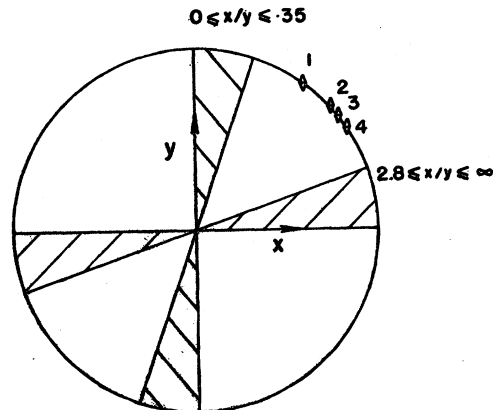


FIG. 23. C^{14} ground-state wave function. 1, jj limit; 2, intermediate coupling (Rosenfeld interaction, $\xi=5$); 3, Visscher and Ferrell (Vi57); 4, Elliott (El56).

($\xi \sim 4$) and that determined directly is not to be regarded as at all significant. On the other hand, the disagreement in the C^{14} case is very real and not at present understandable.

$$N^{14}(d,p)N^{15}; C^{14}(d,n)O^{15}$$

Where they overlap, the three $N^{14}(d,p)N^{15}$ experiments (Sh55, Gr56, Wa57) agree quite well, except for the 8.316-Mev $l=0$ transition.

We have already discussed the $l=1$ transitions. It only remains to use (IV.33) and the ground-state absolute reduced width (Wa56) to obtain

$$0.037 \leq \theta_0^2(1p) \leq 0.044. \quad (\text{IV.40})$$

Between 5 and 9 Mev in N^{15} there are seven positive-parity levels. Halbert (Ha56, Ha57) has carried out detailed shell-model calculations for such states of $A=15$, arising from $1s^4 1p^{10} 2s$, $1s^4 1p^{10} 1d$, $1s^3 1p^{12}$. In the comparison between theory and experiment presented in Table VI, we have used the spin assignments and S values of Halbert.⁶² These spin assignments are consistent with all currently available experimental evidence.

The reduced widths of Sh55 were normalized by taking $[J]\theta^2(5.28) = 0.049$, from Gr56.

We have ignored the doubtful $l=0$ component in the transition to the 7.58-Mev state. There is no conclusive evidence that such a component exists. Its presence would contradict Halbert's spin assignment for the state.

Apart from the data of Wa57 for the 8.316-Mev level and the mixed transition to the 8.571-Mev state, the values of $\theta_0^2(1d)$ and $\theta_0^2(2s)$ are consistent to within $\pm 30^\circ$. In view of the great complexity of the wave functions, this is satisfactory and lends support to

⁶² The N^{14} ground state is represented by an intermediate coupling wave function (Rosenfeld interaction, $\xi=4$) the S values being given in Appendix G of Ha56. In Ha57 the N^{14} wave function of Sherr *et al.* is used, the values of S being very similar.

TABLE VI.

Excitation	J^π	$\mathcal{S}(l=0)$	$\mathcal{S}(2)$	$\theta^2(0)$	$\theta^2(2)$	$\theta_0^2(2s)^a$	$\theta_0^2(1d)^a$	Reference
5.28	$\frac{5}{2}^+$...	0.134	...	0.008		0.061	Gr56
5.31	$\frac{3}{2}^+$	0.110	0.033			Sh55, Gr56
7.165	$\frac{7}{2}^+$...	0.726	...	0.049	0.067	0.056	Gr56
			0.041	0.13	0.056	Sh55
7.314	$\frac{3}{2}^+$	0.642	0.015	0.084	...	0.15		Gr56
				0.095	...			Sh55
7.575	$\frac{5}{2}^+$...	0.622	...	0.058	0.093	0.093	Gr56
					0.063	0.10	0.10	Sh55
					0.068	0.11	0.11	Wa57
8.316	$\frac{1}{2}^+$	0.853	0.005	0.12	...	0.14		Gr56
				0.16	...	0.19	0.19	Sh55
				0.24	...	0.28	0.28	Wa57
8.571	$\frac{3}{2}^+$	0.013	0.594	0.004	0.009	0.30	0.016	Sh55
				0.005	0.011	0.37	0.018	Wa57

^a The entries in the columns headed " $\theta_0^2(2s)$ " and " $\theta_0^2(1d)$ " are not to be regarded as reliable estimates of single-particle reduced widths, but rather as values of the ratios $\theta^2(0)/\mathcal{S}(0)$ and $\theta^2(2)/\mathcal{S}(2)$, evaluated for each transition. Agreement between theory and experiment is then exhibited in the degree of consistency of the ratios so obtained.

Halbert's spin assignments. Taking mean values, we have the rough estimates

$$\theta_0^2(1d) \approx 0.08, \quad \theta_0^2(2s) \approx 0.15. \quad (\text{IV.41})$$

It should be remarked that interchange of the spin assignments for the 7.165- and 7.571-Mev levels would not seriously impair agreement with experiment.

The positive parity levels of N^{15} could obviously be discussed from the weak coupling standpoint. It can be seen from Table VI, or from Fig. 3 of Ha57, that at least the first two states of $A=14$ ($J=1, T=0$ and $J=0, T=1$) contribute jointly to several of the N^{15} states. Now both of these states of $A=14$ are available as ground states of target nuclei (N^{14} and C^{14}). This has the unique consequence that not only can components of $[\varphi_0(N^{14}) \times u_k]$, where $u_k = 1d_{\frac{5}{2}}$ or $2s_{\frac{1}{2}}$, be directly located by $N^{14}(d,p)N^{15}$, but also fragments of $[\varphi_0(C^{14}) \times u_k]$ are accessible by $C^{14}(He^3, d)N^{15}$. A careful $C^{14}(He^3, d)N^{15}$ experiment would therefore yield valuable insight into the weak-coupling structure of positive parity levels in N^{15} .

$$N^{15}(p,d)N^{14}$$

The absolute ground-state reduced width (Be58) agrees well with the value found by $N^{14}(d,p)N^{15}$ (Wa57).

We have already discussed the transitions to the first two states of N^{14} ; it remains to examine the 3.945-Mev level. The reduced width θ_1^2 for this level is subject to large uncertainties; the estimate

$$0.1 \leq \mathcal{S}_1'/\mathcal{S}_1 \leq 0.3 \quad (\text{IV.42})$$

of the stripping ratio is probably reliable. It is found that $\mathcal{S}_1'/\mathcal{S}_1$ calculated as a function of ζ with a Rosenfeld

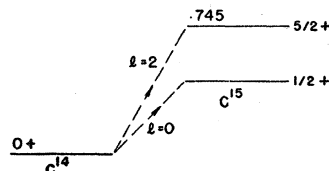


FIG. 24.

interaction varies very little between $\zeta=4$ and the jj limit. The value for $\mathcal{S}_1'/\mathcal{S}_1$ in this region lies between 0.45 and 0.5, significantly higher than (IV.42).

$$C^{14}(d,p)C^{15}$$

Since the first excited state of C^{15} is 6.09 Mev above the ground state, the $\frac{1}{2}^+$ and $\frac{5}{2}^+$ levels at 0 and 0.745 Mev in C^{15} must be nearly pure $2s_{\frac{1}{2}}$ and $1d_{\frac{5}{2}}$ single-particle levels (Fig. 24).

The shell-model calculations of Halbert (Ha56, Ha57) give results consistent with the preceding expectation. The first $T=\frac{3}{2}$ levels of $A=15$ are predicted to be nearly⁶³ degenerate, and to have $J=\frac{1}{2}^+, \frac{5}{2}^+$.

The simple weak-coupling argument and the detailed calculation of Halbert and French agree⁶⁴ in suggesting $\mathcal{S} \approx 1$ for the $l=0$ and $l=2$ transitions under consideration. The absolute reduced widths (Mo58) then yield the rough estimates

$$\theta_0^2(1d) \approx 0.05, \quad \theta_0^2(2s) \approx 0.1 \quad (\text{IV.43})$$

for the single-particle widths.

Angular distributions with clear stripping form were measured for transitions to two higher levels in C^{15} , at 6.4 and 7.3 Mev. At the corresponding values of Q , however, Butler curves with $l=0, 1, 2$, and 3 are almost identical. l values and spins could be determined by $C^{14}(n,n)C^{14}$,⁶⁵ whereupon reliable stripping widths could be extracted.

$$A = 15 \rightleftharpoons 16$$

$$N^{15}(d,p)N^{16}$$

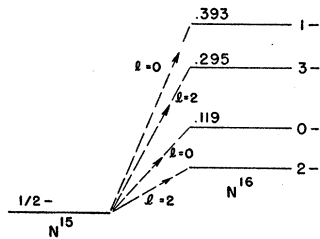
Detailed calculation (El57) indicates that jj coupling is an excellent approximation for the four lowest $T=1$ states of $A=16$ (Fig. 25). The levels in question are accurately represented by $(p_{\frac{1}{2}}^{-1}d_{\frac{5}{2}})_{J=2,3}$ and $(p_{\frac{1}{2}}^{-1}s_{\frac{1}{2}})_{J=0,1}$.

⁶³ The $\frac{5}{2}^+$ level is actually predicted to be 0.2 Mev lower than the $\frac{3}{2}^+$. This could certainly be altered by allowable changes in the parameters of the theory.

⁶⁴ For the $\frac{1}{2}^+$ level, Halbert (Ha56) gives $\mathcal{S}=0.97$.

⁶⁵ Levels above 1.22 Mev in C^{16} are energetically accessible.

FIG. 25.

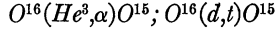


Such an interpretation indicates $S \approx 1$ for each of the four transitions in question, a prediction which is confirmed by the near equality of the respective $l=0$ and $l=2$ reduced widths. In fact, consideration of the reduced widths enabled Warburton and McGruer (Wa57) to fix the spins of the levels in question, illustrating an important practical use of (d,p) widths. The absolute reduced widths yield

$$\theta_0^2(1d) \approx 0.05 \quad (\text{IV.44})$$

and

$$\theta_0^2(2s) \approx 0.18. \quad (\text{IV.45})$$



In the pickup reactions on O^{16} , we expect to see two strong $l=1$ transitions ($S=4$ and $S=8$, respectively) to the one-hole $p_{\frac{1}{2}}$ and $p_{\frac{3}{2}}$ states in O^{15} and N^{15} (Fig. 26).

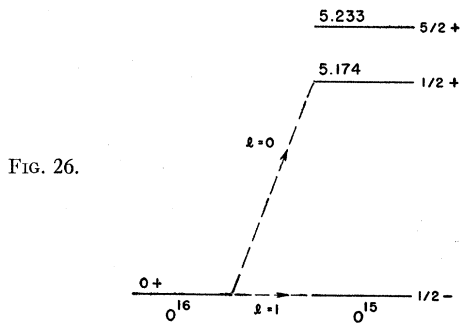
An $O^{16}(He^3,\alpha)$ experiment has been carried out with a 9.2-Mev He^3 beam (Hi59). A very clear $l=0$ transition is observed to the $\frac{1}{2}^+$ member of the positive-parity doublet near 5.2 Mev in O^{15} . This implies either a $(2s_{\frac{1}{2}})_0$ admixture in the O^{16} ground state, sizeable $1s_{\frac{1}{2}}^3 1p_{\frac{1}{2}}^2$ contributions in the 5.174-Mev level in O^{15} , or possibly both. It will be noticed that the $\frac{1}{2}^+$ member of the O^{15} doublet lies lower, the reverse of what is found in N^{15} .

The ground-state (d,t) transition has recently been studied (Ke60) at a deuteron energy of 14.9 Mev. The measured absolute cross section yields $\Lambda\theta^2 = 2.4$, which is unexpectedly small; for example, with $S=4$, $\theta_0^2(1p) \approx 0.04$ from (IV.28) and (IV.40), and $\Lambda = 190$ from (II.38), we would expect $\Lambda\theta^2 \approx 30$. Several factors may contribute to the observed diminution of $\Lambda\theta^2$:

(1) In the $O^{16}(d,t)O^{15}$ experiment under consideration (Ke60), the energy of the outgoing tritons is only 4.7 Mev. $\theta_0^2(1p)$ seems to decrease at very low projectile energies.

(2) There is consistent evidence (see Sec. VII.2) that single-particle reduced widths decrease as the binding energy of the transferred nucleon increases. In the case of $O^{16}(d,t)O^{15}$ (ground state), this binding energy has the large value of 15.65 Mev.

(3) Very little is known about the energy-dependence of the (d,t) normalization factor Λ . In view of the large release of binding energy and the small triton energy involved, it is possible that the above rough estimate of Λ , as well as that of $\theta_0^2(1p)$, is a substantial overestimate.



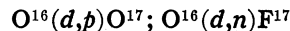
mate. In order to clarify the situation, it would be worthwhile to repeat the $O^{16}(d,t)O^{15}$ experiment at a deuteron energy of 20 Mev or higher and to study $O^{16}(p,d)O^{15}$ with protons of similar energy.

In concluding this section on the $1p$ shell, we remark that our two most serious sources of difficulty, encountered in $Li^7(d,He^3)He^6$ and $O^{16}(d,t)O^{15}$, have involved (d,t) or (d,He^3) and not the simpler deuteron-nucleon reactions.

V. STRIPPING AND PICKUP REACTIONS ON ds -SHELL NUCLEI

In Sec. IV, we had something to say about most of the $1p$ -shell transitions for which experimental data are available. Since the ds shell is not well understood spectroscopically and because, in several instances, the experimental situation is unsatisfactory, such thoroughness is not attempted in the present section. In discussing the ds shell, we analyze in detail only those reactions from which we can obtain useful spectroscopic information.

Stripping reactions in the ds shell have been discussed by several authors; $l=0$ and $l=2$ transitions in $O^{17}(d,p)O^{18}$ by Bilaniuk and Hough (Bi57); $Mg^{24}(d,p)Mg^{25}$ and $Si^{28}(d,p)Si^{29}$ from the viewpoint of the rotational model by Litherland *et al.* (Li58) and Bromley *et al.* (Br57); the mixed $l=0+2$ ground-state transition in $P^{31}(d,p)P^{32}$ by Parkinson (Pa58); $l=1$ transitions in the last-named reaction by Pandya (Pa57a).



Since the next levels of the same spin and parity are 5 Mev higher, the ground and first excited states of O^{17} and F^{17} are, without doubt, good single-particle $1d_{\frac{3}{2}}$ and $2s_{\frac{1}{2}}$ levels (Fig. 27). The (d,p) and (d,n) reactions on O^{16} therefore provide an ideal means of studying the d and s single-particle reduced widths and their dependence on bombarding energy.

The values of the reduced-width ratio θ^{2*}/θ_0^2 for the first two levels of O^{17} and F^{17} , obtained in (d,p) (Bu51a, Gr56) and (d,n) (Mi53) experiments with 8- to 9-Mev deuterons, are 2 and 4.3, respectively. It seems unlikely that this large discrepancy reflects a real difference between (d,p) and (d,n) reduced widths. Pre-

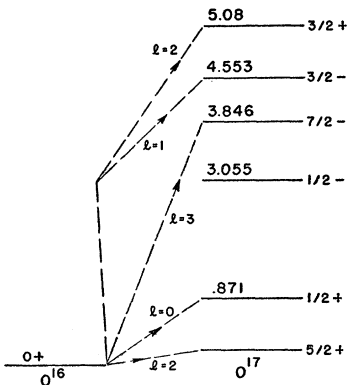


FIG. 27.

liminary measurements with 15-Mev deuterons (Ke59) yield a value of 3.4 for θ_0^2/θ_g^2 , intermediate between the preceding extremes.

At bombarding energies up to 4 Mev, the angular distribution of the ground-state deuterons does not have the characteristic stripping form (Gr56a, St55, Ba57). At 8 and 19 Mev, respectively, the measured ground-state reduced widths (Bu51a, Fr53) of 0.058 and 0.044, respectively,⁶⁶ are consistent with the preliminary value of 0.05 (Ke59) at 15 Mev. There is, therefore, no evidence of a significant variation in $\theta_0^2(1d)$ between 8 and 19 Mev. Furthermore, the resulting value

$$\theta_0^2(1d) \approx 0.05 \quad (\text{V.1})$$

is in good agreement with the values (0.05 to 0.07) obtained in Sec. IV from $1p$ -shell studies.

The reduced width θ_0^2 of the 0.872-Mev level of O^{17} appears to increase steadily with bombarding energy from 0.013 at 2.1 Mev (Gr56a) to 0.11 at 8 Mev (Bu51a). It is not clear whether the larger value of 0.17 at 15 Mev (Ke59) indicates a real energy variation or experimental uncertainties. At any rate, the main energy variation occurs for low energies, as we have already noted in the case of $\theta_0^2(1p)$. Using the 15-Mev data (Ke59) because it is probably the most reliable, we have

$$\theta_0^2(2s) \approx 0.17, \quad (\text{V.2})$$

in good agreement with $1p$ -shell estimates (0.15 to 0.18).

Further $O^{16}(d,p)O^{17}$ experiments, in which absolute cross sections are measured at different deuteron energies, are needed to clarify the dependence of $\theta_0^2(1d)$ and $\theta_0^2(2s)$ on bombarding energy.

The $l=2$ reduced width of the 5.08-Mev level is nearly equal to that of the ground state, the observed values being 0.8 θ_0^2 (Gr56) and 0.9 θ_0^2 (Ke59). This suggests that the level in question, whose spin is $\frac{3}{2}^+$, is predominantly single-particle $1d_{\frac{3}{2}}$. However, we cannot rule out the possibility of an energy variation

of $\theta_0^2(1d)$; stripping data on higher levels of O^{17} are needed before a final conclusion can be reached.

A detailed discussion of the negative-parity levels of O^{17} has already been given in Example 2 of Sec. III.11. We concluded that the 3.856-Mev level in O^{17} is a good single-particle $1f_{7/2}$ state. On using (V.1) and the measured ratio (Gr56) of its reduced width to θ_0^2 , we obtain

$$\theta_0^2(1f) \approx 0.012. \quad (\text{V.3})$$

We conclude by repeating that further $O^{16}(d,p)O^{17}$ and $O^{16}(\text{He}^3,d)F^{17}$ experiments, studying levels in the final nucleus at least up to 8 Mev, would be well worthwhile.

$O^{17}(d,p)O^{18}$

Transitions leading to the three lowest levels of O^{18} have been studied experimentally (Bi57) (Fig. 28). On the basis of these results, spins of 0^+ , 2^+ , and 4^+ were suggested for the corresponding states in O^{18} . These assignments have now been confirmed by $C^{14}(\alpha,\gamma)O^{18}$. (See Aj59.) No absolute cross sections have been measured.

Wave functions for O^{18} have been calculated by Redlich (Re54, Re58), and by Elliott and Flowers (El55a), with very similar results. On using Redlich's wave functions, we find $s^*/s_g \approx 1.2$ for the 3.55-Mev and ground states of O^{18} . This is in good agreement with the observed reduced-width ratio of 1.1.

The mixed $l=0+2$ transition to the 1.99-Mev level has been discussed in detail as Example 2 of Sec. III.9.

$O^{18}(d,t)O^{17}$

Transitions to low-lying negative-parity levels in O^{17} (Ar60) indicate that the O^{18} ground-state wave function contains sizeable $(1f_{7/2})_0$ and $(2p_{3/2})_0$ admixtures (Fig. 29). Neglecting core excitation, the O^{18} ground-state wave function is

$$\Psi(O^{18}) = \alpha(1d_{\frac{3}{2}})_0 + \beta(2s_{\frac{1}{2}})_0 + \gamma(1d_{\frac{5}{2}})_0 + \delta(1f_{7/2})_0 + \epsilon(2p_{\frac{3}{2}})_0. \quad (\text{V.4})$$

The pickup data are now used to determine the size of the amplitudes in (V.4).

Consider first the $l=1$ transitions. A strong triton group is observed (Ar60) belonging to the $\frac{1}{2}^-$ level at

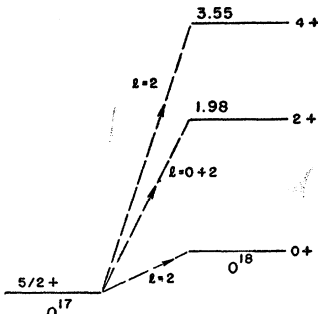


FIG. 28.

⁶⁶ The reduced widths quoted here and in Table I for the two lowest transitions in $O^{16}(d,p)O^{17}$ are smaller by a factor of three than those extracted by Fairbairn (Fa54) from the same experimental data, but in reasonable agreement with the values given by Fujimoto *et al.* (Fu54).

3.058 Mev in O^{17} , but no angular distribution could be measured because of the presence of elastically scattered deuterons. Since the level in question shows no stripping from O^{16} (Gr56, Ke59), its predominant configurations clearly involve $1p_{\frac{1}{2}}$ core excitation.

The total $l=1$ reduced width in $O^{16}(d,p)O^{17}$ of the $\frac{3}{2}^-$ states at 4.555 and 5.38 Mev is markedly smaller than $\theta_0^2(2p)$ (Ke59), again implying significant amounts of $1p$ -core excitation. $1p$ and $2p$ contributions to pickup to these levels add coherently so that we cannot say much about the $2p_{\frac{3}{2}}^2$ amplitude in (V.4). To obtain a solution, we take

$$\epsilon = \frac{1}{2}\delta, \quad (V.5)$$

a relation which emerges from the shell-model calculation cited in the following. The size of the $2p_{\frac{3}{2}}^2$ component is too small to have much influence on the remaining amplitudes.

The relevant final states being good single-particle levels, the spectroscopic factors for the $1d_{\frac{3}{2}}$, $2s_{\frac{1}{2}}$, $1d_{\frac{5}{2}}$, and $1f_{7/2}$ transitions are

$$S(1d_{\frac{3}{2}}) = 2\alpha^2, \quad S(2s_{\frac{1}{2}}) = 2\beta^2, \quad \dots \quad (V.6)$$

The transitions to the $1d_{\frac{3}{2}}$ and $2s_{\frac{1}{2}}$ levels in O^{17} have Q values similar to those for low-lying $l=0$ and $l=2$ transitions later in the ds shell. We therefore take

$$\theta_0^2(2s)/\theta_0^2(1d) \approx 2, \quad \theta_0^2(1f)/(\theta_0^2(1d)) \approx \frac{1}{2}, \quad (V.7)$$

differing from the values appropriate to $O^{16}(d,p)O^{17}$ in the direction indicated by stripping data on heavier ds -shell nuclei.

Using the observed reduced widths $\Lambda\theta^2$ given in Sec. II.3, Table II, (V.5)–(V.7) enable us to solve for the (squared) amplitudes in (V.4). The resulting percentage composition of the O^{18} ground-state wave function is exhibited in Table VII. We also list, for comparison, the intensities obtained in the shell-model calculations of Elliott and Flowers (El55a) and Redlich (Re58), and in a similar calculation⁶⁷ including $1f_{7/2}^2$ and $2p_{\frac{3}{2}}^2$ contributions.

In view of the various uncertainties involved (particularly in the ratios of the single-particle reduced widths) over-all agreement is very satisfactory. The shell-model calculation gives $1f_{7/2}^2$ and $2p_{\frac{3}{2}}^2$ admixtures

TABLE VII.

Wave function \ of	Intensity	$1d_{\frac{3}{2}}^2$	$2s_{\frac{1}{2}}^2$	$1d_{\frac{5}{2}}^2$	$1f_{7/2}$	$2p_{\frac{3}{2}}^2$
From pickup data	75.2%	14.5	3.3	5.5	1.4	
Shell model ^a	66.9	21.2	5.2	2.9	0.7	
Redlich	74	16	9.6	
Elliott and Flowers	79	15.2	5.8	

^a See footnote 67.

⁶⁷ The effective two-body interaction used had a Gaussian radial dependence with range parameter (Fr56) $\lambda=1$, strength $V_0=30$ Mev, and Rosenfeld exchange dependence. The necessary single-particle level positions were taken from the spectrum of O^{16} .

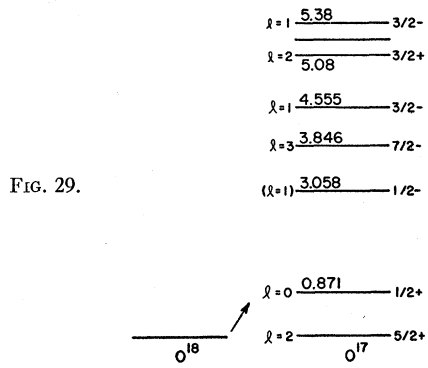


FIG. 29.

considerably smaller than those indicated by the pickup data. This situation could certainly be improved by reasonable changes in the parameters of the shell-model interaction. It is also noteworthy that the ratio of $1d_{\frac{5}{2}}$ to $2s_{\frac{1}{2}}$ intensities obtained from the pickup data is in good agreement with shell-model predictions.

The observed (Ar60) ground-state reduced width of $\Lambda\theta^2=5.7$ and the value of α^2 obtained before imply

$$\Lambda\theta_0^2(1d)=3.8. \quad (V.8)$$

Because of the jump in Q value between $O^{16}(d,p)O^{17}$ and $O^{17}(d,p)O^{18}$, $\theta_0^2(1d)$ in (V.8) cannot be regarded as a known quantity. However, the normalization constant Λ has been determined from $C^{14}(d,t)C^{18}$ (Mo58) and $Mg^{25}(d,t)Mg^{24}$ (Ha60) where the Q values are within a few hundred kilovolts of that encountered in the present example. Furthermore, the values of Λ obtained from C^{14} (165) and Mg^{25} (150) are in excellent agreement and all three experiments under consideration involve the same deuteron energy.⁶⁸ Thus, the value $\Lambda=160$ in the present situation should be reliable. From (V.8) and (V.7) we then have, for the single-particle reduced widths,

$$\theta_0^2(1d)=0.024, \quad \theta_0^2(1f)=0.012, \quad \theta_0^2(2s)=0.05. \quad (V.9)$$

The preceding value of $\theta_0^2(1f)$ is in excellent agreement with the very consistent values obtained in several experiments involving nuclei between O^{17} and Ca^{45} , supporting the reliability of our analysis.

On comparing (V.9) with (V.2) and (V.3), we see that both $\theta_0^2(1d)$ and $\theta_0^2(2s)$ have decreased by a factor of two to three between $O^{16} \rightleftharpoons O^{17}$ and $O^{17} \rightleftharpoons O^{18}$. They appear to remain fairly constant up to $A=28$. These observations suggest that the dramatic decrease in the single-particle reduced widths reveals a strong dependence on Q (especially close to $Q=0$), since Q (for low-lying transitions) changes by about 4 Mev between $O^{16} \rightleftharpoons O^{17}$ and $O^{17} \rightleftharpoons O^{18}$ and then varies relatively little.

$$F^{19}(p,d)F^{18}$$

In the only relevant experiment (Be58), the four levels near 1 Mev in F^{18} were not resolved (Fig. 30).

⁶⁸ All were carried out on the University of Pittsburgh cyclotron.

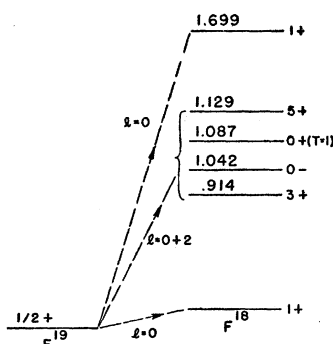


FIG. 30.

Other studies (Ku58, Aj59, Hi59a) clearly indicate that the spins of the 0.94- and 1.129-Mev members of this quartet are 3⁺ and 5⁺, respectively. There is, however, some disagreement about the remaining two states. Kuehner *et al.* (Ku58) identify the level at 1.087 Mev as the lowest $T=1$ state in F^{18} , with $J=0^+$, the 1.042-Mev level probably having $J=0^-$. Hinds and Middleton (Hi59a) reverse these spin assignments, asserting that the $J=0^+$, $T=1$ level lies at 1.042 Mev. We have adopted the spin assignments of Kuehner *et al.* (Ku58, Aj59), but our analysis would not be affected by an interchange of the spins. The essential conclusion, on the basis of conservation of angular momentum, is that the $l=0$ and $l=2$ components of Bennett's (Be58) combined angular distribution correspond, respectively, to the $J=0^+$, $T=1$ and $J=3^+$, $T=0$ levels in the quartet near 1 Mev in F^{18} .

We have an independent check on the absolute (p,d) reduced widths of Be58. The reduced width of the $J=0^+$, $T=1$ ground state of O^{18} has been measured in $F^{19}(n,d)O^{18}$ (Ri57a), the value of 0.017 so obtained being in reasonable agreement with the (p,d) reduced width (0.023) of the analog level in F^{18} .

We can calculate S values for the $l=0$ and $l=2$ transitions of interest using either of the very similar sets of wave functions calculated by Redlich (Re55, Re58) and Elliott and Flowers (El55a). Redlich's wave functions give the results shown in Table VIII. Agreement between theory and experiment for the $l=0$ transitions is good.⁶⁹ To fit the relative reduced width of the $l=2$ transition to the first excited state of F^{18} , we must take

$$\theta_0^2(2s)/\theta_0^2(1d) \approx 1.5. \quad (V.10)$$

From the observed ground-state reduced width of 0.017 (Be58) and the calculated value of S , we obtain

$$\theta_0^2(2s) \approx 0.03. \quad (V.11)$$

This is smaller by a factor of five than the value (V.2) obtained from $O^{16}(d,p)O^{17}$ and smaller by a factor of two than the value (V.9) obtained from $O^{18}(d,t)O^{17}$. The Q values of these reactions are 1.1 and 5.8 Mev,

⁶⁹ An $l=2$ reduced width of about 0.016 of the $l=0$ reduced width is predicted for the F^{18} ground state. No $l=2$ component is observed (Be58) as expected.

respectively, compared with 8.2 Mev for $F^{19}(p,d)F^{18}$ (ground state). We therefore have striking evidence that $\theta_0^2(2s)$ decreases strongly as Q increases. $\theta_0^2(1d)$ seems to exhibit similar tendencies although a comparison of (V.1), (V.7), and (V.10) indicates a slower rate of decrease.

In conclusion, we note that Bennett's (Be58) combined angular distribution to the four levels near 1 Mev in F^{18} may include some $l=1$ contributions involving $1p_{1/2}$ pickup to the 0^- level.

$F^{19}(d,t)F^{18}$

Two experiments have been reported, with 9-Mev deuterons (El57c) and 15-Mev deuterons (Ha60a). The low value $\Lambda = 105$ obtained for the (d,t) normalization constant in the 15-Mev experiment perhaps indicates a tendency for Λ to decrease as Q increases.

No ground-state reduced width could be obtained from the 9-Mev data since the differential cross section was not measured at sufficiently small angles to locate the main forward peak.

TABLE VIII.

$T_0 J_0$	Excitation energy in F^{18} (Mev)	l	S	S/S_g	θ_0^2/θ_0^2 (Be58)
01	0	0	0.6	1	1
03	0.94	2	0.7	1.1	1.5
10	{ 1.042 1.087	0	0.6	1.0	1.4
01	1.699	0	0.1	0.21	0.12

The four levels near 1 Mev were not completely resolved, the triton angular distributions being interpreted (El57c) as showing an $l=1$ transition to a level around 0.94 Mev and an $l=0$ transition to a level near 1.07 Mev. The presence of a strong $l=1$ transition at this excitation is not confirmed by the (p,d) data (Be58); furthermore, the purported $l=1$ angular distribution must certainly include a sizeable contribution from $l=2$ tritons to the 3^+ level at 0.94 Mev. We conclude that, although an $l=1$ transition to the 0^- level at 1.042 Mev is possible, its presence is not established by available data. Further experimental study of $F^{19}(d,t)F^{18}$ and also of $F^{19}(d,He^3)O^{18}$ is clearly desirable.

$F^{19}(d,p)F^{20}$

No shell-model wave functions are available for low-lying positive-parity states of F^{20} . Such wave functions are probably very complex, could not be obtained without laborious calculation, and in any case would be of questionable reliability. We therefore do not discuss the predictions of the shell model for $l=0$ and $l=2$ transitions in $F^{19}(d,p)F^{20}$.

However, the Nilsson form of the rotational model has been applied to F^{19} with considerable success

(Pa57, Ra57). The $\frac{1}{2}^+$ ground state of F^{19} is identified as the lowest of a $K_0=\frac{1}{2}$ rotational band,⁷⁰ whose intrinsic configuration is illustrated in Fig. 31. In this figure we exhibit the value of Ω and the Nilsson orbit-number for each orbit; a neutron is symbolized by an open circle, a proton by a cross.

Let us consider the rotational bands in F^{20} that can be reached by adding a neutron to the ground-state configuration of F^{19} . The lowest orbit in which there is a vacancy is No. 7, with $\Omega=\frac{3}{2}^+$. The two bands, with $K=1$ and $K=2$, which arise from the resulting intrinsic configurations probably lie close in energy with the $K=2$ band lower (Br59); they certainly interact strongly.

The spin of the F^{20} ground state is known (Aj59) to be either 2^+ or 3^+ . We feel that the 2^+ assignment is more plausible, for the following reasons:

(1) The interaction between the $K=1$ and $K=2$ bands depresses the $J=2$ and $J=3$ members of the $K=2$ band by considerable amounts. In order that the

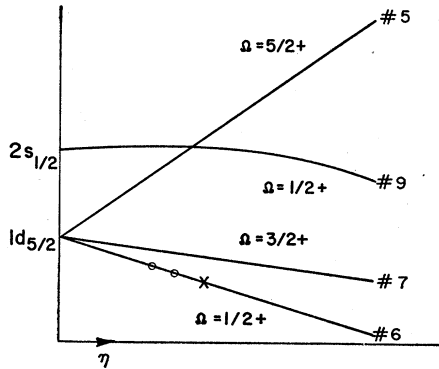


FIG. 31.

$J=3$ state lie lower, the difference between these depressions must exceed their zero-order energy difference taking the moment of inertia parameter from the spectrum of Ne^{20} , we find a separation of about 1.5 Mev which is probably too large to be overcome by the interaction between bands.

(2) On using Nilsson's single-particle wave functions (Ni55), we find $S < 0.1$ for the $l=2$ transitions to the $J=2$ members of both the $K=1$ and the $K=2$ bands, this result being insensitive to changes in deformation. It is clear that no interaction between bands can alter the fact that the lowest $J=2^+$ state should have a small stripping width. On the other hand, the $J=3^+$ members of both bands have sizeable S values, in the vicinity of 0.25. The fact that no stripping has been observed to the F^{20} ground state is then a clear argument in favor of a spin of 2^+ .

⁷⁰ This $K_0=\frac{1}{2}$ band mixes strongly with a nearby $K_0=\frac{3}{2}^+$ band. Since a $K_0=\frac{3}{2}^+$ band contains no state with $J_0=\frac{1}{2}^+$, the mixing does not influence the wave function of the $K_0=\frac{1}{2}$ ground state.

We therefore suggest that the ground state of F^{20} has $J=2^+$, the first excited state $J=3^+$. K is probably strongly mixed in both states.

Eight $l=1$ transitions are observed (El56) to levels of F^{20} between 5.04 and 7.20 Mev. Since $\phi_0(F^{19})$ has $J=\frac{1}{2}^+$, there are four basic $l=1$ components:

$$[\phi_0 \times 2p_{\frac{1}{2}}]_J: J=1, 2^-;$$

$$[\phi_0 \times 2p_{\frac{3}{2}}]_J: J=0, 1^-.$$

Since no spins and parities are known, we confine ourselves to an application of the gross sum rule (III.185), which yields

$$\phi_0^2(2p) \geq 0.021. \quad (V.12)$$

$F^{19}(d,n)Ne^{20}$

We again analyze the stripping data in terms of the rotational model. The intrinsic configuration of the Ne^{20} ground state is formed by adding an $\Omega=\frac{1}{2}^+$ proton in orbit No. 6, to the F^{19} ground-state configuration (Fig. 32). Band mixing should be relatively unimportant here (Br59). Calculated values of S for positive values of Nilsson's (Ni55) deformation parameter η^{71} are given below for the $J=0^+$ and $J=2^+$ states, the 4^+ state being excluded by conservation of angular momentum:

$\eta =$	2	4	6	l
$S(J=0)=$	0.31	0.49	0.57	0
$S(J=2)=$	0.34	0.31	0.29	2.

Agreement with the experimental reduced-width ratio $\theta_0^2/\theta_g^2 = 1.1$ (Ca55a) can be achieved only by taking

$$\theta_0^2(2s)/\theta_0^2(1d) < 1. \quad (V.13)$$

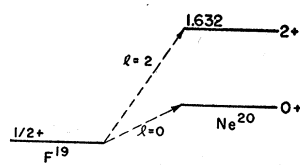
In view of the very large Q values involved (≈ 10 Mev) and the apparently rapid decrease of $\theta_0^2(2s)$ as Q increases, this, perhaps, is not unreasonable.

$Ne^{20}(d,p)Ne^{21}$

No absolute cross sections were measured in the only available experiment (Bu56). The only point on which we wish to comment is the fact that no stripping is observed to the $\frac{3}{2}^+$ ground state of Ne^{21} . From the standpoint of extreme jj coupling, this is to be expected since the transition in question must involve a $d_{\frac{5}{2}}$ nucleon and is therefore j -forbidden.

4.248 4^+

FIG. 32.



⁷¹ η measures the relative importance of the deformation and the spin-orbit coupling. $\eta=0$ corresponds to zero deformation.

Ne²²(d,p)Ne²³

In contrast to Ne²⁰(d,p)Ne²¹, a strong $l=2$ ground-state transition is observed, implying that the spin of Ne²³ is $\frac{5}{2}^+$ (Bu56) (Fig. 33).

In examining the predictions of the rotational model let us refer to Fig. 31 [the intrinsic structure given in discussing F¹⁹(d,p)F²⁰]. The Ne²² ground state ($K_0=0^+$) has four nucleons in the $\Omega=\frac{1}{2}^+$ (No. 6) orbit and two neutrons (the full complement) in the $\Omega=\frac{3}{2}^+$ (No. 7) orbit. Low-lying bands of positive parity in Ne²³ are constructed by adding a neutron in orbit No. 5, with $\Omega=\frac{5}{2}^+$, and No. 9 with $\Omega=\frac{1}{2}^+$.

We identify the ground and first excited states of Ne²³ with the lowest states of the resulting rotational bands (with $K=\frac{5}{2}$ and $K=\frac{1}{2}$) on observing that the decoupling parameter (Ke56) of the $K=\frac{1}{2}$ band is such that it has a $\frac{1}{2}^+$ ground state for positive deformations with the $\frac{5}{2}^+$ member more than 1 Mev higher. Since $\Delta K=2$, the two bands in question do not interact directly (Ke56); indirect interaction, through positive parity bands arising from the $2s_{\frac{1}{2}}$ and $1d_{\frac{3}{2}}$ states of the spherical shell model, is discouraged by the fact that interactions between bands arising from different spherical orbits are relatively weak. The pure-band approximation should therefore be adequate in the present situation.

The ground-state transition has $S_g=\frac{1}{3}$. This result is independent of the deformation because an intrinsic state with $\Omega=\frac{5}{2}^+$ receives no contributions from $2s_{\frac{1}{2}}$ and $1d_{\frac{3}{2}}$ and therefore has a definite value ($\frac{5}{2}^+$) of j . In contrast, the s value of the first excited state is sensitively dependent on η , decreasing rapidly from the value $s=1$ as η increases from 0. In order to obtain the observed reduced-width ratio $\theta^2/\theta_g^2=4$ (Bu56) for the reasonable deformation $\eta \sim 4$, we must have

$$\theta^2(2s)/\theta^2(1d) > 2. \quad (\text{V.14})$$

This is a very reasonable result since the Q values concerned are quite small (between 2 and 3 Mev), so that we would expect to find a reduced-width ratio close to what was found in O¹⁶(d,p)O¹⁷ and markedly larger than the values obtained in O¹⁸(d,t)O¹⁷ and F¹⁹(d,n)Ne²⁰.

Na²³(p,d)Na²²; Na²³(d,t)Na²²

Both the (p,d) and the (d,t) experiments have been performed (Be58, Vo58) (Fig. 34). They disagree concerning the ratio of the $l=2$ reduced widths of the lowest two states of Na²². The (p,d) experiment gives $\theta^2/\theta_g^2 \approx 1$,

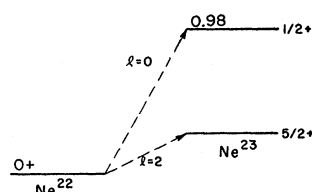


FIG. 33.

while the (d,t) value is 0.33. It is probable that the 0.59-Mev angular distribution of Be58 contains deuterons from the 0.89-Mev level in Na²², for which the (d,t) experiment (Vo58) gives $\theta^2/\theta_g^2 = 0.59$.

We do not give a detailed theoretical analysis of the relative reduced widths since nothing is known about the spins of the relevant excited states of Na²² and since we are dealing with an odd-odd nucleus in which interactions between the bands of the simple rotational model are probably important.

Na²³(d,p)Na²⁴

The results of the three available experiments (Sh54, Da60, Vo58) are in fair agreement where they overlap. We cannot give a detailed analysis of the positive-parity transitions because of the spectroscopic difficulty of dealing with an odd-odd nucleus and because of insufficient information about excited-state spins.

Nine $l=1$ transitions (Da60) are seen to levels in Na²⁴ up to 4.5 Mev. On using the gross sum rule (III.185) and normalizing the relative reduced widths of Da60 with the aid of the absolute ground-state cross

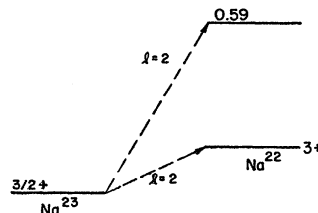


FIG. 34.

section of Vo58, we obtain

$$\theta^2(2p) \geq 0.028, \quad (\text{V.15})$$

where the inequality refers to the possible presence of unobserved $2p$ contributions above 5.4 Mev in Na²⁴.

Na²³(d,n)Mg²⁴

We consider, first, the theoretical predictions for the first three levels (Fig. 35). These have been discussed by Litherland *et al.* (Li58).

Ground State

According to the jj -coupling shell model, the Na²³(d,n)Mg²⁴ (g.s.) reaction is j -forbidden. On using the Nilsson rotational model, we have $S_g \approx 0.08$ for $\eta \approx 4$, the s value being so small that the reaction is, once again, effectively forbidden.

1.368-Mev Level

Both $l=0$ and $l=2$ are allowed by angular momentum conservation, but the $l=0$ component is forbidden by a K selection rule, $\delta(|\Omega|, |K \pm K_0|)$, since $K_0 = \frac{3}{2}$, $\Omega = \frac{1}{2}$, and $K=0$. For $\eta=4$, the predicted s value is given by $s(1.368)=0.69$.

4.122-Mev Level

Independently of the deformation, (III.204) yields

$$9s(J=4^+; K=0)/5s(J=2^+; K=0) = \frac{1}{6}, \quad (\text{V.16})$$

provided that we make the approximation of ignoring $j=\frac{3}{2}$ contributions to the 2^+ level. We can verify directly that such contributions are of no consequence.

The only available experiment (Ca^{55}) is, unfortunately, inadequate to provide a thorough test of these predictions. The angular distribution of neutrons to the 2^+ level apparently shows no stripping although the cross-section is quite large ($\sim 5 \times \text{g.s. cross section}$). The 4.122-Mev 4^+ level is not resolved from a nearby 2^+ state whose $l=0$ component dominates the combined angular distribution.

Probably only two significant points emerge from the available experimental results. These are the absence of a ground-state transition, and the absence of an $l=0$ component in the 1.368-Mev angular distribution, vindicating the j and K selection rules. It is surprising that the $l=2$ component of the first excited state should not have appeared quite clearly, since

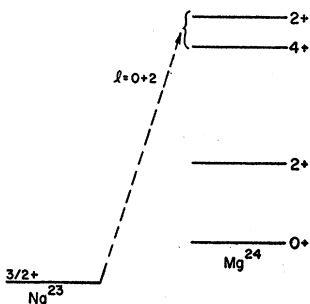


FIG. 35.

$[J]_S = 24/7$ and $\theta_0^2(1d)$ is not less than 0.02, implying $[J]\theta_0^2 \approx 0.07$.

A high-resolution $\text{Na}^{23}(\text{He}^3, d)\text{Mg}^{24}$ experiment would be valuable.

 $\text{Mg}^{24}(d, p)\text{Mg}^{25}; \text{Mg}^{24}(d, n)\text{Al}^{25}$

Three $\text{Mg}^{24}(d, p)\text{Mg}^{25}$ and one $\text{Mg}^{24}(d, n)\text{Al}^{25}$ experiments have been performed [Fig. 36(a)]. The three (d, p) experiments (Ho53d, Hi58, Ha60) give reduced widths in excellent agreement with each other. The (d, n) experiment, at the low deuteron energy of 4 Mev, yields reduced widths whose ratios agree well with the (d, p) results, but whose absolute values are much smaller. This reduction in reduced widths probably reflects the influence of the low bombarding energy.

The ground-state angular distribution at a deuteron energy of 14.8 Mev (Ha60) exhibits a sharp forward spike superposed on a normal $l=2$ curve, an anomaly which is not visible in the 8-Mev (Ho53d) or the 9-Mev (Hi58) data. It is not clear what produces this forward peak in the angular distribution; careful measurements

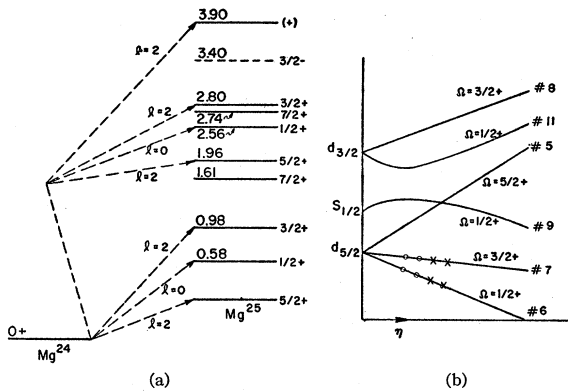


FIG. 36.

at successively smaller deuteron energies (Ha60) reveal a gradual diminution in the forward spike until, at about 9 Mev, an $l=2$ curve of the usual form remains. It is not likely that the anomalous behavior in question stems from contaminants in the target (Ha60); the effect seems to be real.

We discuss $l=0$ and $l=2$ transitions to levels in Mg^{25} below 4 Mev on the basis of the rotational model, which was first applied to Al^{25} and Mg^{25} by Litherland *et al.* (Li58).

The intrinsic structure of the ground state of Mg^{24} is illustrated in Fig. 36(b); for notation, see Fig. 31. Low-lying positive-parity levels of Mg^{25} (or Al^{25}) involve four bands, with $T=\frac{1}{2}$ and $K=\frac{1}{2}^+, \frac{5}{2}^+, \frac{1}{2}^+$, and $\frac{3}{2}^+$, respectively, formed by adding a nucleon in orbits Nos. 9, 5, 11, and 8. Rotational bands interact strongly only if they arise from the same spherical shell-model orbits and differ in K by 1.⁷² We therefore expect the two lowest bands, with $K=\frac{1}{2}^+$ and $K=\frac{5}{2}^+$, to be fairly pure. The two higher bands undoubtedly interact so strongly that statements made on the basis of a pure-band approximation would be valueless.

We therefore treat the bands based on Nilsson orbits No. 9 ($K=\frac{1}{2}$) and No. 5 ($K=\frac{5}{2}^+$) as pure, but take account of the interaction between the bands based on orbit No. 11 ($K=\frac{1}{2}$) and No. 8 ($K=\frac{3}{2}$) in the manner described by Kerman (Ke56). Since, in the present case, only the $J=\frac{3}{2}^+$ states of the last-mentioned bands enter into the band-mixing problem, we need only diagonalize a 2×2 matrix. A brief description of the procedure is given in connection with $\text{Si}^{28}(d, p)\text{Si}^{29}$. We do not consider here the problem of fitting the observed energy spectrum of Mg^{25} by the eigenvalues of the rotational Hamiltonian; this can, in fact, be done with fair accuracy (Li58). Rather, we content ourselves with identifying the levels of Mg^{25} as members of the various rotational bands, calculating δ values on this basis.

Satisfactory agreement with the observed relative reduced widths of levels below 2.8 Mev is obtained with

⁷² Two different $K=\frac{1}{2}$ bands can also interact.

TABLE IX.

Excitation (Mev)	J^π	K	Orbit No.	l	$\frac{S\theta_0^2(l)}{S_0\theta_0^2(1d)}$	$\frac{\theta^2}{\theta_0^2}$ (Ho53d)	(Hi58)	(Ha60)
0	$\frac{5}{2}^+$	$\frac{5}{2}$	5	2	1	1	1	1
0.58	$\frac{3}{2}^+$	$\frac{1}{2}$	9	0	1.8	2.0	2.1	...
0.98	$\frac{3}{2}^+$	$\frac{1}{2}$	9	2	0.45	0.75	0.76	...
1.61	$\frac{7}{2}^+$	$\frac{5}{2}$	5
1.96	$\frac{5}{2}^+$	$\frac{1}{2}$	9	2	0.21	0.44	0.45	0.37
2.56	$\frac{3}{2}^+$	$\frac{1}{2}$	11	0	1.2	...	1.0	...
2.74	$\frac{7}{2}^+$	$\frac{1}{2}$	9

the reasonable values

$$\eta = 3, \quad \frac{\theta_0^2(2s)}{\theta_0^2(1d)} = 1.2 \quad (\text{V.17})$$

of the relevant parameters (see Table IX). The ground-state spectroscopic factor is $S_g = \frac{1}{3}$ and is independent of the deformation parameter η .

It remains to discuss two positive-parity levels, at 2.80 and 3.90 Mev, which were found in Hi58 to have large $l=2$ reduced widths. There is little doubt that the spin of the lower level is $\frac{3}{2}^+$, but that of the upper may be either $\frac{3}{2}^+$ or $\frac{5}{2}^+$. We consider two possible interpretations.

(1) Both levels have spin $\frac{3}{2}^+$ and arise from the interaction of the $\frac{3}{2}^+$ members of the rotational bands, with $K = \frac{1}{2}$ and $K = \frac{3}{2}$, respectively, based on Nilsson's orbits Nos. 11 and 8. On using the momentum of inertia indicated by the spectrum of Mg^{24} , and a deformation parameter $\eta = 3$, we find that the two states in question are 3 Mev apart and that the K values are very strongly mixed.⁷³ The entire $1d_{\frac{5}{2}}$ reduced width is concentrated on the lower $\frac{3}{2}^+$ state, which has $S \approx 0.8$, compared with $S < 0.01$ for the higher.

(2) Litherland *et al.* (Li58) identify the levels at 2.80 and 3.90 Mev in Mg^{25} as the $\frac{3}{2}^+$ and $\frac{5}{2}^+$ members, respectively, of a pure $K = \frac{1}{2}$ band based on orbit No. 11. We have seen that a calculation based on the full rotational Hamiltonian (Ke56) reveals that the pure-band approximation is very poor in the case under consideration. It is nevertheless possible that the 3.90-Mev level has $J = \frac{5}{2}^+$, with $K = \frac{1}{2}$ and $K = \frac{3}{2}$ strongly mixed.

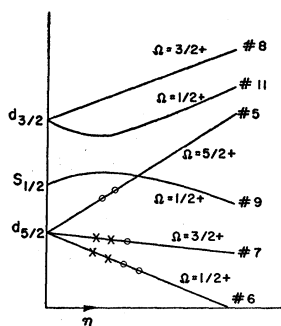


FIG. 37.

⁷³ The lower state is about 60% $K = \frac{1}{2}$ and 40% $K = \frac{3}{2}$.

Such a state would certainly have a very small $l=2$ reduced width since most of the available $d_{\frac{5}{2}}$ intensity has been used up to the lower $\frac{3}{2}^+$ levels of Mg^{25} . The 2.80-Mev level would be interpreted as before.

Both of the foregoing interpretations lead to $S/S_g \approx 2.4$ for the 2.80-Mev level, considerably larger than the observed (Hi58) ratio $\theta^2/\theta_0^2 \approx 1.3$ of reduced widths. A more serious objection is that the 3.90-Mev level is predicted in both cases to have an unobservably small reduced width, in direct contrast to the finding of Hi58. The latter discrepancy may be less severe than now appears because the 3.90-Mev level was not resolved in Hi58 from the nearby single-particle $1f_{7/2}$ state at 3.97 Mev; the observed $l=2$ reduced width is accordingly subject to large error. A (d, p) experiment resolving these states would help clarify the situation.

At an excitation energy of 3 Mev or higher, positive-parity bands arising from breakup of the Mg^{24} core might enter into consideration (Br59). The intrinsic structure of one such band, with $K = \frac{3}{2}^+$, is shown in Fig. 37. Another $K = \frac{3}{2}^+$ band of comparable energy has the two promoted neutrons in orbit No. 9. However, if we neglect pairing forces of the kind considered by Brink and Kerman (Br59), these core-excited bands are connected by sizeable off-diagonal interaction matrix elements only to the two lowest bands, based on orbits No. 9 and No. 5. Since the zero-order separation is 3 Mev or more, the resulting mixing of bands is probably small. This is confirmed by the $\text{Mg}^{25}(d, t)\text{Mg}^{24}$ experiments of Hamburger and Blair (Ha60), wherein only the members of the ground-state band in Mg^{24} are excited with appreciable probability. Accordingly, since members of core-excited bands show no stripping from Mg^{24} , their neglect should have little influence on our analysis of the stripping data.

On using the observed reduced widths (Hi58) and calculated S values for the two lowest states of Mg^{25} , we obtain the estimates

$$\theta_0^2(1d) \approx 0.03, \quad \theta_0^2(2s) \approx 0.04 \quad (\text{V.18})$$

of the relevant single-particle reduced widths.

Observed $l=1$ and $l=3$ transitions are indicated in Table X. Litherland *et al.* (Li58) suggested that the levels at 3.40, 3.97, and 4.27 Mev are the $\frac{3}{2}^-$, $\frac{7}{2}^-$, and $\frac{1}{2}^-$ members of a $K = \frac{1}{2}$ band arising from Nilsson's orbit No. 4, the lowest orbit arising from the $1f_{7/2}$ state of the

spherical shell model. The spectroscopic factors so implied for $\eta=4$ are 0.11, 0.19, and 0.006, respectively. $\theta_0^2(1f)$ and $\theta_0^2(2p)$ are known with reasonable accuracy; using the values 0.010 and 0.025, respectively, we obtain the calculated reduced widths shown in Table X. It is clear that the observed reduced widths are at variance with the proposed interpretation, the predicted values being too small by factors of five or more. A valid application of the rotational model to negative-parity levels in Mg^{25} should include all four bands arising from $1f_{7/2}$ and their interaction, both $2p_{3/2}$ bands and their interactions, and possibly also the mixing of $1f_{7/2}$, $2p_{3/2}$, and $2p_{1/2}$ bands. Too few of the relevant levels and their spins are known to make such a large undertaking worthwhile.

Let us now use the weak-coupling formalism of Sec. III.11 considering first the $l=1$ transitions. Five levels in Mg^{25} were assigned $l=1$ in Hi58⁷⁴; of these, only the lowest, a $\frac{3}{2}^-$ level at 3.40 Mev, is of definitely known spin. The levels in question, with their reduced widths, are given in Table XI.

It was stressed in Sec. III.11 that strongly interacting levels must have the same spin and parity and should lie within 1 or 2 Mev of each other. Accordingly, $J=\frac{3}{2}^-$ is strongly favored for the 4.27-Mev level because of the proximity of the 3.40-Mev level with its large $l=1$ reduced width and spin $\frac{3}{2}^-$. Similarly, $J=\frac{1}{2}^-$ for the 6.80-Mev level is suggested by its large separation from the main $[\phi_0 \times 2p_{3/2}]$ component at 3.40 Mev.

Interpretation of the stripping data on the 7.40- and 7.58-Mev levels is complicated by the fact that $l=1$ and $l=2$ Butler curves are not very different at these excitations. If we accept the $l=1$ assignments of Hi58, the foregoing arguments strongly favor $J=\frac{1}{2}^-$ for both levels. Assuming, for example, that the 7.40-Mev state has spin $\frac{3}{2}^-$, and ignoring the relatively weak level at 4.27 Mev, since its influence on the argument would be slight, the observed reduced widths of the 3.40- and 7.40-Mev levels would demand an incredibly large interaction matrix element of close to 2 Mev. We conclude that strong $\frac{3}{2}^-$ levels at 7.40 or 7.58 Mev would be very hard to explain.⁷⁶ If, however, we assume $J=\frac{1}{2}^-$ for both levels, we find that the total $2p_{3/2}$ and $2p_{1/2}$ intensities are almost the same, in serious disagreement with the expected statistical ratio of two. An alternative possibility presents itself on observing that the angular distribution of the 7.58-Mev level is rather

⁷⁴ Ignoring a possible small component in the 5.79-Mev level, whose presence would not significantly influence the ensuing discussion.

⁷⁵ The 7.40-Mev level appears as an 85-kev resonance in $Mg^{24}(n,n)Mg^{24}$. Consideration of the total cross section at this resonance led Fields and Walt (Fi50) to $J=\frac{1}{2}^-$, and Haeberli *et al.* (Ha58) to $J=\frac{3}{2}^-$. The different spin assignments reflect a disagreement by a factor of two in the measured cross sections. Haeberli *et al.* also found $J=\frac{3}{2}^-$ to be in accord with differential cross sections measured at $\theta(c.m.)=90^\circ$ and 180° . A level near 7.58 Mev appears as a 275-kev resonance in $Mg^{24}(n,n)Mg^{24}$. From the total cross section, Fields and Walt assigned $J=\frac{1}{2}^-$. However, this assignment is by no means certain; indeed, these authors suggested that the "level" in question might be a doublet.

TABLE X.

Level of Mg^{25}	J^π	$\theta^2(\text{calc})$	$\theta^2(\text{obs})$ (Hi58)
3.40	$\frac{3}{2}^-$	0.003	0.019
3.97	$\frac{7}{2}^-$	0.002	0.010
4.27	$(\frac{1}{2}^-)$	0.0002	0.011

different from that of the 7.40-Mev level, bearing a closer resemblance to the 8.05-Mev angular distribution. $l=2$ produces a reasonably good fit in both cases. From the viewpoint of the weak-coupling formalism, the most attractive interpretation of the levels in question is then the following:

$$\left. \begin{array}{ll} 3.40 \text{ Mev} & J = \frac{3}{2}^- \quad [\phi_0 \times 2p_{3/2}] \quad \theta_0^2(2p_{3/2}) \approx 0.024, \\ 4.27 \text{ Mev} & \\ 6.80 \text{ Mev} & J = \frac{1}{2}^- \quad [\phi_0 \times 2p_{3/2}] \quad \theta_0^2(2p_{3/2}) \approx 0.031, \\ 7.40 \text{ Mev} & \\ 7.18 \text{ Mev} & J = \frac{5}{2}^+ \quad [\phi_0 \times 2d_{5/2}] \quad \theta_0^2(2d_{5/2}) \approx 0.020. \\ 7.58 \text{ Mev} & \\ 8.05 \text{ Mev} & \end{array} \right\}$$

The matter should be settled by an experimental determination of the relevant spins and parities.

Applying the sum rule (III.185) to all observed $l=1$ transitions (excluding the transition to the 7.58-Mev level), we have

$$\sum_{2p_{3/2}, 2p_{1/2}} [J]S = (4+2) = 6,$$

whence

$$\theta_0^2(2p) \approx 0.026, \quad (\text{V.19})$$

in good agreement with other estimates.

Three $l=3$ transitions have been observed (Hi58), to levels at 3.97, 4.72, and 7.24 Mev in Mg^{25} . The spin of the 3.97-Mev level is known to be $\frac{7}{2}^-$. Arguing again that strongly interacting levels should be within 1 or 2 Mev of each other, we conclude that the probable spins of the 4.72- and 7.23-Mev levels are $\frac{7}{2}^-$ and $\frac{5}{2}^-$, respectively.

The two $\frac{7}{2}^-$ levels (Fig. 38) involve components of $[\phi_0 \times 1f_{7/2}]$. Since $[\phi_0 \times 2p_{3/2}]$ appears to be about 0.6 Mev below $[\phi_0 \times 1f_{7/2}]$ in Mg^{25} , it is possible that $[\phi_1 \times 2p_{3/2}]$ is less than 1 Mev from $[\phi_0 \times 1f_{7/2}]$ and interacts with it quite strongly. Proceeding in the manner described in

TABLE XI.

Excitation (Mev)	J	l	$[J]\theta^2$
3.40	$\frac{3}{2}^-$	1	0.076
4.27		1	0.022
6.80		1	0.014
7.40		1	0.048
7.58	$\left\{ \begin{array}{l} \frac{5}{2}^+ \\ (\frac{1}{2}^-) \end{array} \right.$	1	0.042
		2	0.055

⁷⁶ This estimate agrees well with the value 0.019 found from $Ca^{40}(d,p)Ca^{41}$ (Ho53).

$$\phi_0 \xrightarrow{1.368} 2^+$$

FIG. 38.

$$\phi_0 \xrightarrow{\text{Mg}^{24}} 0^+$$

Sec. III.11 (Example 1), the reduced widths of the 3.97 and 4.72 Mev levels indicate a zero-order separation of 450 kev and an interaction matrix element of 300 kev. The absolute reduced widths of the $\frac{7}{2}^-$ levels indicate that

$$\theta_0^2(1f_{7/2}) = 0.012, \quad (\text{V.20})$$

in excellent agreement with (V.3).

The 7.23-Mev state must⁷⁷ be predominantly $[\phi_0 \dot{\times} 1f_{\frac{5}{2}}]$, providing the only identification to date of a single-particle $1f_{\frac{5}{2}}$ level in a ds -shell nucleus. The absolute reduced width of the 7.23-Mev level gives

$$\theta_0^2(1f_{\frac{5}{2}}) = 0.013. \quad (\text{V.21})$$

The ordering of single-particle levels in Mg^{25} differs in several respects from what is found⁷⁸ elsewhere in the region $16 < A < 50$. Firstly, values of the p -doublet splitting fall consistently between 1 and 2.5 Mev, with the single exception that in $\text{Mg}^{25}[2p_{\frac{1}{2}}] - [2p_{\frac{3}{2}}] \approx 3.5$ Mev. On the other hand, the f -doublet splitting in Mg^{25} is only 3 Mev, smaller than in Sc^{41} and the Ca isotopes, where $[1f_{\frac{5}{2}}] - [1f_{7/2}] > 6$ Mev. Lastly, Mg^{25} is the only known nucleus where $2p_{\frac{3}{2}}$ lies below $1f_{7/2}$.

A very strong $l=0$ transition is assigned in Hi58 to a level at 5.49 Mev in Mg^{25} . It is very hard to account for a very large $2s_{\frac{1}{2}}$ component as high as 5.5 Mev in Mg^{25} . The Q value of the transition in question is within 10 kev of that of the intense $l=0$ transition to the first excited level of C^{18} . In separating these groups, Hinds *et al.* (Hi58) may have underestimated the C contribution.

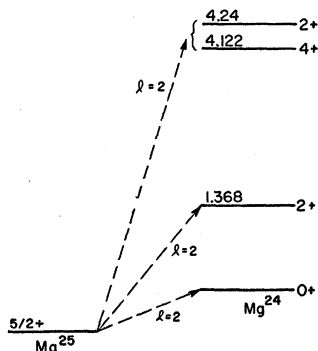


FIG. 39.

$$\text{Mg}^{25}(p,d)\text{Mg}^{24}, \text{Mg}^{25}(d,t)\text{Mg}^{24}$$

Two closely-spaced levels near 4.2 Mev in Mg^{24} were not resolved in the only available (p,d) experiment (Be58) (Fig. 39). A (d,t) experiment (Ha60) indicates that most of the combined $l=2$ transition proceeds to the 4^+ level at 4.122 Mev. The (d,t) and (p,d) results are in satisfactory accord except that the (p,d) experiment indicates a markedly stronger transition to the 4.2-Mev doublet.

The intrinsic structure of the ground states of Mg^{24} and Mg^{25} was described in connection with the inverse experiment $\text{Mg}^{24}(d,p)\text{Mg}^{25}$. The fact that, of the levels of Mg^{24} up to 7.6 Mev, only the members of the ground-state band were excited with appreciable intensity in the (d,t) experiment, indicates that the $K=\frac{5}{2}^+$ ground state of Mg^{25} is very pure.⁷⁹ The small reduced width of the 2^+ state at 4.24 Mev probably arises from a residual interaction with the 2^+ member of the ground-state band.

According to (III.204), the spin- J member of the 0^+ rotational band in Mg^{24} has a spectroscopic factor proportional to $C(J, \frac{5}{2}, 0, \frac{5}{2})^2$. The resulting reduced-width ratios are given in Table XII. The (d,t) reduced widths

TABLE XII.

Level in Mg^{24}	J^π	$\frac{S}{S_g}$	$\frac{\theta^2}{\theta_0^2}(d,t)$	$\frac{\theta^2}{\theta_0^2}(p,d)$
0	0^+	1	1	1
1.368	2^+	$25/14 = 1.8$	2.0	2.7
4.122	4^+	$3/14 = 0.21$	0.33	1.0

are in excellent agreement with the predictions of the rotational model; agreement for the (p,d) reduced widths is markedly poorer.

In Example 1 of Sec. III.10, we applied the jj -coupling sum rule

$$S_2 + S_4 = 8S_g$$

to the (p,d) reduced widths. Agreement with the observed reduced widths is unimpressive and becomes rather worse if we use the (d,t) data. The preceding sum rule is to be contrasted with

$$S_2 + S_4 = 2S_g,$$

obtained with the aid of the rotational model. The rotational sum rule is obviously in much better agreement with experiment than the jj -coupling sum rule.

$$\text{Mg}^{25}(d,p)\text{Mg}^{26}$$

Since we are again dealing with the transfer of a nucleon with $\Omega = \frac{5}{2}$, for which j has the specified value of $\frac{5}{2}$, the reduced widths of levels in the $K=0$ ground-state band of Mg^{26} are independent of the deformation (Fig. 40). We find, for the spectroscopic factors of the

⁷⁷ From the viewpoint of the Nilsson brand of rotational model.

⁷⁸ The 7.23-Mev level was not completely resolved in Hi58 from a nearby $l=2$ level at 7.18 Mev. The separation of the combined angular distribution into $l=2$ and $l=3$ components is quite convincing.

⁷⁹ The positions of single-particle levels in the region $30 < A < 60$ have been discussed in detail by Nussbaum (Nu56).

ground and first excited states of Mg^{26} , the values $s_g = 2$ and $s^* = 5/7$.

In the only available experiment (Ho53d), the ground-state angular distribution was not measured. Since $l=2$ is demanded by conservation of angular momentum, an upper limit $\theta_g^2 \leq 0.04$ was set on the reduced width. The $l=2$ assignment has now been confirmed in the reaction (Ha60) $Mg^{26}(d,t)Mg^{25}$; using the value $\Lambda = 150$ of the (d,t) normalization factor obtained from $Mg^{25}(d,t)Mg^{24}$, the ground-state reduced was found to be 0.031 which is consistent with the foregoing upper limit and is used in the following discussion. The ratio of the $l=2$ reduced widths of the two lowest states of Mg^{26} is then found to be

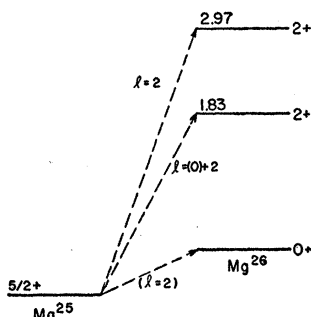
$$\theta^2/\theta_g^2 = 0.7.$$

Considering the uncertainty involved in our indirect determination of θ_g^2 and the fact that both the states under consideration are found to contain small admixtures of excited bands, agreement with the predicted ratio

$$s/s_g = 5/14 \approx 0.4$$

is tolerably good.

FIG. 40.



As discussed by Satchler (Sa58) and by Sawicki (Sa58a), the presence of an $l=0$ admixture in the transition to the 1.83-Mev level reveals $2s_{\frac{1}{2}}$ components in its wave function. The most likely origin of such components is through interaction with the 2^+ level at 2.97 Mev. Geometrical effects cannot contribute (Sa58b). Since rotation-particle coupling (Ke56) does not connect bands with $\Delta K = 2$ directly, the interaction in question probably arises mainly from residual two-body forces.

$Mg^{26}(d,t)Mg^{25}$

If the last two nucleons in the Mg^{26} ground state were entirely in Nilsson's orbit No. 5, only the ground-state of Mg^{26} would be excited in $Mg^{26}(d,t)Mg^{25}$. The fact that other levels show appreciable pickup (Ha60) reveals the presence of admixture in the Mg^{26} intrinsics wave function. Let us write

$$\Psi(Mg^{26}) = \alpha(\text{No. } 5)^2 + \beta(\text{No. } 9)^2 + \gamma(\text{No. } 11)^2 \quad (\text{V.22})$$

TABLE XIII.

Excitation (Mev)	J^π	K	Orbit No.	l	$s(\eta=2)$	$s(\eta=4)$	θ^2/θ_g^2 (Ha60)
0	$\frac{5}{2}^+$	$\frac{5}{2}$	5	2	$2\alpha^2$	$2\alpha^2$	1
0.58	$\frac{1}{2}^+$	$\frac{1}{2}$	9	0	$1.3\beta^2$	$0.56\beta^2$	0.080
2.56	$\frac{3}{2}^+$	$\frac{3}{2}$	11	0	$0.39\gamma^2$	$0.94\gamma^2$	0.023

for the relevant intrinsic wave function; we use the observed pickup widths to evaluate α^2 , β^2 , and γ^2 . A similar analysis has been given in Ha60.

First, we consider the ground states of the rotational bands based on orbits No. 5, No. 9, and No. 11 in Mg^{25} . The respective values of s , obtained from (III.204) with the aid of Nilsson's single-particle wave functions (Ni55), are given in Table XIII.

In order to obtain estimates of the amplitudes we must have a suitable value for $\theta_0^2(2s)/\theta_0^2(1d)$. We have encountered consistent evidence that this ratio decreases as Q increases; since the Q values for the transitions in question are much higher than those encountered in $Mg^{24}(d,p)Mg^{25}$ and almost as large as that for $F^{19}(d,n)Ne^{20}$, (V.17) and (V.13) suggest that

$$\theta_0^2(2s)/\theta_0^2(1d) \approx 1 \quad (\text{V.23})$$

is acceptable as a reasonable estimate. We then obtain

$$\alpha^2 = 0.80 \quad \beta^2 = 0.10 \quad \gamma^2 = 0.10 \quad (\eta=2), \quad (\text{V.24})$$

$$\alpha^2 = 0.75 \quad \beta^2 = 0.22 \quad \gamma^2 = 0.03 \quad (\eta=4). \quad (\text{V.25})$$

Using the ground-state spectroscopic factor (which is insensitive to η) and the corresponding observed absolute reduced width (Ha60) of 0.031, we have

$$\theta_0^2(1d) \approx 0.02. \quad (\text{V.26})$$

Comparison with (V.18) again reveals the tendency of single-particle reduced widths to decrease with increasing Q .

According to (III.204), the reduced widths of levels of the same band in Mg^{25} are proportional to the appropriate (squared) Nilsson amplitudes. Relevant experimental data is available only for the $K = \frac{1}{2}$ band based on orbit No. 9, for which we have the data given in Table XIV. The ratios are very sensitive functions of the deformation, and it is patently impossible to obtain reasonable agreement for both the $\frac{3}{2}^+$ and $\frac{5}{2}^+$ states. For $\eta=3$, the reduced-width ratio of the $\frac{5}{2}^+$

TABLE XIV.

Excitation (Mev)	J^π	l	$\frac{s}{s_{J=\frac{1}{2}}}(\eta=2)$	$\frac{s}{s_{J=\frac{1}{2}}}(\eta=4)$	$\frac{\theta^2}{\theta_{J=\frac{1}{2}}^2}$ (Ha60)
0.58	$\frac{1}{2}^+$	0	1	1	1
0.98	$\frac{3}{2}^+$	2	0.28	1.6	0.16
1.96	$\frac{5}{2}^+$	2	0.26	1.7	0.72

state is reasonably reproduced but the $\frac{3}{2}^+$ level is much too strongly excited.

The $\frac{3}{2}^+$ level at 2.80 Mev in Mg^{26} , which we have seen to be an intimate mixture of $K=\frac{1}{2}$ and $K=\frac{3}{2}$, also has a small observed $l=2$ reduced width. The value of δ for this state, calculated for $\eta=3$ on the assumption that the (No. 8)² admixture in (V.22) is negligible, is found to be 0.028_g , in fair accord with the observed reduced-width ratio of 0.03 (Ha60).

$Mg^{26}(d,p)Mg^{27}$

Two experiments have been reported, one with 8.9-Mev deuterons studying levels in Mg^{27} up to 4.75 Mev (Hi58), the other studying only the ground and first excited states of Mg^{27} at a deuteron energy of 8 Mev (Ho53d). The absolute reduced widths measured in these two experiments disagree by a factor of two.

Let us study the $l=1$ transitions first in order to get a better idea of the correct Mg^{27} absolute reduced widths. A strong $l=1$ level appears at 3.56 Mev in Mg^{27} , analogous to the $2p_{\frac{1}{2}}$ level at 3.40 Mev in Mg^{27} . There is probably a weak $l=1$ level at 4.75 Mev in Mg^{27} , similar to the 4.27-Mev level in Mg^{26} . The reduced widths of Hi58 then yield $\theta_0^2(2p) \approx 0.035$, significantly larger than other estimates, suggesting that the absolute Mg^{27} reduced widths of Hi58 are too large. Let us, therefore, renormalize the reduced widths of Hi58 to $\theta_0^2(2p) = 0.026$ [(V.19), (V.33), and (V.34)]. The resulting reduced widths are intermediate in value between those of Ho53d and Hi58, and are given in Fig. 41.

The deformations of the four Mg isotopes with $A=24$ to 27 appear to be quite similar (Ra57). The rotational model therefore predicts that the spacings and reduced widths of low-lying levels of Mg^{27} should resemble those of Mg^{26} with the ground-state $K=\frac{5}{2}$ band removed. Because of the different effects of residual two-body forces (Br59) in the two cases, we do not expect this similarity in structure to be more than qualitative.

That the predicted qualitative similarity is exhibited by the observed level sequences and reduced widths can be seen from Fig. 41.

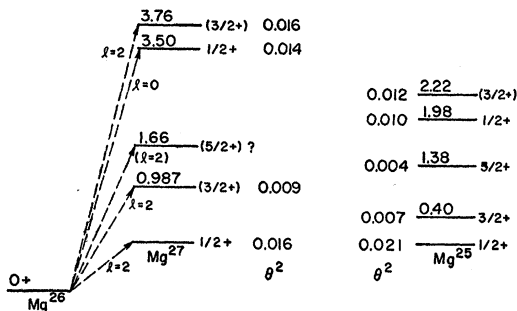


FIG. 41.

$Al^{27}(d,p)Al^{28}$

A high-resolution experiment has been performed with 6-Mev deuterons (En56), studying levels up to 5.14 Mev in Al^{28} , but measuring no absolute cross sections [Fig. 42(a)]. The reduced widths so obtained can, however, be normalized with the aid of an earlier less-detailed experiment (Ho53a) at a bombarding energy of 8 Mev.

We start by discussing the possibility of applying the rotational model to the low-lying positive-parity levels of Al^{28} and their reduced widths. The intrinsic structure of the Al^{27} ground state is as shown in Fig. 42(b). The lowest $T=1$ bands of $A=28$ have $K=2$ and $K=3$, being formed from the Al^{27} ground state by adding a nucleon in the No. 9 ($\Omega=\frac{1}{2}^+$) orbit [see Fig. 42(b)]. Low-lying excited bands can be formed in two different ways. Firstly, excited $T=1$ bands with $K=0$ and $K=1$ are constructed by putting two nucleons in each of orbits No. 5 and No. 9. Secondly, a nucleon can be added to the Al^{27} ground-state configuration in either of the $1d_{\frac{3}{2}}$ orbits, No. 11 and No. 8. We may enumerate the various bands in the following fashion:

- A. $\{6^4 7^4 5^3 9^1\} T=1; K=2, 3,$
- B. $\{6^4 7^4 5^2 9^2\} T=1; K=0, 1,$
- C. $\{6^4 7^4 5^3 11^1\} T=1; K=2, 3,$
- D. $\{6^4 7^4 5^3 8^1\} T=1; K=1, 4.$

The number of nucleons in each orbit is given by the superscripts. Sheline (Sh56) has discussed levels of Al^{28} up to 2.3 Mev in terms of the rotational model. He assumes that the only rotational bands of importance are those arising from the intrinsic configurations A and B , the $1d_{\frac{3}{2}}$ orbits making no significant contribution. The observed reduced widths indicate that such an assumption is unjustified. The crux of the matter lies in the large $l=2$ reduced widths (En56) of the levels at 1.02 and 2.28 Mev in Al^{28} , reduced widths which correspond to δ values close to one. None of the rotational states discussed by Sheline could possibly have sufficiently large $l=2$ reduced widths; members of the

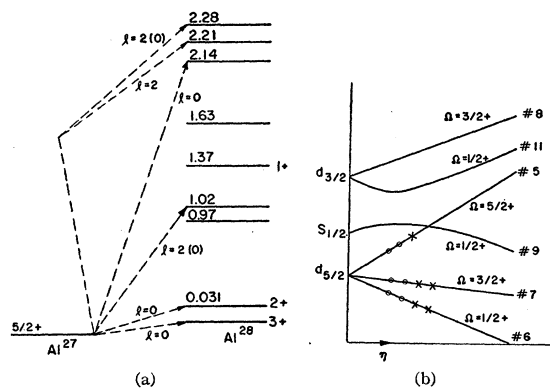


FIG. 42.

ground-state $K=3$ and $K=2$ bands have $S(l=2) < 0.2$ for any reasonable deformation,⁸⁰ while states arising from the intrinsic configuration B cannot be reached by stripping from Al^{27} and so have $S=0$. In fact, $l=2$ reduced widths of the desired size demand large $1d_{\frac{3}{2}}$ contributions. For reasonable deformations, such contributions can be found only in members of the first kind of excited band discussed previously, wherein the added nucleon is in one of the $1d_{\frac{3}{2}}$ orbits, No. 11 and No. 8.

Thus a correct application of the rotational model to low-lying levels in Al^{28} must include all the rotational bands enumerated previously and interactions between them. This is obviously a large undertaking and is hardly worthwhile since only three of the relevant levels are of definitely known spin and parity.

Let us proceed to examine the negative-parity transitions. Strong $l=1$ transitions are observed to levels in Al^{28} between 3.4 and 5.2 Mev. There are six basic $l=1$ components:

$$\begin{aligned} [\phi_0 \times 2p_{\frac{1}{2}}]J, \quad J = 1, 2, 3, 4^- \\ [\phi_0 \times 2p_{\frac{3}{2}}]J, \quad J = 2, 3^- \end{aligned}$$

Applying the sum rule (III.185), we deduce from

$$\sum [J]S = (3+5+7+9)+(5+7) = 36$$

and⁸¹

$$\sum [J]\theta^2 \geq 0.7,$$

that

$$\theta_0^2(2p) \geq 0.02. \quad (\text{V.27})$$

Since no spins are known and since $2p_{\frac{1}{2}}$ and $2p_{\frac{3}{2}}$ components can both contribute to $J=2^+$ and $J=3^+$ states, we cannot separate $2p_{\frac{1}{2}}$ and $2p_{\frac{3}{2}}$ contributions. However, the large $[J]\theta^2$ values of the 3.59-, 4.69-, and 4.77-Mev levels indicate that they must have $J>1$ and probably $J>2$ also.

No $l=3$ transitions were observed (En56). This is probably due to competition with $l=1$; $l=1+3$ superpositions are allowed by conservation of angular momentum when $J_0 \geq 2$. (Al^{27} has $J_0 = \frac{5}{2}$.)

$\text{Al}^{27}(d,n)\text{Si}^{28}$

The two available experiments, at deuteron energies of 6 and 9 Mev (Ru57 and Ca55), are in poor agreement. We accept the 9-Mev data of Ca55 as more reliable.

Binding-energy calculations on the basis of the rotational model (Br57) suggest that the equilibrium deformation of ds -shell nuclei changes sign near Si^{28} . This expectation has been supported by applications of the

⁸⁰ The equilibrium deformation of Al^{28} is probably (Ra57) rather smaller than that of Mg^{26} or Al^{26} ; $\eta=2$ is probably a reasonable estimate.

⁸¹ The inequality allows for the possibility that sizeable $l=1$ components lie above the limit of the experiment in question (En56). We quote only one significant digit because the reduced widths of En56 were normalized indirectly, using those of Ho53a.

rotational model to Si^{29} (Br57) and P^{31} (Br58), where reasonable agreement with experiment is achieved for deformation parameters of between -2 and -3 , prolate shapes being rather definitely excluded. The change of sign in question appears to take place quite suddenly; the adjacent nuclei Al^{28} and Si^{29} probably have stable equilibrium deformations of roughly equal magnitude and opposite sign. The existence (but not the sign) of a stable equilibrium deformation in the "closed-shell" nucleus Si^{28} is indicated by its successful inclusion in Brink and Kerman's (Br59) calculation of relative binding energies of light deformed nuclei. By minimizing the total energy of the nucleus with respect to η , it is found (Br57) that the equilibrium deformations of Si^{28} and Si^{29} should be almost the same. This prediction is much less sensitive to the details of the model used than the precise value obtained for the deformation at minimum energy. We therefore conclude that Si^{28} is, in all likelihood, an oblate nucleus, with $\eta \approx -2$.

Having assigned very different equilibrium deformations to Al^{27} and Si^{28} , we cannot give a quantitative discussion of the $\text{Al}^{27}(d,n)\text{Si}^{28}$ reduced widths on the basis of the rotational model. Not only is the core overlap factor $\langle f|i \rangle$ in (III.204) now an unknown quantity, but also the single-particle Nilsson orbits in Al^{27} and Si^{28} are no longer even approximately orthogonal.

The existence of stable deformations for Al^{27} and Si^{28} implies, in the language of the shell model, sizeable contributions to the corresponding wave functions from the $1d_{\frac{3}{2}}$ and $2s_{\frac{1}{2}}$ orbits. We later encounter very direct experimental evidence of such admixtures in discussing the reactions $\text{Si}^{28}(\text{He}^3, \alpha)\text{Si}^{27}$ and $\text{Si}^{28}(d, p)\text{Si}^{29}$; first we examine the implications of the $\text{Al}^{27}(d, n)\text{Si}^{28}$ reduced widths.

In jj coupling, the Al^{27} ground state is simply $d_{\frac{5}{2}}^{-1}$ and that of Si^{28} a closed-shell state. The $\text{Al}^{27}(d, n)\text{Si}^{28}$ (ground state) reaction would then have $S=12$, as described in Example 4 of Sec. III.9. Since $\theta_0^2(1d)$ is about 0.02 for reactions of the relevant Q value (V.26), the observed reduced width of 0.039 (Ca55) reveals a discrepancy of a factor of six. Since it is unlikely⁸² that there is such a large error in the measured absolute cross section of Ca55, we are forced to the conclusion that the preceding simple wave functions for Al^{27} and Si^{28} are seriously inadequate.

In the following calculation, our aim is to find the smallest $2s_{\frac{1}{2}}$ and $1d_{\frac{3}{2}}$ admixtures consistent with the observed ground-state reduced width. We assume optimal cooperation of phases and make the approximation of using extreme jj wave functions, of lowest

⁸² The strong $l=0$ transition(s) to level(s) near 9.3 Mev in Si^{28} probably excites the analog of the Al^{28} ground-state doublet. Reasonable agreement is found between the values, 0.31 and 0.22, respectively, of $\sum [J]\theta^2$ for this lowest $T=1$ doublet measured by $\text{Al}^{27}(d, n)\text{Si}^{28}$ (Ca55) and $\text{Al}^{27}(d, p)\text{Al}^{28}$ (En56).

symplectic symmetry,⁸³ for states of $d_{\frac{5}{2}}^n$. We obtain an upper limit to, rather than an estimate of, the one-hole and closed-shell components in Al²⁷ and Si²⁸, respectively.

$$\Psi(\text{Si}^{28}) = \beta_1 \left(\begin{array}{c} d_{\frac{5}{2}}^{-2} \\ \frac{1}{2} \end{array} \right)_{00} + \beta_2 \left(\begin{array}{c} c_2 \\ \frac{1}{2} \end{array} \right)_{01} + \beta_3 \left(\begin{array}{c} c_3 \\ \frac{1}{2} \end{array} \right)_{10} + \beta_4 \left(\begin{array}{c} c_4 \\ \frac{1}{2} \end{array} \right)_{00}, \quad (\text{V.28})$$

where c_2 , c_3 , and c_4 describe configurations involving $s_{\frac{1}{2}}$ and $d_{\frac{5}{2}}$. For example, c_2 represents some linear combination of $(s_{\frac{1}{2}}^2)_{01}$ and $(d_{\frac{5}{2}}^2)_{01}$. We are not interested in the precise nature of the c_i ; apart from additional overlap factors to be mentioned in the following, the

$$\Psi(\text{Al}^{27}) = \alpha_1 \left(\begin{array}{c} d_{\frac{5}{2}}^{-1} \\ \frac{1}{2} \end{array} \right)_{\frac{1}{2}\frac{1}{2}} + \alpha_2 \left(\begin{array}{c} c'_2 \\ \frac{1}{2} \end{array} \right)_{\frac{1}{2}\frac{1}{2}} + \alpha_3 \left(\begin{array}{c} c'_3 \\ \frac{1}{2} \end{array} \right)_{\frac{1}{2}\frac{1}{2}} + \alpha_4 \left(\begin{array}{c} c'_4 \\ \frac{1}{2} \end{array} \right)_{\frac{1}{2}\frac{1}{2}}. \quad (\text{V.29})$$

Corresponding terms in (V.28) and (V.29) are connected by the transfer of a $1d_{\frac{5}{2}}$ nucleon. On using (III.64),⁸⁵ the overlap integrals are, respectively,

$$g(d_{\frac{5}{2}}) = 1, -(1/14)^{\frac{1}{2}} \langle c_2 | c'_2 \rangle, -(7/18)^{\frac{1}{2}} \langle c_3 | c'_3 \rangle, -(\frac{2}{3})^{\frac{1}{2}} \langle c_4 | c'_4 \rangle.$$

The overlap factors $\langle c_i | c'_i \rangle$ clearly depend on the exact nature of the $2s_{\frac{1}{2}}$ and $1d_{\frac{5}{2}}$ contributions c_i and c'_i to Si²⁸ and Al²⁷. In accordance with our aim of setting a lower limit on such core-excited components, we take $\langle c_i | c'_i \rangle = 1$. If the overlap factors are, in fact, significantly smaller than one, then the amount of core excitation implied by the observed reduced widths will be correspondingly larger.

The spectroscopic factor is therefore

$$S(1d_{\frac{5}{2}}) = 12[\alpha_1 \beta_1 - (1/14)^{\frac{1}{2}} \alpha_2 \beta_2 - (7/18)^{\frac{1}{2}} \alpha_3 \beta_3 - (\frac{2}{3})^{\frac{1}{2}} \alpha_4 \beta_4]. \quad (\text{V.30})$$

It is clear that if the phases (especially of the last two components) cooperate, a large reduction in the spectroscopic factor can be produced by a moderate amount of core excitation. Let us suppose, for example, that

⁸³ Symplectic symmetry may not be very "good" for $d_{\frac{5}{2}}^n$, but is probably as good as jj coupling and quite satisfactory in the present context. For states of $d_{\frac{5}{2}}^{-2}$ no assumptions need be made concerning symplectic symmetry since each such state is uniquely specified by T and J .

⁸⁴ Notice that, in writing the pair of quantum numbers (TJ), we place T first.

⁸⁵ In evaluating the last of these four overlap integrals, we need the cfp $\langle d_{\frac{5}{2}}^5 \frac{1}{2} \frac{5}{2} | d_{\frac{5}{2}}^4 0 0 \rangle$, which is not given by Edmonds and Flowers (Ed52). However, using explicit expressions given by Grayson and Nordheim (Gr56b) for the cases of lowest symplectic symmetry, we find $\langle d_{\frac{5}{2}}^5 \frac{1}{2} \frac{5}{2} | d_{\frac{5}{2}}^4 0 0 \rangle = -(2/15)^{\frac{1}{2}}$.

As in the case of Ne²⁰, paired excitations from the $1d_{\frac{5}{2}}$ to the $2s_{\frac{1}{2}}$ and $1d_{\frac{5}{2}}$ shells are energetically favored. Let us, therefore, exclude such configurations as $d_{\frac{5}{2}}^{-3} s_{\frac{1}{2}}^3$, and write⁸⁴ for the Si²⁸ ground-state wave function,

$$\Psi(\text{Si}^{28}) = \beta_1 \left(\begin{array}{c} d_{\frac{5}{2}}^{-2} \\ \frac{1}{2} \end{array} \right)_{00} + \beta_2 \left(\begin{array}{c} c_2 \\ \frac{1}{2} \end{array} \right)_{01} + \beta_3 \left(\begin{array}{c} c_3 \\ \frac{1}{2} \end{array} \right)_{10} + \beta_4 \left(\begin{array}{c} c_4 \\ \frac{1}{2} \end{array} \right)_{00}, \quad (\text{V.28})$$

reduced widths in which we are interested here (those involving transfer of a $1d_{\frac{5}{2}}$ nucleon) depend on the c_i only through the total quantum numbers.

In similar fashion Al²⁷ may be represented by

the Al²⁷ and Si²⁸ ground states are 60% $d_{\frac{5}{2}}^{-1}$ and $d_{\frac{5}{2}}^{-2}$, respectively, and that the phases cooperate. Let us take, in fact,

$$\langle \alpha_1 \alpha_2 \alpha_3 \alpha_4 \rangle = (\beta_1 \beta_2 \beta_3 \beta_4) = [(6/10)^{\frac{1}{2}}, (1/10)^{\frac{1}{2}}, (1/10)^{\frac{1}{2}}, (2/10)^{\frac{1}{2}}]$$

and substitute in (V.30). We obtain $S \approx 1.45$, in place of the value 12 found in pure jj coupling.

Thus the small Al²⁷(d,n)Si²⁸ ground-state reduced width places an upper limit of about 60% on the closed-shell component in $\Psi(\text{Si}^{28})$. The remaining $1d_{\frac{5}{2}}$ contributions must appear in higher excited 0^+ states of Si²⁸; the corresponding $l=2$ transitions should be sought in high-resolution Al²⁷(d,n)Si²⁸ or Al²⁷(He³, d)Si²⁸ experiments.

Si²⁸(He³, d)Si²⁷

If Si²⁸ were a true closed-shell nucleus, the only positive-parity transition to be observed to low-lying levels of Si²⁸ would be the $l=2$ ground-state transition. The observation (Hi60) of a strong $l=0$ transition to the $\frac{1}{2}^+$ first excited state of Si²⁷ and a second $l=2$ transition to the $\frac{3}{2}^+$ second excited state, constitutes a direct verification that the Si²⁸ ground-state wave function contains large $2s_{\frac{1}{2}}$ and $1d_{\frac{5}{2}}$ contributions (Fig. 43).

Si²⁸(d,p)Si²⁹; Si²⁸(d,n)P²⁹

The measured (d,p) and (d,n) reduced widths (Ho53, Ca57) of the first excited states of Si²⁹ and P²⁹ disagree by a factor of two. Since the first excited state of P²⁹

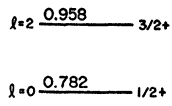
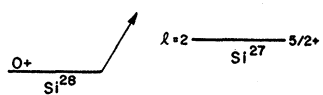


FIG. 43.



is within 1.5 Mev of the proton separation energy, we regard the (d,p) reduced width as more significant.

The observed $l=2$ reduced widths of $\frac{5}{2}^+$ states in Si^{29} are a further indication of core excitation in Si^{28} . For, by conservation of angular momentum, such transitions must involve the capture of a $d_{\frac{5}{2}}$ nucleon; only $1d_{\frac{5}{2}}$ seems likely at the excitations in question and would be ruled out by a closed-shell assumption for Si^{28} .

Although the reduced widths involved are small, they imply large amounts of core excitation in the ground state of Si^{28} . Summing over all $\frac{5}{2}^+$ states (or their fragments) which can be formed from (V.28) by capture of a $1d_{\frac{5}{2}}$ nucleon, we obtain the sum rule

$$\sum S(1d_{\frac{5}{2}}) = \frac{1}{6}(\beta_2^2 + \beta_3^2 + 2\beta_4^2). \quad (\text{V.31})$$

Adopting $\theta_0^2(1d) \approx 0.025$ as a suitable value of the single-particle reduced width for the Q values in question, the wave function

$$(\beta_1\beta_2\beta_3\beta_4) = [(6/10)^{\frac{1}{2}}(1/10)^{\frac{1}{2}}(1/10)^{\frac{1}{2}}(2/10)^{\frac{1}{2}}]$$

used in connection with $\text{Al}^{27}(d,n)\text{Si}^{28}$ gives

$$\sum \theta^2(1d_{\frac{5}{2}}) \approx 0.0025,$$

considerably smaller than the measured sum of 0.006. This discrepancy indicates either an even larger degree of core excitation in Si^{28} or coherent $2d_{\frac{5}{2}}$ contributions to the observed $l=2$ reduced widths.

There is little doubt that the well-isolated strong $l=3$ and $l=1$ transitions to levels at 3.62, 4.9, and 6.38 Mev in Si^{29} reveal good single-particle $1f_{7/2}$, $2p_{\frac{3}{2}}$, and $2p_{\frac{1}{2}}$ levels, respectively. The absolute reduced widths yield

$$\theta_0^2(1f) \approx 0.013, \quad (\text{V.32})$$

$$\theta_0^2(2p_{\frac{3}{2}}) \approx 0.029, \quad (\text{V.33})$$

$$\theta_0^2(2p_{\frac{1}{2}}) \approx 0.023, \quad (\text{V.34})$$

in reasonable agreement with earlier estimates. The p -doublet splitting is 1.5 Mev and the relative positions of $1f_{7/2}$ and $2p_{\frac{3}{2}}$ levels is reversed from what is observed in Mg^{26} .

Bromley *et al.* (Br57) have pointed out that nuclei between Si^{28} and S^{32} possess oblate equilibrium shapes, and therefore suggest that the Nilsson rotational model is applicable. The intrinsic structure of the Si^{28} ground

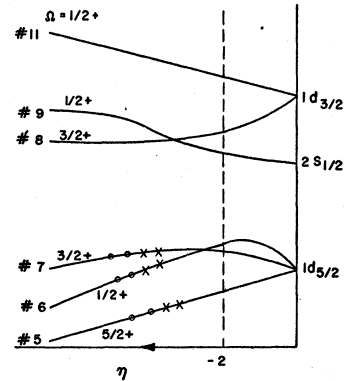


FIG. 44.

state is shown in Fig. 44. It can be seen that, for oblate shapes, three positive-parity bands are expected among the low-lying levels of Si^{29} , based on the $\Omega = \frac{1}{2}^+$ (No. 9), $\Omega = \frac{3}{2}^+$ (No. 8), and $\Omega = \frac{5}{2}^+$ (No. 11) Nilsson orbits.

Bromley *et al.* neglected the mixing of bands and assigned the five lowest levels of Si^{29} to the first two of these bands. Such a model is at variance with observed $l=2$ transitions to $\frac{3}{2}^+$ states, as can readily be seen as follows. The reduced width of the $\frac{3}{2}^+$ state arising from the $K = \frac{3}{2}$ (No. 8) band is

$$S = \frac{1}{2}c_{\frac{3}{2}}^2(\text{No. 8}),$$

where $c_{\frac{3}{2}}$ is the $d_{\frac{5}{2}}$ amplitude in the single-particle Nilsson function. The same expressions hold for the $\frac{3}{2}^+$ states arising from the No. 9 and No. 11 $K = \frac{1}{2}$ bands. For small deformations $c_{\frac{3}{2}}^2(\text{No. 8}) \approx 1$, $c_{\frac{3}{2}}^2(\text{No. 9}) \approx 0$, and $c_{\frac{3}{2}}^2(\text{No. 11}) \approx 1$. The prediction is therefore that two $l=2$ transitions with about one-half of the full single-particle strength will be observed to $\frac{3}{2}^+$ levels of Si^{29} . In fact, only one $d_{\frac{5}{2}}$ transition is seen (Ho53) and this has a full single-particle reduced width. We now show that the discrepancy stems from the unwarranted neglect of band mixing and disappears when the complete rotational Hamiltonian is used.

Pure rotational bands are obtained by neglecting a "Coriolis" term

$$-(\hbar/2g)(\mathbf{J} \cdot \mathbf{j}) \quad (\text{V.35})$$

in the rotational Hamiltonian (Ke56), where J is the total nuclear angular momentum and j is that of the intrinsic nucleon motion. The operator (V.35) connects states differing in K by 1, or two $K = \frac{1}{2}$ bands; for moderate deformations (of the kind encountered in calculations of nuclear energy levels) it has large off-diagonal matrix elements between states of rotational bands arising from the same shell-model orbits. In the case of Si^{29} , such strongly interacting states are encountered in the $K = \frac{1}{2}$ and $K = \frac{3}{2}$ bands based on Nilsson's orbits No. 11 and No. 8.

We therefore must carry out a calculation for Si^{29} based on the full rotational Hamiltonian described by Kerman (Ke56). The Hamiltonian matrix is set up and diagonalized in a representation spanned by the pure-

δ	θ^2
$3/2 + \frac{2.45}{2.45} .03$	$(5/2+) \frac{3.07}{2.43} .0002$
$5/2 + \frac{2.39}{2.39} .02$	$3/2 + \frac{2.43}{2.03} .0005$
$5/2 + \frac{1.75}{1.75} .12$	$5/2 + \frac{2.03}{1.28} .019$
$3/2 + \frac{0.65}{Si^{29}} .90$	$3/2 + \frac{1.28}{Si^{29}} .022$
$1/2 + \frac{.56}{Si^{29}} .56$	$1/2 + \frac{.56}{Si^{29}} .022$
Rotational Model	Observed (Ho53)

FIG. 45.

band states from Nilsson orbits No. 8, No. 9, and No. 11. The matrices encountered are 2×2 for $J = \frac{1}{2}^+$ and 3×3 for $J = \frac{3}{2}^+, \frac{5}{2}^+, \dots$. The calculation has two adjustable parameters, the deformation η and the moment of inertia δ ; we take the zero-order positions of the ground states of the interacting bands to be given by the rotational Hamiltonian and Nilsson's intrinsic eigenvalues. The energy levels and spectroscopic factors shown in Fig. 45 are obtained with a deformation $\eta = -2$ and a moment of inertia parameter $\hbar^2/2\delta = 0.35$ Mev suggested by the value (0.37) obtained from the excitation of the first 2^+ state in Si^{30} .

(1) No states in addition to the ones shown in Fig. 45 are predicted below 3.5 Mev; none of the higher states have $\delta > 0.05$. Thus agreement with the spins, order, and positions of positive-parity states of Si^{29} is fairly good. The general tendency of the predicted levels to crowd too closely together could be improved by using a rather larger value of $\hbar^2/2\delta$. Our results favor a spin of $\frac{5}{2}^+$ for the 3.07-Mev level.

(2) The calculated δ values are in satisfactory accord with the observed reduced widths. In particular, it is striking that interaction between bands results in all the observable $d_{\frac{5}{2}}$ reduced width being concentrated in the first excited state. The $d_{\frac{5}{2}}$ reduced width of the second excited state is found to be larger than predicted by much the same factor as was encountered in our shell-model discussion of this transition. A larger $1d_{\frac{5}{2}}$ reduced width could be obtained only by increasing the deformation and this would push the $\frac{3}{2}^+$ first excited state too close to the $\frac{1}{2}^+$ ground state.

(3) In using the rotational model to interpret the data on $Si^{28}(d,p)Si^{29}$, we must assume that Si^{28} and Si^{29} possess nearly equal equilibrium deformations. We have discussed this question in connection with $Al^{27}(d,n)Si^{28}$.

Detailed agreement could obviously be improved by minor adjustments in the parameters η and $\hbar^2/2\delta$. The significant points which have emerged are that a good over-all picture of both spectrum and reduced widths has been obtained with a reasonable choice of parameters and, of particular interest here, that agreement for the reduced widths cannot be obtained without taking correct account of the interaction between the two $1d_{\frac{5}{2}}$ bands.

Using the δ values given in Fig. 45 and the observed reduced widths (Ho53) of the ground and first excited

states of Si^{29} , we obtain

$$\theta_0^2(2s) \approx 0.04, \quad (V.36)$$

$$\theta_0^2(1d) \approx 0.021. \quad (V.37)$$

The $2s$ reduced width is sensitively dependent of the deformation, while the $1d$ reduced width is not. The value (V.37) of $\theta_0^2(1d)$ is consistent with (V.24), obtained from $Mg^{24}(d,p)Mg^{25}$, where the Q value is comparable.

$P^{31}(p,d)P^{30}$

The intrinsic configuration of the lowest bands in P^{30} may involve a mixture of $(\Omega = \frac{1}{2}^+)^2$ and $(\Omega = \frac{3}{2}^+)^2$, the two nucleons occupying Nilsson orbits No. 9 and No. 8, respectively. Each configuration gives rise to three bands, two with $T=0$ and one with $T=1$ ($K=0$); since we are dealing with an odd-odd nucleus, all six bands may be (in zero order) below 2 Mev (Br59). The bands arising from $(\Omega = \frac{1}{2}^+)^2$ and $(\Omega = \frac{3}{2}^+)^2$ interact with each other only through residual two-body forces since the Coriolis term (V.35) is a one-body operator. The fact that Nilsson orbits Nos. 9 and 8 lie very close in energy for small negative deformations, and our earlier conclusions concerning the Mg^{26} ground state (where conditions are less favorable for interaction), suggest that strong mixing may occur. The situation is clearly quite complicated. Accordingly, since the only available experiment (Be58) locates only two $l=0$ transitions to levels of P^{30} , (one of them to an unresolved doublet of levels near 0.7 Mev) and since little is known about the spins of low-lying levels of P^{30} , we do not give a detailed discussion of the $P^{31}(p,d)P^{30}$ data.

$P^{31}(d,p)P^{32}$

Experimental studies of levels in P^{32} up to 6.56 Mev (Da57) and of the ground-state doublet (Pa58) have been reported. No absolute cross-sections have been measured. We therefore depart from our usual order and discuss $l=1$ transitions first; from such considerations we obtain a rough normalization of the $l=0$ and $l=2$ reduced widths.

There are four basic $2p$ single-particle components (Fig. 46):

$$[\phi_0 \times 2p_{\frac{1}{2}}]_J, \quad J=1, 2^-; \quad [\phi_0 \times 2p_{\frac{3}{2}}]_J, \quad J=0, 1^-.$$

The fact that nine $l=1$ transitions are observed indi-

$$\phi_2 \xrightarrow{2.232} 5/2^+$$

$$\phi_1 \xrightarrow{1.265} 3/2^+$$

FIG. 46.

$$\phi_0 \xrightarrow{\text{P}^{31}} 1/2^+$$

cates fragmentation of these single-particle states. This fragmentation could be produced by interaction with such states as $[\phi_1 \times 1f_{\frac{3}{2}}]_{2^-}$, $[\phi_2 \times 1f_{\frac{7}{2}}]_{1,2^-}$, $[\phi_1 \times 2p_{\frac{1}{2}}]_{0,1^-}$, and $[\phi_2 \times 2p_{\frac{3}{2}}]_{1^-}$, independently of the detailed fashion in which $2s_{\frac{1}{2}}$ and $1d_{\frac{3}{2}}$ contributions are mixed in the P^{31} ground-state wave function. In particular, the fact that nine rather than four $l=1$ transitions are seen cannot be taken to imply that the P^{31} ground state involves large departures from jj coupling⁸⁶; we may be forced to invoke such departures in interpreting other data.

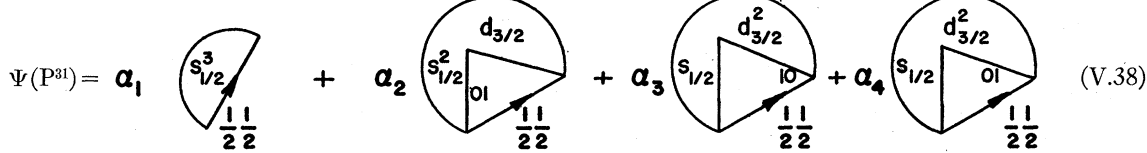
The two $1f_{\frac{7}{2}}$ components $[\phi_0 \times 1f_{\frac{7}{2}}]_J$, $J=3, 4^-$ have not been identified.

Let us now apply the sum rule (III.185) to the $l=1$ transitions. If C is the factor which normalizes the relative cross sections of Da57, we have

$$44C = 12\theta_0^2(2p).$$

Taking $\theta_0^2(2p)=0.027$, we obtain

$$C \approx 0.0074.$$



taking account of all $(\frac{1}{2}, \frac{1}{2})$ states of $s_{\frac{1}{2}}^3$, $s_{\frac{1}{2}}^2 d_{\frac{3}{2}}$, and $s_{\frac{1}{2}} d_{\frac{3}{2}}^2$.

We use the observed $l=0$ reduced widths to estimate the size of the amplitudes α_1 , α_2 , α_3 , and α_4 in (V.38) and hence the amount of core excitation in the ground state of P^{31} .

We take account of all states of $s_{\frac{1}{2}}^3 d_{\frac{3}{2}}$ and $s_{\frac{1}{2}}^2 d_{\frac{3}{2}}^2$ which can be reached by $l=0$ stripping from P^{31} ; such states have $T=1$ and $J=0$ or 1 . $s_{\frac{1}{2}}^3 d_{\frac{3}{2}}$ contains no $T=1$ states with $J=0$ and only one with $J=1$, the latter state being identified with the ground state of P^{32} . There are three $J=1$ states and one $J=0$ state with $T=1$ in $s_{\frac{1}{2}}^2 d_{\frac{3}{2}}^2$. Energy estimates based on the spectra of P^{30} , Cl^{34} , and S^{34} indicate that the $J=0$ state should be lowest. It is therefore likely that the 0.515-Mev level in P^{32} has $J=0^+$. We can then assign⁸⁸ states of $s_{\frac{1}{2}}^3 d_{\frac{3}{2}}$ and $s_{\frac{1}{2}}^2 d_{\frac{3}{2}}^2$ to observed levels of P^{32} in the following plausible fashion; the corresponding \mathcal{S} values, obtained with the aid of (III.65), (III.68), and the wave function (V.38) for the ground state of P^{31} , are given alongside:

$$P^{32}(0) : [(s_{\frac{1}{2}}^3)_{\frac{1}{2}} (1d_{\frac{3}{2}})]_{(TJ)=(11)} \\ \mathcal{S}(l=2) = \alpha_1^2, \quad \mathcal{S}(l=0) = \frac{2}{3} \alpha_2^2 \quad (V.39)$$

$$P^{32}(0.515) : [(s_{\frac{1}{2}}^2)_{10} (1d_{\frac{3}{2}})_{10}]_{(TJ)=(10)} \\ \mathcal{S}(l=0) = \frac{4}{3} \alpha_3^2 \quad (V.40)$$

⁸⁶ This point has been made by Pandya (Pa57a) in a rather different fashion.

⁸⁷ The analogous $1d_{\frac{3}{2}}$ transitions in $Al^{27}(d,p)Al^{28}$ give no such direct information because of competition with $1d_{\frac{5}{2}}$ contributions. The situation for $A=32$ is otherwise very similar to that for $A=28$.

⁸⁸ Similar assignments have been made by Pandya (Pa57a).

TABLE XV.

Excitation	J	$[J]\theta^2$	Reference
0	1^+	2	0.022
		0	0.0015
0.077	2^+	2	0.031
0.515		0	0.005
1.15		0	0.009
2.2		0	0.004
4.21		0	0.005

^a We assume that only one member of the doublet at 2.2 Mev has an $l=0$ angular distribution.

With this normalization, the reduced widths of $l=0$ and $l=2$ transitions in $P^{31}(d,p)P^{32}$ are then as given in Table XV.

The presence of $l=0$ transitions to low-lying levels of P^{32} is a clear⁸⁷ indication that the single-hole wave function $s_{\frac{1}{2}}^3$ is not an accurate representation of the P^{31} ground state. Let us write, in fact,

$$P^{32} \left\{ \begin{array}{l} 1.15 \\ 2.2 \\ 4.21 \end{array} \right\} : [(s_{\frac{1}{2}}^2)_{01} (d_{\frac{3}{2}}^2)_{10}]_{11} + [(s_{\frac{1}{2}}^2)_{10} (d_{\frac{3}{2}}^2)_{01}]_{11} \\ + [(s_{\frac{1}{2}}^2)_{01} (d_{\frac{3}{2}}^2)_{12}]_{11} \\ \sum \mathcal{S}(l=0) = \frac{2}{3} (\alpha_3^2 + \alpha_4^2). \quad (V.41)$$

From the appropriate measured reduced widths (Da57); (V.40) and (V.41) determine α_3^2 and α_4^2 ; the ratio of the $l=0$ and $l=2$ reduced widths in the ground-state transition (Pa58) yields α_2^2/α_1 through (V.39); since $\alpha_1^2 + \alpha_2^2$ is known from the normalization of (V.38), the squares of all amplitudes in (V.38) are now determined.

It remains to select suitable values of $\theta_0^2(2s)$ and $\theta_0^2(1d)$. The Q value for $P^{31}(d,p)P^{32}$ is close to that of $Si^{28}(d,p)Si^{29}$, where $\theta_0^2(1d)$ has been estimated rather reliably as 0.02. Since the corresponding value of $\theta_0^2(2s)$ is sensitive to the deformation assumed for Si^{29} in extracting it, we prefer to use the rather smaller value of 0.03 indicated by determinations of $\theta_0^2(2s)/\theta_0^2(1d)$ elsewhere in the ds shell. [See, for example, (V.17).] With

$$\theta_0^2(1d) \approx 0.02, \quad \theta_0^2(2s) \approx 0.03, \quad (V.42)$$

we find

$$\alpha_1^2 = 0.66, \quad \alpha_2^2 = 0.04, \quad \alpha_3^2 = 0.04, \quad \alpha_4^2 = 0.26. \quad (V.43)$$

Our treatment of the ground-state transition is the same, in principle, as the original one of Parkinson

(Pa58; see also Fr60). The fact that the preceding value of α_2^2 is considerably smaller than Parkinson's reflects our different assumptions concerning $\theta_0^2(1d)/\theta_0^2(2s)$ and the change of normalization implied by the presence of the third and fourth terms in (V.38).

A reasonable picture of the $P^{31}(d,p)P^{32}$ reduced widths has thus been obtained. In the process, it has been estimated that the P^{31} ground state is between 60 and 70% $s_{\frac{1}{2}}^{-1}$. This should be regarded as a rough estimate in view of the uncertainties introduced by our indirect normalization of the reduced widths of Da57 and by our assumed values of the single-particle reduced widths.

The rotational model has been applied with some success to P^{31} by Broude *et al.* (Br58), and P^{32} may also be an oblate nucleus. However, we do not discuss the rotational interpretation of the $P^{31}(d,p)P^{32}$ reduced widths because of the difficulty, described in connection with P^{30} , of dealing with the many bands at low excitation in an odd-odd nucleus.

$P^{31}(d,n)S^{32}$

If the P^{31} ground state were well described as a single-hole $s_{\frac{1}{2}}$ state and the S^{32} ground state as a closed shell, we would have $S=4$ for the $P^{31}(d,n)S^{32}$ ground-state reaction. The observed $l=0$ reduced width (Ca55) $\theta_0^2=0.006$, smaller by a factor of at least 10 than such an S value would demand, reveals the inadequacy of the preceding simple wave functions. We have already reached this conclusion from our analysis of $P^{31}(d,p)P^{32}$; it is also suggested by the fact that a second $l=0$ transition is observed (Ca55) to level(s) around 4 Mev in S^{32} .

The situation is very similar to that encountered in $Al^{27}(d,n)Si^{28}$; the arguments presented in detail there need not be repeated. Suffice it to say that with the wave function (V.38) and (V.42) for P^{31} , the observed diminution of the $P^{31}(d,n)S^{32}$ ground-state reduced width sets a rough lower limit of 40% on the amount of core excitation in S^{32} .

A more detailed consideration of the excited levels of S^{32} is not worthwhile since so little is known of their properties, particularly spins and parities.

$S^{32}(d,p)S^{33}; S^{32}(d,n)Cl^{33}$

The (d,p) and (d,n) reduced-width ratios (Ho53, Mi53) of the first two levels in S^{33} and Cl^{33} , respectively, are in marked disagreement. We regard the (d,p) data as more significant because the Q value of $S^{32}(d,n)Cl^{33}$ (0.84 Mev) is -0.746 Mev, so that the level in question is close to the proton separation energy.

Since no absolute cross sections have been measured, we confine ourselves to a brief qualitative discussion of the observed reduced widths. We start with the $l=1$ transitions.

$$\phi_2 \xrightarrow{3.78}$$

$$\phi_1 \xrightarrow{2.24} 2+$$

FIG. 47.

$$\phi_0 \xrightarrow{s^{32}} 0+$$

There are two basic $2p$ single-particle components (Fig. 47)

$$[\phi_0 \times 2p_{\frac{1}{2}}]_{\frac{1}{2}}, [\phi_1 \times 2p_{\frac{1}{2}}]_{\frac{1}{2}}.$$

Four $l=1$ transitions are, in fact, observed, the levels and reduced widths being as shown in Table XVI.

The only state of a weak-coupling representation based on S^{32} (see Sec. III.11) which could possibly interact significantly with $[\phi_0 \times 2p_{\frac{1}{2}}]$ is $[\phi_1 \times 1f_{7/2}]$. Similarly, only one state, namely, $[\phi_1 \times 2p_{\frac{1}{2}}]$, seems likely to interact strongly with $[\phi_0 \times 2p_{\frac{1}{2}}]$. We therefore suggest that the 4.2- and 4.9-Mev $l=1$ levels have $J=\frac{3}{2}^-$ and $\frac{1}{2}^-$, respectively. The values of $\sum[J]\theta^2$ for the $\frac{3}{2}^-$ and $\frac{1}{2}^-$ states are in the ratio $12.1/8.1 \approx 1.5$, compared with the predicted value of two.

A strong $l=3$ transition to a level near 2.8 Mev in S^{33} reveals the dominant $1f_{7/2}$ single-particle component. The reduced-width ratios imply

$$\theta_0^2(2p)/\theta_0^2(1f) \approx 1.7 \quad (V.44)$$

in good agreement with other estimates of this ratio.

We have already mentioned that the presence of an $l=0$ transition to the first excited state of S^{33} implies core excitation in S^{32} . Apart from this, the most significant point about the positive-parity transitions is the absence of observable $l=2$ transitions to $\frac{5}{2}^+$ states in S^{33} . In the first place, it indicates that we are justified in ignoring $1d_{\frac{5}{2}}$ excitations in S^{32} , and, by implication, in P^{31} also; secondly, since $2d_{\frac{5}{2}}$ contributions are at least as likely among low-lying $S^{32}(d,p)S^{33}$ transitions as in $Si^{28}(d,p)Si^{29}$, it suggests that $2d_{\frac{5}{2}}$ contributions to observed $d_{\frac{5}{2}}$ transitions in $Si^{28}(d,p)Si^{29}$ are too small to be of importance.

Region $33 \leq A \leq 38$

If the earlier part of the ds shell, with $A \leq 32$, we have seen that $1d$ and $2s$ configurations are strongly mixed; at the end of the shell, on the other hand, around $A=40$, the jj -coupling shell model seems to be quite successful. It is unfortunate that so little experimental information is available concerning the interesting transitional region. We would like to know whether low-lying levels of nuclei in this region can be adequately described as belonging to $1d_{\frac{5}{2}}^n$ and to what extent excitation of the $2s_{\frac{1}{2}}$ core is important. A related question concerns the equilibrium shapes of nuclei beyond Si^{28} . We have seen that nuclei from $A=28$ to

$A=31$ can be treated with some success in terms of a rotational model, assuming oblate equilibrium deformations. Further experimental study is needed to find out whether and, if so, to what extent the region of oblate nuclei extends beyond S^{32} .

$\text{Cl}^{35}(d,p)\text{Cl}^{36}$

The only available stripping experiment (Ki52) concerns the $\text{Cl}^{35}(d,p)\text{Cl}^{36}$ ground-state reaction, a mixture of $l=0$ and $l=2$. No absolute cross section is available.

This isolated piece of data does not, in fact, tell us much about the importance of core excitation in Cl^{35} . For the Cl^{36} ground state is expected to be mainly $(d_{\frac{3}{2}}^4)_{(TJ)=(12)}$ (the configuration $d_{\frac{3}{2}}^3$ containing only one such state); thus the small $l=0$ admixture in the ground-state angular distribution reveals a small component of $[(s_{\frac{1}{2}}^{-1})_{\frac{1}{2}}(d_{\frac{3}{2}}^4)_{12}]_{\frac{1}{2}}$ in the Cl^{35} ground-state wave function.

But this admixture is not the one most likely to contribute significantly to the Cl^{35} ground state. $[(s_{\frac{1}{2}}^{-1})_{\frac{1}{2}}(d_{\frac{3}{2}}^4)_{02}]_{\frac{1}{2}}$ is energetically more favorable and is not connected to the dominant component in the Cl^{36} ground state by transfer of a single nucleon. Furthermore, we cannot be sure that other kinds of excitation of the $2s$ shell can be ignored in Cl^{35} and Cl^{36} .

We conclude that much more experimental information is needed before we can say anything significant about the Cl^{35} and Cl^{36} wave functions. Probably the best way to study such matters would be to perform high-resolution $\text{Cl}^{35}(d,p)\text{Cl}^{36}$ and $\text{Cl}^{35}(\text{He}^3,d)\text{Ar}^{36}$ experiments. Points of interest raised by such investigations could then be further examined by suitably chosen experiments on S^{34} , Cl^{36} , and perhaps Ar^{36} .

VI. STRIPPING AND PICKUP REACTIONS ON HEAVIER NUCLEI ($A>40$)

Since there are few data concerning nuclei with $A>70$, this section concerns stripping widths in the region $40 \leq A < 70$. In our theoretical discussions we use the jj -coupling shell model and the weak-coupling formalism described in Sec. III.11.

$\text{K}^{39}(d,p)\text{K}^{40}$

Two experiments have been performed, at deuteron energies of 6 Mev (En59) and 8.9 Mev (Da59). The results of these two studies agree very well, within the limitations imposed by the lower energy resolution and

TABLE XVI.

Excitation (Mev)	J^π	l	Relative $[J]\theta^2$	Reference
3.22	$\frac{3}{2}^-$	1	10.5	Ho53
4.2	$(\frac{3}{2}^-)$	1	1.6	Ho53
4.9	$(\frac{1}{2}^-)$	1	0.8	Ho53
5.71	$\frac{1}{2}^-$	1	7.3	Ho53

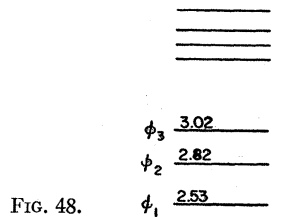
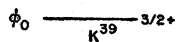


FIG. 48.



the lack of absolute cross sections in the 8.9-Mev experiment.

The strong $l=3$ transitions to the first four levels of K^{40} have already been discussed in detail as Example 3 of Sec. III.9. The four levels in question being, as we have seen, good single-particle $1f_{7/2}$ states, the absolute reduced widths of En59 yield

$$\theta_0^2(1f_{7/2}) \approx 0.010, \quad (\text{VI.1})$$

quite close to the values found in the ds shell ($\theta_0^2(1f_{7/2}) \approx 0.012$ [(V.3), (V.20), (V.32)]).

Some 30 $l=1$ transitions are observed to levels between 1.6 and 5 Mev in K^{40} . We discuss them in terms of the weak-coupling formalism, since $2p$ contributions to the K^{39} ground-state wave function are assuredly negligible.

There are six basic single-particle $2p$ components (see Fig. 48):

$$\begin{aligned} [\varphi_0 \times 2p_{\frac{1}{2}}], \quad J=0, 1, 2, 3^-; \\ [\varphi_0 \times 2p_{\frac{3}{2}}], \quad J=1, 2-. \end{aligned}$$

The experimental results indicate that these states are split into many fragments. Such a situation is not hard to understand qualitatively; on the reasonable assumption that some of the low-lying excited states of K^{39} have positive parity, we can clearly have many interacting states of the type $[\varphi_0 \times u_k]$, where $u_k = 1f_{7/2}, 2p_{\frac{1}{2}}$, or $2p_{\frac{3}{2}}$. The situation is too complex to attempt any detailed enumeration of the final-state interactions involved.

On summing over all $l=1$ levels, we have, using (III.185),

$$\sum [J]\theta^2 = 24\theta_0^2(2p).$$

The observed values of $[J]\theta^2$ (En59) yield $\sum [J]\theta^2 \approx 0.49$, whence

$$\theta_0^2(2p) \approx 0.021, \quad (\text{VI.2})$$

in reasonable agreement with ds -shell estimates.

Let us now say a few words about $2p_{\frac{1}{2}}$ and $2p_{\frac{3}{2}}$ components separately.

$2p_{\frac{1}{2}}$ Levels

The large $l=1$ reduced widths of levels at 2.042, 2.064, 2.099, and 2.622 Mev indicate the presence of major components of $[\varphi_0 \times 2p_{\frac{1}{2}}]$. The $[J]\theta^2$ values of these levels enable us to make the plausible spin assignments given in Table XVII.

 $2p_{\frac{1}{2}}$ Levels

We cannot say much about the detailed nature of the $2p_{\frac{1}{2}}$ levels. Apparently the degree of fragmentation of the $2p_{\frac{1}{2}}$ components is greater than that of the $2p_{\frac{3}{2}}$, which is not surprising in view of the higher excitation.

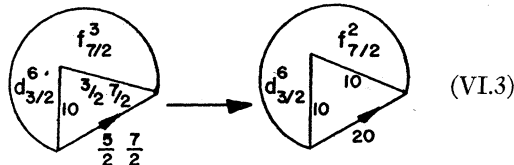
Three weak $l=0$ transitions are observed to levels of K^{40} between 3 and 4 Mev. Their significance is discussed later.

 $Ar^{40}(d,p)Ar^{41}$

The only available experiment (Bu56) gives no absolute cross sections. On using the ground-state peak cross section given in an early study (Gi52), a rough normalization can be obtained. The accuracy of the resulting absolute reduced widths is quite uncertain.

 $l=3$ Transitions

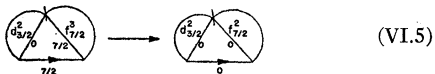
Only one $l=3$ transition is observed, connecting the ground states of Ar^{40} and Ar^{41} . We ignore core excitation and discuss this transition in terms of the jj -coupling shell model, taking the lowest state of each configuration compatible with the given total quantum numbers. The ground-state transition is then described by⁸⁹



the appropriate S value being $\frac{3}{4}$, from (III.65). The absolute ground-state reduced width (Bu56, Gi52) then leads to the reasonable estimate

$$\theta_0^2(1f_{7/2}) \approx 0.013. \quad (VI.4)$$

⁸⁹ As an academic point, we note that since the $d_{\frac{5}{2}}$ neutron shell is filled in both states, the reaction (VI.3) can be described more simply without the isotopic-spin formalism as



or (since the $d_{\frac{5}{2}}$ group has spin zero) more simply still as



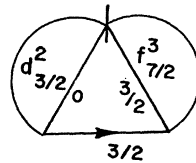
In situations such as this, to use the isotopic-spin formalism is to make things unnecessarily complicated.

TABLE XVII.

State of K^{40}	J^π	$[J]\theta^2(l=1)$	$\theta^2(l=1)$
2.042 Mev	3^-	0.086	0.012
2.064	2^-	0.078	0.016
2.099	1^-	0.053	0.018
2.622	0^-	0.018	0.018

 $l=1$ Transitions

The two basic $2p$ single-particle components are distributed among seven observed $l=1$ transitions. The large $[J]\theta^2$ value of the 1.39-Mev level in Ar^{41} indicates that it contains a large fragment of $[\varphi_0 \times 2p_{\frac{1}{2}}]$ and, accordingly, has spin $\frac{3}{2}$. The low-lying $l=1$ level at 0.57 Mev must also contain a component of the $2p_{\frac{1}{2}}$ single-particle state (and hence must also have spin $\frac{3}{2}$), probably arising from an interaction between



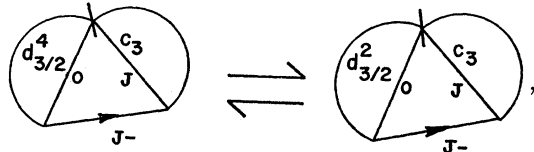
and $[\varphi_0 \times 2p_{\frac{1}{2}}]$.

On applying the sum rule (III.185), we find $\theta_0^2(2p) \approx 0.035$. If we use (VI.4) to express $\theta_0^2(2p)$ in units of $\theta_0^2(1f)$ (thereby avoiding any reference to our doubtful indirect normalization of the reduced widths of Bu56), we have

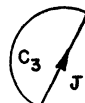
$$\theta_0^2(2p)/\theta_0^2(1f) \approx 2.6. \quad (VI.6)$$

This value of the ratio of single-particle reduced widths is to be compared with 2.1 from $K^{39}(d,p)K^{40}$ [(VI.1) and VI.2)] and 1.7 from the (d,p) experiments on Ca [(VI.7) and (VI.8)].

In view of the correspondence

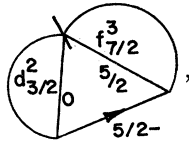


where



is some state of three particles in the $1f-2p$ shell, we expect a qualitative similarity between the positions and reduced widths of low-lying levels in Ca^{43} and Ar^{41} . This expectation is clearly borne out by the results of available $Ca^{42}(d,p)Ca^{43}$ (Bo57) and $Ar^{40}(d,p)Ar^{41}$ (Bu56) experiments; the similarity even seems to extend to two weak positive-parity levels found at nearly the same excitations in Ca^{43} and Ar^{41} . The main difference is that many levels are known below 4 Mev in Ca^{43} which show no stripping from Ca^{42} , while no analogous levels

have been found in Ar^{41} . In particular, no low-lying $\frac{5}{2}^-$ level of Ar^{41} of the form



corresponding to the first excited state of Ca^{43} , has yet been observed. Most of these apparent differences probably stem from the lower resolution in the only available $\text{Ar}^{40}(d,p)\text{Ar}^{41}$ experiment (Bu56).

Low-lying positive-parity transitions in $\text{Ar}^{40}(d,p)\text{Ar}^{41}$ are discussed later.

$\text{Ca}^{40}(d,p)\text{Ca}^{41}$; $\text{Ca}^{42}(d,p)\text{Ca}^{43}$; $\text{Ca}^{44}(d,p)\text{Ca}^{45}$

(d,p) experiments on Ca^{40} (Bo57a), Ca^{42} (Bo57), and Ca^{44} (Co57), have been performed with 7-Mev deuterons. The cross sections are given in the same relative units. The reduced widths extracted from the data obtained in these three experiments can be normalized with the help of an earlier study (Ho53) with 8-Mev deuterons.

We find it convenient to discuss the three Ca experiments simultaneously. Many aspects of these reactions have been discussed by French and Raz⁶⁰ (Fr56), whose main interest was in using the (d,p) results to study certain matrix elements of the effective two-nucleon interaction. We are not concerned with that topic here.

The ground-state $l=3$ transitions have already been discussed in Example 5 of Sec. III.9. The ratios of the three ground-state reduced widths agree well with the jj -coupling predictions. The absolute reduced widths indicate

$$\theta_0^2(1f) \approx 0.013, \quad (\text{VI.7})$$

in good agreement with other estimates.

Stripping to the low-lying $\frac{5}{2}^-$ state at 0.373 Mev in Ca^{43} and to a similar state (probably at 0.176 Mev) in Ca^{45} can only involve $1f_{\frac{5}{2}}$, by conservation of angular momentum. Since the main $1f_{\frac{5}{2}}$ components appear at 6 Mev or higher (Cl59), transfer of a $1f_{\frac{5}{2}}$ nucleon at such an excitation is strongly unfavored. The fact that no stripping is observed (Bo57, Co57) suggests that jj coupling is a reasonable approximation. The foregoing considerations have no bearing on the possibility of core excitation.

In considering $l=1$ transitions, we use the weak-coupling formalism of Sec. III.11, on the assumption that $2p_{\frac{1}{2}}$ and $2p_{\frac{3}{2}}$ do not contribute significantly to the ground states of the even- A Ca isotopes. Let us first separate $2p_{\frac{1}{2}}$ from $2p_{\frac{3}{2}}$. To do this, we note that $2p_{\frac{1}{2}}$ levels are expected to lie above $2p_{\frac{3}{2}}$ levels and that the total $2p_{\frac{1}{2}}$ intensity ($\sum [J]\theta^2$) should be twice that of $2p_{\frac{3}{2}}$.

The results of the most plausible such separation are given in Table XVIII. The values of $\theta_0^2(p)$ obtained by

TABLE XVIII.

Orbit	Excitation of state	$[J]\theta^2$	$\theta_0^2(2p)$
$\text{Ca}^{40}(d,p)\text{Ca}^{41}$			
$2p_{\frac{1}{2}}$	1.947	0.080	0.026
	2.469	0.027	
$2p_{\frac{3}{2}}$	2.967	0.002	
	3.619	0.005	
	3.736	0.003	0.021
	3.950	0.032	
$\text{Ca}^{42}(d,p)\text{Ca}^{43}$			
$2p_{\frac{1}{2}}$	0.593	0.005	0.021
	2.048	0.080	
$2p_{\frac{3}{2}}$	2.607	0.008	
	2.880	0.005	
	2.947	0.005	0.012
	3.584	0.005	
$\text{Ca}^{44}(d,p)\text{Ca}^{45}$			
$2p_{\frac{1}{2}}$	1.432	0.011	
	1.902	0.054	0.019
	2.249	0.009	
$2p_{\frac{3}{2}}$	2.844	0.009	
	3.244	0.004	
	3.419	0.018	0.016

applying the sum rule (III.185) to each set of $2p_{\frac{1}{2}}$ and $2p_{\frac{3}{2}}$ transitions constitute a test of the consistency of our interpretation.

Several remarks should be made concerning this table.

(1) The identification of the 2.47-Mev level in Ca^{41} as single-particle $2p_{\frac{1}{2}}$ is strongly unfavored. Apart from upsetting the relative amounts of $[\varphi_0 \times 2p_{\frac{1}{2}}]$ and $[\varphi_0 \times 2p_{\frac{3}{2}}]$, such an interpretation would demand an equal division of $[\varphi_0 \times 2p_{\frac{1}{2}}]$ between levels 1.5 Mev apart.

(2) $\theta_0^2(2p_{\frac{1}{2}}) < \theta_0^2(2p_{\frac{3}{2}})$, especially in $\text{Ca}^{42}(d,p)\text{Ca}^{43}$. It is probable that this difference is due to the existence of $2p_{\frac{1}{2}}$ levels above the excitation reached in the relevant experiments.

(3) It should be stressed that Table XVIII lists only those $\frac{3}{2}^-$ and $\frac{1}{2}^-$ states which have observable $l=1$ reduced widths. There are many levels below 4 Mev in the odd- A Ca isotopes which show no stripping and of these there must surely be some with spin $\frac{3}{2}^-$, some with spin $\frac{1}{2}^-$.

(4) In both Ca^{43} and Ca^{45} the lowest $l=1$ level is weak, arising mainly from $(f_{7/2})_{\frac{3}{2}^-}, (f_{7/2})_{\frac{5}{2}^-}$.

The values of $\theta_0^2(2p)$ determined in Table XVIII cluster around the value

$$\theta_0^2(2p) \approx 0.022, \quad (\text{VI.8})$$

excluding the $2p_{\frac{1}{2}}$ levels in Ca^{43} and Ca^{45} [see (2)].

Strong $l=2$ transitions to levels at 4.76 and 5.72 Mev (Ho53) indicate large single-particle $2d_{\frac{5}{2}}$ contributions. Such an interpretation is supported by the gross-structure studies of Schiffer and Lee (Sc59), who find that, in the region $49 \leq A \leq 66$, $2d_{\frac{5}{2}}$ levels lie 1 to 2 Mev above $2p_{\frac{3}{2}}$. The usual sum rule (III.185) then gives

$$\theta_0^2(2d_{\frac{5}{2}}) \geq 0.016. \quad (\text{VI.9})$$

⁶⁰ See Fr56, particularly Table I.

No single-particle $1f_{\frac{1}{2}}$ or $1g_{\frac{9}{2}}$ components have been reported in (d,p) studies of the Ca isotopes. It is now almost certain, from a study of the structure of Sc⁴¹ by $\text{Ca}^{40}(p,p)\text{Ca}^{40}$ (Cl59), that such components lie above the range of excitations studied, around 6 Mev.

Core Excitation in the Region $A \sim 40$

In the (d,p) reactions on K³⁹, Ar⁴⁰, Ca⁴⁰, Ca⁴², and Ca⁴⁴, weak $l=0$ and $l=2$ transitions are observed to low-lying levels of the residual nuclei. Detailed discussion of these transitions in terms of minor components in the target ground state is more difficult than for $A \sim 30$ because of the greater likelihood of coherent $1d$ and $2d$, $2s$ and $3s$ contributions and because of uncertainty concerning the relevant single-particle reduced widths. We therefore confine ourselves to a brief qualitative discussion.

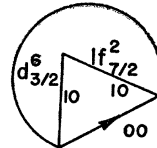
Let us start with the $l=0$ transitions. Even if these were to arise only from excitations of the $2s$ shell, the amount of $2s$ core excitation implied by the observed reduced widths would be less than 10%. Since possible $3s$ contributions are coherent with $2s$, it is possible that the actual amount of core excitation is considerably smaller.

Since no $l=2$ transitions have been identified in

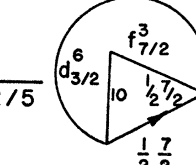
K³⁹(d,p)K⁴⁰, we discuss the similar cases of Ar⁴¹ and the odd- A Ca isotopes. Here the situation is quite different. If core excitation is responsible for the observed transitions it must involve $1d_{\frac{3}{2}}$; the amount of core excitation implied by the measured reduced widths is between 10 and 20%. $2d_{\frac{5}{2}}$ contributions, coherent with $1d_{\frac{3}{2}}$, are probably of little importance. Such an interpretation implies $J=\frac{3}{2}^+$ for the low-lying positive-parity levels in question. If, on the other hand, we are dealing with low-lying fragments of $[\varphi_0 \times 2d_{\frac{5}{2}}]$, the correct spin assignment is $J=\frac{5}{2}^+$. But the $2d_{\frac{5}{2}}$ single-particle component must certainly be small, so that core excitation must predominate. Since $J=\frac{5}{2}^+$ is strongly unfavored for low-lying core-excited levels in Ar⁴¹, Ca⁴¹, or Ca⁴³, we conclude that the probable spin is $\frac{3}{2}^+$.

Sizeable amounts of $1d_{\frac{3}{2}}$ and $2s_{\frac{1}{2}}$ core excitation in the ground states of the Ar and Ca isotopes may have surprisingly little effect on the $2p$ and $1f$ reduced widths. This is obvious in the case of $2p$; for $1f$, it is a consequence of the fact that $1d_{\frac{3}{2}}$ and $2s_{\frac{1}{2}}$ nucleons are promoted in pairs. The essential point here is that the δ values of $f_{7/2}^{2n+1} \rightarrow f_{7/2}^{2n}$ and $f_{7/2}^{2n-1} \rightarrow f_{7/2}^{2n-2}$ differ only by $\frac{1}{4}$ [see (III.150)]. For example, if we replace the simple ground-state wave functions of Ca⁴⁰ and Ca⁴¹ by

$$\Psi(\text{Ca}^{40}) = \sqrt{\frac{3}{5}} \begin{array}{c} d_{3/2}^8 \\ \diagdown \quad \diagup \\ 00 \end{array} + \sqrt{\frac{2}{5}} \begin{array}{c} f_{7/2}^2 \\ \diagdown \quad \diagup \\ 10 \quad 10 \\ \diagdown \quad \diagup \\ 00 \end{array}$$



$$\Psi(\text{Ca}^{41}) = \sqrt{\frac{3}{5}} \begin{array}{c} d_{3/2}^8 \\ \diagdown \quad \diagup \\ 00 \\ \diagdown \quad \diagup \\ \frac{1}{2} \quad \frac{7}{2} \end{array} + \sqrt{\frac{2}{5}} \begin{array}{c} f_{7/2}^3 \\ \diagdown \quad \diagup \\ 10 \quad \frac{1}{2} \quad \frac{7}{2} \\ \diagdown \quad \diagup \\ \frac{1}{2} \quad \frac{7}{2} \end{array}$$



and

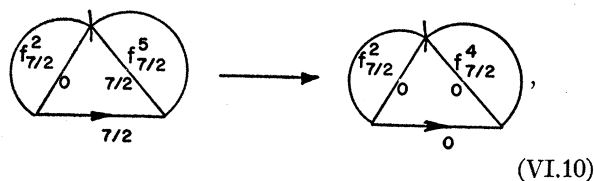
involving 40% excitation of the $1d_{\frac{3}{2}}$ shell, we have $\delta=0.90$. In other words, 40% core excitation changes δ only from 1 to 0.9, assuming that the phases cooperate in the desired way.

Ti⁴⁶(d,p)Ti⁴⁷

Preliminary results of an experiment by Rietjens and Bilaniuk (Ri60) with 7.8-Mev deuterons reveal one $l=3$ transition, proceeding to the first excited state of Ti⁴⁷, and five $l=1$ transitions to levels of Ti⁴⁷ between 1.56 and 3.31 Mev (see Fig. 49).

The reaction to the ground state of Ti⁴⁷, whose spin is known to be $\frac{5}{2}^-$, shows no stripping. From the jj -coupling viewpoint, this is to be expected since the transition must involve a $1f_{\frac{1}{2}}$ nucleon and is therefore j -forbidden.

If we use the jj -coupling approximation and treat neutrons and protons separately, the transition to the $\frac{7}{2}^-$ first excited state of Ti⁴⁷ is described⁹¹ by



⁹¹ On using the isotopic-spin formalism and assuming that symplectic symmetry σ is a good quantum number, the transition in question becomes

$(f_{7/2}^7)TJ=\frac{3}{2} \frac{7}{2}$, $\sigma=(1000) \rightarrow (f_{7/2}^6)T_0J_0=00$, $\sigma_0=(0000)$, the δ value being $\frac{1}{2}$, exactly as before. A similar comment holds for Ti⁴⁸(d,p)Ti⁴⁹(g.s.).

with $S=\frac{1}{2}$. Although no absolute cross sections are available, Rietjens and Bilaniuk (Ri60) have also studied $\text{Ti}^{48}(d,p)\text{Ti}^{49}$, measuring the cross sections for Ti^{47} and Ti^{49} in the same relative units. They find, for the ratio of the $f_{7/2}$ reduced widths,

$$\theta^{2*}(\text{Ti}^{47}, 0.16 \text{ Mev})/\theta_g^2(\text{Ti}^{49}) = 2.2 \pm 0.7. \quad (\text{VI.11})$$

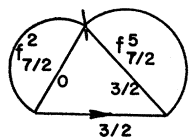
On representing the $\text{Ti}^{48}(d,p)\text{Ti}^{49}$ ground-state transition by the appropriate modification of (VI.10), we obtain $S_g(\text{Ti}^{49}) = \frac{1}{4}$ and, accordingly,

$$S^*(\text{Ti}^{47}, 0.16 \text{ Mev})/S_g(\text{Ti}^{49}) = 2,$$

in agreement with (VI.11).

The lowest $l=1$ level, at 1.56 Mev, undoubtedly contains a large fragment of the $2p_{\frac{1}{2}}$ single-particle state $[\varphi_0 \times 2p_{\frac{1}{2}}]$, its spin being, therefore, $\frac{3}{2}-$. It is likely that the nearby 1.80-Mev level also contains a $2p_{\frac{1}{2}}$ contribution. With these exceptions, we cannot separate $2p_{\frac{1}{2}}$ and $2p_{\frac{3}{2}}$ among the observed $l=1$ transitions; it is, in fact, doubtful that all $2p$ contributions have been accounted for. Levels with large cross sections at $\theta_{\text{Lab}}=20^\circ$ are found at 3.60 and 3.71 Mev in Ti^{47} , either or both of which may have an $l=1$ stripping pattern.

The 0.55-Mev, level probably has spin $\frac{3}{2}-$, belonging predominantly to



The fact that no stripping is observed indicates a negligible interaction with $[\varphi_0 \times 2p_{\frac{1}{2}}]$, in contrast with analogous levels in Ca^{43} and Ca^{45} .

$\text{Ti}^{48}(d,p)\text{Ti}^{49}$

There are two relevant experiments. Preliminary results of the first of these (Ri60) are indicated in Fig. 50(a). The second is a study (Sc59) of gross structure in the proton spectra from $\text{Ti}^{48}(d,p)$, with energy resolution poorer than the average spacing of levels in this mass region. The purpose of this work is to locate

FIG. 49.

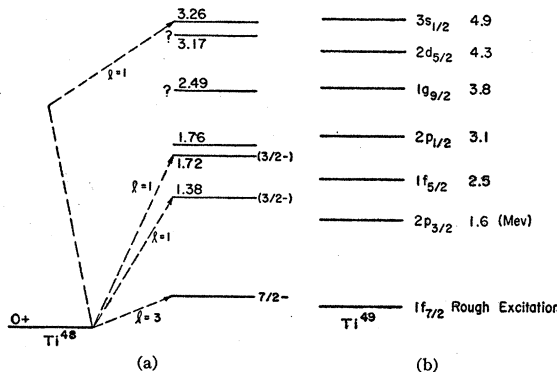
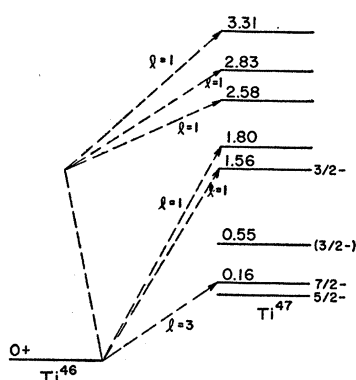


FIG. 50.

single-particle levels in the residual nucleus, the low resolution having the effect of reassembling the various fragments of the basic single-particle states. No absolute cross sections are available.

We have already discussed the $l=3$ ground-state transition in comparing $1f_{7/2}$ reduced widths in Ti^{47} and Ti^{49} . Let us therefore proceed to discuss the higher single-particle levels. The rough positions of single-particle levels in Ti^{49} found by Schiffer *et al.* are shown in Fig. 50(b).

The results of Rietjens and Bilaniuk are consistent with these findings. The $l=1$ transitions to levels at 1.38 and 1.72 Mev clearly⁹² involve the major portion of the $2p_{\frac{1}{2}}$ level $[\varphi_0(\text{Ti}^{48}) \times 2p_{\frac{1}{2}}]$. On using the sum rule (III.185) and the fact that $S_g(\text{Ti}^{49}) = \frac{1}{4}$, the observed reduced widths of the first three observed states of Ti^{49} lead to

$$\theta^{2*}(2p)/\theta_g^2(1f) \approx 1.3, \quad (\text{VI.12})$$

rather smaller than the value 1.7 implied by (VI.7) and (VI.8). The findings of Schiffer *et al.* suggest that the 2.49-Mev level in Ti^{49} is single-particle $1f_{\frac{5}{2}}$; no angular distribution is available for this level at the time of writing, but the cross section at $\theta_{\text{Lab}}=20^\circ$ is consistent with the foregoing interpretation. The 3.26-Mev level involves a large fragment of $[\varphi_0 \times 2p_{\frac{1}{2}}]$, and the nearby 3.17-Mev level may do so as well.

The level density of known levels of Ti^{47} and Ti^{49} up to about 3 Mev is markedly lower than in Ca^{41} , Ca^{43} , Ca^{45} . It is likely that other levels, which show no stripping from Ti^{46} and Ti^{48} , actually exist in the relevant parts of the spectra of Ti^{47} and Ti^{49} .

$\text{Ca}^{48}(d,p)\text{Ca}^{49}$

Angular-distribution measurements (Bu54) show that the reactions to the first two states of Ca^{49} have $l=1$ (see Fig. 51). The levels in question being, undoubtedly, single-particle $2p_{\frac{1}{2}}$ and $2p_{\frac{3}{2}}$, the absolute cross sections

⁹² In an experimental study of the circular polarization of γ rays following the capture of polarized neutrons by Ti^{48} , Trumppy (Tr57) assigned a spin of $\frac{1}{2}$ to the 1.72-Mev level in Ti^{49} . Since the measurements involved in the polarization experiment are very delicate, we prefer the spin-assignment of $\frac{3}{2}-$, which is definitely favored by the stripping data.

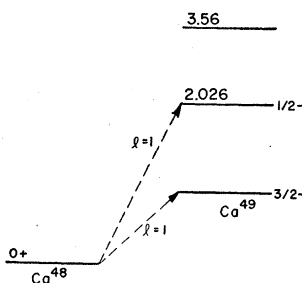


FIG. 51.

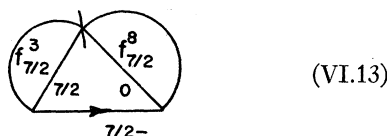
of the corresponding transitions would provide a reliable determination of $\theta_0^2(2p)$ in this mass region. No cross sections, relative or absolute, are available.

The $1f_{\frac{1}{2}}$ single-particle level is no lower than 3.56 Mev in Ca⁴⁹. This is to be contrasted with the situation in Ti⁴⁹, where the $1f_{\frac{1}{2}}$ level seems to lie below $2p_{\frac{1}{2}}$, and bears a close resemblance to what is found in Ca⁴¹. It is clear that the filling of $1f_{7/2}$ proton shell has a profound influence on the $1f_{\frac{1}{2}}$ neutron levels. Further experimental information, in particular a determination of the position of $1f_{\frac{1}{2}}$ levels in Ca⁴¹, Ca⁴³, Ca⁴⁵, Ca⁴⁷, and Ti⁴⁷, is needed to shed light on this matter.

$$V^{51}(d,p)V^{52}$$

Three experiments have been performed, two (El58, Da60a) with moderate energy-resolution for levels up to 2.8 Mev in V⁵², the other (Sc59) a "gross structure" study with low resolution. The two moderate-resolution experiments are in good agreement.

The V⁵¹ ground state is expected to be predominantly



with a complete shell of $f_{7/2}$ neutrons. Thus, $V^{51}(d,p)V^{52}$ should involve $2p_{\frac{1}{2}}$, $2p_{\frac{3}{2}}$, $1f_{\frac{1}{2}}$, ... single-particle levels and their fragments. Let us consider $l=1$ levels first. There are four basic $2p_{\frac{1}{2}}$ components, $[\varphi_0 \times 2p_{\frac{1}{2}}]J = 2, 3, 4, 5^+$, and two basic $2p_{\frac{3}{2}}$ components $[\varphi_0 \times 2p_{\frac{3}{2}}]J = 3, 4^+$. If the main $2p_{\frac{1}{2}}$ and $2p_{\frac{3}{2}}$ components do not overlap, we can separate them in the usual way with the aid of the relation⁹³

$$\sum [J]\theta^2(2p) = 2 \sum [J]\theta^2(2p)$$

obtained from (III.185).

Experimental information concerning $l=1$ levels in V⁵² is summarized in Fig. 52. The reduced widths $[J]\theta^2$ of the various proton groups resolved in El58 (taken from Table I) are exhibited graphically to the right. Proton groups which are known (Sc52) to correspond to more than one level in V⁵² are indicated by a vertical bar (—|). On the left, the positions of the $2p_{\frac{1}{2}}$ and $2p_{\frac{3}{2}}$ single-particle levels, found in the work of Schiffer *et al.*

(Sc59) are given. It is clear that the two sets of results are consistent with each other.

The foregoing interpretation of the $2p$ levels assumes that the lower $l=1$ transitions (below 1 Mev) involve predominantly $2p_{\frac{1}{2}}$ nucleons, those above 1.4 Mev involving $2p_{\frac{3}{2}}$. This assumption is suggested by the "break" between 0.9 and 1.4 Mev in the sequence of $l=1$ levels and receives support from the good agreement between the observed ratio

$$\sum_{\text{Exc. } < 1 \text{ Mev}} [J]\theta^2(l=1) / \sum_{\text{Exc. } > 1 \text{ Mev}} [J]\theta^2(l=1) = 2.5,$$

and the statistical ratio of two.

The fractions of the total $2p_{\frac{1}{2}}$ contribution

$$\sum [J]\theta^2(2p_{\frac{1}{2}})$$

belonging to levels with $J=2, 3, 4$, and 5^+ , are $\frac{5}{32}$, $\frac{7}{32}$, $\frac{9}{32}$, and $\frac{1}{32}$, respectively. The ground state of V⁵² possesses almost 0.6 of the observed (El58) total value of $\sum [J]\theta^2$ for $l=1$ levels below 1 Mev, suggesting a large ground-state spin. On the other hand, the β^- decay V⁵² → Cr⁵² is allowed and proceeds entirely to the 2^+ excited state of Cr⁵², so that the spin of the V⁵² ground state must be either 2^+ or 3^+ . The difficulty would be resolved if the ground state of V⁵² were a close doublet, probably consisting of a 3^+ ground state and a 5^+ first excited state. Such a doublet would contain $18/32 \approx 0.56$ of the total $2p_{\frac{1}{2}}$ contribution.

On using the absolute cross sections of Da60a and the sum rule (III.185), we have

$$\theta_0^2(2p) \approx 0.019, \quad (\text{VI.14})$$

in good agreement with earlier estimates.

There is a definite break in the succession of strong stripping transitions between 2.307 and 2.8 Mev in V⁵². Dalton *et al.* (Da60a) then find five more strong stripping transitions to levels up to 4.43 Mev in V⁵². It is impossible to decide on the basis of the simple Butler theory whether the appropriate l value for these transitions is 1 or 2. All that is known about the systematics of single-particle levels and single-particle reduced widths in this mass region conclusively indicates $l=2$; we have assumed this to be the correct assignment in the foregoing discussion.

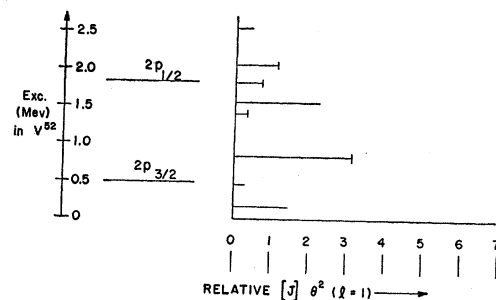


FIG. 52.

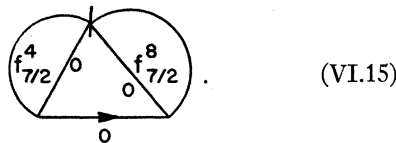
⁹³ True independently of the ground-state target spin.

Similar difficulties in distinguishing adjacent l values are encountered in (d,p) experiments on the Ca isotopes (Bo57, Bo57a, Co57) and in $\text{Cr}^{52}(d,p)\text{Cr}^{53}$ (El58b) where the transition to the 2.31-Mev level may have either $l=1$ or $l=2$. The difficulty may stem from the fact that each of the experiments in question was performed at deuteron energies of 6 to 9 Mev, very close to the height of the Coulomb barrier (6 to 7 Mev) in this mass region. This point is also raised in Secs. II.4 and VII.

No $1f_{\frac{5}{2}}$ level was found in the low-resolution $\text{V}^{51}(d,p)-\text{V}^{52}$ work of Schiffer *et al.* (Sc59). This is not surprising since $1f_{\frac{5}{2}}$ components are expected, in this region to lie close to the main $2p$ contributions, in which case $l=1$ would probably swamp $l=3$. El-Bedewi and Tadros (El58) find large $l=3$ admixtures in groups of levels near 1.8 and 2.1 Mev in V^{52} . It is certain that sizeable $1f_{\frac{5}{2}}$ contributions have as yet escaped detection.

$\text{Cr}^{52}(d,p)\text{Cr}^{53}$

The ground state of Cr^{52} [Fig. 53(a)] should be adequately represented by the wave function



The fact that the $1f_{7/2}$ neutron shell is fully occupied, while the $2p$ and $1f_{\frac{5}{2}}$ shells are empty, permits the use of the weak-coupling formalism of Sec. III.11 in discussing $l=1$ and $l=3$ levels in Cr^{53} . We consider $l=1$ transitions first.

There is no doubt that the ground state of Cr^{53} contains a large fragment of the $2p_{\frac{3}{2}}$ single-particle state $[\varphi_0 \times 2p_{\frac{3}{2}}]$ [Fig. 53(b)]. The experimental stripping data (El58b) then present us with the puzzling phenomenon of two $l=1$ transitions, to levels 1.74 Mev apart, each with roughly the intensity relative to the ground state to be expected of a full single-particle $2p_{\frac{3}{2}}$ transition. We examine three possible interpretations of this situation.

(1) It has usually been assumed (Nu56, El58b) that the spin of the 0.57-Mev level of Cr^{53} is $\frac{1}{2}-$, the corresponding $l=1$ transition involving $2p_{\frac{3}{2}}$. If the transition to the 2.31-Mev level has been correctly assigned $l=1$,⁹⁴ it must surely proceed through $2p_{\frac{3}{2}}$ also. The presence of two approximately equal fragments of $[\varphi_0 \times 2p_{\frac{3}{2}}]$ 1.74 Mev apart then demands the existence of a $\frac{1}{2}-$ state (possibly $[\varphi_1 \times 2p_{\frac{3}{2}}]$) nearly degenerate with $[\varphi_0 \times 2p_{\frac{3}{2}}]$, and an implausibly large interaction matrix element of close to 1 Mev. A further objection to the present interpretation is that it implies

$$\sum[J]\theta^2(2p_{\frac{3}{2}}) \approx 0.85 \sum[J]\theta^2(2p_{\frac{3}{2}}),$$

⁹⁴ We later discuss the possibility that the $l=1$ assignment is incorrect.

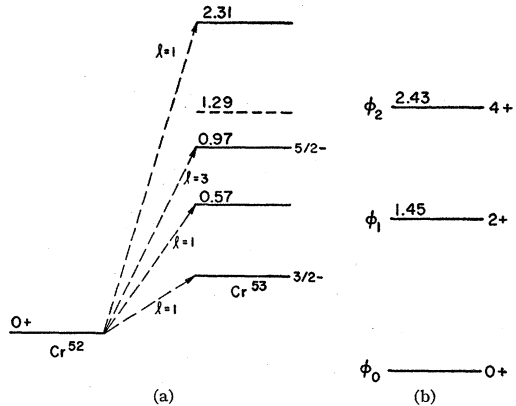


FIG. 53.

in serious disagreement with the expected statistical ratio of two.

(2) Another possibility is that the two lowest $l=1$ levels, at 0 and 0.57 Mev in Cr^{53} , have spin $\frac{3}{2}-$ while that at 2.31 Mev has spin $\frac{1}{2}-$. At first sight, this suggestion is rather attractive. It implies

$$\sum[J]\theta^2(2p_{\frac{3}{2}}) \approx 2.3 \sum[J]\theta^2(2p_{\frac{3}{2}}),$$

satisfactorily close to the statistical ratio of two; furthermore, the two fragments of $[\varphi_0 \times 2p_{\frac{3}{2}}]$ do not appear to be unreasonably far apart.

The observed (El58b) $l=1$ reduced widths of the ground and 0.57-Mev levels of Cr^{53} then demand the existence of a $\frac{3}{2}-$ state only 180 kev above $[\varphi_0 \times 2p_{\frac{3}{2}}]$ and connected to it by a moderately large interaction matrix element of 270 kev. The only reasonable possibility for such a state is $[\varphi_1 \times 2p_{\frac{3}{2}}]$. A calculation of the energy of this state relative to $[\varphi_0 \times 2p_{\frac{3}{2}}]$, describing φ_0 and φ_1 by the appropriate states of the neutron configuration $f_{7/2}^4$ and choosing an effective two-body interaction consistent with certain features of the spectra and stripping widths of nuclei near $A=40$ (Pa57a), places it nearly 2 Mev above $[\varphi_0 \times 2p_{\frac{3}{2}}]$. The effective interaction appropriate to this mass region is not well understood and our detailed prediction correspondingly uncertain.⁹⁵ Nevertheless, it is very hard to produce a reasonable interaction which depresses $[\varphi_1 \times 2p_{\frac{3}{2}}]$ even to within 1 Mev of $[\varphi_0 \times 2p_{\frac{3}{2}}]$; the difficulty of reducing the separation to the desired

⁹⁵ In discussing some projection theorems relating the level structures of nuclei in the vicinity of $A=60$, Lawson and Uretsky (La57) identify the 0.57-, 1.29-, and 2.31-Mev levels as the $\frac{3}{2}+$, $\frac{7}{2}+$, and $\frac{1}{2}-$ members, respectively, of the group $[\varphi_1 \times 2p_{\frac{3}{2}}]$, $J=\frac{3}{2}, \frac{5}{2}, \frac{7}{2}, \frac{1}{2}$, predicting that the missing $\frac{5}{2}-$ state should be around 1.8 Mev. Apart from the difficulty (discussed before) of producing a low-lying $\frac{5}{2}-$ state, these assignments are open to the objections that they do not account for the $l=1$ reduced widths of the 0.57- and 2.31-Mev levels (they imply a zero reduced width in each case) and that the 2.31-Mev level, if indeed its parity is negative, must surely involve $2p_{\frac{3}{2}}$. However, the theorems used by Lawson and Uretsky, in particular their "center-of-gravity theorem," are of a very general nature. If the foregoing detailed assignments are incorrect, we would expect to find levels of Cr^{53} , as yet undetected, below 2.5 Mev, to which the theorems in question apply.

value of 180 kev is sufficiently extreme to constitute a serious objection to the present interpretation of the Cr⁵³ reduced widths.

(3) The angular distribution of the 2.31-Mev level in Cr⁵³ is not reproduced very well by Elwyn and Shull's (El58b) Butler curve with $l=1$ and $r_0=5.6$ f; almost as good a fit is obtained with $l=2$ and the larger, but reasonable, radius of 7 f. On the basis of the angular distribution alone, $l=1$ is more likely but $l=2$ cannot be definitely excluded.

We therefore have a third possible interpretation of the Cr⁵³ results, according to which the ground, 0.57-, and 2.31-Mev levels are single-particle $2p_{\frac{1}{2}}$, $2p_{\frac{3}{2}}$, and $2d_{\frac{5}{2}}$ states, respectively. The observed reduced widths (El58b) lend support to such an interpretation. The values of $[J]\theta^2$ for the ground and 0.57-Mev states of Cr⁵³ are in the ratio 1.9, agreeing well with the statistical ratio of 2; the $l=2$ reduced width of the 2.31 Mev level yields⁹⁶

$$\theta_0^2(2d)/\theta_0^2(2p) \approx 1.1,$$

in good agreement with the values found for this ratio in the (d,p) experiments on Zn⁶⁴(VI.16), Zn⁶⁶(VI.17), and Zn⁶⁸(VI.18), and also in the gross-structure studies of Schiffer *et al.* (Sc59). A $2p$ -doublet splitting of 0.6 Mev is markedly smaller than the values $[2p_{\frac{1}{2}}] - [2p_{\frac{3}{2}}] \approx 1.5$ Mev found in nearby nuclei; on the other hand, $[2d_{\frac{5}{2}}] - [2p_{\frac{3}{2}}] \approx 2.3$ Mev is close to what is found in Ti⁴⁹ (2.7 Mev), V⁵² (2.1 Mev), and Mn⁵⁶ (2.3 Mev).

We therefore have three alternative interpretations of the Cr⁵³ reduced widths, of which the third is, perhaps, the most attractive. The matter should now be settled experimentally; probably the best way to do this would be to determine the spin and parity of the 2.31-Mev level and the spin of the 0.57-Mev level independently of the stripping results. A Cr⁵²(d,p)Cr⁵³ experiment studying levels up to 5 Mev in Cr⁵³ would also be useful in identifying the main $2d_{\frac{5}{2}}$ contributions and thereby either supporting or excluding interpretation (3).

There is no doubt that the 0.97-Mev level is predominantly $[2p_{\frac{3}{2}} \times 1f_{\frac{5}{2}}]$. Indeed, this experiment (El58b) was the first in which a $1f_{\frac{5}{2}}$ single-particle state was definitely identified.

Cr⁵³(d,p)Cr⁵⁴

It is likely that some of the proton groups observed in the only available experiment (El58b) correspond to unresolved groups of levels in Cr⁵⁴ and that sizeable $l=3$ components have been swamped by the dominant $l=1$ contributions (Fig. 54). No absolute cross sections are available.

The observed $l=1$ reduced widths do not lend themselves to any simple interpretation. We might be

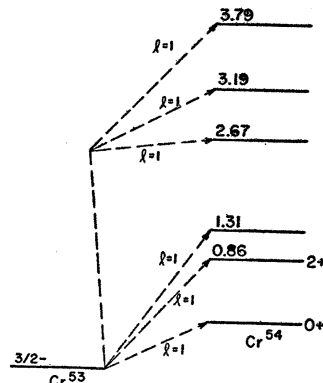


FIG. 54.

tempted by the marked break between 1.31 and 2.67 Mev in the pattern of observed $l=1$ transitions to suggest that $l=1$ levels below 1.5 Mev involve mainly $2p_{\frac{3}{2}}$, those above 2.5 Mev being predominantly $2p_{\frac{1}{2}}$. The proposed $2p_{\frac{3}{2}}$ transitions are, however, too strong relative to $2p_{\frac{1}{2}}$ by a factor of about four to support such an interpretation. Detailed analysis of the low-lying levels of Cr⁵⁴ and their reduced widths must await identification of possible $l=3$ contributions and, possibly, further information concerning the spins of the relevant states.

Co⁵⁹(d,p)Co⁶⁰

There are two relevant experiments, one (El58a), with moderate resolution, reaching levels up to 1 Mev in Co⁶⁰, the other (Sc59) being a low-resolution study of single-particle neutron levels in Co⁶⁰.

In the latter experiment, the proton energy-spectrum reveals only one low-lying $l=1$ peak; above this $l=1$ peak, $2d_{\frac{5}{2}}$ contributions are found to be centered around 2.7 Mev, $3s_{\frac{1}{2}}$ near 4 Mev, while $1g_{9/2}$ components are tentatively identified close to $2d_{\frac{5}{2}}$. No $1f_{\frac{5}{2}}$ contributions are found, a conclusion which is paralleled in the moderate-resolution work of El58a. However, preliminary results of a high-resolution Co⁵⁹(d,p)Co⁶⁰ experiment (En57) indicate that there are many $l=1$ levels below 2.5 Mev in Co⁶⁰ with sizeable $l=3$ admixtures, and a few pure $l=3$ levels as well. It is therefore almost certain that, in the low-resolution work of Sc59, $1f_{\frac{5}{2}}$ contributions are concealed in the single $l=1$ peak.

The simplest interpretation (Sc59) of the existence of only one $l=1$ peak is that, in $^{27}\text{Co}_{32}^{59}$, the $2p_{\frac{3}{2}}$ neutron shell is complete. The single $l=1$ peak would then correspond to $2p_{\frac{3}{2}}$. Since, however, $2p_{\frac{3}{2}}$ and $2p_{\frac{1}{2}}$ contributions are experimentally indistinguishable, it is by no means clear that this extreme assumption is justified. Further work is needed to find out how the $2p_{\frac{3}{2}}$ and $1f_{\frac{5}{2}}$ neutron shells fill in the region $50 < A < 70$, (p,d) or (d,t) pickup experiments are particularly useful in this connection.⁹⁷

⁹⁶ The l value of the 2.31-Mev level being uncertain, this is to be regarded as test of the consistency of our interpretation rather than an independent estimate of the ratio of single-particle reduced widths.

⁹⁷ See the discussion of the (d,t) experiments of Zeidman *et al.* (Ze60) at the end of this section.

$Zn^{64}(d,p)Zn^{65}$; $Zn^{66}(d,p)Zn^{67}$; $Zn^{67}(d,p)Zn^{68}$;
 $Zn^{68}(d,p)Zn^{69}$

(d,p) experiments on Zn^{64} , Zn^{66} , and Zn^{67} have been performed with 10-Mev deuterons (Sh59), $Zn^{68}(d,p)Zn^{69}$ with both 10-Mev (Sh59) and 11.9-Mev (Eb54) deuterons. The 10- and 11.9-Mev $Zn^{68}(d,p)$ results are in reasonable agreement, although the $l=4$ transition to the first excited state of Zn^{69} is markedly stronger in the 10-Mev experiment. We use the 10-Mev data of Sh59⁹⁸ in the following discussion. Although no absolute cross sections are available, the various $Zn(d,p)$ cross sections of Sh59 are given in the same relative units.

The presence of $l=1$ and $l=3$ transitions to low-lying levels with $J=\frac{3}{2}^-$ and $\frac{5}{2}^-$, respectively, in Zn^{65} and Zn^{67} indicates that neither the $2p_{\frac{1}{2}}$ nor the $1f_{\frac{5}{2}}$ neutron shell can be regarded as closed in the Zn^{64} and Zn^{66} ground-state wave functions. We cannot make quantitative estimates of the structure of these wave functions on the basis of the stripping widths alone.

Above the $1f_{\frac{5}{2}}$ and $2p_{\frac{1}{2}}$ contributions in $Zn^{64}(d,p)Zn^{65}$ and $Zn^{66}(d,p)Zn^{67}$, strong transitions are observed with $l=1$, $l=4$, and $l=2$, similar to the three lowest transitions in $Zn^{68}(d,p)Zn^{69}$. But the Zn^{68} ground-state wave function is expected to involve, predominantly, closed $1f_{\frac{5}{2}}$ and $2p_{\frac{1}{2}}$ shells. Thus, the Zn^{69} levels in question can be plausibly interpreted as single-particle $2p_{\frac{1}{2}}$, $1g_{9/2}$, and $2d_{\frac{5}{2}}$, the spins ($\frac{1}{2}^-$ and $9/2^+$) of the first two states being otherwise known. We see later that the $Zn^{67}(d,p)-Zn^{68}$ ground-state reduced widths lends some support to our hope that $(p_{\frac{1}{2}})^2_0$, $(1d_{\frac{5}{2}})_0$, and $(1g_{\frac{9}{2}})_0$ contributions to the Zn^{68} ground state are small.

We would like to give a similar single-particle interpretation of the $l=1$, $l=4$, and $l=2$ levels in Zn^{65} and Zn^{67} . Such an interpretation demands that the reduced widths of analogous levels in Zn^{65} , Zn^{67} , and Zn^{69} be the same, since each $S=1$. On using the data of Sh59 and expressing the reduced widths in the same units, we have the values shown in Table XIX. The reduced widths of corresponding levels are seen to agree moderately well, their ratios very much better. It seems, in fact, that the proposed single-particle interpretation⁹⁹ of the levels in question is a reasonable approximation, probably rather better in Zn^{69} than in Zn^{65} and Zn^{67} .

From Table XIX, then, we obtain for the ratios of $2p$, $1g$, and $2d$ reduced widths:

$$\theta_0^2(1g)/\theta_0^2(2p) \approx 2.1, \quad \theta_0^2(2d)/\theta_0^2(2p) \approx 1.1, \\ \text{from } Zn^{65}; \quad (VI.16)$$

⁹⁸ Sh59 suggest that the transitions in question may have $l=3$ rather than $l=4$, arising from excitation of the $1f_{7/2}$ shell in Zn^{64} and Zn^{68} . Apart from the difficulty of producing a core-excited transition of the requisite strength [remember the $1d_{\frac{5}{2}}$ transitions in $Si^{28}(d,p)Si^{29}$], we regard $l=3$ as unlikely because the 0.44-Mev transitions in Zn^{69} , which certainly has $l=4$, has a very similar angular distribution.

⁹⁹ We have incidentally suggested spins for the relevant levels of Zn^{65} and Zn^{67} .

TABLE XIX.

J^π	l	$\theta^2(Zn^{65})$	$\theta^2(Zn^{67})$	$\theta^2(Zn^{69})$
$1/2^+$	1	0.90	0.85	1.4
$9/2^+$	4	1.9	1.6	2.5
$5/2^+$	2	1.0	0.89	1.4

$$\theta_0^2(1g)/\theta_0^2(2p) \approx 1.9, \quad \theta_0^2(2d)/\theta_0^2(2p) \approx 1.0, \\ \text{from } Zn^{67}; \quad (VI.17)$$

$$\theta_0^2(1g)/\theta_0^2(2p) \approx 1.8, \quad \theta_0^2(2d)/\theta_0^2(2p) \approx 1.0, \\ \text{from } Zn^{69}. \quad (VI.18)$$

These estimates of $\theta_0^2(1g)/\theta_0^2(2p)$ constitute the only information about $\theta_0^2(1g)$ encountered in this study; they are rather larger than the values quoted in the gross-structure study of Sc59 (~ 1.0).

If the closed-shell interpretation of the Zn^{68} ground state is a reasonable approximation, the $Zn^{67}(d,p)Zn^{68}$ ground-state transition should be well represented by $(2p_{\frac{1}{2}})_0(1f_{\frac{5}{2}})_0 \rightarrow (2p_{\frac{1}{2}})_0(1f_{\frac{5}{2}})_\frac{5}{2}$, ignoring the zero-coupled group of protons. The S value of this transition is six (the number of particles in the $1f_{\frac{5}{2}}$ neutron shell). If we regard the transition $Zn^{68}(d,p)Zn^{69}$ as single-particle $2p_{\frac{1}{2}}$, so that $S=1$, and use the estimate $\theta_0^2(2p) \approx 2\theta_0^2(1f)$, the measured ratio (Sh59)

$$\theta_g^2[Zn^{67}(d,p)Zn^{68}]/\theta_g^2[Zn^{68}(d,p)Zn^{69}] = 2.4$$

indicates $S_g[Zn^{67}(d,p)Zn^{68}] \approx 5$.

This is sufficiently close to the predicted value of six to suggest that core excitation in the Zn^{68} ground state is relatively unimportant.

(d,t) Reactions on Nuclei with $51 \leq A \leq 68$

(d,t) reactions on a number of nuclei with mass numbers between 51 and 68 have been studied by Zeidman, Yntema, and Raz (Ze60, Ra60) at a deuteron energy of 21.5 Mev. In many of the (d,t) experiments individual levels of the residual nucleus were not resolved; even if they were, far too little is known about the spectroscopy of nuclei with $A \approx 60$ for us to provide an explicit wave function for each state. Accordingly, the kind of analysis used in connection with $O^{18}(d,t)O^{17}$ or $Mg^{26}(d,t)Mg^{25}$ is no longer possible. Instead, we use the sum rules of Appendix 2, where the summations extend over all observed transitions of given l and the information obtained primarily concerns the target ground state.

We could proceed directly and simply by substitution in (III.120') or (III.140') of Appendix 2. Instead, it is instructive to derive the desired sum rule explicitly in one particular case, that of $Zn^{64}(d,t)Zn^{63}$. We assume charge independence, so that the Zn^{64} ground state has $T=2$, $M_T=2$. Since the isotopic spins of the final states in Zn^{63} are not known, we need sum rules for the quantity $(C)^2\theta^2$, where $(C)^2$ is the isotopic-spin coupling

factor in (II.30) or (II.37). It is reasonable to write

$$\begin{aligned}\Psi(\text{Zn}^{64}) = & \alpha(f_{\frac{1}{2}}^0)_{20} + \beta\{(f_{\frac{1}{2}}^6)_{10}(p_{\frac{1}{2}}^2)_{10}\}_{20} \\ & + \gamma\{(f_{\frac{1}{2}}^4)_{20}(p_{\frac{1}{2}}^4)_{00}\}_{20} + \delta\{(f_{\frac{1}{2}}^4)_{00}(p_{\frac{1}{2}}^4)_{20}\}_{20} \\ & + \epsilon\{(f_{\frac{1}{2}}^2)_{10}(p_{\frac{1}{2}}^6)_{10}\}_{20} \quad (\text{VI.19})\end{aligned}$$

for the ground-state wave function of Zn^{64} , with $TJ=20$. Other components which might be required could be included in the following discussion without difficulty.

Let us now list the components in the Zn^{63} wave functions which can be reached by pickup from (VI.19). We consider $l=3$ transitions first and use (III.64) or (III.67) to evaluate the necessary overlap integrals (reduced-width amplitudes):

$$\begin{aligned}T_0=\frac{3}{2}: \quad & \chi_1=(f_{\frac{1}{2}}^7)_{\frac{1}{2}} \quad g_1=(7/10)^{\frac{1}{2}}\alpha \\ & \chi_2=\{(f_{\frac{1}{2}}^5)_{\frac{1}{2}}(p_{\frac{1}{2}}^2)_{10}\} \quad g_2=(5/12)^{\frac{1}{2}}\beta \\ & \chi_3=\{(f_{\frac{1}{2}}^5)_{\frac{1}{2}}(p_{\frac{1}{2}}^2)_{10}\} \quad g_3=(1/30)^{\frac{1}{2}}\beta \\ & \chi_4=\{(f_{\frac{1}{2}}^3)_{\frac{1}{2}}(p_{\frac{1}{2}}^4)_{00}\} \quad g_4=(1/2)^{\frac{1}{2}}\gamma \\ & \chi_5=\{(f_{\frac{1}{2}}^3)_{\frac{1}{2}}(p_{\frac{1}{2}}^4)_{20}\} \quad g_5=(1/5)^{\frac{1}{2}}\delta \\ & \chi_6=\{(f_{\frac{1}{2}})_{\frac{1}{2}}(p_{\frac{1}{2}}^6)_{10}\} \quad g_6=(1/4)^{\frac{1}{2}}\epsilon \\ T_0=\frac{5}{2}: \quad & \chi'_1=(f_{\frac{1}{2}}^7)_{\frac{1}{2}} \quad g'_1=(3/10)^{\frac{1}{2}}\alpha \\ & \chi'_2=\{(f_{\frac{1}{2}}^5)_{\frac{1}{2}}(p_{\frac{1}{2}}^2)_{10}\} \quad g'_2=(3/10)^{\frac{1}{2}}\beta \quad (\text{VI.20}') \\ & \chi'_3=\{(f_{\frac{1}{2}}^3)_{\frac{1}{2}}(p_{\frac{1}{2}}^2)_{20}\} \quad g'_3=(3/10)^{\frac{1}{2}}\delta\end{aligned} \quad (\text{VI.20})$$

Consider the $T_0=\frac{3}{2}$ states first. Actual states ϕ_j of Zn^{63} with $J_0=\frac{5}{2}-$ and $T_0=\frac{3}{2}$ are linear combinations of $\chi_1, \chi_2, \dots, \chi_6$ and of other $\frac{5}{2}-$ states $\chi_7 \dots \chi_s$ which are not reached by $f_{\frac{1}{2}}$ pickup from (VI.19). Specifically, we have

$$\phi_j = \sum_{k=1}^s c_{jk} \chi_k, \quad (\text{VI.21})$$

where s is the number of states in Zn^{63} which contain significant components of $\chi_1 \dots \chi_6$ and $g_k=0$ for $k>3$. As described at the end of Sec. III.7, the spectroscopic factor S_j of ϕ_j is

$$\begin{aligned}S_j(f_{\frac{1}{2}}) = & 8\left\{\sum_{k=1}^s c_{jk} g_k\right\}^2 \\ = & 8\left\{\sum_k c_{jk}^2 g_k^2 + 2 \sum_{k<l} c_{jk} c_{jl} g_k g_l\right\}. \quad (\text{VI.22})\end{aligned}$$

We now sum (VI.22) over all states of Zn^{63} with $T_0 J_0 = \frac{3}{2} \frac{5}{2}-$ and observable $f_{\frac{1}{2}}$ pickup reduced widths; in other words, we sum over j :

$$\sum_j S_j(f_{\frac{1}{2}}) = 8\left\{\sum_k \left(\sum_i c_{jk}^2\right) g_k^2 + 2 \sum_{k<l} \left(\sum_i c_{jk} c_{jl}\right) g_k g_l\right\}. \quad (\text{VI.23})$$

Since the matrix $[c_{jk}]$ transforms one (real) orthonormal set of functions into another, it must be orthogonal. Thus

$$\sum_j c_{jk} c_{jl} = \delta(k,l). \quad (\text{VI.24})$$

Substituting (VI.24) in (VI.23), we see that the cross terms vanish and the sum rule

$$\sum_j S_j(f_{\frac{1}{2}}) = 8 \sum_k g_k^2 \quad (\text{VI.25})$$

is obtained. The foregoing argument refers explicitly to states of Zn^{63} with $T_0=\frac{3}{2}$. It is, however, obvious that (VI.25) and the arguments which led to it are equally applicable to the states with $T_0=\frac{5}{2}$.

The amplitudes (VI.20) and (VI.20') then lead to

$$\begin{aligned}\sum_{f_{\frac{1}{2}}} S\left(f_{\frac{1}{2}}: T_0 = \frac{3}{2}\right) \\ = 8\left(\frac{7}{10}\alpha^2 + \frac{9}{20}\beta^2 + \frac{1}{2}\gamma^2 + \frac{1}{5}\delta^2 + \frac{1}{4}\epsilon^2\right), \quad (\text{VI.26})\end{aligned}$$

$$\sum_{f_{\frac{1}{2}}} S\left(f_{\frac{1}{2}}: T_0 = \frac{5}{2}\right) = 8\left(\frac{3}{10}\alpha^2 + \frac{3}{10}\beta^2 + \frac{3}{10}\delta^2\right). \quad (\text{VI.26}')$$

It remains to combine (VI.26) and (VI.26') into a sum rule for $(C^2)S(f_{\frac{1}{2}})$. The relevant isotopic-spin coupling factor $\{C[T_0 \frac{1}{2}T : M_{T_0}, M_T - M_{T_0}]\}^2$ has the value 1 for each $T_0=\frac{3}{2}$ state, $\frac{1}{6}$ for $T_0=\frac{5}{2}$. Thus, multiplying (VI.26) by 1, (VI.26') by $\frac{1}{6}$, and adding, we obtain the final sum rule

$$\sum_{f_{\frac{1}{2}}} (C^2)S(f_{\frac{1}{2}}) = 6\alpha^2 + 4\beta^2 + 4\gamma^2 + 2\delta^2 + 2\epsilon^2. \quad (\text{VI.27})$$

We verify immediately that (VI.27) is precisely what is obtained by applying the general sum rule (III.140') of Appendix 2 to each separate component of (VI.19) and adding the results. We have thus verified the assertion at the end of Appendix 2 that the contributions to the sum rule from different components of the target wave function do not interfere. The argument is clearly quite general. For $2p_{\frac{1}{2}}$ pickup, we obtain in similar fashion

$$\sum_{2p_{\frac{1}{2}}} (C^2)S(2p_{\frac{1}{2}}) = 2\beta^2 + 2\gamma^2 + 4\delta^2 + 4\epsilon^2. \quad (\text{VI.27}')$$

Finally, summing over all states of Zn^{63} which are reached from Zn^{64} by pickup of either an $f_{\frac{1}{2}}$ or a $2p_{\frac{1}{2}}$ neutron, we have

$$\sum_{f_{\frac{1}{2}}, 2p_{\frac{1}{2}}} (C)S = 6, \quad (\text{VI.28})$$

the number of neutrons outside closed shells.

It is easy to see that, in the general case of pickup on a nucleus with isotopic spin $T (= M_T)$ and n nucleons outside closed shells, we have

$$\sum (C)S = \frac{n}{2} + M_T, \quad (\text{VI.29})$$

where the summation extends over all transitions involving nucleons outside closed shells.

Raz *et al.* (Ra60) have used sum rules similar to those under consideration to interpret the results of (d,t) experiments on nuclei with mass number $A \approx 60$. These authors adopt what we describe, in Appendix 1, as an " n - p formalism." Components in ground-state wave functions are formed by placing neutrons and protons separately in low-energy states. Although, as we have emphasized repeatedly, this procedure is not charge-independent, the sum rules obtained by Raz *et al.* (for $\sum S$) do not differ greatly from what is found [for $\sum(C)^2 S$] with the aid of (III.140') of Appendix 2. This reflects the fact that the T admixtures in the lowest states of the n - p formalism are usually small. It is clear that the sum rule (VI.29), the right-hand side of which depends only on n (the number of nucleons) and M_T (the neutron excess), also emerges in the n - p formalism.

We encounter two main difficulties in applying our sum rules to the results of (d,t) experiments (Ze60) in the region from V to Zn. Firstly, $l=3$ levels are sometimes unresolved from nearby $l=1$ levels, making it difficult to measure the $l=3$ reduced width. In such cases we accept the upper limit given in Ze60 as a rough estimate of the $l=3$ reduced width. Secondly, $f_{7/2}$ contributions to pickup are experimentally indistinguishable from $f_{5/2}$. We assume that $f_{7/2}$ transitions to levels below 4 Mev in nuclei between Cr⁵² and Zn⁶⁸ are unimportant. Too little is known about the systematics of single-hole states for us to be certain that this is a good approximation.

Let us, then, apply the "total" sum rule (VI.29). To do so, we need to know the values of three phenomenological parameters, the (d,t) normalization factor Λ , and the single-particle reduced widths $\theta_0^2(1f)$ and $\theta_0^2(2p)$. We take

$$\theta_0^2(2p)/\theta_0^2(1f) = 2,$$

(see Figs. 58 and 59) and use measured values of $(C)^2 \Lambda \theta^2$ (Ze60) to "evaluate" $\Lambda \theta_0^2(1f)$. The results are shown in Table XX.

Results are reasonably consistent; the tendency of $\Lambda \theta_0^2(1f)$ to decrease with mass number probably reflects the presence of sizeable $1f_{5/2}$ and $2p_{3/2}$ contributions above the highest excitations reached in the relevant experiments (Ze60). The small value of $\Lambda \theta_0^2(1f)$ found in Zn⁶⁷(d,t)Zn⁶⁶ is, however, quite disturbing since all sizeable $l=1$ and $l=3$ contributions up to about 5 Mev in Zn⁶⁶ have been identified. Elsewhere in this study we have found $\Lambda \approx 190$ (II.38) and $\theta_0^2(1f) \approx 0.012$ (Fig. 58), yielding $\Lambda \theta_0^2(1f) \approx 2.3$, in satisfactory agreement with the values in Table XX.

The separate $f_{5/2}$ and $2p_{3/2}$ sum rules give only two relations between the amplitudes in the target ground-state wave function and therefore do not, in general, determine these (squared) amplitudes completely. Sometimes it is possible to obtain a solution with the aid of other experimental data, as in the case of Fe⁵⁷ discussed in Ra60.

The main qualitative conclusions to be drawn from

TABLE XX.

Target nucleus	Mn ⁵⁵	Fe ⁵⁶	Fe ⁵⁷	Co ⁵⁹	Zn ⁶⁴	Cu ⁶⁵	Zn ⁶⁶	Zn ⁶⁷	Zn ⁶⁸
$\Delta \theta_0^2(1f)$	3.0	2.7	2.0	2.4	1.9	1.8	1.5	0.8	1.2

the experiments of Zeidman *et al.* (Ze60) are the following:

(1) The absence of $l=1$ transitions in V⁵¹(d,t)V⁵⁰ and Cr⁵²(d,t)Cr⁵¹ provide further indications that $2p_{3/2}$ admixtures in the configurations $1f_{7/2}^n$ are small.

(2) The $f_{5/2}$ and $2p_{3/2}$ orbits mix very strongly. There is some evidence that the $f_{5/2}$ orbit contributes more to even-even nuclei than to even-odd nuclei (Sc59, Ra60).

Many more pickup experiments in this mass region are needed, not only in order to examine the wave functions of the target ground states but also, and probably more important, to study the properties of single-hole states in the residual nuclei.

VII. REVIEW OF THE INFORMATION OBTAINED FROM THE ANALYSIS OF EMPIRICAL REDUCED WIDTHS

It is clear from the wide variety of useful applications in Secs. IV to VI that the Born-approximation analysis of stripping widths is very useful in the study of nuclear spectroscopy. The central assumption of our procedure is that the shortcomings of the simple Born-approximation theory of stripping can be absorbed in an empirical single-particle reduced width θ_0^2 , which varies smoothly as a function of the relevant parameters. The most convincing justification of this assumption is the body of consistent information deduced with its aid about the properties of nuclear levels. In Sec. VII.1, we give a brief résumé of the different kinds of information which can be obtained from an analysis of stripping widths.

The properties of θ_0^2 provide another, more direct, test of our basic assumption. If this assumption is justified, we should now have a fairly detailed picture of the magnitude of θ_0^2 and of its dependence on its parameters. In Sec. VII.2 we collect the information about θ_0^2 obtained in Secs. IV to VI. It is seen that the behavior of the empirical single-particle reduced width is sufficiently consistent to confirm the reliability of our procedure.

Finally, in Sec. VII.3, we discuss some experiments and types of experiment which are of particular interest for future study.

1. Information about the Properties of Nuclear States

In this subsection, we review the different ways in which a stripping width can tell us something about the structure of nuclei. Many of the procedures to be described have been used extensively in Secs. IV-VI.

(a) *Spin Determinations*

The best-known application of the stripping reaction in nuclear spectroscopy is in determining spins and parities. Such applications vary in sophistication from cases which involve only simple kinematical considerations to those where we use relatively detailed information about the structure of the nuclear states involved and about the systematics of stripping reactions.

Purely on the basis of kinematics, measured l values fix parities and restrict spins to one of a few possible values. Assuming that (as is nearly always the case) the spin and parity $J_0\Pi_0$ of the target ground state are known, the parity Π of the final state is fixed as $\Pi=\Pi_0(-)^l$, while its spin J must lie between $J_0+l+\frac{1}{2}$ and the smaller of $|J_0-l\pm\frac{1}{2}|$. In the special case $J_0=l=0$, J is determined uniquely, having the value $\frac{1}{2}$.

At the next level of sophistication, suppose that in a (d,p) [or (d,n)] reaction involving the addition of a nucleon inequivalent to those in the target ground state, a large value of $[J]\theta^2$ is found. Since in such a case it is known from (III.73') that $s \leq 1$, a knowledge of the appropriate single-particle reduced width $\theta_0^2(l)$ may impose a lower limit on J and, in some cases, determine it completely. A good example of this kind is provided by the work of Warburton and McGruer (Wa57) on $N^{15}(d,p)N^{16}$. They find an $l=0$ transition to a level at 0.393 Mev in N^{16} , with $[J]\theta^2=0.54$. Since $s \leq 1$ and $\theta_0^2(2s)$ in this mass region is known to lie between 0.1 and 0.2, it is clear that $J \geq 1$. However, since the target spin is $\frac{1}{2}$, the only possible spins are 0 and 1, so that the level in question must have $J=1$.

The spin determinations considered so far make no assumptions about the structure of nuclei beyond what is involved in deciding that the transferred nucleon in certain situations is inequivalent to those in the target ground state. In order to make more specific use of our knowledge of nuclear structure, we usually proceed to introduce some nuclear model. Now each model, in its simplest form, makes general statements concerning reduced widths, of the form of selection rules, predicting that certain reduced widths should be large, others small. These selection rules are frequently useful in fixing spins. For example, in the region $20 \leq A \leq 28$, $1d_{\frac{3}{2}}$ transitions to low-lying levels (below about 3 Mev) are j -forbidden or, in other words, are predicted to have zero reduced widths by the extreme jj -coupling shell model. The fact, therefore, that the $Ne^{20}(d,p)Ne^{21}$ ground-state transition shows no stripping, while $Ne^{22}(d,p)Ne^{23}$ (ground state) has $l=2$, implies spins of $\frac{3}{2}^+$ and $\frac{5}{2}^+$ for the ground states of Ne^{21} and Ne^{23} , respectively. Other models, for example, the rotational model, can be used in similar fashion.

Selection rules are far from exploiting fully the possibilities of a nuclear model in analyzing reduced widths. We need not be satisfied with statements as to whether certain reduced widths are large or small, but

may demand, instead, quantitative expressions for them. Initial and final nuclear states are then described by the appropriate model wave functions and the reduced widths calculated by the techniques described in Sec. III; finally, the calculated reduced widths are compared with experiment. This procedure, exemplified many times in Secs. IV to VI, often leads to the assignment of spins. For instance, the spins of several positive-parity levels in N^{15} were assigned by comparing their observed stripping widths in $N^{14}(d,p)N^{15}$ (Sh55, Gr56, Wa57) with the predictions of Halbert's (Ha57) detailed shell-model calculation.

Arguments based on the weak-coupling formalism of Sec. III.11, where we are dealing with single-particle states and the manner in which they are "spread out" over adjacent bands of excitation, give rise to another important class of spin determinations. If the target nucleus has $J_0=0$, spins of levels in the residual nucleus can sometimes be assigned on the expectation that sizeable fragments of each basic single-particle state should be found quite close together, probably within 1 or 2 Mev. In other words, there is a tendency in odd- A nuclei for levels of the same spin and parity which do not belong to the ground-state configurations and which are excited by stripping from adjacent even-even nuclei, to appear in clusters. This tendency is confined to levels which show stripping and does not apply to levels of the same spin and parity in general. Spins are suggested on this basis for $l=1$ levels in Ca^{41} , Ca^{43} , and Ca^{45} in Sec. VI. When the target spin is nonzero, there are several single-particle states of each kind, with different spins, in the residual nucleus. If these basic single-particle components have suffered sufficiently slight loss by fragmentation, each such state has $s \approx 1$ and the corresponding values of $[J]\theta^2$ are proportional to $(2J+1)$. Considerations of this kind, first emphasized by Enge (En53), yield the spins of the four lowest levels in K^{40} which are well described by $[d_{\frac{3}{2}}^{-1}f_{7/2}]J=2, 3, 4, 5^-$, and also of four $l=1$ levels around 2 Mev in the same nucleus arising from $[d_{\frac{3}{2}}^{-1}2p_{\frac{3}{2}}]J=0, 1, 2, 3^-$.

(b) *Determination of Amplitudes and Interaction Matrix Elements*

The reduced width of an unfavored transition often measures an admixed amplitude in a wave function whose major component has some simple coupling scheme. Furthermore, the determination of such admixed amplitudes, in addition to being useful in itself, can yield a measure of the size of interaction matrix elements. A good illustration is encountered in Example 3 of Sec. III.9. Here we consider possible $l=1$ admixtures in the $l=3$ transition in $K^{39}(d,p)K^{40}$ to a 3^- level at 0.028 Mev in K^{40} . The dominant configuration of this level is $[d_{\frac{3}{2}}^{-1}1f_{7/2}]_{3^-}$; an $l=1$ admixture could be produced by an interaction with the $2p_{\frac{3}{2}}$ state $[d_{\frac{3}{2}}^{-1}2p_{\frac{3}{2}}]_{3^-}$, whose main component is at 2.042 Mev in K^{40} . A measurement of the $l=1$ reduced width of the

0.028-Mev level would determine the admixed $2p_{\frac{1}{2}}$ amplitude and hence the interaction matrix element $\langle [d_{\frac{3}{2}}^{-1}1f_{7/2}]_{\text{s}-} | H | [d_{\frac{3}{2}}^{-1}2p_{\frac{1}{2}}]_{\text{s}-} \rangle$. Any interaction matrix element is a significant quantity and can tell us something about the effective two-body interaction in nuclei. In the actual case under consideration, only an upper limit on the observed $l=1$ admixture is available (En59).

(c) Nuclear Models

Reduced widths measured in stripping and pickup reactions provide important tests of the wave functions of nuclear models. The main emphasis here is on giving a reasonable interpretation of enhanced and inhibited transitions and on correctly predicting the number of strong transitions of given l . Many such examples are found in Secs. IV to VI. In favorable cases, we hope to give a quantitative estimate of each observed reduced width with the help of the model wave functions.

In Sec. IV, low-lying $l=1$ transitions in the $1p$ shell have been analyzed in terms of the intermediate-coupling shell model. Satisfactory agreement with experiment can generally be obtained with values of the interaction parameters similar to those found necessary in studies of other properties of $1p$ -shell nuclei (In53, Ku56).

At the beginning of the ds shell, up to $A=19$, similar intermediate-coupling calculations have been carried out. Reduced-width data is too scanty to provide, as yet, a searching test of such predictions. The rotational model has also been used for $A=19$, but it is quite possible that the two models agree better with each other than they do with the experimental data. Later in the ds shell, from $A=20$ to $A=33$, the data bear a qualitative resemblance to the jj -coupling predictions. Closer inspection reveals that, in detail, the jj approximation is very crude in the region in question. In particular, $l=0$ and $l=2$ reduced widths in the vicinity of $A=28$ and $A=32$ reveal that the "closed-shell" nuclei Si^{28} and S^{32} involve large amounts of core-excited configurations. However, the Nilsson form of rotational model (Ni55) gives a satisfactory description of stripping data in the region $20 \leq A \leq 33$, but only if correct account is taken of the mixing of rotational bands arising from the $1d_{\frac{5}{2}}$, $2s_{\frac{1}{2}}$, and $1d_{\frac{3}{2}}$ orbits of the spherical shell model. These applications of the rotational model enable us to understand both the qualitative success and the quantitative failure of the jj -coupling shell model. For, although the low levels of ds -shell nuclei belong predominantly to the same (ds) shell, the success of the rotational model indicates that the d and s subshells are intimately mixed. Very little is known about late ds -shell model nuclei, with $33 \leq A \leq 38$.

In Sec. VI we have discussed "intermediate" nuclei, with $38 \leq A < 70$; much more data is needed before any clear picture can emerge. Qualitatively, however, the jj -coupling shell model within the configuration $1f_{7/2}$

has some success in interpreting the properties of low-lying levels in $1f_{7/2}$ nuclei ($A < 52$). The results of stripping and pickup reactions on nuclei in the mass region $52 < A < 68$ indicate that the $1f_{\frac{5}{2}}$ and $2p_{\frac{3}{2}}$ orbitals are very strongly mixed.

Since most of the available data refer to light and intermediate nuclei, with $A < 70$, the only detailed models used in our study are the rotational model and various species of shell model. However, as further stripping data become available in the region $70 \leq A \leq 150$, the vibrational collective model, whose predictions are considered in Sec. III.13, may become important.

(d) Single-Particle Levels¹⁰⁰ and Stripping Reactions

The stripping experiment $[A] \rightarrow [A+1]$ is a natural means of studying single-particle levels in the nucleus $[A+1]$, their fragmentation, their relative positions and separations, and how such properties vary from nucleus to nucleus. Detailed information of this kind should yield valuable insight into the effective two-body interaction in nuclei. The weak-coupling formalism described in Sec. III.11 provides a very convenient framework for the discussion of stripping transitions to single-particle states.

When the single-particle states under consideration are split by final-state interactions into large numbers of fragments, it is usually impracticable to discuss the reduced width of each individual level. Instead, we consider sums of the reduced widths of many levels, using the sum rule (III.185). In such studies, it may not be essential to resolve individual levels of $[A+1]$, the desired information being obtainable from low-resolution measurements of the kind carried out by Schiffer, Lee, and Zeidman (Sc59). It should be observed, however, that low-resolution studies have certain important limitations. Whenever the fragments of two single-particle states with different l values overlap, there is a danger that the state with higher l will be obscured. For example, in the work of Schiffer *et al.* (Sc59) on $f\ell$ -shell nuclei, $1f_{\frac{5}{2}}$ components often escape observation.

(e) Pickup Reactions and Single-Hole States

In contrast to a stripping reaction which reveals the properties of single-particle states in the residual nucleus, the pickup reaction $[A+1] \rightarrow [A]$ can be used to focus attention on the ground-state wave function of the target nucleus $[A+1]$. A pickup reaction can often measure small amplitudes in a ground-state wave function which could not readily be detected by any other means. Striking illustrations of this technique are

¹⁰⁰ The term "single-particle level" has been defined at the end of Sec. III.9 and in Sec. III.11. We are talking here of cases where the "single particle" is inequivalent to all nucleons in the ground state of $[A]$.

found in the analysis of the reaction $C^{14}(d,t)C^{13}$ in Sec. IV, and of $O^{18}(d,t)O^{17}$ and $Mg^{26}(d,t)Mg^{25}$ in Sec. V.

Just as stripping reactions reveal single-particle states, pickup reactions seek single-hole states in the residual nucleus. Little is known about the properties of such single-hole states, but the subject promises to be important in the future.

2. Information about the Mechanism of Stripping Reactions: Single-Particle Reduced Widths

The quantity of spectroscopic interest in a reduced width

$$\theta^2 = S\theta_0^2 \quad (\text{VII.1})$$

is the spectroscopic factor S . In this study we have used the Born approximation to extract values of θ^2 from the measured differential cross sections of stripping and pickup reactions, treating the single-particle reduced width θ_0^2 as an empirical parameter. If this procedure is reliable, we should find that θ_0^2 is a smoothly varying function of its parameters, namely, n, l, j, r_0, Q , and one of the projectile energies (E_0 or E).

It would be very surprising if θ_0^2 were found to depend significantly on j for fixed n and l , and, indeed, there is convincing evidence that it does not. Furthermore, we have already pointed out that our reduced widths depend strongly on r_0 only when the Butler theory finds difficulty in providing a stable fit to the observed differential cross section. On the other hand,

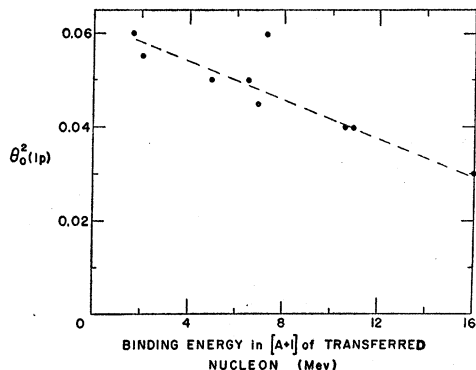


FIG. 55. $\theta_0^2(1p)$ as a function of binding energy.

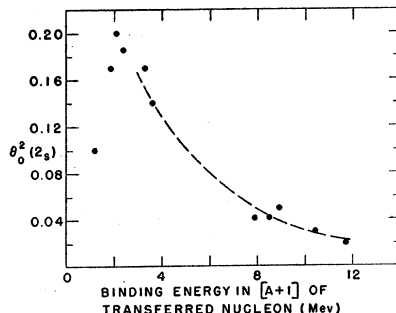


FIG. 56. $\theta_0^2(2s)$ as a function of binding energy.

θ_0^2 is certainly different for different values of n and l . We therefore consider a separate reduced width $\theta_0^2(n,l)$ for each pair of values (n,l) , and study the dependence of these quantities on the energy parameters.

(a) Dependence of θ_0^2 on the Projectile Energies

Absolute cross sections for the reactions $Be^9(d,p)Be^{10}$, $C^{12}(d,p)C^{13}$, $O^{16}(d,p)O^{17}$, $Mg^{24}(d,p)Mg^{25}$, and $Mg^{24}(d,n)Al^{25}$ have been measured at several different bombarding energies. From Table I, we find in each case that the observed reduced widths, and therefore $\theta_0^2(1p)$, $\theta_0^2(2s)$, and $\theta_0^2(1d)$, increase by factors of two to three as the deuteron energy increases from, roughly, 3 to 7 Mev. All available evidence, including the cases just cited, indicates that the single-particle reduced widths do not change much as the deuteron energy is further increased to 15 Mev and perhaps to even higher energies.

Accordingly, let us consider only "moderate-energy" single-particle reduced widths obtained from reactions wherein neither projectile energy lies outside the approximate range of 6 to 20 Mev. We understand this restriction to apply when we speak of reduced widths without further qualification. Our task is therefore to study the dependence of each single-particle reduced width $\theta_0^2(n,l)$ on the remaining energy parameter Q .

(b) Dependence of θ_0^2 on Q

Instead of the Q value of the reaction

$$[A] + [a] \rightarrow [A+1] + [a-1], \quad (\text{VII.2})$$

we introduce the binding energy B of the transferred nucleon in the nucleus $[A+1]$. According to (II.8), we have

$$B = Q + \epsilon_a - \epsilon_{a-1}. \quad (\text{VII.3})$$

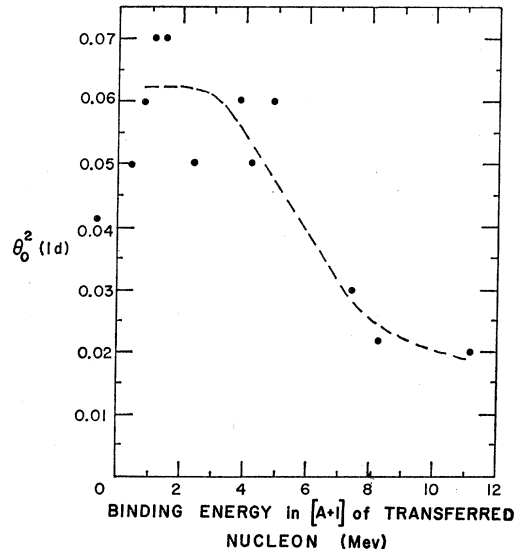


FIG. 57. $\theta_0^2(1d)$ as a function of binding energy.

Let us now use the values of $\theta_0^2(n,l)$ obtained in Secs. IV to VI to plot each single-particle reduced width as a function of B . The results for $\theta_0^2(1p)$, $\theta_0^2(2s)$, $\theta_0^2(1d)$, $\theta_0^2(1f)$, and $\theta_0^2(2p)$ are shown in Figs. 55 to 59. In view of the uncertainties involved in extracting these single-particle reduced widths—experimental error, inaccuracy of model wave functions, and the shortcomings associated with the Born approximation—their over-all consistency is remarkable and confirms the reliability of our semiempirical procedure for analyzing stripping data.

The salient qualitative features of Figs. 55 to 59 are¹⁰¹:

- (1) With the exception of $\theta_0^2(1f)$, each of the single-particle reduced widths under consideration decreases monotonically with increasing B for $B > 2$ Mev.
- (2) $\theta_0^2(1f)$ does not change significantly between $B=0$ and $B=8$ Mev.

For binding energies in the ranges covered by Figs. 55 to 59, the foregoing five single-particle reduced widths fluctuate by less than 20% about their central values. [$\theta_0^2(2s)$ for $B < 2$ Mev should be excluded from this statement since $l=0$ reduced widths of levels close to the nucleon separation energy ($B=0$) are often pathologically sensitive to r_0]. Consistency to within $\pm 20\%$ is very satisfactory.

It is now shown that an interpretation can be given of the salient characteristics of θ_0^2 in terms of a simple potential-well model of the process of nucleon capture.

Let us therefore suppose that, in the reaction (VII.2), the transferred nucleon is captured by a spherically symmetric potential well representing the nucleus [A]. The reduced width for this process is, by definition, a

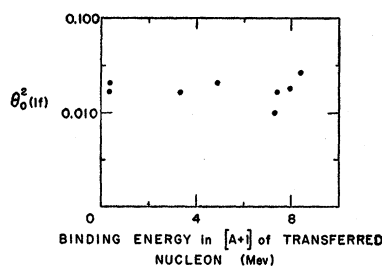


FIG. 58. $\theta_0^2(1f)$ as a function of binding energy.

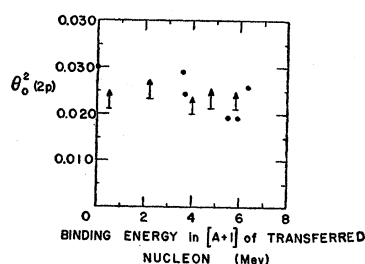


FIG. 59. $\theta_0^2(2p)$ as a function of binding energy.

¹⁰¹ The symbol “↑” in Fig. 59 refers to cases [for example, (V.12)] where only a lower limit is available for the relevant single-particle reduced width.

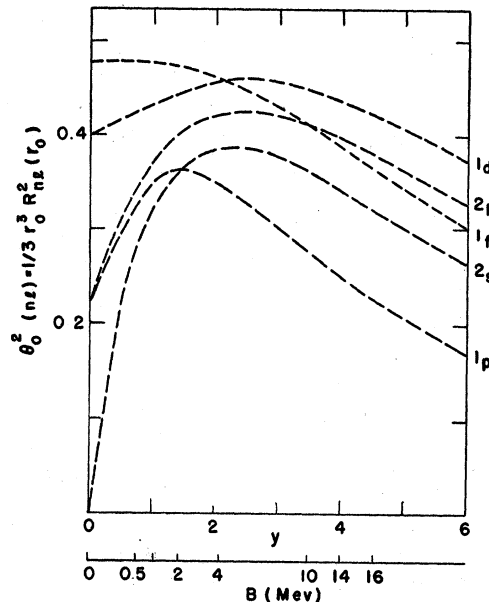


FIG. 60. Single-particle reduced widths for a square-well potential.

single-particle reduced width. It is given (II.14) by

$$\theta_0^2(n,l) = \frac{1}{3} r_0^3 R_{nl}^2(r_0), \quad (\text{VII.4})$$

where $R_{nl}(r_0)$ is the radial wave function, evaluated at the nuclear surface, of the captured nucleon in the potential well representing [A]. The quantity (VII.4) can be evaluated numerically for a suitably chosen potential well. It is found to be a function of the single parameter y , which is related to the binding energy of the captured nucleon in the capturing potential by

$$y = r_0 [2\mu B]^{\frac{1}{2}}, \quad (\text{VII.5})$$

where μ is the reduced mass of the nucleon.

$\theta_0^2(n,l)$ has been evaluated by Lubitz¹⁰³ (Lu57) and by Lane (La54a), for various values of n and l , using normalized square-well eigenfunctions. Lubitz's results are shown in Fig. 60 (taken from Fig. 2 of Lu57). To facilitate comparison with Figs. 55 to 59, we have chosen the representative parameter values $\mu=0.95$ and $r_0=5$ f, and give values of B corresponding to a few values of y .

It is obvious that several of the characteristics of the empirical single-particle reduced widths are reproduced by the potential-well model. Such features include:

- (1a) Each single-particle reduced width decreases monotonically with increasing y for $y > 2.5$.
- (2a) $\theta_0^2(1f)$ varies by only 10% between $y=0$ and $y=3$.

¹⁰² The well depth is determined by n , l , B , and r_0 and can be evaluated very simply for specific parameter values with the aid of Fig. 3 of Lu57.

¹⁰³ We are indebted to Dr. Lubitz for correspondence on this topic.

A comparison of predictions (1a) and (2a) of the potential-well model with characteristics (1) and (2) of the empirical single-particle widths reveals qualitative similarity. There are equally obvious quantitative disparities. For example, the maxima predicted by the square-well model occur at larger binding energies than do the empirical maxima. Furthermore, the well-known tendency of the Born-approximation theory to overestimate cross sections manifests itself in the fact that the square-well reduced widths are an order of magnitude larger than the empirical values. Again, the relative values of the different single-particle reduced widths predicted by the potential-well model bear little resemblance to what is found empirically.

In view of the uncertainties involved in extracting empirical reduced widths and since a square well does not provide the best possible equivalent potential well for the nucleus [A], we do not expect to find quantitative agreement between the potential-well model and empirical values of θ_0^2 . However, the success of the potential-well model in reproducing the qualitative features of the empirical single-particle reduced widths provides further confirmation of the validity of our procedure.

The single-particle reduced widths $\theta_0^2(2d)$ and $\theta_0^2(1g)$ also appear in a few instances in Secs. V and VI. Much less is known about them than about the five single-particle reduced widths discussed afore. Available data indicate rather consistently that

$$\theta_0^2(2d) \simeq \theta_0^2(2p) \quad (\text{VII.6})$$

and

$$\theta_0^2(1g) > 1.3\theta_0^2(2p). \quad (\text{VII.7})$$

Similar findings have been reported by Schiffer, Lee, and Zeidman (Sc59).

Nothing is known about single-particle reduced widths for bombarding energies above 18 Mev and essentially nothing for capture into unbound levels of [$A+1$] ($B<0$). Both these topics merit experimental study. Further experiments should also be undertaken to verify that θ_0^2 does not vary significantly with projectile energies in the range 6 to 20 Mev. The direct evidence on which we have based this conclusion is rather scanty, but the consistent picture which has emerged of the dependence of θ_0^2 on the binding energy of the transferred nucleon argues in its favor.

3. Suggested Experiments for Future Study

We conclude our study of stripping widths with a discussion of some experiments and types of experiment of particular interest. In some of these experiments the main objective is to study the properties of a specific nucleus; others are more concerned with the mechanism of stripping reactions and aim to sharpen our semi-phenomenological procedure for analyzing stripping

widths by determining its parameters with greater precision. Many of the experiments in the ensuing list have already been discussed elsewhere in our study; in such cases we are content to give a reference to the section wherein the relevant discussion may be found.

(1) The successful application of our procedure for analyzing stripping data depends on an accurate knowledge of the appropriate single-particle reduced widths. Any stripping or pickup experiment can contribute to our store of information about θ_0^2 and should therefore include measurements of absolute cross section.

In addition, several specific aspects of the single-particle reduced widths merit experimental investigation; some of these aspects have already been mentioned in Sec. VII.2.

(a) The same transitions should be studied at several different bombarding energies in order to study the dependence of θ_0^2 on projectile energies. See Sec. VII.2.

(b) We know very little about single-particle reduced widths of unbound levels ($B<0$). It would be interesting to examine how such quantities are related to the corresponding resonant reduced widths and to Born-approximation reduced widths for bound levels.

(c) The behavior of single-particle reduced widths close to the nucleon separation energy should be studied and compared to the behavior predicted in Fig. 60. See Sec. II.4.

(d) The relation between (d,p) and (d,n) reduced widths of analog levels in mirror nuclei is poorly understood. Since the binding energy of the nucleons captured into such states often differ significantly, it is by no means certain that $\theta^2(d,p) = \theta^2(d,n)$.

(e) We see from Figs. 55 to 59 that little is known about the behavior of θ_0^2 for $B>12$ Mev. This could be studied by pickup reactions on closed-shell nuclei (or the inverse stripping reactions). The bombarding energy should be 20 Mev or higher in order to keep the energy of the outgoing particles well above the Coulomb barrier.

(2) The (d,t) and (d,He^3) normalization factors $\Lambda(t)$ and $\Lambda(\text{He}^3)$ must be evaluated more precisely. Available data (see Sec. II.3) indicate that it is probably possible to extend our analysis to include such more complex processes, but our knowledge of the normalization factors is inadequate. This is reflected in the fact, noted at the end of Sec. IV, that the most serious difficulties encountered in our study involve (d,t) or (d,He^3) reactions. The (d,t) and (d,He^3) normalization factors may be quite different and should be evaluated separately. See Sec. II.3.

(3) In Sec. II.4 we remarked that (d,p) experiments with 6- to 8-Mev deuterons on nuclei with $A \geq 40$ (Bo57, Bo57a, Da60a) have repeatedly found difficulty in distinguishing $l=1$ from $l=2$, $l=2$ from $l=3$. Since the bombarding energies involved are very close to the

relevant Coulomb barrier heights (6 to 7 Mev), we suggest that experiments with higher-energy projectiles might distinguish l values more clearly.

(4) (d,p) experiments should be carried out with deuterons of 20 Mev or more in order to test the validity of the Born approximation at higher bombarding energies. See Sec. II.4.

(5) In discussing the $Mg^{24}(d,p)Mg^{25}$ ground-state transition in Sec. IV, we mentioned the anomalous forward spike found in the $l=2$ angular distribution at a deuteron energy of 14.8 Mev (Ha60). Such a phenomenon could not be due to an $l=0$ admixture, even allowing for the possibility of spin-flip. Recent work by Parkinson (Pa60) with 8-Mev deuterons has revealed a similar spike in the $l=2$ transition $Mg^{25}(d,p)Mg^{26}$ (1.83 Mev). In this case an $l=0$ admixture is allowed, but the forward peak, as was the case in $Mg^{24}(d,p)Mg^{25}$, is much more sharply localized in the forward direction than an $l=0$ Butler curve. It would be very interesting to find out whether a distorted-wave calculation predicts these sharp forward spikes. Such calculations might also give some indication where to seek other instances of the anomalous forward peak.

(6) Available data on vibrational ($100 \leq A \leq 150$) and rotational ($150 < A < 190$) nuclei have for the most part been obtained from the analysis of β -decay schemes and from Coulomb-excitation studies. Such information is subject to rather severe restrictions since only a limited number of levels are energetically accessible to β decay and since the probability of Coulomb excitation decreases rapidly with increasing excitation energy. Stripping and pickup experiments provide an ideal means of studying vibrational and rotational nuclei.

In order to carry out this program, the systematics of stripping reactions for $A > 70$ must be studied in detail.

(7) $Li^7(n,d)He^6$, because of the puzzling $Li^7(d,He^3)He^6$ results. See Sec. IV. Measurements of the (n,d) reduced widths of the first two states of He^6 would yield valuable information about the energy dependence of $\Lambda(He^3)$.

(8) $B^{11}(d,n)C^{12}$ or $B^{11}(He^3,d)C^{12}$, especially to the 7.65 Mev 0^+ state of C^{12} . See Sec. IV.

(9) $C^{13}(He^3,d)N^{14}$, up to 10 Mev in N^{14} , because of special interest in the $A=14$ levels. See Sec. IV.

(10) $C^{14}(He^3,d)N^{15}$, up to 10 Mev in N^{15} , in order to

(a) fix the S_0 parameter of the $A=14$ states (see Sec. IV and also the end of Sec. III.10) and

(b) use the fact that both C^{14} and N^{14} are available as targets to examine the weak-coupling structure of the levels of N^{15} .

(11) $N^{15}(He^3,d)O^{16}$, up to 10 Mev in O^{16} , with particular attention to the following features:

(a) The ground-state reduced width ($S=4$) should be compared with the surprisingly small value obtained in $O^{16}(d,t)O^{15}$.

(b) Information can be obtained concerning the 0^+ state at 6.04 Mev in precisely the same way as in $B^{11}(He^3,d)C^{12}$ (7.65 Mev).

(c) $l=0$ and $l=2$ transitions measure $p_{\frac{1}{2}}^{-1}s_{\frac{1}{2}}$ and $p_{\frac{3}{2}}^{-1}d_{\frac{3}{2}}$ components in negative-parity levels of O^{16} above 6 Mev.

(d) Shell-model wave functions for the levels mentioned in (c) have been calculated by Elliott (El57).

(12) $O^{16}(p,d)O^{15}$; $O^{16}(d,He^3)N^{15}$. See Sec. IV.

(13) $O^{16}(d,p)O^{17}$ up to 10 Mev in O^{17} , in order to study single-particle levels, their positions, and how they are fragmented by final-state interactions.

(14) $O^{17}(d,t)O^{16}$ (6.06 Mev), to supplement 11(b).

(15) $O^{18}(d,p)O^{19}$; $O^{18}(He^3,d)F^{19}$. These experiments would test available shell-model wave functions (El55a, Re58) for $A=18$ and $A=19$. Although the first three levels of F^{19} , $\frac{1}{2}^+$ ground state, $\frac{1}{2}^-$ at 110 kev, $\frac{5}{2}^+$ at 198 kev, are only about 100 kev apart, the energy resolution necessary for complete separation is no better than 200 kev because the $\frac{1}{2}^-$ level at 110 kev should show no stripping.

(16) $F^{19}(d,t)F^{18}$; $F^{19}(d,He^3)O^{18}$, as in (15).

(17) $Al^{27}(He^3,d)Si^{28}$. If α is the $1d_{\frac{3}{2}}^{-1}$ amplitude in the Al^{27} ground-state wave function, then $\sum S$ for all $1d_{\frac{3}{2}}$ transitions to 0^+ states of Si^{28} is $12\alpha^2$. On using the rough value $\alpha^2 \approx 0.6$ obtained in Sec. V, we obtain $\sum S \approx 7$. The observed ground-state reduced width implies $S \approx 2$, accounting for only a minor portion of the sum. We therefore expect to find $1d_{\frac{3}{2}}$ transitions of considerable strength to higher 0^+ levels in Si^{28} . (The $l=2$ transitions in question may be obscured by coherent $2d_{\frac{5}{2}}$ admixtures and, since the relevant spins are not known, by $1d_{\frac{5}{2}}$ transitions to levels of Si^{28} with $J \neq 0$.)

(18) $Si^{28}(d,He^3)Al^{27}$, because of interest in the Si^{28} ground-state wave function. See Sec. V.

(19) $Si^{28}(d,p)Si^{29}$, up to 10 Mev in Si^{29} . See Sec. V.

(20) $Si^{29}(d,t)Si^{28}$, to supplement (17).

(21) $S^{33}(d,n)Cl^{34}$; $S^{33}(d,p)S^{34}$. The single-particle levels with $l=3$ or $l=1$ are of interest. There are, for example, two sets of $f_{7/2}$ single-particle levels (identified by strong $l=3$ reactions), namely, $J=2, 3, 4, 5$ with $T=0, 1$. Both are observable in the (d,n) [or (He^3,d)] reaction, only one set in the (d,p) . There is a strong prediction (Fr60a) that the average of the $T=0, 1$ spectra should be identical with the low-lying spectrum of Cl^{38} , which is well known. Even if only the $T=1$ spectrum were known, we could combine this with that of Cl^{38} to get a complete account of the shell-model interaction for a $(d_{\frac{5}{2}}, f_{7/2})$ pair. A similar argument applies to the $p_{\frac{3}{2}}$ levels; in Cl^{38} the $p_{\frac{3}{2}}$ levels are unknown but could be deduced from those of K^{40} for which we have a plausible assignment (see Sec. VI). There are a great many possible examples of this sort (see Fr60a).

(22) $Cl^{35}(d,p)Cl^{36}$; $Cl^{35}(He^3,d)Ar^{36}$, particularly to the Cl^{36} ground state and the first excited 2^+ state of Ar^{36} . See end of Sec. V.

(23) The $[J]\theta^2$ values of the expected $l=3$ transitions to the first four levels of Cl^{38} , whose predominant configuration is $[(d_{\frac{5}{2}})_2 \times 1f_{7/2}]_{(TJ=2J)}$, $J=2, 3, 4, 5^-$, should verify the correctness of the theoretical spin assignments of Goldstein and Talmi (Go56) and of Pandya (Pa56) for these levels.

(24) $\text{Ar}^{38}(d,p)\text{Ar}^{39}$ should resemble $\text{Ca}^{40}(d,p)\text{Ca}^{41}$ quite closely. A level at 1.52 Mev in Ar^{39} is known to have spin $\frac{3}{2}^+$. If a weak $l=2$ transition is observed to this level, $J=\frac{3}{2}^+$ would be strongly favored for the 2.014-Mev level in Ca^{41} . See Sec. VI.

(25) $\text{K}^{39}(\text{He}^3,d)\text{Ca}^{40}$. Since the ground-state transition completes the $1d_{\frac{5}{2}}$ shell, we have $S \approx 8$. The observed ground-state reduced width would yield information about core-excitation in K^{39} , and Ca^{40} , as in the similar cases of $\text{Al}^{27}(d,n)\text{Si}^{28}$ and $\text{P}^{31}(d,n)\text{S}^{32}$ discussed in Sec. V.

(26) Ground-state reactions involving the calcium isotopes are of very great interest. One would like to know the variation of S with n (Sec. III.10, Example 2) for the entire chain of n values. At present only three points are available on the $S \leq 1$ branch; the $S \geq 1$ branch is of particular interest because this branch effectively measures the m degeneracy of the single-particle $f_{7/2}$ state and thus gives a sensitive indication of the validity of the spherical shell model in a region where one has a strong *a priori* feeling that it should be good. (Observe that the strong cooperative effect is found in the shell model; the rotational collective model gives at most a weak cooperative effect.)

Of course, excited-state reactions in the calcium isotopes as well as in the other $f_{7/2}^-$ shell nuclei are of general interest too.

(27) $\text{Ca}^{48}(d,t)\text{Ca}^{47}$; $\text{Ga}^{48}(d,\text{He}^3)\text{Sc}^{47}$. The β^- decay $\text{Ca}^{47} \rightarrow \text{Sc}^{47}(\frac{7}{2}^- \rightarrow \frac{7}{2}^-)$ with $\log ft = 8.6$, is strongly inhibited. If this is due to very different ground-state configurations for Ca^{47} and Sc^{47} , the ground-state (d,t) and (d,He^3) reduced widths will reflect such differences. By simultaneously performing $\text{Ca}^{48}(d,p)\text{Ca}^{49}$ to the $1f_{\frac{5}{2}}$ single-particle level, $\theta_0^2(1f_{\frac{5}{2}})$ could be determined for use in analyzing the pickup results.

(28) As indicated in Appendix 2, (He^3,d) and (d,t) experiments with heavy nuclei lead to configurations which contain two T values. Very often we should be able to determine the T value simply by the magnitude of $(C)^2\theta^2$, where $(C)^2$ is the isotopic-spin coupling factor. For example, if we should observe an excited-configuration reaction with a near single-particle strength in $\text{Cr}^{52}(\text{He}^3,d)\text{Mn}^{53}$, we could argue that the Mn^{53} state has $T = \frac{3}{2}$, since $(C)^2 = \frac{4}{5}, \frac{1}{5}$ for $T = \frac{3}{2}, \frac{5}{2}$, respectively.

A related point which does not seem to have been emphasized sufficiently in the literature is that (d,n) or (He^3,d) reactions on nuclei with $T > 0$ (and a positive neutron excess) should reveal *two* sets of single-particle states, with $T = T_0 \pm \frac{1}{2}$. Such an effect should be sought

in gross-structure experiments of the kind carried out [for (d,p)] by Schiffer *et al.* (Sc59). Similarly, two sets of single-hole states are expected in (d,t) reactions, while (d,He^3) or (n,d) , like (d,p) , should show no T doubling.

(29) There has recently been considerable interest in the statistics of the spacing of levels of given Π, J, T , one question being, for example, whether the spectrum shows the expected "repulsion" between levels (Po60). Stripping experiments with zero-spin targets to individual levels in a giant resonance peak produce a set of such levels and might then be of some utility in studying the statistical behavior. In fact, combining the reduced widths with the spacings might facilitate a more subtle study of the statistical behavior than is possible via the energies alone.

CONCLUSION

The analysis of stripping data with the aid of the Born approximation has had a good measure of success. A large body of information has been obtained about the structure of nuclei with $A < 70$, checking at many points with findings based on other experimental data. The empirical single-particle reduced widths behave in consistent fashion as functions of their parameters. Available evidence indicates that, in addition to deuteron-nucleon reactions, more complex processes such as (d,t) , (d,He^3) , and perhaps (He^3,α) and (α,t) , which involve transfer of a single nucleon, can be included in the same general framework. This will require further experimental work to determine the empirical constants normalizing the differential cross sections of these more complex reactions.

APPENDIX 1

Isotopic Spin in the $n-p$ Formalism

It has been suggested several times in the foregoing that the isotopic-spin formalism may in some cases, particularly for heavier nuclei, be replaced by a simpler one in which neutrons and protons are treated separately (using what we call the " $n-p$ formalism"). There are really two questions involved here.

The first question is whether in reactions involving heavier nuclei the isotopic-spin Clebsch-Gordan factor which we abbreviate as $(C)^2$ should be included in the equations relating $d\sigma/d\omega$ and θ^2 [e.g., (II.29) and (II.30)], one being often tempted to omit this factor on the vague ground that isotopic spin does not have much to do with heavier nuclei which have a neutron excess and whose active neutrons and protons are in different orbits. We see that in fact $(C)^2$ should always be included in the equation. In a large class of cases, however, $(C)^2 = 1$ so that the question then has no con-

tent; but if $(C)^2 \neq 1$, the use, e.g., of Eq. (II.29) without the $(C)^2$ factor gives a reduced width which has built into it a fluctuating isotopic-spin dependence which may disguise its real significance. The $(C)^2$ factor should then be included in the equation for exactly the same reason as one uses in lighter nuclei. The second question is for the person who wishes to calculate a relative reduced width S from a model. Should he use the T formalism or the $n-p$ formalism? The answer here is that only when $(C)^2$ is automatically unity is the $n-p$ formalism as a general rule more convenient. In this special case the closed neutron subshells behave in the reaction as entirely inert objects.

We observe first that no matter which formalism we choose, the isotopic spin of both states in a reaction is definite.¹⁰⁴ In order, then, for a wave function to be described *simply* in terms of an $n-p$ configuration, it must be that the states of such a configuration should have a definite T , for otherwise we would have to use an appropriate mixture of $n-p$ configurations. It is easy to show (see Fr60a) that T is definite in an $n-p$ configuration and has the value $|T_z| = \frac{1}{2}(N-Z)$ if and only if every orbit which contains one or more protons is completely filled for neutrons.¹⁰⁵ Configurations of this type we may call $(n-p)_T$ configurations. The low-lying states of heavier nuclei belong to $(n-p)_T$ configurations and, moreover, any (d,p) reaction starting with such a configuration necessarily leads to another. The $(C)^2$ factor has the form $(C[T_{0\frac{1}{2}}T_0+\frac{1}{2}; -T_0, -\frac{1}{2}])^2$ which is automatically unity. The neutron subshell which in the target nucleus has the same orbit as the active protons may be regarded as entirely inert and ignored.

For a (d,n) or (He^3,d) experiment things may be different. If the added proton enters an orbit which is neutron-filled, we have once again a final $(n-p)_T$ configuration, $(C)^2=1$, and things are as before. If the added proton enters a higher orbit which is neutron-empty, the resultant configuration is not an $(n-p)_T$ configuration and $(C)^2 \neq 1$. The point is that final states with two different T values are available¹⁰⁶ and the two

¹⁰⁴ We ignore the admixing of isotopic spins caused by Coulomb effects since for all the nuclei we consider this should be negligibly small except in the special circumstance that two states of the same (J,π) but different T come very close together. Observe, too, that when the reaction involves two $(n-p)_T$ configurations (see the following for the definition) isotopic-spin admixtures which would arise from a different radial dependence of neutron and proton have no effect except to make unequal the single-particle neutron and proton widths.

¹⁰⁵ If the state has a proton excess the words proton and neutron should be interchanged here. Note, too, that certain states involving equivalent protons and neutrons, not in filled subshells, also necessarily have a definite T (for example, a proton and equivalent neutron). These are of no interest to us here and we may exclude them without modifying the definition of an $(n-p)_T$ configuration by observing that their T value depends on J .

¹⁰⁶ Or counting differently, more than one $n-p$ configuration contributes, the proton being added in the j orbit, sinking to another ($j \rightarrow j'$) while a neutron makes the inverse transition. The number of $n-p$ configurations which are excited may be

$(C)^2$ factors simply determine the way in which the total cross section divides among the states of different T . It is obvious that [when the $(C)^2$ factor is properly taken account of] we have¹⁰⁷ $S=1$ for final states of either T . This simple result would have been entirely disguised if reduced widths were extracted without considering the $(C)^2$ factor and, for example, we would find a different reduced width for the (d,n) experiment than for the (d,p) experiment to the corresponding level. The same argument applies to the case where the added proton enters an orbit which contains some neutrons but is not filled except that here we do not have the simple case $S=1$. S instead should be determined by a detailed calculation which is simpler in the T formalism, but in any case the reduced widths should always be extracted using an equation containing the $(C)^2$ factor. If the T value is not known, the quantity determined should be stated as $(C)^{\theta 2}$, and it sometimes happens that the numerical value of this class does, in fact, indicate what the T value must be.

The same remarks apply to the pickup reactions. Here the (d,He^3) experiments starting with a heavier nucleus always lead to an $(n-p)_T$ configuration with $(C)^2=1$. The (d,t) experiments, on the other hand, lead to more complicated situations unless the neutron is removed from a proton-empty orbit. If the orbit is not proton-empty, then once again states of two different T values are available, $(C)^2 \neq 1$, calculations via the T formalism are usually much simpler, and the reduced width should be extracted by means of an equation containing the $(C)^2$ factor.

APPENDIX 2

Further Sum Rules

In many cases, particularly when dealing with (d,t) and (He^3,d) reactions with heavier nuclei, the isotopic spin of many of the final levels is not known and then the sum rules given in Sec. III.10 cannot be immediately applied. Instead, we need sum rules for the quantity $(C)^{\theta 2}$, where $(C)^2$ is the isotopic-spin Clebsch-Gordan coupling factor in (II.30) and (II.37). Since in (III.127) and (III.128) we have given, for the transfer of an equivalent particle, separate sum rules for each final T value, and since (III.140) and (III.141) enable us to generalize these to the most complex configurations,¹⁰⁸ it is not difficult to produce the required sum rules and we give the results without proof.

larger than two (corresponding to different values of j'), but the exclusion principle for the neutrons reduces the number of degrees of freedom to two.

¹⁰⁷ We ignore here the possibility that the initial nucleons couple differently in the final state since we already know how to handle this complication.

¹⁰⁸ Note that in (III.138) the inert group $(\rho_1 \tau_1)$ may be replaced by any group whatever of particles inequivalent to ρ_2 , without changing the results.

$$\sum_{x_0 J_0 T_0} \{C[T_{0\frac{1}{2}}T; M_{T_0 m}]\}^2 S(j^n x JT \rightarrow j^{n-1} x_0 J_0 T_0) = \frac{n}{2} + 2mM_T, \quad (\text{III.120}')$$

$$\sum_{x J T} \{C[T_{0\frac{1}{2}}T; M_{T_0 m}]\}^2 [J] S(j^n x JT \rightarrow j^{n-1} x_0 J_0 T_0) = [J_0] \left\{ \frac{(N-n+1)}{2} - 2mM_{T_0} \right\}, \quad (\text{III.121}')$$

$$\begin{aligned} \sum_{\substack{J_0 T_0 \\ x_2 J_2 T_2}} \{C[T_{0\frac{1}{2}}T; M_{T_0 m}]\}^2 S(J_1 T_1; j^n x_2 J_2 T_2; JT \rightarrow J_1 T_1; j^{n-1} x_3 J_3 T_3; J_0 T_0) \\ = \frac{n}{2} + mM_T \cdot \left\{ \frac{T(T+1) + T_2(T_2+1) - T_1(T_1+1)}{T(T+1)} \right\}, \quad (\text{III.140}') \end{aligned}$$

$$\begin{aligned} \sum_{\substack{J T \\ x_2 J_2 T_2}} \{C[T_{0\frac{1}{2}}T; M_{T_0 m}]\}^2 [J] S(J_1 T_1; j^n x_2 J_2 T_2; JT \rightarrow J_1 T_1; j^{n-1} x_3 J_3 T_3; J_0 T_0) \\ = [J_0] \left\{ \frac{N-n+1}{2} - mM_{T_0} \cdot \left[\frac{T_0(T_0+1) + T_3(T_3+1) - T_1(T_1+1)}{T_0(T_0+1)} \right] \right\}. \quad (\text{III.141}') \end{aligned}$$

We have numbered these equations to coincide with the corresponding sum rules of Sec. III.10 for θ^2 without the $(C)^2$ factor. In the last two, the notation $(J_1 T_1; j^n x_2 J_2 T_2; JT)$ denotes a group $J_1 T_1$ vector coupled to the j^n group $x_2 J_2 T_2$, the resultant angular momenta being JT . The transitions are those of (III.38) with $\alpha_1 \equiv J_1 T_1$, $\alpha_2 \equiv J_2 T_2$, $\beta_2 \equiv J_3 T_3$, etc., remembering, as just mentioned, that the internal structure of the inert group is of no consequence. The first two equations are special cases ($T_1 \rightarrow 0$) of the second two, while the second and fourth are the hole-particle complements of the other two. The trivial case $T=0$ causes no difficulty in the last two equations, the m -dependent term simply vanishing when $T=0$. The equations could be written more formally in terms of a Clebsch-Gordan coefficient and (for the last two) a Racah coefficient. For example, the sum in the first equation is

$$n \left\{ C \left[\frac{n}{2} \frac{1}{2} \frac{n+1}{2}; M_{T_0 m} \right] \right\},$$

which sheds an interesting light on the structure of the equation.

The equations inform us immediately about such phenomena as the relative magnitudes (apart from the purely dynamical effects) of a giant resonance peak reached from a given nucleus by (d,p) and (d,n) reactions, and when more data of this type become available they will be of considerable value.

We stress once again that the equations given here and in Sec. III.10 enable us to evaluate the desired sum for any case whatever for which a target wave function is available. When dealing with a j^n group the symbols in question do not require that the symplectic symmetry or seniority should be good; there is, in general, such a requirement for the sum rules of Eqs. (III.132), (III.136), and (III.137), but we have not felt it worthwhile to write the equations for these cases.

Finally, if the target wave function is represented as a linear combination of orthogonal states with ampli-

tudes A_i , it is clear that in any sum rule there is no interference between the different components, and the sums are then a linear combination with amplitudes $|A_i|^2$ of the sums for each orthogonal state. The vanishing of these interference terms is shown in a specific example at the end of Sec. VI.

ACKNOWLEDGMENTS

We would like to express our gratitude to J. C. Armstrong, R. S. Bender, E. F. Bennett, A. G. Blair, O. M. Bilaniuk, C. K. Bockelman, W. W. Buechner, H. A. Enge, E. W. and A. I. Hamburger, S. Hinds, E. L. Keller, L. L. Lee, J. N. McGruer, W. C. Parkinson, G. Parry, J. B. Reynolds, H. T. Richards, J. P. Schiffer, K. G. Standing, E. K. Warburton, D. H. Wilkinson, J. L. Yntema, and B. Zeidman for sending us experimental data before publication. Thanks are due to W. P. Alford, O. M. Bilaniuk, D. A. Bromley, B. L. Cohen, H. A. Enge, A. I. and E. W. Hamburger, H. Neupert, and E. K. Warburton for discussions of experimental data, and to N. Austern, E. Baranger, L. S. Kisslinger, R. D. Lawson, C. Lubitz, S. P. Pandya, and B. J. Raz for comments, criticism, and suggestions. Finally, we are grateful to Dr. A. J. Allen for hospitality at the Radiation Laboratory, University of Pittsburgh, where part of this work was carried out.

BIBLIOGRAPHY

- Aj52 F. Ajzenberg, Phys. Rev. 88, 298 (1952).
- Aj59 F. Ajzenberg-Selove and T. Lauritsen, Nuclear Phys. 11, 1 (1959).
- Am59 R. D. Amado, Phys. Rev. Letters 2, 399 (1959).
- Ar60 J. Armstrong (private communication).
- As59 V. J. Ashby and H. C. Catron, UCRL Rept. 5419 (1959).
- Au54 T. Auerbach, University of Rochester Ph.D. thesis, 1954.
- Au55 T. Auerbach and J. B. French, Phys. Rev. 98, 1276 (1955).
- Au56 T. Auerbach and J. B. French, NYO Rept. 3478 (1956).
- Au60 N. Austern, "Direct reaction theories," in J. B. Marion and J. L. Fowler, Editors, *Fast Neutron Physics* (Interscience Publishers Inc., New York, 1960), Chap. V.
- Ba57 E. Baumgartner and H. W. Fulbright, Phys. Rev. 107, 219 (1957).

- Ba58 E. Baranger and S. Meshkov, Phys. Rev. Letters **1**, 30 (1958).
- Ba59 R. Batchelor and J. H. Towle, Proc. Phys. Soc. (London) **73**, 307 (1959).
- Be53 R. E. Benenson, Phys. Rev. **90**, 420 (1953).
- Be56 R. E. Benenson, K. W. Jones, and M. T. McEllistrem, Phys. Rev. **101**, 308 (1956).
- Be58 E. F. Bennett, NYO Rept. 8082 (1958); Princeton University Ph.D. thesis, 1958.
- Be59 E. F. Bennett and D. R. Maxson, Phys. Rev. **116**, 131 (1959).
- Bh52 A. B. Bhatia, K. Huang, R. Huby, and H. C. Newns, Phil. Mag. **43**, 485 (1952).
- Bi57 O. M. Bilaniuk and P. V. C. Hough, Phys. Rev. **108**, 305 (1957).
- Bi58 O. M. Bilaniuk and J. C. Hensel (private communication).
- Bi59 O. M. Bilaniuk and J. B. French (to be published).
- Bo52 A. Bohr, Kgl. Danske Videnskab. Selskab. Math.-fys. Medd. **29**, No. 14 (1952).
- Bo53 A. Bohr and B. R. Mottelson, Kgl. Danske Videnskab. Selskab. Math.-fys. Medd. **27**, No. 16 (1953).
- Bo55 H. Boerner, *Darstellungen von Gruppen* (Springer-Verlag, Berlin, 1955).
- Bo57 C. K. Bockelman, C. M. Braams, C. P. Browne, W. W. Buechner, R. R. Sharp, and A. Sperduto, Phys. Rev. **108**, 176 (1957).
- Bo57a C. K. Bockelman and W. W. Buechner, Phys. Rev. **107**, 1366 (1957).
- Br53 D. A. Bromley, J. A. Bruner, and H. W. Fulbright, Phys. Rev. **89**, 396 (1953).
- Br55 C. P. Browne and W. C. Cobb, Phys. Rev. **99**, 644(A) (1955).
- Br55a C. P. Browne, MIT Progr. Rept., May 31, 1955.
- Br57 D. A. Bromley, H. E. Gove, and A. E. Litherland, Can. J. Phys. **35**, 1057 (1957).
- Br58 C. Broude, L. L. Green, and J. C. Willmott, Proc. Phys. Soc. (London) **72**, 1122 (1958).
- Br59 D. M. Brink and A. K. Kerman, Nuclear Phys. **12**, 314 (1959).
- Bu51 S. T. Butler, Proc. Roy. Soc. **A208**, 559 (1951).
- Bu51a E. J. Burge, H. B. Burrows, W. M. Gibson, and J. Rotblat, Proc. Roy. Soc. (London) **A210**, 534 (1951).
- Bu56 H. B. Burrows, T. S. Green, S. Hinds, and R. Middleton, Proc. Phys. Soc. (London) **A69**, 310 (1956).
- Bu57 S. T. Butler, *Nuclear Stripping Reactions* (John Wiley & Sons, Inc., New York, 1957).
- Ca52 F. L. Canavan, Phys. Rev. **87**, 136 (1952).
- Ca55 J. M. Calvert, A. A. Jaffe, A. E. Litherland, and E. E. Maslin, Proc. Phys. Soc. (London) **A68**, 1008 (1955).
- Ca55a J. M. Calvert, A. A. Jaffe, and E. E. Maslin, Proc. Phys. Soc. (London) **A68**, 1017 (1955).
- Ca57 J. M. Calvert, A. A. Jaffe, A. E. Litherland, and E. E. Maslin, Proc. Phys. Soc. (London) **A70**, 78 (1957).
- Ca57a R. R. Carlson, Phys. Rev. **107**, 1094 (1957).
- Ca58 J. R. Cameron, Bull. Am. Phys. Soc. Ser. II, **3**, 187 (1958).
- Ce56 M. Cerineo, Nuclear Phys. **2**, 113 (1956).
- Cl59 C. M. Class, R. H. Davis, and J. H. Johnson, Phys. Rev. Letters **3**, 41 (1959).
- Co35 E. U. Condon and G. H. Shortley, *Theory of Atomic Spectra* (Cambridge University Press, New York, 1935).
- Co57 S. A. Cox and R. M. Williamson, Phys. Rev. **105**, 1799 (1957).
- Co57a W. R. Cobb and D. B. Guthe, Phys. Rev. **107**, 181 (1957).
- Da52 P. B. Daitch and J. B. French, Phys. Rev. **87**, 900 (1952).
- Da53 R. H. Dalitz, Proc. Phys. Soc. (London) **A66**, 28 (1953).
- Da57 A. W. Dalton, S. Hinds, and G. Parry, Proc. Phys. Soc. (London) **A70**, 586 (1957).
- Da59 A. W. Dalton, G. Parry, and H. D. Scott, Proc. Phys. Soc. (London) **73**, 677 (1959).
- Da60 A. W. Dalton, G. Parry, and H. D. Scott (to be published).
- Da60a A. W. Dalton, A. Kirk, G. Parry, and H. D. Scott, Proc. Phys. Soc. (London) **75**, 95 (1960).
- Eb54 F. S. Eby, Phys. Rev. **96**, 1355 (1954).
- Ed52 A. R. Edmonds and B. H. Flowers, Proc. Roy. Soc. (London) **A214**, 512 (1952).
- Ed57 A. R. Edmonds, *Angular Momentum in Quantum Mechanics* (Princeton University Press, Princeton, New Jersey, 1957).
- El52 F. A. El-Bedewi, Proc. Phys. Soc. (London) **A65**, 64 (1952).
- El54 J. P. Elliott, J. Hope, and H. A. Jahn, Phil. Trans. Roy. Soc. (London) **A246**, 241 (1954).
- El55 J. P. Elliott and T. H. R. Skyrme, Proc. Roy. Soc. (London) **A232**, 561 (1955).
- El55a J. P. Elliott and B. H. Flowers, Proc. Roy. Soc. (London) **A229**, 536 (1955).
- El56 F. A. El-Bedewi, Proc. Phys. Soc. (London) **A69**, 221 (1956).
- El57 J. P. Elliott and A. M. Lane, "The nuclear shell model," *Handbuch der Physik* (Springer-Verlag, Berlin, 1957), Vol. XXXIX, p. 214.
- El57a F. A. El-Bedewi and M. A. El-Wahab, Nuclear Phys. **3**, 385 (1957).
- El57b J. P. Elliott and B. H. Flowers, Proc. Roy. Soc. (London) **A242**, 57 (1957).
- El57c F. A. El-Bedewi and I. Hussein, Proc. Phys. Soc. (London) **A70**, 233 (1957).
- El58 F. A. El-Bedewi and S. Tadros, Nuclear Phys. **8**, 71 (1958).
- El58a F. A. El-Bedewi and S. Tadros, Nuclear Phys. **8**, 79 (1958).
- El58b A. J. Elwyn and F. B. Shull, Phys. Rev. **111**, 925 (1958).
- En56 H. A. Enge, A. Sperduto, W. W. Buechner, and M. Mazari, MIT Progr. Rept. XV (1955-56).
- En57 P. M. Endt and C. M. Braams, Revs. Modern Phys. **29**, 683 (1957).
- En59 H. A. Enge, E. J. Irwin, Jr., and D. H. Weaner, Phys. Rev. **115**, 949 (1959).
- Ev53 W. H. Evans, T. S. Green, and R. Middleton, Proc. Phys. Soc. (London) **A66**, 108 (1953).
- Ev54 N. T. S. Evans and W. C. Parkinson, Proc. Phys. Soc. (London) **A67**, 684 (1954).
- Ev58 N. T. S. Evans and A. P. French, Phys. Rev. **109**, 1272 (1958).
- Fa51 U. Fano, Natl. Bur. Standards Rept. No. 1214 (1951).
- Fa54 W. M. Fairbairn, Proc. Phys. Soc. (London) **A67**, 564 (1954).
- Fe37 E. Feenberg and E. P. Wigner, Phys. Rev. **51**, 95 (1937).
- Fe37a E. Feenberg and M. Phillips, Phys. Rev. **51**, 597 (1937).
- Fe55 E. Feenberg, *Shell Theory of the Nucleus* (Princeton University Press, Princeton, New Jersey, 1955).
- Fi51 R. E. Fields and M. Walt, Phys. Rev. **83**, 479 (L) (1951).
- Fi52 B. H. Flowers, Proc. Roy. Soc. (London) **A212**, 248 (1952).
- Fo54 G. M. Fogelsong and D. G. Foxwell, Phys. Rev. **96**, 1001 (1954).
- Fr53 R. G. Freemantle, W. M. Gibson, D. J. Prowse, and J. Rotblat, Phys. Rev. **92**, 1268 (1953).
- Fr56 J. B. French and B. J. Raz, Phys. Rev. **104**, 1411 (1956).
- Fr56a J. B. French, Phys. Rev. **103**, 1391 (1956).
- Fr57 J. B. French and A. Fujii, Phys. Rev. **105**, 652 (1957).
- Fr58 J. B. French, University of Pittsburgh Tech. Rept. No. IX, NR022-068 (1958).
- Fr60 J. B. French, "The analysis of reduced widths," in F. Ajzenberg-Selove, Editor, *Nuclear Spectroscopy* (Academic Press, Inc., New York, 1960).
- Fr60a J. B. French (to be published).
- Fu52 H. W. Fulbright, J. A. Bruner, D. A. Bromley, and L. M. Goldman, Phys. Rev. **88**, 700 (1952).
- Fu54 Y. Fujimoto, K. Kikuchi, and S. Yoshida, Progr. Theoret. Phys. Kyoto **11**, 264 (1954).
- Ge53 E. Gerjuoy, Phys. Rev. **91**, 645 (1953).
- Gi52 W. M. Gibson and E. E. Thomas, Proc. Roy. Soc. (London) **A210**, 543 (1952).

- Gi54 W. M. Gibson, Phil. Mag. **44**, 297 (1953).
 Go34 S. Goudsmit and R. F. Bacher, Phys. Rev. **46**, 948 (1934).
 Go53 E. Goldberg, Phys. Rev. **89**, 760 (1953).
 Go56 S. Goldstein and I. Talmi, Phys. Rev. **102**, 589 (1956).
 Gr56 T. S. Green and R. Middleton, Proc. Phys. Soc. (London) **A69**, 28 (1956).
 Gr56a J. C. Grosskreutz, Phys. Rev. **101**, 706 (1956).
 Gr56b W. C. Grayson, Jr., and L. W. Nordheim, Phys. Rev. **102**, 1084 (1956).
 Ha49 O. Haxel, J. H. D. Jensen, and H. E. Suess, Phys. Rev. **75**, 1766 (1949).
 Ha50 O. Haxel, J. H. D. Jensen, and H. E. Suess, Z. Physik **128**, 295 (1950).
 Ha56 E. C. Halbert, University of Rochester Ph.D. thesis, 1956.
 Ha58 A. I. and E. W. Hamburger, Bull. Am. Phys. Soc. Ser. II, **3**, 222 (1958).
 Ha59 E. W. Hamburger, University of Pittsburgh thesis, Tech. Rept. No. XII, NRO22-068 (1959).
 Ha59a E. W. Hamburger (private communication).
 Ha60 E. W. Hamburger and A. G. Blair, Phys. Rev. **119**, 777 (1960).
 Ha60a A. I. Hamburger, Phys. Rev. (to be published).
 Hi57 S. Hinds (private communication).
 Hi58 S. Hinds, R. Middleton, and G. Parry, Proc. Phys. Soc. (London) **71**, 49 (1958).
 Hi59 S. Hinds and R. Middleton, Proc. Phys. Soc. (London) **74**, 775 (1959).
 Hi59a S. Hinds and R. Middleton, Proc. Phys. Soc. (London) **74**, 762 (1959).
 Hi59b S. Hinds and R. Middleton, Proc. Phys. Soc. (London) **74**, 196 (1959).
 Ho50 J. R. Holt and C. T. Young, Proc. Phys. Soc. (London) **A63**, 835 (1950).
 Ho53 J. R. Holt and T. N. Marsham, Proc. Phys. Soc. (London) **A66**, 467 (1953).
 Ho53a J. R. Holt and T. N. Marsham, Proc. Phys. Soc. (London) **A66**, 249 (1953).
 Ho53b J. R. Holt and T. N. Marsham, Proc. Phys. Soc. (London) **A66**, 565 (1953).
 Ho53c J. R. Holt and T. N. Marsham, Proc. Phys. Soc. (London) **A66**, 1032 (1953).
 Ho53d J. R. Holt and T. N. Marsham, Proc. Phys. Soc. (London) **A66**, 258 (1953).
 Ho53e J. Horowitz and A. M. L. Messiah, J. phys. radium **14**, 695 (1953).
 Ho53f J. Horowitz and A. M. L. Messiah, J. phys. radium **14**, 731 (1953).
 Ho54 J. Horowitz and A. M. L. Messiah, J. phys. radium **15**, 142 (1954).
 Ho54a H. D. Holmgren, J. D. Blair, B. E. Simmons, T. F. Stratton, and J. F. Stuart, Phys. Rev. **95**, 1544 (1954).
 Hu37 F. Hund, Z. Phys. **105**, 202 (1937).
 Hu53 R. Huby, Progr. Nuclear Phys. **3**, 177 (1953).
 In53 D. R. Inglis, Revs. Modern Phys. **25**, 390 (1953).
 Ir51 J. Irving, Phil. Mag. **42**, 338 (1952).
 Ja50 H. A. Jahn, Proc. Roy. Soc. (London) **A201**, 516 (1950).
 Ja51 H. A. Jahn and H. van Wieringen, Proc. Roy. Soc. (London) **A209**, 502 (1951).
 Ke56 A. K. Kerman, Kgl. Danske Videnskab. Selskab. Math.-fys. Medd. **30**, No. 15 (1956).
 Ke59 E. L. Keller (private communication).
 Ke60 E. L. Keller (private communication).
 Ki52 J. S. King and W. C. Parkinson, Phys. Rev. **88**, 141(L), (1952).
 Ki53 J. S. King and W. C. Parkinson, Phys. Rev. **89**, 1080 (1953).
 Ki53a J. S. King and W. C. Parkinson, Phys. Rev. **90**, 381(A) (1953).
 Ku56 D. Kurath, Phys. Rev. **101**, 216 (1956).
 Ku58 J. A. Kuehner, E. Almqvist, and D. A. Bromley, Phys. Rev. Letters **1**, 260 (1958).
 La53 A. M. Lane, Proc. Phys. Soc. (London) **A66**, 977 (1953).
 La54 A. M. Lane and L. A. Radicati, Proc. Phys. Soc. (London) **A67**, 167 (1954).
 La54a A. M. Lane, Rept. T/R 1289, Harwell (unpublished) (1954).
 La55 A. M. Lane, R. G. Thomas, and E. P. Wigner, Phys. Rev. **98**, 1524 (1955).
 La55a A. M. Lane, "On states of non-normal parity in light nuclei," MIT (unpublished) (1955).
 La57 R. D. Lawson and J. L. Uretsky, Phys. Rev. **108**, 1300 (1957).
 La58 A. M. Lane and R. G. Thomas, Revs. Modern Phys. **30**, 257 (1958).
 Le55 S. H. Levine, R. S. Bender, and T. N. McGruer, Phys. Rev. **97**, 1249 (1955).
 Le56 C. Van der Leun and P. M. Endt, Physica **22**, 134(L), (1956).
 Li50 D. E. Littlewood, *Theory of Group Characters* (Oxford University Press, New York, 1950).
 Li58 A. E. Litherland, H. McManus, E. B. Paul, D. A. Bromley, and H. E. Gove, Can. J. Phys. **36**, 378 (1958).
 Lu57 C. R. Lubitz, "Numerical table of Butler-Born approximation stripping cross-sections," University of Michigan Rept. (unpublished) (1957).
 Ma49 M. G. Mayer, Phys. Rev. **75**, 1969 (1959).
 Ma50 M. G. Mayer, Phys. Rev. **78**, 16 (1950).
 Ma50a M. G. Mayer, Phys. Rev. **78**, 22 (1950).
 Ma55 M. G. Mayer and J. H. D. Jensen, *Theory of Nuclear Shell Structure* (John Wiley & Sons, Inc., New York, 1955).
 Ma56 E. E. Maslin, J. M. Calvert, and A. A. Jaffe, Proc. Phys. Soc. (London) **A69**, 754 (1956).
 Ma57 J. B. Marion, Nuclear Phys. **4**, 282 (1957).
 Ma59 M. H. Macfarlane and J. B. French, NYO Rept. 2846 (1959).
 Ma60 S. Mayo and A. I. Hamburger, Phys. Rev. (to be published).
 Mc56 J. N. McGruer, E. K. Warburton, and R. S. Bender, Phys. Rev. **100**, 235 (1956).
 Me56 S. Meshkov and C. W. Ufford, Phys. Rev. **101**, 258 (1956).
 Me58 W. E. Meyerhof and L. F. Chase, Jr., Phys. Rev. **111**, 1348 (1958).
 Mi53 R. Middleton, E. A. El-Bedewi, and C. T. Tai, Proc. Phys. Soc. (London) **A66**, 95 (1953).
 Mo57 S. A. Moszkowski, "Nuclear models," *Handbuch der Physik* (Springer-Verlag, Berlin, 1957), Vol. XXXIX, p. 411.
 Mo58 W. E. Moore, J. N. McGruer, and A. I. Hamburger, Phys. Rev. Letters **1**, 29 (1958).
 Mo59 W. E. Moore, University of Pittsburgh Ph.D. thesis, 1959 (unpublished).
 Na58 M. El-Nadi and L. Abou Hadid, Nuclear Phys. **8**, 51 (1958).
 Ne58 H. Neuert (private communication).
 Ni54 W. E. Nickell, Phys. Rev. **95**, 426 (1954).
 Ni55 S. G. Nilsson, Kgl. Danske Videnskab. Selskab. Math.-fys. Medd. **29**, No. 16 (1955).
 No50 L. W. Nordheim, Phys. Rev. **78**, 294 (1950).
 Nu56 R. H. Nussbaum, Revs. Modern Phys. **28**, 423 (1956).
 Ok55 S. Okai and M. Sano, Progr. Theoret. Phys. Kyoto **14**, 399(L) (1955).
 Pa56 S. P. Pandya, Phys. Rev. **103**, 956 (1956).
 Pa57 E. B. Paul, Phil. Mag. **15**, 311 (1957).
 Pa57a S. P. Pandya, Progr. Theoret. Phys. Kyoto **18**, 668 (1957).
 Pa57b S. P. Pandya and J. B. French, Ann. Phys. **2**, 166 (1957).
 Pa58 W. C. Parkinson, Phys. Rev. **110**, 485 (1958).
 Pa60 W. C. Parkinson (private communication).
 Po60 C. E. Porter and N. Rosenzweig, Suomalaisen Tiedeakat. Toimituksia (to be published).
 Ra42 G. Racah, Phys. Rev. **62**, 438 (1942).
 Ra43 G. Racah, Phys. Rev. **63**, 367 (1943).

- Ra49 G. Racah, Phys. Rev. **76**, 1352 (1949).
 Ra50 G. Racah, Helv. Phys. Acta, Suppl. III **23**, 229 (1950).
 Ra57 G. Rakavy, Nuclear Phys. **4**, 375 (1957).
 Ra60 B. J. Raz, B. Zeidman, and J. L. Yntema, Phys. Rev. (to be published).
 Re51 I. Resnick and S. S. Hanna, Phys. Rev. **82**, 463 (1951).
 Re54 M. G. Redlich, Phys. Rev. **95**, 448 (1954).
 Re55 M. G. Redlich, Phys. Rev. **98**, 199 (1955).
 Re56 J. B. Reynolds and K. G. Standing, Phys. Rev. **101**, 158 (1956).
 Re58 M. G. Redlich, Phys. Rev. **110**, 468 (1958).
 Rh54 K. B. Rhodes, University of Pittsburgh Ph.D. thesis, 1954 (unpublished).
 Ri54 F. L. Ribe and J. D. Seagrave, Phys. Rev. **94**, 934 (1954).
 Ri57 H. T. Richards and A. Chiba (private communication).
 Ri57a F. L. Ribe, Phys. Rev. **106**, 767 (1957).
 Ri60 L. H. Th. Rietjens, O. M. Bilaniuk, and M. H. Macfarlane (to be published).
 Ro48 L. Rosenfeld, *Nuclear Forces* (North-Holland Publishing Company, Amsterdam, 1948).
 Ro51 J. Rotblat, Phys. Rev. **83**, 1271 (1951).
 Ro51a J. Rotblat, Nature **167**, 1027 (1951).
 Ro57 M. E. Rose, *Elementary Theory of Angular Momentum* (John Wiley & Sons, Inc., New York, 1957).
 Ru57 A. G. Rubin, Phys. Rev. **108**, 62 (1957).
 Sa54 G. R. Satchler, Proc. Phys. Soc. (London) **A67**, 471 (1954).
 Sa55 G. R. Satchler, Phys. Rev. **97**, 1416 (1955).
 Sa58 G. R. Satchler, Ann. Phys. **3**, 275 (1958).
 Sa58a J. Sawicki, Nuclear Phys. **6**, 575 (1958).
 Sa58b J. Sawicki and G. R. Satchler, Nuclear Phys. **7**, 289 (1958).
 Sc53 J. E. Schwager and L. A. Cox, Phys. Rev. **92**, 102 (1953).
 Sc54 G. Scharff-Goldhaber and J. Weneser, Phys. Rev. **98**, 212 (1954).
 Sc59 J. P. Schiffer, L. L. Lee, Jr., and B. Zeidman, preprint (1959).
 Se57 F. D. Seward, I. Slaus, and H. W. Fulbright, Phys. Rev. **107**, 159 (1957).
 Sh54 R. Shapiro, Phys. Rev. **93**, 290 (1954).
 Sh55 R. D. Sharp and A. Sperduto, MIT Progr. Rept. 1954-55, and private communication.
 Sh56 R. K. Sheline, Nuclear Phys. **2**, 382 (1956).
 Sh59 F. B. Shull and A. J. Elwyn, Phys. Rev. **112**, 1667 (1959).
 Sm57 R. K. Smith, Phys. Rev. **107**, 196 (1957).
 St55 T. F. Stratton, J. M. Blair, K. F. Famularo, and R. V. Stuart, Phys. Rev. **98**, 629 (1955).
 St56 K. G. Standing, Phys. Rev. **101**, 152 (1956).
 Su58 R. G. Summers-Gill, Phys. Rev. **109**, 1591 (1958).
 Te58 G. M. Temmer and N. P. Heydenburg, Bull. Am. Phys. Soc. Ser. II, **3**, 200 (1958).
 Th55 R. G. Thomas, Phys. Rev. **100**, 25 (1955).
 To54 W. Tobocman, Phys. Rev. **94**, 1655 (1954).
 To55 W. Tobocman and M. H. Kalos, Phys. Rev. **97**, 132 (1955).
 To56 W. Tobocman, Case Institute of Technology Tech. Rept. No. 29 (1956).
 Tr57 G. Trumpy, Nuclear Phys. **2**, 664 (1957).
 Vo58 W. F. Vogelsang and J. N. McGruer, Phys. Rev. **109**, 1663 (1958).
 Wa57 E. K. Warburton and J. N. McGruer, Phys. Rev. **105**, 639 (1957).
 Wa58 A. H. Wapstra, "Atomic masses of nuclides," *Handbuch der Physik* (Springer-Verlag, Berlin, 1958), Vol. XXXVIII, p. 1.
 Wa58a E. K. Warburton and H. J. Rose, Phys. Rev. **109**, 1199 (1958).
 Wa60 E. K. Warburton and W. T. Pinkston, Phys. Rev. (to be published).
 We28 H. Weyl, *Group Theory and Quantum Mechanics* (Dover Publications, New York, 1928).
 We46 H. Weyl, *The Classical Groups* (Princeton University Press, Princeton, New Jersey, 1946).
 We56 A. Werner, Nuclear Phys. **1**, 9 (1956).
 We60 H. E. Wegner and W. S. Hall (to be published).
 Wi55 H. B. Willard, J. K. Bair, and J. D. Kington, Phys. Rev. **98**, 669 (1955).
 Wi55a E. P. Wigner, Ann. Math. **62**, 548 (1955).
 Wi56 H. B. Willard, J. K. Bair, J. D. Kington, and H. O. Cohn, Phys. Rev. **101**, 765 (1956).
 Wi57 D. H. Wilkinson, Phys. Rev. **105**, 666 (1957).
 Wi60 D. H. Wilkinson (private communication, 1960).
 Yo54 S. Yoshida, Progr. Theoret. Phys. Kyoto **12**, 141 (1954).
 Ze58 B. Zeidman and J. M. Fowler, Phys. Rev. **112**, 2020 (1958).
 Ze60 B. Zeidman, J. L. Yntema, and B. J. Raz, Phys. Rev. (to be published).
 Ze60a B. Zeidman (private communication).